UNIVERSITÀ DEGLI STUDI DI FIRENZE
Dipartimento di Sistemi e Informatica
Dottorato di Ricerca in Informatica e Applicazioni
XXV Ciclo

ALGORITHMS FOR BIOLOGICAL GRAPHS: ANALYSIS AND ENUMERATION

ANDREA MARINO

Supervisor: *Prof. Pierluigi Crescenzi*

PhD Coordinator: *Prof. Rosario Pugliese*

December, 2012

Andrea Marino: *Algorithms for Biological Graphs: Analysis and Enumeration,* Dottorato di Ricerca in Informatica e Applicazioni, © December, 2012

ABSTRACT

Some biological networks are designed for sequencing purposes. Others, i.e. Protein-Protein Interaction, Metabolic, and Gene Regulatory Networks are implicitly dynamic in the sense that not all the vertices and links are active at the same time. In such a context, the structural analysis must take into account more biological information, whenever this is possible, or it requires to enumerate all the feasible structures (given some set of constraints) in order to select a posteriori the realistic ones from a biological point of view.

Enumerating all the most and less *central vertices* in a network according to their *eccentricity* is an example of an enumeration problem whose solutions are polynomial and can be listed in polynomial time, very often in linear or *almost* linear time in practice.

Enumerating *stories*, i.e. all maximal directed acyclic subgraphs of a graph G whose sources and targets belong to a predefined subset of the vertices, is on the other hand an example of an enumeration problem with an exponential number of solutions, that can be solved by using a non trivial brute-force approach. Given a metabolic network, each individual story should explain how some interesting metabolites are derived from some others through a chain of reactions, by keeping all alternative pathways between sources and targets.

Enumerating *cycles* or *paths* in an undirected graph, such as a protein-protein interaction undirected network, is an example of an enumeration problem in which all the solutions can be listed through an optimal algorithm, i.e. the time required to list all the solutions is dominated by the time to read the graph plus the time required to print all of them. By extending this result to directed graphs, it would be possible to deal more efficiently with *feedback loops* and *signed paths* analysis in signed or interaction directed graphs, such as gene regulatory networks.

Finally, enumerating *mouths* or *bubbles* with a source s in a directed graph, that is enumerating all the two vertex-disjoint directed paths between the source s and all the possible targets, is an example of an enumeration problem in which all the solutions can be listed through a linear delay algorithm, meaning that the delay between any two consecutive solutions is linear, by turning the problem into a constrained cycle enumeration problem. Such patterns, in a de Bruijn graph representation of the reads obtained by sequencing, are related to polymorphisms in DNA- or RNA-seq data.

Happiness only real when shared
— Christopher McCandless

RINGRAZIAMENTI

Grazie alla mia famiglia, i miei genitori, Maria, Giovanna e Marco, a Lucilla e a chi ha mi ha donato la tranquillità per lavorare serenamente in questi anni. Grazie a Pierluigi, da cui ho avuto l'onore di essere guidato e con cui ho avuto il piacere di lavorare. Grazie a Roberto Grossi e Maria Cecilia Verri; grazie a Leonardo e Beatrice. Grazie agli amici del Dipartimento di Sistemi e Informatica, agli amici del laboratorio 102 del plesso didattico di Viale Morgagni e agli amici frequentatori del Dipartimento Ulisse Dini dell'Università di Firenze.

ACKNOWLEDGMENTS

I would like to thank Marie-France Sagot and BAMBOO & BAOBAB Team of INRIA Grenoble Rhône-Alpes in Lyon, that supported a big part of this work. Thanks to Florence, Paulo, Gustavo, Etienne, Vicente, Rui, Susan, Matteo, Cecilia, Blerina, and Vincent. Thanks to Michel Habib and LIAFA of University Paris Diderot, Paris 7. Thanks to Fedor Fomin and Andrea Pietracaprina, who kindly accepted to read and review this thesis, for their helpful comments and suggestions.

SOUNDTRACK

Carlos Paredes *O Melhor de Carlos Paredes: Guitarra*, Andrés Segovia *The Art of Segovia*, Eddie Vedder *Ukulele Songs* and *Into the Wild*, Cat Power *The Covers Record*, Daft Punk *Tron: Legacy*, Joy Division *Unknown Pleasures* and *Closer*, Pino Daniele *Terra mia*, *Pino Daniele*, and *Nero a metà*, Vinicio Capossela *L'indispensabile*.

CONTENTS

1 INTRODUCTION

The aim of enumeration is to list all the feasible solutions of a given problem satisfying some constraints. Enumeration algorithms are particularly useful whenever the goal of a problem is not clear and all its solutions need to be checked. The number of solutions of an enumeration problem usually increases with the size of the input. Whenever this size is small, brute force algorithms are helpful, and simple implementations can successfully solve the problem. On the other hand, for large scale data more sophisticated approaches from algorithm theory are required in order to guarantee a bounded increase of the computation time when the input size increases.

Since one peculiar property of biological networks is the uncertainty, a scenario in which enumeration algorithms can be helpful is biological network analysis. Modelling biological networks indeed introduce bias: arc dependencies are neglected and underlying hyper-graph behaviours are forced in simple graph representations to avoid intractability. Moreover regulatory interactions between all the biological networks are omitted, even if none of the different biological layers is truly isolated. Last but not least, the dynamical behaviours of biological networks are often not considered: indeed most of the currently available biological network reconstructions are potential networks, where all the possible connections are indicated, even if edges/arcs and vertices are hardly present all together at the same time. We have discussed these aspects of the biological networks in the following work, in which I was involved to understand the modelling mechanism underlying biological networks and to review the measures used to highlight vertices, such as centralities measures.

[1] Cecilia Klein, Andrea Marino, Marie-France Sagot, Paulo Vieira Milreu, and Matteo Brilli. Structural and dynamical analysis of biological networks. *Briefings in functional genomics*, August 2012.

1.1 CONTRIBUTION OF THE THESIS

In this thesis we will show four examples of enumeration algorithms that can be applied to efficiently deal with some biological problems modelled by using biological networks: enumerating central and peripheral nodes of a network, enumerating stories, enumerating paths or cycles, and enumerating bubbles. Notice that the corresponding computational problems we define are of more general interest and our results hold in the case of arbitrary networks. In order to briefly overview our results, in the following we will use the standard notations and definitions, described in Section 1.2.

1.1.1 *Enumerating Central and Peripheral vertices*

Structural analysis allows the identification of important and not important vertices within a network and for this reason has become very popular in many disciplines. In the biological domain, the importance of a vertex can be defined in many different ways. With neighbourhood-based centrality measures, such as degree, the importance of the vertices is inferred from their local connectivity and the more connections a vertex has the more central it is. Closeness, eccentricity, and shortest path based betweenness relies on global properties of a network, such as distance between vertices.

We will focus on the enumeration of the radial and diametral vertices, i.e. vertices that are central and peripheral according to the eccentricity notion of centrality, and on the computation of the radius and diameter of biological networks and of real world graphs in general. The diameter and radius of a graph are respectively the maximum and minimum eccentricity among all its nodes, where the eccentricity of a node x is the distance from x to its farthest node. Thus, intuitively, the diametral source vertices are the vertices that hardly reach the other ones, the diametral target vertices are the vertices hardly reachable from the other ones, and the radial vertices are the vertices that easily reach all the vertices of the network. In order to calculate the vertices that can be easily reached from any other vertex, it is sufficient to consider the transposed graph.

We will present the DiFUB Algorithm, which is able to list all the diametral sources and targets and to compute the diameter of (strongly) connected components of a graph $G = (V, E)$ in time $O(|E|)$ in practice, even if, in the worst case, the complexity is $\Theta(|V||E|)$. Analogously, we will present a new algorithm to list all the central vertices and to compute the radius of (strongly) connected components of a graph in *almost* $O(|E|)$ time in practice.

The analysis of real world networks in general, such as citation, collaboration, communication, road, social, and web networks, has attracted a lot of attention. The fundamental analysis measures have been reviewed in [2]. Moreover the size of these networks has been increasing rapidly, so that in order to study such measures, algorithms able to handle huge amount of data are needed. Since the algorithms available until now were not able to compute diameter and radius in the case of huge real world graphs, the contribution of our algorithms is not just limited to biological networks analysis, but extends also to the analysis of complex networks in general. We thus have shown their effectiveness also for several other kinds of complex networks.

Our work appeared in the following.

[3] Pierluigi Crescenzi, Roberto Grossi, Leonardo Lanzi, and Andrea Marino. On computing the diameter of real-world directed (weighted) graphs. In *SEA*, pages 99–110, 2012.

This has been the generalization of the following works.

[4] P. Crescenzi, R. Grossi, C. Imbrenda, L. Lanzi, and A. Marino. Finding the Diameter in Real-World Graphs: Experimentally Turning a Lower Bound into an Upper Bound. In Mark de Berg and Ulrich Meyer, editor, *Algorithms - ESA 2010, 18th Annual European Symposium. Proceedings, Part I*, volume 6346 of *Lecture Notes in Computer Science*. Springer, 2010.

[5] P. Crescenzi, R. Grossi, M. Habib, L. Lanzi, and A. Marino. On Computing the Diameter of Real-World Undirected Graphs. Presented at Workshop on Graph Algorithms and Applications (Zurich–July 3, 2011) and selected for submission to the special issue of Theoretical Computer Science in honour of Giorgio Ausiello in the occasion of his 70th birthday, 2011.

[6] P. Crescenzi, R. Grossi, M. Habib, L. Lanzi, and A. Marino. On computing the diameter of real-world undirected graphs. *Theoretical Computer Science*, 2012.

Our algorithm in [6], has been used to compute the diameter of Facebook Network (721.1M vertices, 68.7G edges, and diameter 41) with just 17 BFSes in a popular work ([7, 8], divulged by New York Times on November 22, 2011).

The work in [3] has been presented also at WBA 2012 (Workshop in Bioinformatics and Algorithms), held in São Paulo on April 2nd and 3rd, 2012.

In all these works my contribution has been in the design of the algorithms, proving their correctness, and testing their effectiveness on a dataset of real world huge graphs.

1.1.2 *Enumerating Stories*

The problem of enumerating stories was motivated initially by the biological question in [9] related to Metabolic networks, in particular to compound graphs, in which vertices are compounds and there is an arc from a compound x to a compound y if there is a metabolic reaction that consumes x and produces y (see Section 2.2.2). A subset $\mathbb{B}$ corresponds to compounds that have been experimentally identified as having a significantly higher or lower production in a given condition (for instance when an organism is exposed to some stress). The aim is then to extract all the interaction dependencies among the compounds in $\mathbb{B}$ which do not create cycles but at the same time involve as many compounds as possible. These may require intermediate steps that concern compounds not in $\mathbb{B}$, but the initial and final steps must involve only compounds in $\mathbb{B}$.

A solution, that is a possible scenario of metabolic dependencies, is called a *(metabolic) story*.

A metabolic story has to capture the relationship between the vertices of interest in a way that allows us to define a flow of matter from a set of sources to a set of target compounds. The need for this hierarchy between the compounds led us to consider acyclic solutions. The maximality condition has been added in order to capture all alternative paths between the sources and the targets. The problem is then to “tell" all possible stories given as input a graph G and a subset $\mathbb{B}$ of the vertices of G.

We will present a polynomial algorithm to find one story and an exact but exponential approach for the enumeration problem [10, 11]. This definition is a generalization of a well-known problem which is the *feedback arc set* problem. However, any polynomial-delay algorithm to enumerate feedback arc sets (ex: [12]) can only be used in some particular instances that, as we have shown in [10, 11], correspond to graphs encoding a Metabolic network which do not contain the so-called “bad vertices", which are any not interesting vertex v such that for any predecessor p of v and for any successor s of v, there exists a cycle containing the arcs (p, v) and (v, s). Moreover we will show that finding a story with a specified set of sources or targets is NP-hard.

Our contribution appeared in the following works.

[10] Vicente Acuña, Etienne Birmelé, Ludovic Cottret, Pierluigi Crescenzi, Vincent Lacroix, Alberto Marchetti-Spaccamela, Andrea Marino, Paulo Vieira Milreu, Marie-France Sagot, and Leen Stougie. Telling stories. Presented at Workshop on Graph Algorithms and Applications (Zurich–July 3, 2011).

[11] Vicente Acuña, Etienne Birmelé, Ludovic Cottret, Pierluigi Crescenzi, Fabien Jourdan, Vincent Lacroix, Alberto Marchetti-Spaccamela, Andrea Marino, Paulo Vieira Milreu, Marie-France Sagot, and Leen Stougie. Telling stories: Enumerating maximal directed acyclic graphs with a constrained set of sources and targets. *Theor. Comput. Sci.*, 457:1–9, October 2012.

This latter work has been presented also at WBA 2012 (Workshop in Bioinformatics and Algorithms), held in São Paulo on April 2nd and 3rd, 2012.

The open problems arising from our works have been selected and presented in the following workshop.

[13] V. Acuña, E. Birmelé, L. Cottret, P. Crescenzi, F. Jourdan, V. Lacroix, A. Marchetti-Spaccamela, A. Marino, P.V. Milreu, M.-F.Sagot, and L. Stougie. Metabolic stories: uncovering all possible scenarios for interpreting metabolomics data. In First RECOMB Satellite Conference on Open Problems in Algorithmic Biology (RECOMB-AB), August 27-29, 2012, St. Petersburg, Russia., 2012.

In these works, I contributed to the design of the algorithms (to simplify the networks without losing solutions, to find one story, and to enumerate all the stories), proving their correctness, and showing that finding one story with specified set of sources and targets is NP-hard.

1.1.3 *Enumerating Cycles or Paths*

Studying paths or cycles of biological networks can be useful for several purposes. In the case of interaction graphs, such as Gene Regulatory networks, the importance of enumeration has been shown in [14]. These networks are directed, their vertices are genes, and their arcs are signed, where the sign or weight of the arcs indicates the causal relationship between the vertices, such as activation or inhibition (see Section 2.2.3). In particular cycles and paths can be useful for studying dependencies among vertices, the steady state and multistationarity of dynamic models. Moreover cycles and paths respectively correspond to feedback loops [15, 16] related to robustness in cell signaling networks [17], and signaling paths, i.e. the different positive and negative routes along which a molecule can affect another.

We have considered the problem of enumerating paths and cycles in the case of undirected graphs. This result can be useful for undirected Protein-Protein Interaction networks, where nodes are proteins and edges are interactions (see Section 2.2.1), but in the case of interaction networks in general, our approach neglects the effects of the controls, i.e. the sign and direction of the arcs. In this latter case, the cycles can be enumerated in the underlying undirected graph and *a posteriori* filtered or *ad hoc* algorithms can be applied. The main question arising from our work, is whether it is possible to extend our result to directed graphs in order to efficiently deal also with this kind of networks.

On the other hand, our contribution is not just restricted to biological undirected networks, but extends also to arbitrary undirected graphs. Listing all the paths and cycles in a graph is a classical problem whose efficient solutions date back to the early 70s. The best known solution in the literature is given by Johnson's algorithm [18] and takes $O((|\mathcal{C}(G)| + 1)(|E| + |V|))$ and $O((|\mathcal{P}_{st}(G)| + 1)(|E| + |V|))$ time for a graph $G = (V, E)$, where $\mathcal{C}(G)$ and $\mathcal{P}_{st}(G)$ denote respectively the set of cycles and (s, t)-paths in G. However there exists graphs for which this algorithm is not optimal.

We will present the first optimal algorithm to list all the paths and cycles in an undirected graph G. Our algorithm requires $O(|E| + \sum_{c \in \mathcal{C}(G)} |c|)$ time and is asymptotically optimal: indeed, $\Omega(|E|)$ time is necessarily required to read G as input, and $\Omega(\sum_{c \in \mathcal{C}(G)} |c|)$ time is necessarily required to list the output. Moreover, our algorithm lists all the (s, t)-paths in G optimally in $O(|E| + \sum_{\pi \in \mathcal{P}_{st}(G)} |\pi|)$ time, observing that $\Omega(\sum_{\pi \in \mathcal{P}_{st}(G)} |\pi|)$ time is necessarily required to list the output.

Our algorithm exploits the decomposition of the graph into biconnected components and without loss of generality restricts to study paths and cycles in a same biconnected component. Thus it recursively lists the cycles or (s,t)-paths using the classical binary partition: given an edge e in G, list all the solutions containing e, and then all the solutions not containing e, at each time modifying the graph. In order to avoid recursive calls (in the binary partition) that do not list solutions, we will use a *certificate*, as a data structure, whose cost for dynamically updating is constant with respect to the number of solutions produced. In order to prove the complexity obtained, we will exploit the properties of the binary recursion tree corresponding to the binary partition.

This work appeared in the following.

[19] E. Birmelé, R. Ferreira, R. Grossi, A. Marino, N. Pisanti, R. Rizzi, and G. Sacomoto. Optimal listing of cycles and st-paths in undirected graphs. In *ACM-SIAM Symposium on Discrete Algorithms, SODA 2013*.

In this work, I contributed in the first part of the paper, involving the algorithm design and the general amortization strategy.

1.1.4 *Enumerating Bubbles*

A DNA fragment, that is an RNA-coding sequence, is transformed in a Pre-mRNA sequence, through the transcription phase, in which sequences of *exons* and sequences of *introns* alternatively occur. The removal of all the sequences of introns and of some sequences of exons leads to the mRNA sequence, that is a protein-coding sequence, that translated leads to a protein. Since not any exon is transcribed in the mRNA sequence, there can be many possible mRNA sequences. For instance, let $\langle e_1, i_1, e_2, i_2, e_3, i_3, e_4, i_4 \rangle$ be a fragment of DNA, where for any j, with $1 \leqslant j \leqslant 3$, e_j and i_j are the j-th sequence of exons and introns respectively. The possible resulting mRNA sequences containing e_1 are $\langle e_1, e_2, e_3, e_4 \rangle$, $\langle e_1, e_2, e_3 \rangle$, $\langle e_1, e_2, e_4 \rangle$, $\langle e_1, e_3, e_4 \rangle$, $\langle e_1, e_2 \rangle$, $\langle e_1, e_3 \rangle$, $\langle e_1, e_4 \rangle$. The underlying phenomenon is called alternative splicing and checking all the alternative events has been shown in [20] to correspond to checking recognisable patterns in a de Bruijn graph built from the reads provided by a sequencing project (see Section 2.2.4). The pattern corresponds to an (s,t)-bubble: an (s,t)-bubble is a pair of vertex-disjoint (s,t)-paths that only shares s and t.

Since the k-mers correspond to all words of length k present in the reads (strings) of the input dataset, and only those, in relation to the classical de Bruijn graph for all possible words of size k, the de Bruijn graph for NGS data may then not be complete. We will ignore all the details related to the treatment of NGS data using De Bruijn graphs, and consider instead the more general case of finding all (s,t)-bubbles in an arbitrary directed graph. In particular we show the first linear delay algorithm to identify all bubbles. A previous known algorithm presented in [20] was an adaptation of Tiernan's algorithm for cycle enumeration [21] which does not have a polynomial delay. In the worst case the time elapsed between the output of two solutions is proportional to the number of paths in the graph, i.e. exponential in the size of the graph. Our algorithm is a non trivial adaptation of Johnson's cycle enumeration algorithm [18] in a directed graph with the same theoretical complexity. Notably, the method we propose enumerates all bubbles with a given source with $O(|V| + |E|)$ delay. The algorithm requires an initial transformation of the graph, for each source s, that takes $O(|V| + |E|)$ time and space; this transformation reduces the enumeration of bubbles to the enumeration of constrained cycles in a special graph.

Our algorithm is the result of the following work, in which I was involved for the algorithm design, correctness proof, and time complexity proof.

[22] Etienne Birmelé, Pierluigi Crescenzi, Rui A. Ferreira, Roberto Grossi, Vincent Lacroix, Andrea Marino, Nadia Pisanti, Gustavo Akio Tominaga Sacomoto, and Marie-France Sagot. Efficient bubble enumeration in directed graphs. In *SPIRE*, pages 118–129, 2012.

1.2 BASIC DEFINITIONS AND NOTATIONS

Given a set $X = \{x_1, \ldots, x_n\}$, the cardinality of X is denoted by $|X|$. The power set 2^X is the set of all subsets (including the empty set) of X. A sequence S is an ordered set and is denoted by $\langle s_1, \ldots, s_n \rangle$. The length of the sequence is also denoted by $|S|$. The concatenation of S with an element s_{n+1} is the sequence $\langle s_1, \ldots, s_n, s_{n+1} \rangle$ and is denoted by $\langle S, s_{n+1} \rangle$.

A graph G is a pair of sets (V, E), where the elements of V are called vertices and the elements of E are pairs of vertices, so that $E \subseteq V \times V$. In the case of undirected graphs, these pairs are not ordered, so that $(x, y) \in E$ implies $(y, x) \in E$, and we refer to them as *edges*, while for directed graphs, these pairs are ordered and called *arcs*. In the following we will denote by $n = |V|$ the number of vertices and $m = |E|$ the number of edges or arcs. For any arc (x, y), we say that it is from x to y, or it is incoming to y and out-going from x, or x is the out-neighbour of y and y is the in-neighbour of x, or y is a successor of x and x is a predecessor of y. For any edge (x, y) we say that x and y are neighbours. Any edge or arc (x, x) is called self-loop.

If E is a multi-set, then G is called multi-graph, otherwise it is called simple graph. If not specified, we will refer to simple graphs simply as graphs.

For a vertex $u \in V$, for an undirected graph we denote by $N(u)$ its neighbourhood and by $d(u) = |N(u)|$ its degree, while for a directed graph we denote by $N^+(u)$ and $N^-(u)$ its out- and in- neighbourhood respectively, and by $d^+(u) = |N^+(u)|$ and $d^-(u) = |N^-(u)|$ its out- and in- degree respectively. Vertex u is called *source* if $d^+(u) = 0$ and $d^-(u) > 0$ and *target* if $d^-(u) = 0$ and $d^+(u) > 0$.

For a directed graph $G = (V, E)$, we define its transposed graph as $G' = (V, E')$, where $E' = \{(u, v) : (v, u) \in E\}$.

A path π is a sequence of vertices $\langle v_1, \dots, v_k \rangle$, such that for any i with $1 < i \leqslant k$, v_i is neighbour or out-neighbour of v_{i-1}. Thus we refer to a path π by its natural sequence of vertices or arcs/edges. A path π from s to t, or (s,t)-*path*, is denoted by $\pi = s \rightsquigarrow t$. Additionally, $\mathcal{P}(G)$ is the set of all paths in G and $\mathcal{P}_{s,t}(G)$ is the set of all (s,t)-paths in G. When $s = t$ we have cycles, and $\mathcal{C}(G)$ denotes the set of all cycles in G. If a directed graph does not contain cycles, then it is called Directed Acyclic graph (in short, DAG). Whenever for any pair of vertices u, v, there is a path from u to v, we say that the graph is connected if G is undirected, or strongly connected if G is directed.

The number of arcs or edges in a path π is called length and denoted by $|\pi|$. Analogously the number of arcs or edges in a cycle c is called length and denoted by $|c|$. In this work, we will consider just simple paths and simple cycles.

For any two vertices u, v, the length of the shortest path from u to v is called *distance* and denoted by $d(u,v)$, that is $d(u,v) = \min_{\pi \in \mathcal{P}_{u,v}(G)} |\pi|$. Whenever there is no path from u to v, v is said to be not reachable from u and $d(u,v) = \infty$. The diameter of G is the minimum D such that for any pair of vertices u, v, $d(u,v)$ is less or equal than D, that is $D = \max_{u,v \in V \times V} d(u,v)$. We define the forward (respectively, backward) eccentricity of u and denote it by $ecc_F(u)$ (respectively, $ecc_B(u)$) the $\max_{v \in V} d(u,v)$ (respectively, $\max_{v \in V} d(v,u)$). In the case of undirected graphs, forward and backward eccentricities coincide and are both called simply eccentricity and denoted by $ecc(u)$. Thus the diameter is defined as the maximum forward or the maximum backward eccentricity, i.e. $D = \max_{u \in V} ecc_F(u) = \max_{u \in V} ecc_B(u)$. The radius R of G is the minimum forward eccentricity of its vertices, i.e. $R = \min_{u \in V} ecc_F(u)$, or, in the case of undirected graphs, $R = \min_{u \in V} ecc(u)$. Notice that in general, in directed graphs $\min_{u \in V} ecc_F(u) \neq \min_{u \in V} ecc_B(u)$. We denote by T_u^F (respectively, T_u^B) a forward (respectively, backward) Breadth-First Search (in short, BFS) tree rooted at node u, so that $ecc_F(u)$ (respectively, $ecc_B(u)$) is its height. In an undirected graph for any vertex u in V, the levels of the forward breadth-first search tree rooted at node u, T_u^F, coincide with a backward BFS tree rooted at the same node, T_u^B: thus we refer to both trees simply by T_u.

For a vertex $v \in V$, the *postorder* DFS number of v is the relative time in which v was *last* visited in a Depth-First Search (in short, DFS) traversal, i.e. the position of v in the vertex list ordered by the last visiting time of each vertex in the DFS.

The subgraph *induced* by a set of vertices $V' \subseteq V$ is a graph $G' = (V', E')$, where $E' = \{(u,v) : (u,v) \in E, u, v \in V'\}$. Thus $G[V']$ denotes the subgraph induced by V', and $G - u$ is the induced subgraph $G[V \setminus \{u\}]$ for $u \in V$. Likewise for $e \in E$, we adopt the notation $G - e = (V, E \setminus \{e\})$, and, for any $F \subseteq E$, $G - F = (V, E \setminus F)$.

A *rooted tree* T is an undirected graph such that any two vertices are connected by a unique path and there is one special vertex r called root. The *parent* of a vertex v in T is the vertex connected to it on the path to the root. A *child* of v is a vertex of which v is the parent. The set of all children of v is denoted by

$N^+(v)$. The subtree of T rooted at v is denoted by $T(r)$. The *depth* of a vertex is the length of its unique path to the root. The *height* of a vertex is the length of the longest downward path to a leaf from that node.

In order to avoid confusions, we use the term *node* exclusively when referring to trees. For a given recursive algorithm, in its recursion tree T, each node $x \in T$ corresponds to a call of the algorithm, each $y \in N^+(x)$, child of x, corresponds to a recursive call done inside (the call corresponding to) x, and the root is the initial call to the algorithm. We will use the terms node (of the recursion tree), call (to the algorithm) and iteration (of the algorithm) interchangeably. Moreover, when analysing the time complexity of recursive algorithms, we consider that the cost of an iteration does not include the cost of its recursive calls.

1.3 STRUCTURE OF THE THESIS

The thesis is structured as follows: in Chapter 2, we overview the main kinds of biological networks and we highlight the dynamical structure of the biological networks: we argue the importance of enumeration algorithms for biological network analysis; in Chapter 3, we overview the main computation issues related to enumeration problems and the main techniques to design algorithms and proving their complexity; in the subsequent chapters we show four examples of enumeration algorithms related to biological problems: in Chapter 4 we discuss the problem of enumerating central and peripheral nodes, in Chapter 5 we discuss the problem of enumerating stories, in Chapter 6 we discuss the problem of enumerating cycles or paths, and in Chapter 7 we discuss the problem of enumerating bubbles; we conclude in Chapter 8, summarizing and reporting some open problems.

2 ANALYSIS OF BIOLOGICAL NETWORKS

In this chapter we present an overview of the main kinds of biological networks, highlighting the neglected aspects of each model. In such a context, when analysing biological networks, we argue the need of enumeration algorithms to check all the solutions of a given problem in order to select the realistic ones from a biological point of view.

2.1 INTRODUCTION

Biological networks, are currently being studied with approaches derived from the mathematical and physical sciences. Their structural analysis enables to highlight vertices or structures with special properties that have sometimes been correlated with the biological importance of a gene/protein or event. However, the way in which the biological networks are modelled often neglects the condition-dependencies and the relationship of their links, since a complex behaviour is forced in a form of representation of a simple graph, instead of a directed weighted hypergraph. Moreover biological networks are dynamic both on the evolutionary time-scale, as well as on the much shorter time-scale of physiological processes. There is therefore not a unique network for a given cellular process, but potentially many realizations, each with different properties as a consequence of regulatory mechanisms. Such realizations provide snapshots of a same network in different conditions, enabling the study of condition-dependent structural properties. In such a context, by defining and solving a problem on this simplified form of representations, we need to check all its solutions in order to select the realistic ones.

STRUCTURE OF THE CHAPTER The chapter is structured as follows: in Section 2.2 we report the overview of biological networks; in Section 2.3 we highlight the dynamical structure of the biological networks and we argue the importance of enumeration algorithms for biological network analysis. This second part of the chapter appeared in [1].

2.2 BIOLOGICAL NETWORKS

High-throughput technologies have recently allowed a new perspective in biology, where the cell is interpreted as a large and complex system composed of highly integrated sub-systems. Interpretation of these systems as networks of interactions has spurred the application of analytical tools developed since long by mathematicians and physicists to biological networks.

Several kind of biological networks have been defined, such as Protein-Protein Interaction networks (see Section 2.2.1), Metabolic networks (see Section 2.2.2), Gene Regulatory networks (see Section 2.2.3), de Bruijn graph (see Section 2.2.4).

2.2.1 *Protein-Protein Interaction network*

Proteins form an essential part of organisms and participate in virtually every process within cells. They can be enzymes that catalyse biochemical reactions, or they can have structural or mechanical functions. Moreover they can be involved in cell signalling, immune responses, cell adhesion, and in the cell cycle.

Proteins are biochemical compounds consisting of one or more polypeptides. A polypeptide is a single linear polymer chain of amino acids bonded together by peptide bonds between the carboxyl (carbon double linked with oxygen) and amino (nitrogen linked to two hidrogen) groups of adjacent amino acid residues. The sequence of amino acids in a protein is defined by the sequence of a gene, which is encoded in the genetic code. In general, the genetic code specifies 20 standard amino acids. In the cell, a protein is produced by applying *transcription* and after *translation*.

Protein-protein interactions occur when two or more proteins bind together, often to carry out their biological function.

In a Protein-Protein Interaction network (in short PPIN), vertices are proteins and edges, that are undirected, represent physical interaction between them. Since these interactions can be further combined among them and can happen at different times, in a simple graph representation, whenever a protein has more than one partner (protein complex) we do not know if the different interactions take place together or at different times.

2.2.2 *Metabolic network*

Metabolism is the set of chemical reactions that happen in the cells of living organisms to sustain life. These processes allow organisms to grow and reproduce, maintain their structures, and respond to their environments. A reaction transforms some chemical molecules into others. The molecules that describe a reaction are called chemical compounds, or shortly compounds, and in particular the chemical compounds involved in metabolism are called metabolites. The input compounds of a reaction are called substrates, while the output compounds are called products. Reactions may be reversible, meaning that it is possible to transform its set of products into its set of substrates.

A Metabolic network (in short MN) represents the set of chemical reactions involved in the metabolism of an organism, together performing tasks of putting together and breaking apart molecules in a living cell, e.g. photosynthesis, glycolysis. These chemical reactions are organized into metabolic pathways, in which one or more chemical are transformed through a series of steps into other chemicals, by a sequence of reactions. Enzymes allow organisms to drive desirable reactions that require energy and will not occur by themselves, by coupling them to spontaneous reactions that release energy.

A Metabolic network may be interpreted and built in different ways: vertices can be metabolites or reactions (respectively giving rise to the compound and the reaction graphs), and arcs can be reactions or shared metabolites (see [23, 24]).

In particular a Metabolic network can be modelled as a bipartite directed graph, whose set of vertices can be divided into a set of reactions $\mathcal{R}$ and a set of compounds $\mathcal{C}$, and whose set of arcs can be from a reaction to a compound and vice versa: a reaction has an incoming arc for each one of its substrates and one outgoing arc for each of its products. Alternatively a Metabolic network can be modelled as a directed hypergraph, whose vertices are compounds and hyperarcs are reactions: an hyperarc is a pair $(V_S(r), V_P(r))$, where $V_S(r)$ and $V_P(r)$ are respectively the set of substrates and the set of products of reaction r (see [25] for other examples of hypergraphs applied to biological questions and the associated computational problems). The reconstruction may lead to a loss of fundamental information, as for instance *stoichiometry*, that is the relative amount produced and consumed by each reaction. The stoichiometric matrix $S \in \mathbb{R}_{|C| \times |R|}$, is defined for any compound c and reaction r as follows.

$$S_{c,r} = \begin{cases} k & \text{if } r \text{ produces } k \text{ units of } c \\ -k & \text{if } r \text{ consumes } k \text{ units of } c \\ 0 & \text{otherwise} \end{cases}$$

Since Metabolic networks describe the reactions taking place inside a cell, there might be external compounds to the network: *input* (e.g. nutrients) and *output* (final product of a cell) compounds.

The problems modelled by using hypergraphs (or directed bipartite graphs) are usually hard, so that very often Metabolic networks are studied as Compound graphs, in which the vertices correspond to compounds and there is an arc between two compounds if there is a reaction where one is a substrate and the other is a product. For the sake of completeness, we will mention also Reaction graphs that are the graphs in which the vertices correspond to reactions and there is an arc between two reactions if there is a compound produced by one and consumed by the other [26].

In Figure 1 we summarize these graph models to represent Metabolic networks by considering the reactions R_1, R_2, and R_3 involved in the *Gluconeogenesis* metabolic pathway.

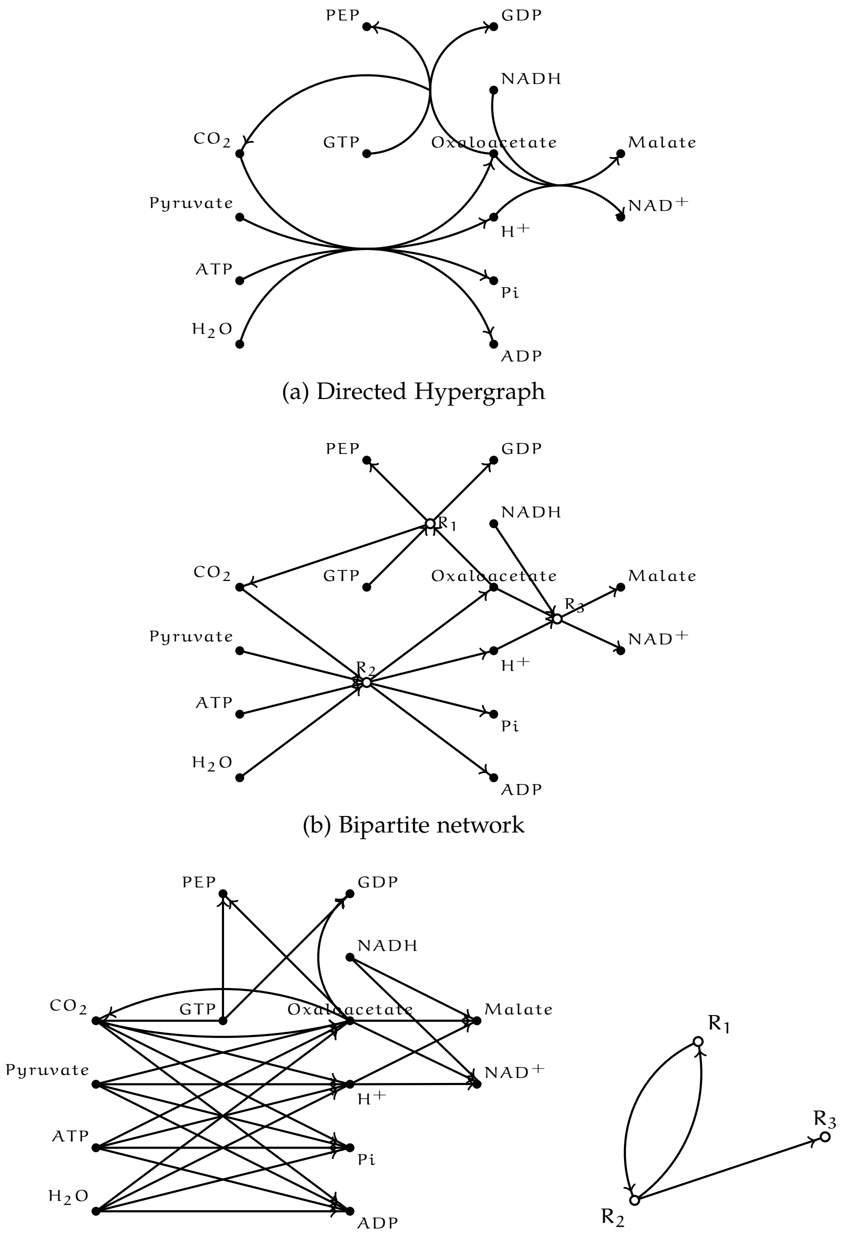

(a) Directed Hypergraph

(b) Bipartite network

(c) Compound network

(d) Reaction network

$$
\begin{aligned}
R_1 &: \quad GTP + Oxaloacetate \longrightarrow CO_2 + PEP + GDP \\
R_2 &: \quad Pyruvate + CO_2 + ATP + H_2O \longrightarrow Oxaloacetate + H^+ + Pi + ADP \\
R_3 &: \quad NADH + Oxaloacetate + 2H^+ \longrightarrow Malate + NAD^+
\end{aligned}
$$

Figure 1: Modelling Metabolic networks

2.2.3 *Gene Regulatory network*

Regulation of gene expression (or gene regulation) includes the processes that cells and viruses use to regulate the way that the information in genes is turned into gene products. Although a functional gene product can be an RNA, the majority of known mechanisms regulates protein coding genes. Gene regulation drives the processes of cellular differentiation and cell living cycle.

A Gene Regulatory network (GRN) models a collection of DNA segments in a cell which interact with each other indirectly, through their RNA and protein expression products, and with other substances in the cell, thereby governing the rates at which genes in the network are transcribed into mRNA.

In a Gene Regulatory network, vertices representing transcriptional regulators are connected by signed arcs to the nodes corresponding to their targets. The sign or weight of such arcs indicates the effect of the control. Because of combinatorial regulation whose output depends on the architecture of promoters which is not encoded in a basic Gene Regulatory network, an hypergraph representation could also be better for these networks [27, 28, 29].

Moreover the system can have as input proteins such as transcription factors, and as output the level of gene expression. The dependencies among links can be modelled using new vertices that correspond to functions which can be obtained by combining basic functions upon the inputs (in a Boolean network model these are boolean functions, typically AND, OR, and NOT). These functions have been interpreted as performing a kind of information processing within the cell, which determines the cellular behaviour.

In Figure 2 we summarize the main forms of representation of a Gene Regulatory network. A genetic circuit is a visual representation of a biological system. The bipartite graph has vertices for proteins and different logical gates for combinatorial regulation: AND requires the presence of both regulators to have transcription, while OR means that it can be activated by one of the regulators alone. The information on the promoter logics is lost in a simple representation, while it is encoded in a hypergraph representation. If a regulator z is removed, when analysing a simple network, one may infer that the auto-regulation of w continues to take place, which is not true, as correctly predicted by the bipartite graph.

2.2.4 *De Bruijn graph*

Ever since Watson and Crick elucidated the structure of the DNA molecule in 1953, thus proving that it carried the genetic information, the challenge of reading the DNA sequence became central for biological research. The earliest chemical methods for DNA sequencing were extremely inefficient, laborious and costly. Over the next few decades, sequencing became more efficient by orders of

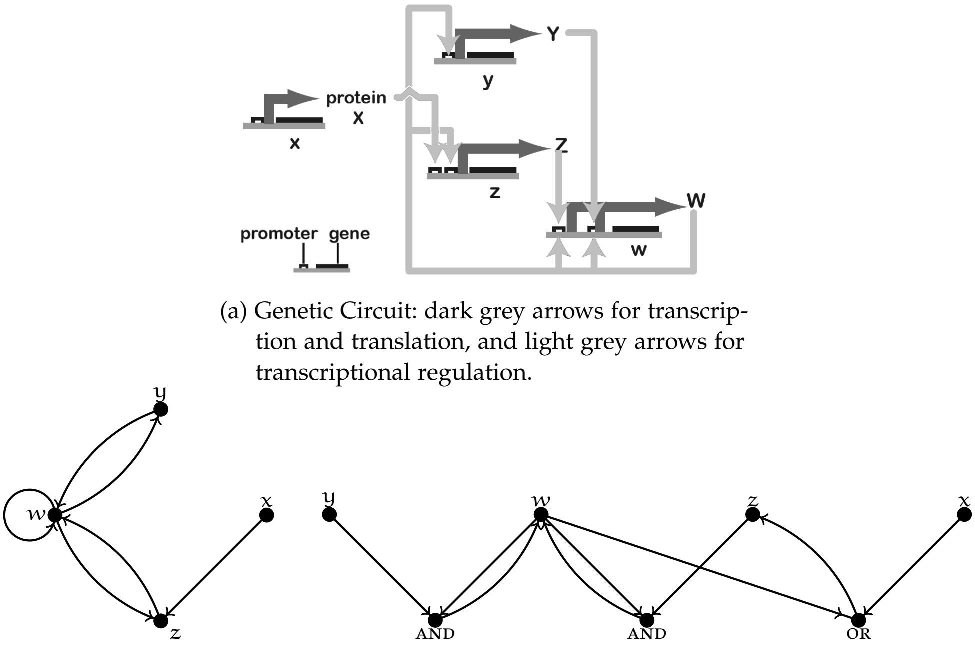

(a) Genetic Circuit: dark grey arrows for transcription and translation, and light grey arrows for transcriptional regulation.

(b) Simple network

(c) Bipartite network

Figure 2: Modelling Gene Regulatory networks

magnitude. In the 1970s, two classical methods for sequencing DNA fragments were developed by Sanger and Gilbert, the dominant sequencing technologies from the late 1970s to the late 2000s used for all of the initial genome sequencing projects (*H. influenzae*, *Yeast*, *Drosophila*, *Arabidopsis*, *human*, and so on). In the 1980s these methods were augmented by the advent of partial automation as well as the cloning method.

Over the past couple of years, new sequencing technologies, called Next Generation Sequencing, have emerged. These new techniques sequence millions of fragments efficiently and in parallel. These fragment sequences are called *reads*, and they form the input for the computational problems.

Next generation sequencing can be used for SNP (single nucleotide polymorphism, i.e. a variation of a single nucleotide in the genetic code of a population) detection or even whole genome re-sequencing. In the first case, it requires the knowledge of most of the sequence in order to identify just rare differences among individuals. This can be used to model organisms that already have a high-quality reference genome sequence available. There are three next generation sequencing platforms that are commercially available and in widespread use: 454 (also known as pyrosequencing or Roche GS FLX, the first next generation method to be commercially available and the first to be applied to large-scale sequencing projects, such as sequencing the genome of James Watson), Solexa (also known as Illumina, used to sequence the entire genome of one African and one Asian human, plus the genome of a cancer patient), SOLiD (ABI).

Since all of these methods give short reads, they have mainly been used for resequencing. In this case, it is not necessary to do a complete, independent genome assembly, but the sequence reads can be aligned to a reference genome sequence. For example, the sequence reads from a single person can be aligned to the reference human genome. However, all of the above methods have been modified to produce *paired reads* in which both ends of a DNA fragment of known length are sequenced. This makes it possible to do *de novo* assemblies of genomes [30].

Performing a completely independent genome assembly is still an interesting topic of research: given h l-long reads $S_1, \ldots, S_h$, how to find the sequence of the full genome? In order to answer to this question the de Bruijn graph has been used. A de Bruijn graph (DBG) is a directed graph $G = (V, E)$ whose set of vertices V are labelled by k-mers, i.e. words of length k that are subsequences of the reads. An arc in E links a vertex u to a vertex v if the suffix of length $k-1$ of u is a prefix of v. A path in this graph defines a potential contiguous subsequence in the genome sufficiently covered by the reads. Hence a read can be converted to its corresponding path and the full genome sequence is a *long* walk in this graph.

2.3 analysis and enumeration of biological networks

Network metrics have been mainly developed for non-biological purposes, but in some cases they provided meaningful biological information. Several topological metrics are often used to analyse biological networks, like for instance, centrality to predict essential genes/reactions/compounds/proteins, average distance and diameter to inspect the compactness of a network, assortativity and dyadicity to study the modularity of a network and correlations between the properties of the vertices.

However structural analysis are not always able to take into account regulatory mechanisms: the activity of enzymes is often regulated by one or more effector metabolites but since the effector metabolite is not consumed, they are not encoded in a Metabolic network. This can have profound consequences because these regulations have important roles in stabilizing metabolic states and in generating complex and biologically important dynamic behaviours [31, 32, 33]. These effectors are moreover able to cross the boundaries between different biological levels, such as metabolism and gene regulation; therefore building integrated models taking these cross talks into account represents a major challenge in systems biology. Modelling efforts have demonstrated that none of the different biological layers is truly isolated [34, 35, 36] so that perturbations propagate between them, and that enzymes also have regulatory functions, exerted through their control over the concentration of particular metabolites. These considerations lead to a view of the cell as a network of networks, whose understanding requires considering regulatory interactions not only within but also between biological networks.

Moreover biases in the network reconstructions or manipulation can strongly affect the results of the analysis, confounding (if there exist) the correlations of biological and topological properties [37]. Indeed, topological measures are the result of a partial reconstruction and a lot of measures are strongly affected by the sampling [38, 39].

In general, biological networks are often studied as static entities, but it should be stressed that they are instead very dynamic at widely different time-scales. They are dynamic in evolutionary time like any other biological structure, and even more on short time-scales, since regulatory connections and feedbacks change the connectivity of the network depending on the physiological state. Consequently, we should interpret most of the currently available biological network reconstructions as potential networks, where all the possible connections are indicated. By the term potential, we highlight the fact that edges/arcs and vertices in this network will be hardly present all together in vivo. If we consider for instance a Protein-Protein Interaction network, not all interaction partners of a protein will be expressed in a given condition, reducing the number of actual partners. On the converse, we may speak of network realizations when focusing on the active subgraph of the potential network, defined on the basis of experimental data [40, 41, 42, 43]. The dynamic nature of biological networks is also at the basis of differential network analysis [44], which aims at capturing the subgraphs specific of a given network realization.

These considerations are important since they affect the analysis of biological networks. As there are many condition-specific realizations of a biological network, they plausibly have different structural properties. It has indeed been shown that random subgraphs of a network do not necessarily maintain the same degree distribution as the entire network [45], suggesting that other structural properties may also change. Similarly, it has been shown that power-law degree distributions can be obtained through random sampling of networks with different topology, indicating that it might be not possible to infer the true degree distribution from partial network reconstructions [46].

Several works try to take into account realizations. Han et al. [40] estimated the temporal connectivity of hubs in the *Yeast* Protein-Protein Interaction network by using gene expression data. Luscombe et al., [41] analysed the structural properties of the *Yeast* Gene Regulatory network in different conditions. Starting from a widely validated Gene Regulatory network, they used gene expression data to extract the subnetworks supposed to be active during environmental stress or the cell cycle, highlighting important differences (see also [42, 40, 43]). The use of realization networks is currently limited by the need for high-quality and high-throughput experimental data, today available only for a few organisms. Nevertheless, large-scale experimental data will be more easily obtained in the future, giving the occasion to develop the algorithms required for a similar approach.

Since biological networks are so complex, the structural analysis must take into account more biological information, whenever this is possible, or it requires to enumerate all the feasible structures (given some set of constraints) in order to select *a posteriori* the realistic ones from a biological point of view. Thus, in this scenario, very often enumeration algorithms can be helpful and they have been applied for several purposes, for instance: enumerating interesting vertices [47], central or peripheral vertices (see Chapter 4), enumerating motifs [48, 49, 50], that are statistically overrepresented subgraphs in a network and have been recognized as 'the simple building blocks of complex networks', and enumerating subgraphs [51, 52] (see Chapter 5), enumerating paths or cycles as chains of interactions or feedback loops [14] (see Chapter 6 and 7), enumerating functional clusters [53], dense modules [54], or cliques [55].

3 ENUMERATION ALGORITHMS

In this chapter we present an overview of the main computation issues related to enumeration problems and the main techniques to design algorithms and proving their complexity.

3.1 INTRODUCTION

The aim of enumeration is listing all the feasible solutions of a given problem. For instance, given a graph $G = (V, E)$, enumerating all the paths or the shortest paths from a vertex $s \in V$ to a vertex $t \in V$, enumerating cycles, or enumerating all the feasible solutions of a knapsack problem, are classical examples of *enumeration problems*. An enumeration algorithm solves an enumeration problem.

While an optimization problem aims to find just the best solution according to an objective function, i.e. an extreme case, an enumeration problem aims to find all the solutions satisfying some constraints, i.e. local extreme cases. This is particularly useful whenever the objective function is not clear: in these cases the best solution should be chosen among the results of the enumeration. Moreover sometimes it can be interesting to capture local structures of the data, instead of the global one, so that enumerating all remarkable local structures becomes particularly helpful. This is often the case in computational biology.

In such a context a good model is the result of a tradeoff between the size and the number of the solutions: whenever the sizes of the solutions are huge, it is more desirable to have relatively few solutions. For these reasons, the models usually include some parameters (such as solution size, frequency, and weight) or unify similar solutions.

It is worth observing that the number of solutions increases with the size of the input. Whenever this size is small, brute force algorithms are helpful, and simple implementations can successfully solve the problem. On the other hand, for large scale data more sophisticated approaches from algorithm theory are required in order to guarantee a bounded increase of computation time when the input size increases.

In this chapter we will present an overview of the main computational issues related to enumeration problems and the main techniques to design algorithms and to prove their complexity. These are part of the lecture notes, written together with Gustavo A. T. Sacomoto, taken during the lectures given by Takeaki Uno at the school on Enumeration Algorithms and Exact Methods (ENUMEX) in Bertinoro, Italy, on September 25-26th, 2012.

Algorithm 1: BruteForce(i, X)

```
Input: An integer $i \geqslant 1$, a sequence of values $X = \langle x_0, \ldots, x_{i-1} \rangle$,
       eventually empty
Output: All the feasible sequences of length $n$ whose prefix is $X$
if no solution includes $X$ then return
if $i > n$ then
    if $X$ is a solution then output $X$
else
    foreach feasible value $e$ of $x_i$ do
        BruteForce$(i+1, \langle X, e \rangle)$
    end
end
```

STRUCTURE OF THE CHAPTER. The chapter is structured as follows: in Section 3.2 we exploit the main algorithmic issues related to enumeration and we show some brute force approaches to solve them. In Section 3.3 we report the main technical framework to design efficient enumeration algorithms and in Section 3.4 we show the main amortization schema. In Section 3.5, we briefly discuss the tractability of enumeration problems in practice.

3.2 ALGORITHMIC ISSUES AND BRUTE FORCE APPROACHES

The design of enumeration algorithms involves several aspects that need to be taken into account in order to achieve correctness and effectiveness. Indeed, any enumeration algorithm have to guarantee that each solution is output exactly once, i.e. should avoid duplication. A straightforward way to achieve this is to store in memory all solutions already found, and whenever a new solution is encountered, test whether it has been already output or not. Clearly, this approach can be memory inefficient when the solutions are large with respect to the memory size, or there are too many of them. Dealing with this would require dynamic memory allocation mechanism and efficient search (*hash*). For these reasons, deciding whether a solution has been already output without storing the solutions already generated is a more suitable strategy that many enumeration algorithms try to apply.

Besides that, there are cases in which implicit forms of duplication should also be avoided, i.e. avoid outputting isomorphic solutions. To this aim, it is often useful to define a canonical form of encoding for the solutions allowing easy comparisons. The canonical form should provide a one-to-one mapping between the objects and their representation, without increasing drastically their size. In this way the problem of enumerating certain objects is turned into the enumeration of their canonical forms. However, in some cases, like graphs,

Algorithm 2: BruteForce(X, D)

```
Input: A pattern $X$, a reference to a global database $D$
Output: All the patterns containing $X$ not isomorphic between them and
        to any pattern contained in $D$
$D \leftarrow D \cup \{X\}$
if no solution includes $X$ then return
if $X$ is a solution then output $X$ foreach $X'$ obtained by adding an element to
$X$ do
    if $\nexists Z \in D$ such that $Z$ isomorphic to $X'$ then
        BruteForce$(X', D)$
    end
end
```

sequence data and matrices, checking isomorphism is hard even by defining a canonical form. Nonetheless, in these cases the isomorphism can be still checked by using exponential algorithms that in practice turn out to be often efficient when the number of solutions is small.

Simple structures, such as cliques and paths are generally easy to enumerate, since cliques can be obtained by iteratively adding vertices, and the set of paths can be easily partitioned. More complex structures, such as maximal (nothing can be added to the solution without losing some required property) or minimal (nothing can be subtracted from the solution without losing some required property) structures, or constrained structures, are more difficult to enumerate. In these cases, even if a solution can be found in polynomial time, the main issue is designing a way to generate other solutions from a given one, i.e *defining a solution neighbourhood*, in order to allow visiting all the solutions by moving iteratively through the neighbourhoods.

It should be noted that using an exponential time approach to find each neighbour or having an exponential number of neighbouring solutions, can lead to time inefficiency. When an exponential number of possible choices have to be applied to a solution in order to possibly obtain other solutions, the enumeration process can take an exponential time for each solution, since there is no guarantee that any choice leads to a solution. For example this is very often the case concerning maximal solutions: removing some elements and adding others to get maximality allow to move iteratively to any solution, but, when the number of these combinations is exponential, the final cost per solution is also exponential. In such a context, if possible, restricting the number of neighbours of a solution or applying some pruning strategy to avoid redundant computation, can lead to more efficiency.

More complex cases concern the problems in which even finding a solution is NP-complete, such as SAT or Hamiltonian cycle. Nonetheless, in these cases, heuristics often effectively apply, specially when the problem turn out to be *usually easy*, like SAT, the *solutions are not huge*, like maximal and minimal structure enumeration, and the *size of the solution space is bounded*.

When the instance sizes are small, another approach to these problems, is to use brute force algorithms. For example, using a divide and conquer approach to enumerate all the candidates and selecting all feasible solutions, or by enlarging the solutions one by one and removing the isomorphic ones. Two basic schemas for brute force algorithms are informally described in Algorithm 1 and 2. In Algorithm 1 every solution is seen as an ordered sequence of values: by invoking BruteForce(1,$\emptyset$, the feasible values are recursively found by enlarging the current solution; in this case, just the test whether X is a solution or not is required. Also Algorithm 2 tries to enlarge the current solution, but at each step we check whether the current solution has been already considered in the past computation: the result of the past computation is stored in a database D.

Note that for both the algorithms, it is necessary to know how to transform a candidate X into another candidate X'. Moreover, it is worth observing that, in both cases, an accurate a priori checking whether X is contained in any solution or not could save a lot of useless computation.

3.3 BASIC ALGORITHMS

Since the number of solutions of many enumeration problems are usually exponential in the size of the instance, enumeration algorithms require often at least exponential time. On the other hand, it is quite natural to ask for a polynomial time algorithm whenever the number of solutions is polynomial. In such a context, the complexity classes of enumeration problems are defined depending on the number of solutions, so that if the number of solution is small, an efficient algorithm has to terminate after short (polynomial) time, otherwise it is allowed to spend more time. According to this idea, the following complexity classes have been defined [56].

Definition 1. *An enumeration algorithm is* polynomial total time *if the time required to output all the solutions is bounded by a polynomial in the size of the input and the number of solutions.*

Definition 2. *An enumeration algorithm is* polynomial delay *if it generates the solutions, one after the other in some order, in such a way that the delay until the first is output, and thereafter the delay between any two consecutive solutions, is bounded by a polynomial in the input size.*

Intuitively, the polynomial total time definition means that the delay between any two consecutive solutions has to be polynomial on the average, while the polynomial delay definition implies that the maximum delay has to be polynomial. Hence, Definition 2 implies Definition 1.

The basic technique for designing enumeration algorithms are: backtracking (depth-first search with lexicographic ordering), binary partition (branch and bound like recursive partition algorithm), reverse search (search on traversal tree defined by parent-child relation). The rest of this section is devoted to exploit the features of these schemas. It is worth observing that this categorization is not strict, since very often these technique overlap each other.

3.3.1 *Backtracking*

A set $F \subseteq 2^U$ (of subsets of U) satisfies the *downward closure* if for any $X \in F$ and for any $X' \subseteq X$, we have $X' \in F$, in other words, for any X belonging to F we have that any subset of X also belongs to F. Given a set U and an oracle to decide whether $X \subset U$ belongs to F, an unknown set of 2^U satisfying the downward closure, we consider the problem of enumerating all (maximal) elements of F. The backtracking technique is mainly applied to these problems. In this approach by starting from an empty set, the elements are recursively added to a solution. The elements are usually indexed, so that in each iteration, in order to avoid duplication, only an element whose index is greater than the current maximum element is added. After all the examinations concerning one element, by backtracking, all the other possibilities are exploited. The basic schema of backtracking algorithms is shown by Algorithm 3. Note that whenever it is possible to apply this schema, we obtain a polynomial delay algorithm, whose space complexity is also polynomial. The technique proposed relies on a depth-first search approach. However, it is worth observing that in some cases of enumeration of families of subsets exhibiting the downward closure property, arising in the mining of frequent patterns (e.g., mining of frequent itemsets), besides the depth-first backtracking, a breadth-first approach can be also successfully used. For instance this is the case of the Apriori algorithm for discovering frequent itemsets [57].

Algorithm 3: BACKTRACK(S)

```
Input: $S \subseteq U$ a set (eventually empty)
Output: All the solutions containing $S$
output $S$
Let $\pi(x)$ be the index associated to an element $x \in U$
foreach $e > \max_{x \in S} \pi(x)$ do
    if $S \cup \{e\}$ is a solution then
        BACKTRACK($S \cup \{e\}$)
    end
end
```

Algorithm 4: SubsetSum(S)

```
Input: $S$ a set (eventually empty) of integers belonging to the collection
       $U = \{a_1, \dots, a_n\}$
Output: All the subsets of $U$ containing $S$ whose sum is less than $b$.
ouput $S$
Let $\pi(x)$ be the index associated to an element $x$
foreach $i > \max_{x \in S} \pi(x)$ do
    if $a_i + \sum_{x \in S} x < b$ then
        SubsetSum($S \cup \{a_i\}$)
    end
end
```

Enumerating all the subsets of a collection $U = \{a_1, \dots, a_n\}$ *whose sum is less than* b.

By using the backtracking schema, it is possible to solve the problem as shown by Algorithm 4. Each iteration outputs a solution, and take $O(n)$ time, so that we have $O(n)$ time per solution. It is worth observing that if we sort the elements of U, then each recursive call can generate a solution in $O(1)$ time, so that we have $O(1)$ time per solution.

3.3.2 *Binary Partition*

Let X be a subset of F, the set of solutions, such that all elements of X satisfy a property P. The binary partition method outputs X only if the set is a singleton, otherwise, it partitions X into two sets X_1 and X_2, whose solutions are characterized by the disjoint properties P_1 and P_2 respectively. This procedure is repeated until the current set of solutions is a singleton. The bipartition schema can be successfully applied to the problem of enumeration of paths of a graph connecting two vertices s and t, of the perfect matchings of a bipartite graph [58], of the spanning trees of a graph [59]. If every partition is non-empty, i.e. all the internal nodes of the recursion tree are binary, we have that the number of internal nodes is bounded by the number of leaves. In addition, if we have that the partition oracle takes polynomial time, since every leaf outputs a solution, we have that the resulting algorithm is polynomial total time. On the other hand, even if there are empty partitions, i.e. internal unary nodes in the recursion tree, if the height of tree is bounded by a polynomial in the size of the input and the partition oracle takes polynomial time, then the resulting algorithm is polynomial delay.

Enumerating all the (s,t)-paths in a graph $G = (V, E)$.

The partition schema chooses an arc $e = (s, r)$ incident to s, and partitions the set of all the (s,t)-paths into the ones including e and the ones not including e. The (s,t)-paths including e are obtained by removing all the arcs incident to s, and enumerating the (r,t)-paths in this new graph, denoted by $G - s$. The (s,t)-paths not including e are obtained by removing e and enumerating the (s,t)-paths in the new graph, denoted by $G - e$. The corresponding pseudocode is shown by Algorithm 5. It is worth observing that if the arc e is badly chosen, a subproblem could not generate any solution; in particular, the set of the (r,t)-paths in the graph $G - s$ is empty if t is not reachable from r, while the set of the (s,t)-paths in $G - e$ is empty if t is not reachable from s. Thus before performing the recursive call to the subproblems it could be useful to test the validity of e, by testing the reachability of t in these modified graphs. Notice that the height of the recursion tree is bounded by $O(|V| + |E|)$, since at every level the size of the graph is reduced by one vertex or arc. The cost per iteration is $O(|V| + |E|)$, the reachability test. Therefore, the algorithm has $O((|V| + |E|)^2)$ delay or $O(|E|^2)$ delay for connected graphs.

This problem has been studied in [60, 21, 61], and in [18], guaranteeing a linear delay. In Chapter 7 we will modify this latter algorithm in order to enumerate *bubbles*. In the particular case of undirected graphs, in Chapter 6 we will show an algorithm based on this bipartition approach having an output sensitive amortized complexity, as shown in [19]. In the particular case of shortest paths, the enumeration problem has been studied in [62]. It is worth observing that the problem of enumerating all the (s,t)-paths in a graph is equivalent to the problem of enumerating all the cycles passing through a vertex.

3.3.3 *Reverse Search*

The reverse search schema defines for any solution a solution called *parent solution* [63], in a way that this parent-children relationship does not induce a cyclic graph or DAG, but induces a tree. In this way, in order to enumerate all the solutions, it is sufficient to traverse the tree by performing a depth first search, so that the number of iterations is equal to the number of solutions. It is worth observing that the tree induced by the parent child relationship does not need to be stored in memory, but it is sufficient to use an algorithm for finding all the children of a parent. Moreover it could be preferable to have an algorithm able to find the $(i+1)$-th child of a node, given the i-th child.

Since the number of iterations is equal to the number of solutions, we have that the cost per solution is equal to the cost per iteration. Thus if finding the next child of a node costs $O(f(n))$ time, where n is the input size, the resulting computation time per iteration is $O(f(n))$. Hence the algorithm is polynomial total time whenever $f(n)$ is polynomial. The space complexity is given by the

Algorithm 5: PATHS(G, s, t, S)

```
Input: A graph $G$, the vertices $s$ and $t$, a sequence of vertices $S$
       (eventually empty)
Output: All the paths from $s$ to $t$ in $G$
if $s = t$ then
    output $S$
    return
end
choose an arc $e = (s, r)$
if no $(r, t)$-path in $G - s$ then
    PATHS$(G - e, s, t, S)$
    return
end
if no $(s, t)$-path in $G - e$ then
    PATHS$(G - e, r, t, \langle S, s \rangle)$
    return
end
PATHS$(G - s, r, t, S)$
PATHS$(G - e, s, t, S)$
```

memory usage of an iteration and by the height of the depth first search tree. This latter cost is not required when we have an algorithm able to find the $(i+1)$-th child of a node, given its i-th child. The delay between two successive solutions is also $O(f(n))$ by using the alternative output technique [64].

Indeed alternative output technique aims to reduce the delay, by avoiding that the depth first search backtrack along long paths without outputting any solution. As shown by Algorithm 7 the solutions are outputted before the recursive calls when the current depth first search level is even, otherwise, i.e. in the odd levels, the solutions are output after the recursive calls. In this way for any two successive solutions we have a delay at most $2f(n)$, where $f(n)$ is the cost of an iteration. Indeed suppose that the parent child relationship induces a path of solutions $x_1, \ldots, x_{g(n)}$ and there is a solution $x_{g(n)+1}$ that is a child of x_1, where $g(n)$ is a function of n. If the cost per iteration is $O(f(n))$, by applying Algorithm 6, for any i with $1 \leqslant i \leqslant g(n)$, the delay is

Algorithm 6: REVERSESEARCH(S)

```
output $S$
foreach child $S'$ of $S$ do
    REVERSESEARCH$(S')$
end
```

```
Algorithm 7: AlternativeOutput(S, depth)
Input: A solution S, an integer depth
Output: All the solutions descendants of S in the tree induced by the
        parent-child relationship
if depth is even then output S foreach child S′ of S do
    AlternativeOutput(S, depth + 1)
end
if depth is odd then output S
```

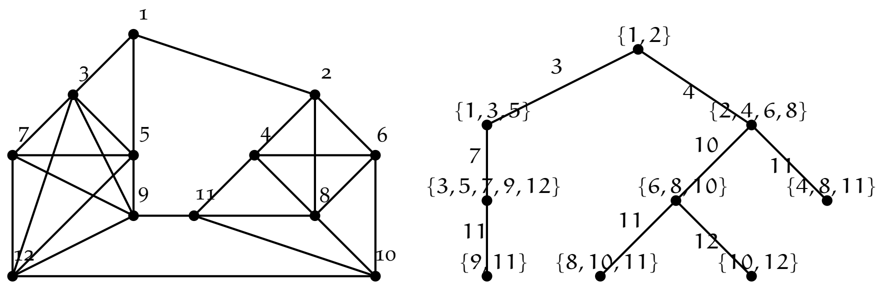

(a) (b)

Figure 3: A graph and the recursion tree induced by Algorithm 8.

$O(f(n))$, and the delay between x_k and x_{k+1} is $O(g(n))$. By applying Algorithm 7, by supposing $g(n)$ odd, the solutions are generated in the following order $x_2, x_4, \ldots x_{g(n)-1}, x_{g(n)}, x_{g(n)-2}, x_{g(n)-4}, \ldots, x_3, x_1, x_{g(n)+1}$, so that the delay is $O(2 \cdot f(n)) = O(f(n))$.

In conclusion, by applying this technique, every time an enumeration algorithm takes $O(f(n))$ time in each iteration and also outputs a solution on each iteration, the delay $O(f(n))$ can be turned into a worst case delay $O(f(n))$.

Maximal Clique Enumeration.

A clique is a complete graph, i.e. a graph in which any two vertices are connected. Finding the clique of maximum size in a graph $G = (V, E)$ is NP-hard [65], while finding a maximal clique is an easy task that can be solved in $O(|E|)$ time: by starting with an arbitrary clique (for instance, a single vertex), grow the current clique one vertex at a time, adding it if connected to each vertex in the current clique, and discarding it otherwise. The clique enumeration problem is the problem of enumerating all the complete subgraph of a given graph in input. This problem has been widely studied by [66, 67, 68]. The bipartite clique enumeration problem is the problem of enumerating all the complete bipartite subgraphs of a bipartite graph and it can be efficiently reduced to a clique enumeration problem [66].

Algorithm 8: EnumMaximalCliques(G, K)

```
Input: A graph $G = (V, E)$, a maximal clique $K \subseteq V$
Output: All the maximal cliques descendants of K in the tree induced by
        the parent-child relationship between maximal cliques
output K
foreach vertex $v \in V$ not in K do
    $K' \leftarrow K[v]$
    if $P(K') = K$ then
        EnumMaximalCliques$(G, K)$
    end
end
```

It is worth observing that the set of cliques is *monotone*, since any subset of the vertices of a clique is also a clique. This means that the backtracking technique can be successfully applied. Checking whether a recursive call is going to produce at least a clique costs $O(|E|)$ time, and has to be repeated for at most $|V|$ recursive calls, so that the final cost is $O(|V||E|)$ per clique.

When the number of solutions increase exponentially when the size of the instance input increases linearly, it seems hard post-processing the solutions found, so that often the simple enumeration problem is turned in enumeration of maximal structures. In this way, the solution set becomes not redundant. More formally, a solution X is maximal if for any $X \subset X'$, X' is not a solution. In general the problem of finding maximal solutions is more difficult, since it is often harder to find a *neighbourhood* relationship between them. However there are some exceptions, like enumerating maximal clique.

Also in real contexts it seems more promising enumerating all the maximal cliques instead of all the cliques: it has been estimated that in real world graphs, even if they are sparse and the size of their cliques is small, the number of maximal cliques is between 0.1% and 0.001% the number of its cliques (see also [69]). Moreover, restricting the enumeration to maximal cliques does not lead to lose any information since any clique is included in at least one maximal clique.

Given a graph $G = (V, E)$, whose vertices are indexed, a set of vertices $X \subseteq V$ is said to be *lexicographically* greater than $Y \subseteq V$ if the vertex whose index is minimum in $(X \setminus Y) \cup (Y \setminus X)$ is contained in X. Moreover, for any $X, Y \subseteq V$, the trichotomy property holds, i.e. exactly one of the following holds: $X < Y$, $X = Y$, or $Y > X$. For any vertex set S, we define $S_{\leqslant i}$ as $S \cap \{v_1, \ldots, v_i\}$.

Let $C(K)$ be the lexicographically smallest maximal clique including a clique $K \subseteq V$, $C(K)$ can be computed by greedily adding vertices to K in lexicographic order of the indices. Observe that for any set K, $C(K)$ is not lexicographically smaller than K.

Given a maximal clique K we define the parent of K, $P(K)$, as $C(K_{\leqslant i-1})$, such that i is the maximum index satisfying $C(K_{\leqslant i-1}) \neq K$. Notice that $C(K_{\leqslant i-1})$ can be efficiently computed by removing the vertices from K by starting from the ones whose index is greater and computing C on the remaining vertices while $C(K) = K$ holds. The lexicographically smallest clique, denoted as K_0, has no parent. Since for any K, $P(K)$ is lexicographically greater than K, and $P(K)$ is uniquely defined, the parent-child relationship induces an acyclic graph, that is a tree.

For any maximal clique K and any vertex v_i, we define $K[v_i]$ as $C((K_{\leqslant i} \cap N(v_i)) \cup \{v_i\})$, where $N(v_i)$ is the neighbourhood of v_i. Thus a maximal clique K' is a child of the maximal clique K, if there exists v_i, with $v_i \notin K$, such that $K' = K[v_i]$. Hence in order to compute the children of a maximal clique K, it is sufficient to check for any v_i whether $P(K[v_i])$ is equal to K.

Observe that for any maximal clique K, $C(K)$ and $P(K)$ can be computed in $O(|E|)$ time. All children of K can be found by at most $|V|$ tests, so that the cost of each iteration is bounded by $O(|V||E|)$ time. Thus, since the number of iterations is equal to the number of solutions, the final cost is $O(|V||E|)$ per maximal clique.

Non-Isomorphic Ordered Tree Enumeration.

Several enumeration problems aim to enumerate all the *substructures* of a given instance, like paths of a graph. However, applications sometimes require solutions satisfying certain constrains, like enumerating path or cycles of a fixed length or enumerating the cliques of a given size. Other problems instead aim to find all the *structures* of a given class, like enumerating the permutations of size n, enumerating trees, crossing lines in a plane, matroids, and binary matrices. Enumerating non trivial structures often implies enumerating non isomorphic structures. In general two structures are isomorphic whenever it is defined a one-to-one correspondence between their elements. For instance a circular sequence is isomorphic to another if and only if it can be transformed in it by using a rotation, a matrix is isomorphic to another matrix if and only if each one can be transformed in the other one by swapping rows and columns, a graph is isomorphic to another graph if and only if their adjacency matrices are isomorphic, i.e. there is a one to one mapping between their vertices that preserves the adjacency.

Let us consider the problem of enumerating ordered trees, trees in which the ordering of the children of each vertex is specified. The isomorphism between two ordered trees is inductively defined as follows: two leaves are isomorphic; two trees rooted on x and y, whose order lists of children are $\langle x_1, \dots, x_p \rangle$ and $\langle y_1, \dots, y_q \rangle$ respectively, are isomorphic if $p = q$ and for any i, with $1 \leqslant i \leqslant p = q$, the subtree rooted on x_i is isomorphic to the subtree rooted on y_i. This problem has been studied in [70], and by fixing the number of leaves in [71].

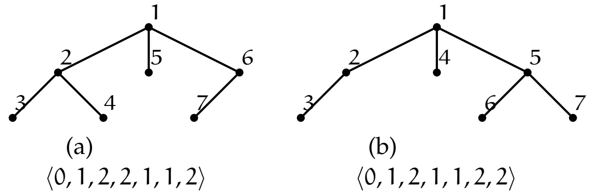

Figure 4: Two non isomorphic ordered trees, labelled by using left-first DFS, and their depth sequences.

Given an ordered tree, we define the indexing of its vertices as the visiting order of a left-first DFS, i.e. a depth first search that visits the children of a vertex following their order. This indexing procedure is unique and isomorphism between two ordered trees, whose vertices are indexed as described, can be checked comparing the edge sets: the two indexed trees are isomorphic if and only if they have the same edge set.

Moreover, the left-first DFS can be used to encode the ordered trees. To this aim, we define the depth sequence as $\langle h_1, \dots, h_n \rangle$, where h_i is the depth of vertex v_i in the left-first DFS tree, where v_i is the i-th vertex visited by a left-first DFS. There is a one-to-one correspondence between the ordered trees and the depth sequences, so that isomorphism can be checked by comparing the depth sequences, as shown by Figure 4.

By following the reverse search schema, we define the parent-child relationship between non-isomorphic trees. In particular the parent of an ordered tree is defined by the tree, obtained by removing the vertex having the largest index, i.e. by removing from a depth sequence its last element (the last element visited by a left-first DFS). Recall that the indexing induced by the left-first DFS is such that the largest index is the leaf of the rightmost branch of the tree. Observe that the size of the parent is smaller than the size of the children, any ordered tree have exact one parent, except the empty tree, so that the relationship induces an acyclic graph.

For any ordered tree T, whose depth-sequence is $\langle h_1, \dots, h_n \rangle$, the children of T according to the parent-child relationship defined before, are all the ordered trees obtained by adding a new vertex v_{n+1} as the rightmost child of a vertex belonging to the rightmost path. Let h_{n+1} be the depth of the new vertex v_{n+1}. Since h_n is the rightmost leaf of T, we have that it belongs to the rightmost path, to be precise, v_n is the last vertex of this path. Thus, the depths of the vertices of the rightmost path of T, from the root to v_n, are exactly the interval $[0, h_n]$. Since the new vertex v_{n+1} is a child of a vertex in this path, the depth h_{n+1} is in the interval $[1, h_n + 1]$. Thus the children of an ordered tree T, with depth-sequence $\langle h_1, \dots, h_n \rangle$, are all the ordered trees whose depth sequence is $\langle h_1, \dots, h_n, h_{n+1} \rangle$, with $1 \leqslant h_{n+1} \leqslant h_n + 1$. An example is given in Figure 5.

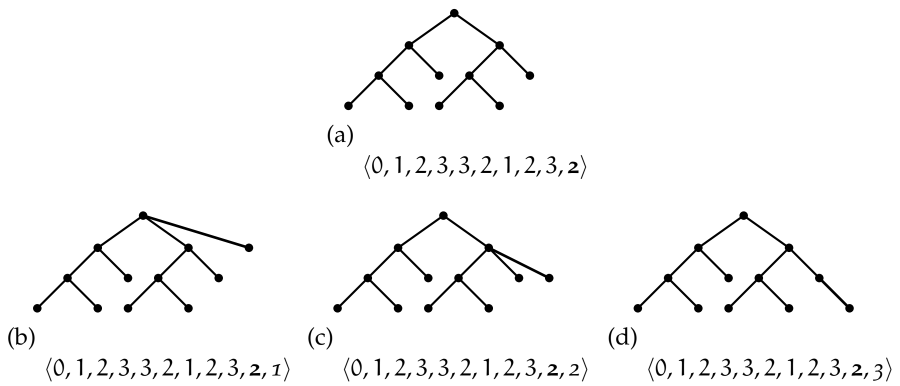

(a) $\langle 0, 1, 2, 3, 3, 2, 1, 2, 3, \mathbf{2} \rangle$

(b) $\langle 0, 1, 2, 3, 3, 2, 1, 2, 3, \mathbf{2}, \mathit{1} \rangle$ (c) $\langle 0, 1, 2, 3, 3, 2, 1, 2, 3, \mathbf{2}, \mathit{2} \rangle$ (d) $\langle 0, 1, 2, 3, 3, 2, 1, 2, 3, \mathbf{2}, \mathit{3} \rangle$

Figure 5: An ordered tree, its depth sequence (a), and its children with their depth sequences (b), (c), and (d).

By using these observations, we can enumerate all the ordered trees of size less than k, as shown by Algorithm 9. Notice that the inner loop takes constant time, so that the time complexity is $O(1)$ per solution.

```
Algorithm 9: EnumOrderedTree(T, k)
  Input: A tree T (eventually empty) and an integer k
  Output: All the non-isomorphic trees of size at most k, whose depth
          sequence contains as prefix the depth sequence of T
  output T
  if size of T = k then return foreach vertex v in the right most path do
      Let T′ be the tree obtained from T by adding a rightmost child to v
      EnumOrderedTree(T′, k)
  end
```

Non-Isomorphic Tree Enumeration.

We now consider the problem of enumerating non-ordered trees, i.e. trees in which the ordering of the children of each vertex is not specified. The isomorphism between two (non-ordered) trees is inductively defined as follows: two leaves are isomorphic; two trees rooted on x and y, whose children lists are X and Y respectively, are isomorphic if $|X| = |Y| = p$ and there exist two permutations of X and Y, $\langle x_1, \ldots, x_p \rangle$ and $\langle y_1, \ldots, y_p \rangle$ respectively, such that for any i, with $1 \leqslant i \leqslant p$, the subtree rooted on x_i is isomorphic to the subtree rooted on y_i. This problem has been studied in [72], by fixing the diameter in [73], and in the more general case of coloured rooted trees in [74].

The näive approach, to use the same algorithm for ordered tree enumeration to enumerate non-ordered trees, would produce many duplicate solutions, since

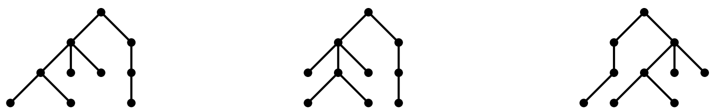

(a) $\langle 0,1,2,3,3,2,2,1,2,3\rangle$ (b) $\langle 0,1,2,2,3,3,2,1,2,3\rangle$ (c) $\langle 0,1,2,3,1,2,3,3,2,2\rangle$

Figure 6: Three isomorphic rooted tree and their depth sequences. The first one is the left heavy embedding.

each non-ordered tree may correspond to an exponential number of ordered trees. Which in turn, would be very inefficient.

In order to define the canonical form of representation of a rooted tree, we use its *left-heavy* embedding, defined as the lexicographically maximum depth sequence among all the ordered trees corresponding to T. Therefore, two non-ordered rooted trees are isomorphic if and only if they have the same left-heavy embedding.

The parent child relationship between canonical forms is defined as follows: the parent of a left-heavy embedding is obtained by the removal of the rightmost leaf of the corresponding tree, the same for ordered trees. Observe that the parent t' of a left-heavy embedding t of T is a left-heavy embedding too, otherwise there would be another sequence greater than t' such that by adding back the rightmost leaf of T we would obtain a depth sequence for T that is lexicographically greater than t.

Hence any child of a rooted tree T is obtained by adding a vertex as children of the vertices belonging of the rightmost path, like for ordered trees. However, some trees obtained by adding a vertex in this way are not children of T, since the resulting sequence does not coincide with their left-heavy embedding. This can happen if there exists a vertex x in the rightmost path of T, such that the depth sequence $t = \langle s_1, \dots, s_p\rangle$ of $T(r)$, where r is the rightmost child of x, is a prefix of the depth sequence $t' = \langle s_1, \dots, s_p, \dots s_q\rangle$ of $T(r')$, where r' is the second rightmost child of x, so that the depth sequence of T ends with t concatenated with t'. Indeed, in this case, by adding a vertex at depth y to $T(r)$ and obtaining $t'' = \langle s_1, \dots, s_p, y\rangle$ as depth sequence of $T(r)$, the depth sequence of T ends with t concatenated with t'': if s_{p+1} is lexicographically smaller than y, this is not a leaf-heavy embedding, since the depth sequence ending with t'' concatenated with t is lexicographically greater. Thus, since s_{p+1} is the depth of the rightmost leaf of $T(r')$, to get all and just the children of T, we have to consider all the possible ways to add a vertex as children of a vertex belonging to the rightmost path, so that its depth is smaller or equal to s_{p+1}.

The *copy vertex* is thus defined as the highest (lowest depth) vertex x in T with at least two[1] children, r and r' (the rightmost and the second rightmost child respectively), such that the depth sequence $\langle s_1, \dots, s_p\rangle$ of $T(r)$ is a prefix of the

[1] If T is a path, the copy vertex is defined as the root.

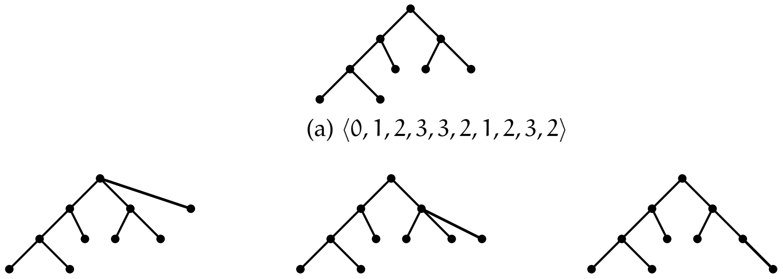

(a) $\langle 0,1,2,3,3,2,1,2,3,2\rangle$

(b) $\langle 0,1,2,3,3,2,1,2,2,1\rangle$ (c) $\langle 0,1,2,3,3,2,1,2,2,2\rangle$ (d) $\langle 0,1,2,3,3,2,1,2,2,3\rangle$

Figure 7: An rooted tree, and its depth sequence (a). (b) and (c) are its children, while (d) is not a child of (a).

depth sequence $\langle s_1, \dots, s_p, \dots s_q\rangle$ of $T(r')$. Given a tree T with copy vertex x, in order to generate the children of T, we have to consider two cases: the prefix of the depth sequences is proper or the depth sequences are equal. In the first case, there exists s_{p+1} and by attaching a new rightmost child to a vertex v, with depth $\leqslant s_{p+1}$, in the rightmost path of T we obtain a new tree T' that is also a left-heavy embedding. Moreover, the new copy vertex of T' is v, if the depth v is not equal to the depth of x; or x, otherwise. On the other case, the subtrees $T(r)$ and $T(r')$ are equal and by attaching a new rightmost child to a vertex v, with depth smaller or equal to the depth of x, in the rightmost path of T we obtain a new tree T' that is also a left-heavy embedding, and the new copy vertex of T' is v. In both cases, we are able to generate the new tree T' and update the copy vertex in constant time. The algorithm is shown by Algorithm 10. Each iteration of the loop costs $O(1)$, so that we have a final cost of $O(1)$ per solution.

3.4 AMORTIZED ANALYSIS

In this section, we explore techniques to analyse the running time of a certain kind of enumeration algorithms. Specifically, enumeration algorithms with a tree-shaped recursion structure.

Suppose a enumeration algorithm with a tree-shaped recursion structure takes $O(n)$ time per node. Based only on this, it is not possible to polynomially bound the time spent to output each solution. We can have exponentially many nodes and a small number of solutions as in, for example, the enumeration of feasible solutions of SAT using a branch-and-bound algorithm. However, if every node outputs a solution, then algorithm takes $O(n)$ per solution. Now, suppose that each leaf outputs a solution and each node takes $O(n)$ time. Again, this is not enough to polynomially bound time per solution, since we can have an exponential number of internal nodes and only few leaves. In addition, we need that either the height of the tree is bounded, in this case the number of nodes is bounded by the number of solutions (leaves) times the height; or each

Algorithm 10: EnumRootedTree(T, x)

```
Input: A tree T (eventually empty), an integer k, and a vertex x
Output: All the non-isomorphic rooted trees of size at most k, whose
        depth sequence contains as prefix the depth sequence of T
output T
if size of T = k then return $r \leftarrow$ the rightmost child of $x$
$r' \leftarrow$ the second rightmost child of $x$
if depth sequence of $(T(r') \neq$ depth sequence of $T(r)$ then
    $y \leftarrow$ the vertex of $T(r')$ after the prefix $T(r)$
else
    $y \leftarrow x$
end
foreach vertex $v$ in the rightmost path of $T$, in increasing depth order do
    add a rightmost child to $v$
    if depth of $v$ = depth of $y$ then
        EnumRootedTree$(T, x)$
        break
    end
    EnumRootedTree$(T, v)$
    remove the rightmost child of $v$
end
```

internal node has at least two children, the number of nodes is bounded by 2 times the number of solutions.

These three scenarios: every node outputs a solution, every leaf outputs a solution and the height of the tree is bounded, and every leaf outputs a solution and each internal nodes has at least two children, are the typical ones in which we can polynomially bound the time complexity. In each case, the time complexity per solution depends on the maximum time complexity $O(n)$ over all nodes. In order to do better, we have to use amortized analysis. The rest of the section is devoted to three amortized analysis techniques: basic amortization, amortization by children and push out amortization.

3.4.1 *Basic Amortization*

A recursive enumeration algorithm usually solves the problem by breaking it into subproblems, which are generally smaller, in both input and output size, than the original problem. The recursion tree for this case has many bottom level nodes taking a short time and a fewer nodes closer to the root taking a long time. We call this effect in the recursion tree *bottom-wideness*. However, this observation alone is not enough to provide good amortized bounds. For instance, Fig. 8a and 8b have bottom level nodes (leaves) taking $O(1)$, but the amortized complexity is still $O(n)$, the maximum cost among the nodes. In both cases, there were a sudden decrease in the computation times.

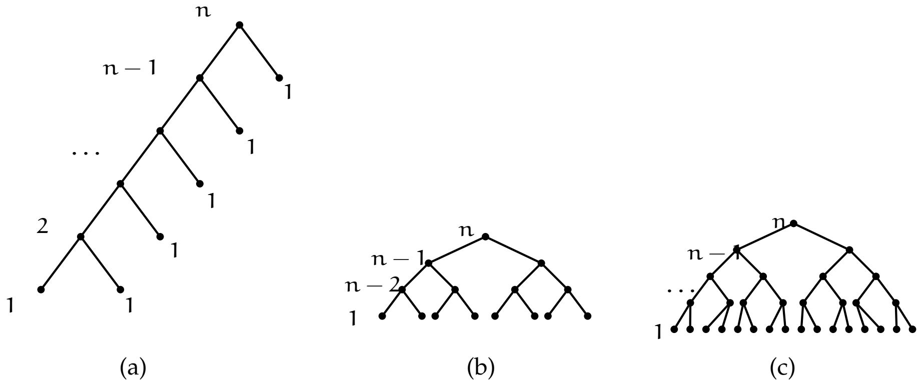

Figure 8: Recursion trees with the cost of each node. (a) The cost of the internal nodes decrease by 1 and the all leaves have cost 1. (b) The nodes in the same level have the same cost, decreasing by 1 from n until $n-2$. The leaves have cost 1. (c) The nodes in the same level have the same cost, decreasing by 1 from n until 1.

In the tree of Fig. 8c each internal node has two children, all the nodes in the same level have the same cost, and the cost of each node decreases by a constant at each level. It is not hard to show that the average complexity per node in this case is $O(1)$. That is, there was a reduction from $O(n)$ to $O(1)$ when considering the amortized complexity. Lemma 2 presents a generalization of this example, every node has two children and the costs are proportional to the height of the node. Technical Lemma 1 is used in the proof of the Lemma 2.

Lemma 1. *For any polynomial* $p(x) = \sum_{k=0}^{m} a_k x^k$, *there exists* δ *and* $\alpha < 1$, *such that* $\frac{p(x+1)}{2p(x)} < \alpha$, *for all* $x > \delta$.

Proof. It is easy to prove that $\lim_{x\to\infty} \frac{p(x+1)}{2p(x)} = 1/2$. Thus, from the definition of limit, there exist ϵ and δ (depending only on ϵ), such $\frac{p(x+1)}{2p(x)} - 1/2 < \epsilon$ for all $x > \delta$. Choosing $\epsilon < 1/2$, we have that $\frac{p(x+1)}{2p(x)} < \epsilon + 1/2 = \alpha < 1$ for all $x > \delta$. □

Lemma 2. *Let* T *be a recursion tree with height* n, *such that every internal node has degree 2; and the cost for each node is* $O(p(i))$, *where* $p(i)$ *is a polynomial and* i *is the height of the node. Then, the amortized cost for each node is* $O(1)$.

Proof. The number of nodes with height i is 2^{n-i}, since the internal nodes have degree 2. The cost of each level i of the tree is bounded by $2^{n-i}p(i)$ and the total cost of the tree is $\sum_{i=1}^{n} 2^{n-i}p(i)$. Let us consider the ratio of the cost of two adjacent levels in the tree,

$$r(i) = \frac{2^{n-(i+1)}p(i+1)}{2^{n-i}p(i)} = \frac{p(i+1)}{2p(i)}.$$

By Lemma 1, $r(i) < \alpha < 1$, for all $i > \delta$. Implying that the cost of each level $i \geqslant \delta$ decrease by α and the sum of the costs of all levels $i \geqslant \delta$ is bounded by the sum of the geometric series, i.e.

$$\sum_{\delta \leqslant i \leqslant n} 2^{n-i}p(i) < 2^{n-\delta}p(\delta) \sum_{\delta \leqslant i \leqslant n} \alpha^{i-\delta} < 2^{n-\delta}p(\delta) \sum_{i=0}^{\infty} \alpha^{i} = \frac{2^{n-\delta}p(\delta)}{1-\alpha}.$$

Therefore, amortized cost of each node in the levels above δ is

$$\frac{\sum_{\delta \leqslant i \leqslant n} 2^{n-i}p(i)}{\sum_{\delta \leqslant i \leqslant n} 2^{n-i}} < \frac{2^{n-\delta}p(\delta)}{1-\alpha}\frac{1}{2^{n-\delta}} = \frac{p(\delta)}{1-\alpha} = O(1).$$

The last equality follows from the fact that α and $delta$ are constants. Moreover, the cost of the nodes with $i \leqslant \delta$ is also $O(1)$. □

Theorem 1 is a straightforward generalization of Lemma 2.

Theorem 1. *Let* T *be a recursion tree with height* n, *such that every internal node has degree* at least *2; and the cost for each node is* $O(p(i))$, *where* $p(i)$ *is a polynomial and* i *is the height of the node. Then, the amortized cost for each node is* $O(1)$.

Enumerating connectivity elimination orderings of a connected graph G*.*

Given a connected graph $G = (V, E)$, a *connectivity elimination ordering* is an ordering of the vertices such that the removal of each vertex keeps the remaining graph connected. Algorithm 11 enumerates all connectivity elimination orderings. Each call of the algorithm takes $O(|V|^3)$ time, since for each $v \in V$ it checks if $G - v$ is connected. Moreover, for any connected graph there are at least two vertices such that their removal maintain the graph connected. Therefore, the hypothesis of Theorem 1 are satisfied, and the amortized complexity per node is $O(1)$. Since, in this case, the number of nodes is at most 2 times the number of leaves, the amortized complexity per solution is also $O(1)$.

Algorithm 11: EnumOrderings($G = (V, E), X$)

```
Input: A graph G and sequence X that is a prefix of a connectivity
       elimination order.
Output: The set of all connectivity elimination orders of G.
if $V = \emptyset$ then
    output X
end
foreach $v \in V$ do
    if $G - v$ is connected then
        EnumOrderings($G - v, \langle X, v \rangle$)
    end
end
```

3.4.2 *Amortization by Children*

The basic amortization strategy presented in the previous section, in the form of Theorem 1, requires that every leaf has the same depth, and the cost of each node depends uniformly on the height. Though there are applications for Theorem 1, these requirements are global, they depend on the tree as whole, imposing a very strict structure in the recursion tree. In this section, we start developing amortization techniques with weaker hypothesis, so that they can be applied also in the case of more biased trees. For this, we focus on local tree structure. Theorem 2 presents a simple amortization scheme using only the parent-children structure.

Theorem 2. *Let* T *be a recursion tree and* $T(x)$ *the cost of node* $x \in T$*. The amortized cost for each node is* $O(\max_{z \in T} \frac{T(z)}{|N^+(z)|+1})$.

Proof. We divide the cost $T(x)$ between the node x and its children $N^+(x)$. In this way the new cost of x is $\frac{T(x)}{|N^+(x)|+1}$ plus the cost received from its parent y. Thus,

$$\begin{aligned} T'(x) &= O(\frac{T(x)}{|N^+(x)|+1} + \frac{T(y)}{|N^+(y)|+1}) \\ &= O(\max_{z \in \{x,y\}} \frac{T(z)}{|N^+(z)|+1}) = O(\max_{z \in T} \frac{T(z)}{|N^+(z)|+1}). \end{aligned}$$

□

Enumerating all simple paths of G *starting from* s.

Given a graph $G = (V, E)$ and a vertex $s \in V$, we consider the problem of enumerating all simple paths of G that start on s. Algorithm 12 solves this problem. Each call outputs a solution and takes $O(|N(s)|)$ time, since we have to explore all edges from s. Moreover, each edge from s generates a recursive call. Therefore, applying Theorem 2 we have that the amortized cost per node is $O(\max_{z \in T} \frac{|N(z)|}{|N(z)|+1}) = O(1)$.

```
Algorithm 12: EnumPaths($G = (V, E), s, \pi$)
    Input: A graph $G$, a vertex $s$ and a path $\pi$ from $s$.
    Output: The set of all paths from $s$ in $G$ with prefix $\pi$.
    output $\pi$
    foreach $v \in N(s)$ do
        EnumPaths($G - s, v, \langle \pi, s \rangle$)
    end
```

3.4.3 *Push out Amortization*

In Lemma 2 the key property was that the total cost on each level increases with a constant factor, by going to the next deeper level. Intuitively, the increase of computation time is good because it forbids a sudden decrease, as the one of the trees in Fig. 8a and 8b. In this section, we apply the same idea locally. Instead of comparing the total cost of two adjacent levels we compare the cost of a node with the total cost of its children. Lemma 3 gives a precise statement for this local increase property. Afterwards, Theorem 3 generalizes Lemma 3, by combining it with the amortization by children of Theorem 2.

Lemma 3. *Let* T *be a recursion tree, such that the cost of each leaf is* $O(T^*)$*; and there exist* $\alpha > 1$ *such that every internal node* $x \in T$ *satisfy* $\sum_{y \in N^+(x)} T(y) \geqslant \alpha T(x)$*, where* $T(x)$ *is the cost of* x*. Then, the amortized cost for each node is* $O(T^*)$*.*

Proof. Consider a node $x \in T$ and define $C(x) = \sum_{y \in N^+(x)} T(y)$. We divide the cost $T(x)$ proportionally among the children, so that each $y \in N^+(x)$ receives $T(x)\frac{T(y)}{C(x)}$. Observe that $\sum_{y \in N^+(x)} T(x)\frac{T(y)}{C(x)} = T(x)$, i.e. all the cost $T(x)$ is divided among the children. By doing this division recursively, starting from the root, we have that a node $z \in T$ receives from its parent at most $\frac{T(z)}{\alpha - 1}$.

Let us prove the last claim by induction on the depth of the node. Assume that all nodes w with depth $d - 1$ receive at most $\frac{T(w)}{\alpha-1}$ from its parent. The base case is trivial, because the root receives no cost. Let z be a node with depth d, its parent w has depth $d - 1$. By the induction hypothesis, the cost received by w from its parent is $\frac{T(w)}{\alpha-1}$ and the total cost of w is $T(w) + \frac{T(w)}{\alpha-1}$. Thus, the cost received by z is:

$$\frac{T(z)}{C(w)}(T(w) + \frac{T(w)}{\alpha - 1}) = T(z)\frac{T(w)}{C(w)}\frac{\alpha}{\alpha - 1} \leqslant T(z)\frac{1}{\alpha}\frac{\alpha}{\alpha - 1} = \frac{T(z)}{\alpha - 1}.$$

The inequality follow from $\frac{T(w)}{C(w)} = \frac{T(w)}{\sum_{y \in N^+(w)} T(y)} \leqslant \frac{1}{\alpha}$. Completing the proof of the claim.

In the end of the cost division process the only nodes that have non-zero cost are the leaves. For any leaf the cost received from its parent is at most $\frac{T^*}{\alpha-1}$. Therefore, the total cost is $O(T^* + \frac{T^*}{\alpha-1}) = O(T^*)$, since α is a constant. □

Theorem 3 is a generalization of Lemma 3. In the theorem, for every node x satisfying item 2 we can use the same amortization strategy of the lemma, i.e. proportionally divide all the cost $T(x)$ among the children. However, instead of stopping this process only on the leaves, we stop on the first node satisfying item 1 or 3. If the node x satisfies item 1 and its ancestrals satisfy item 2, we know that the cost pushed to x is $O(\frac{T^*}{\alpha-1})$ and the total cost of x is $O(T^* + \frac{T^*}{\alpha-1}) = O(T^*)$. On the other hand, if a node x satisfies item 3 we can amortize $T(x)$ among the $\Omega(\frac{T(x)}{T^*})$ children or solutions. In this way, each child receives $O(T^*)$ (that is not passed to its grandchildren), so that the cost of x is $O(T^*)$ and we have the same case of item 1.

Theorem 3. *Let T be a recursion tree, such that each node $x \in T$ satisfy one of the following properties:*

1. $T(x) = O(T^*)$;
2. $\sum_{y \in N^+(x)} T(y) \geqslant \alpha T(x)$, *where* $\alpha > 1$ *is a constant;*
3. x *has* $\Omega(\frac{T(x)}{T^*})$ *children, or outputs* $\Omega(\frac{T(x)}{T^*})$ *solutions.*

Then, the amortized cost for each node is $O(T^*)$.

Matching Enumeration

Given an undirected graph $G = (V, E)$, a *matching* M in G is a set of pairwise non-adjacent edges, i.e. for any two edges $(u, v) \neq (x, y) \in M$, we have that $\{u, v\} \cap \{x, y\} = \emptyset$. The set of all matchings of G is denoted by $\mathcal{M}(G)$. Several variants of matching enumeration have been studied: perfect (every vertex has an incident edge in M) matching enumeration in bipartite graphs [75, 76, 77, 58], perfect matching in general graphs [78], maximal matchings in bipartite graphs [77] and maximal matchings in general graphs [79]. In this section, we consider the problem of enumerating all matchings of a graph. First, we present a simple algorithm (Algorithm 13) that correctly enumerates all matchings. Then, we modify it (Algorithm 14) to satisfy the hypothesis of Theorem 3, so we can use it to improve the algorithm complexity.

Algorithm 13 uses the binary partition method, each recursive call partitions $\mathcal{M}(G)$ in two sets: matchings not including the edge (u, v) and the ones including it. In the first case (line 6), we remove (u, v) from G and leave M unchanged. In the second case (line 7), we add (u, v) to the matching M and remove from G all edges adjacent to (u, v). The cost of a node is bounded by, the number of edges removed, $O(|V|)$. Now let us analyse the structure of the recursion tree. The conditional of line 1 ensures that only leaves output solutions. Moreover, there is always a matching including (u, v) and one not including it, so every node leads to a solution. Thus, in the recursion tree all internal nodes have exactly two children and every leaf output a solution. Therefore, the number of nodes is bounded by $2|\mathcal{M}(G)|$, and Algorithm 13 takes $O(|V|)$ time for each matching.

Algorithm 13: ENUMMATCHING$(G = (V, E), M)$

```
  Input: A graph G and a matching M (eventually empty)
  Output: $\mathcal{M}(G)$, the set of matchings of G
1 if $E = \emptyset$ then
2     output M
3     return
4 end
5 choose an edge $(u, v) \in E$
6 EnumMatching$(G - (u, v), M)$
7 EnumMatching$(G - \{(x, y) \in E | x \in \{u, v\}\}, M \cup \{(u, v)\})$
```

Actually, each node in the recursion tree of Algorithm 13 takes $O(|N(u)| + |N(v)|)$ time. Consider a node x with the input graph $G = (V, E)$, the input graph of its children contain $|E| - 1$ and $|E| - |N(u)| - |N(v)|$ edges. Hereafter, for the sake of clear analysis, we bound the computation time of each node by $c|E|$. In this way, the cost for x is $T(x) = c|E|$ and, $T(y_1) = c(|E| - 1)$ and $T(y_2) = c(|E| - |N(u)| - |N(v)|)$ for each child. Based on this costs we cannot apply Theorem 3. The leaves take $O(1)$ time, satisfying item 1. However, the internal nodes do not satisfy item 2 or item 3. Each internal node has exactly 2 children and do not output solutions, so that item 3 is not satisfied. On the other hand, the total computation time of the children is not increasing by constant factor over the parent, i.e. there is no constant $\alpha > 1$ such that $T(y_1) + T(y_2) \geqslant \alpha T(x)$.

In order to satisfy item 3 of Theorem 3 we need $|N(u)| + |N(v)|$ to be bounded, so that $T(y_2)$ is not too small. The key property is that for any graph either there is an edge (u, v) such that $|N(u)| + |N(v)| < |E|/2$ or there is a node u with $|N(u)| \geqslant |E|/4$. Algorithm 14 is a modified version of Algorithm 13 that uses this property. If there exists an edge (u, v) such that $|N(u)| + |N(v)| < |E|/2$ (line 5), we have that

$$T(y_1) + T(y_2) \geqslant c(|E| - 1) + c\frac{|E|}{2} \geqslant \frac{3}{2}T(x),$$

satisfying item 2. Alternatively, if there exists u such that $|N(u)| \geqslant |E|/4$ (line 8), we create at least $|E|/4$ children, satisfying item 3. Therefore, applying Theorem 3 and using that the number of internal nodes is bounded by $2|\mathcal{M}(G)|$, we have that Algorithm 14 takes $O(1)$ time amortized for each matching enumerated.

Algorithm 14: EnumMatching($G = (V, E), M$)

```
   Input: A graph $G$ and a matching $M$ (eventually empty)
   Output: $\mathcal{M}(G)$, the set of matchings of $G$
1  if $E = \emptyset$ then
2      output $M$
3      return
4  end
5  if $\exists (u, v) \in E$ s.t. $|N(u)| + |N(v)| < |E|/2$ then
6      EnumMatching($G - (u, v), M$)
7      EnumMatching($G - \{(x, y) \in E | x \in \{u, v\}\}, M \cup \{(u, v)\}$)
8  else
9      choose $u$ s.t. $|N(u)| \geqslant |E|/4$
10     EnumMatching($G - u, M$)
11     foreach $v \in N(u)$ do
12         EnumMatching($G - \{(x, y) \in E | x \in \{u, v\}\}, M \cup \{(u, v)\}$)
13     end
14 end
```

3.5 data-driven speed up

Polynomial delay algorithms, especially linear delay, can be considered as being very close to optimal algorithms in practice. Indeed since the delay is defined as a function of the input size, it can be often considered very small or negligible with respect to the usual exponential number of outputted solutions. However, there are certain applications, particularly in data mining, in which the input data are very large (frequent pattern mining, candidate enumeration, community mining, feasible solution enumeration). In such a context, when the number of outputted solutions is expected to be small (polynomial in the input size), the problem is said to be *large-scale tractable*. This is the case of enumerating peripheral or central nodes in large graphs, as shown in Chapter 4.

On the other hand, when the number of solutions increases exponentially with a linear increase in the instance size, we usually have that many solutions are similar and therefore redundant. In these cases, a post processing step is required to suppress the redundant solutions. Since the number of solutions is huge, the post processing is very time consuming or even infeasible, so these problems are considered intractable. This could be potentially the case of the frequent itemset problem, that is the problem of enumerating all the patterns appearing frequently in a large database, where a pattern can be a sequence of items, a short string, or a subgraph (any subset of a frequent itemset is also frequent). However this intractability is very often linked to the application: for example, even if in theory the number of maximal cliques can be exponential in the size of the graph, in practice for large sparse graphs this number is usually polynomial in the size of the graph. On the other hand, however, the number of independent sets in a graph is huge both in theory and in practice.

4

ENUMERATING DIAMETRAL AND RADIAL VERTICES AND COMPUTING DIAMETER AND RADIUS OF A GRAPH

In this chapter we show an example of enumeration problem whose number of solutions is polynomial and for which a polynomial algorithm exists, that is enumerating diametral vertices, i.e. vertices whose eccentricity is the diameter, and radial vertices, i.e. vertices whose eccentricity is the radius. Intuitively they correspond to periphery and center of a network. After an overview on the centrality measures used in the analysis of biological networks, we show an efficient algorithm to list such vertices. The contribution of this work is not just limited to biological networks, but is even more useful for complex huge network analysis in general. Indeed, even if the complexity of our algorithms is theoretically $O(nm)$*, like the text-book algorithm, we show that in practice it runs often in* $O(m)$ *time. This study implies the analysis of the diameter and radius of a network, so that we will evaluate the effectiveness of our algorithms in finding such measures.*

4.1 INTRODUCTION

Structural analysis allows the identification of important and not important vertices within a network and for this reason it has become very popular in many disciplines. In general, the importance of a vertex can be defined in many different ways. The effectiveness of each centrality measure depends on the context of application.

In this chapter, we will focus on the enumeration of the radial and diametral vertices, i.e. central and peripheral vertices according to the eccentricity notion of centrality, and on the computation of the radius and diameter of biological networks and of real world graphs in general. Recall that the diameter D is the maximum distance $d(x, y)$ among all the pairs of vertices x, y. In other words, the diameter of a graph is the maximum forward or backward eccentricity of its vertices, where the forward and backward eccentricities of a vertex x are respectively $ecc_F(x) = max_{y \in V} d(x, y)$ and $ecc_B(x) = max_{y \in V} d(y, x)$. The radius R is instead defined as the minimum forward eccentricity of its vertices. Diametral sources and targets are thus defined as all the vertices x such that $ecc_F(x) = D$ and $ecc_B(x) = D$ respectively; the radial vertices are instead all the vertices x such that $ecc_F(x) = D$.

In the case of an undirected graph, whenever the graph is not connected, i.e. when at least for a pair of vertices x, y there is no path from x to y, the radius and diameter of its connected components are usually studied. In the more general case of a directed graph, whenever the graph is not strongly connected, i.e. at least for a pair of vertices x, y there is no path from x to y, we will consider in this work the radius and diameter of its strongly connected components.

In the case of biological networks, for instance in metabolic networks, the diameter indicates how many reactions have to be performed in order to produce any metabolite from any other metabolite [80]. For several biological networks, it has been studied in [81, 82] and for protein-protein interactions in [83]. The radius can indicate how many reactions have to be performed at least in order to produce all the metabolites from any other metabolite.

The analysis of real world networks in general, such as citations, collaboration, communication, road, social, and web networks, has attracted a lot of attention, and in [2] the fundamental analysis measures have been reviewed. Moreover the size of these networks has been increasing rapidly, so that, in order to study such measures, algorithms able to handle huge amount of data are needed. Hence the contribution of our algorithms is not just limited to biological networks analysis, but extends to complex networks analysis in general. Indeed, in the case of the diameter, for social networks, in which every vertex is an individual and the edges represent their friendship, the diameter has been studied for several social networks in [84, 85, 81], for peer to peer social networks in [86], for mobile social networks in [87], for Facebook in [7, 8]. For several scientific collaboration networks, in which every vertex is a scientist and scientists are linked whenever they have collaborated for a research paper, the diameter has been studied in [88, 81]. In the case of a web network, in which every vertex corresponds to a web page and the arcs correspond to hyper links, the diameter indicates how quickly any page can be reached. For several web networks, this has been estimated in [89, 81, 90]. Because of the huge size of the networks, in almost any of those works, the diameter of the connected components of undirected graphs or the strongly connected components of directed graphs was just estimated. For these reasons, we have shown the effectiveness of our algorithms not only for biological networks but also for several other kinds of complex networks.

PREVIOUS WORK. The *Single-source Shortest Path* (in short SSSP) is the problem of finding all the shortest paths from a given vertex to all the others. In general this problem has complexity $O(m)$ in the case of unweighted graphs by using the traditional BFS algorithm and $O((m+n)\log n)$ in the case of weighted graphs, by using the Dijkstra's Algorithm.

In general algorithms for finding the exact radius or diameter solve the *All Pairs Shortest Path* problem (in short APSP), that is the problem of finding the shortest path between all pairs of vertices of the graph, so that the maximum distance obtained is the diameter. This can be efficiently done by applying the classical *text-book* algorithm, i.e. solving for any vertex the SSSP problem, or by applying fast matrix multiplication with complexity $O(n^{2.376})$[84]. See [91] for a survey. However in the context of huge real world networks, these approaches are not practical and usually just estimations or bounds can be provided.

Some algorithms are able to estimate the cumulative distribution of the shortest path lengths of any kind of graph and can be applied to obtain an estimation of the radius and diameter with a small additive error using much less computations with respect to the APSP. This is the case of ANF (Approximate Neighbourhood Function) in [92], HyperANF in [93], HADI in [94], and Cohen frameworks [95, 96, 97, 98, 99, 100].

A lower bound of the diameter, or an upper bound of the radius can be provided by using a *sample* of the vertices and returning respectively the maximum and the minimum eccentricity found, as done in [101] for the diameter, or by using other heuristics.

In the case of the radius, this sampling method has been exploited for a huge web graph in [89], but as far as we know no other methods have been proposed.

In the case of the diameter, for undirected graphs a lower bound can be provided by using the so called *double sweep* algorithm: pick the farthest vertex from a random vertex and return its eccentricity. The idea can be iterated picking at each step the farthest vertex from the previous one and maintaining the highest eccentricity found as in [81]. In real world networks actually this lower bound is very good and, in order to prove the effectiveness of this approach, several works, like [102] and [4], propose strategies to find a matching or close upper bound. Recent advances have shown that in real cases a matching between a lower and upper bound for the diameter can be found by applying a very small number of computations of SSSP, even if, in the worst case, the time complexity degenerates in the time complexity of the APSP problem. In [5], and independently in [103], a lower and upper bound on the diameter are indeed dynamically refined by calculating the eccentricity of vertices properly chosen, so that also the diameter of huge real world undirected graphs has been discovered.

The algorithm shown in [5] has been integrated into the library in [104], and has been used in order to compute the exact diameter of several quite huge subgraphs of the Facebook graph: a highly parallel version of this method was able to compute the diameter of the largest subgraph (approximately 149.1M of vertices and 15.9G of edges) in twenty minutes [7, 8].

For directed graphs, in order to obtain a lower bound for the diameter, the idea of the *double sweep* has been adapted by [89]: pick the farthest vertex from a random vertex and return its backward eccentricity, i.e. its eccentricity in the transposed graph. In [3] the effectiveness of this directed version of the *double sweep* has been verified and the technique in [5] has been reviewed and generalized in order to calculate the diameter graphs too.

CONTRIBUTION. As a result of our previous works [3, 4, 5, 6], we will present the DiFUB algorithm, which is able to calculate the diameter and to list all the vertices that are sources or targets of a diametral path of (strongly) connected components of huge real world (directed) graphs in time $O(m)$ in practice. Our experimental results are supported by considering an extensive dataset of real world graphs. By using the same technique, we will show an algorithm for efficiently computing the radius and listing all the vertices that are sources of a radial path of such graphs. For the same dataset we will show the effectiveness of this algorithm. It is worth of noting that our algorithms extend also to weighted graphs.

Parts of this chapter appeared in [1, 105].

STRUCTURE OF THE CHAPTER. This chapter is organised as follows: in Section 4.2 we will overview the most popular centrality measures that have been applied to biological networks to discover vertex essentiality; in Section 4.3, respectively Section 4.4, we will show our algorithm to compute the diameter, respectively the radius, and to list all the peripheral, respectively the central, vertices according to the eccentricity notion of centrality; in Section 4.5 we will show how these algorithms work through an example and in Section 4.6, we will report some graphs in which our algorithms achieve the worst performances; in Section 4.7 we will show that this is not the case of real world graphs. Finally in Section 4.8 we conclude with some open problems and in Section 4.9 with some considerations about distance analysis in general.

4.2 OVERVIEW ON CENTRALITY ANALYSIS FOR BIOLOGICAL NETWORKS

Given a network, it is natural to wonder how important each vertex is to the functionality of the network. A number of graph measures have been developed for evaluating vertex centrality [106, 107, 108, 109, 110, 111] and several tools allow to compute network metrics, such as CentiBiN [106], VisANT [112], Visone [113], Pajek [114], CentiScaPe [111], and CentiLib [115]. Centrality measures can be local (or neighbourhood based) or global (distance or feedback based).

LOCAL MEASURES. With neighbourhood-based measures, such as degree, the importance of the vertices is inferred from their local connectivity and the more connections a vertex has the more central it is. Highly connected vertices (hubs) were found to possess special properties in the *Yeast* Protein-Protein Interaction network: they are more often essential than non-hub proteins [116, 117]). They tend to play a central role in the modular organization of a network [118, 40] and seem to be evolutionarily more conserved [119]. Nevertheless, since then, several works have raised doubts on some of these associations [120, 121].

There is no consensus in the literature on how to define a hub, and different criteria have been used: a certain fraction of the highest degree vertices [122];

vertices with a certain fraction of the total connectivity [123]; a degree greater than an arbitrary threshold [40, 124, 125].

In order to have an indication about the homogeneity of the vertices of a network, it is interesting to study the degree distribution that for most biological networks is well fitted by a power-law ($P(k) \propto k^{-\gamma}$) with $\gamma \approx 2$, where k corresponds to the degree. In these networks, a few hubs play a fundamental role for the integrity and navigability of the network [118], while a vast majority of the vertices has only a few connections. This degree distribution has been associated to robustness against random vertex removal. Robustness to the loss of a vertex in the Metabolic network indicates the presence of alternative pathways bypassing the missing reaction; in Gene Regulatory networks it may correspond to the presence of alternative ways of transducing and controlling information. On the contrary, these networks are highly sensitive to directed attacks, because removal of hubs deeply affects network functionality [126]. Even though much research has been done on the power-law distribution and its universality in biological networks, criticisms have been raised [127].

The local connectivity of vertices can be studied in further detail by using either assortativity or dyadicity. The first measure is the correlation between the degree of adjacent vertices [128]. Maslov and Sneppen [129] found that hubs in the *Yeast* Protein-Protein Interaction network are mostly connected to non-hubs, and are therefore well separated from each other. Dyadicity [130] measures the degree to which vertices of a network are connected to vertices sharing some characteristic (functional classification, essentiality, involvement in a disease and so on) and is therefore able to characterize the modular structure of a network, considering the distribution of the functions over the vertices and their connectivity [131]. A network is called heterophilic (heterophobic) when different categories are connected more (less) often than expected following a random model. It has been recently used to study the coupling between structure and functionality in transcriptional and non coding (nc) RNA-protein interactions networks [132]. The results showed that most transcriptional regulators and ncRNAs tend to connect to genes/proteins of other functional classes, suggesting that regulators do not really belong to a functional class and tend to coordinate several of them [132]. On the converse, in Protein-Protein Interaction networks connections more often involve proteins of a same functional category.

GLOBAL MEASURES. Closeness [133], eccentricity, and shortest path based betweenness [134] are based on global properties of a network, in particular to the shortest path length between its vertices. The closeness of a vertex depends on its average distance from the others and is of particular interest for information networks (such as signalling and gene regulatory networks), because it measures how fast information flows from a vertex of interest to all the reachable vertices on the average [135]. It has been recently integrated with biological information in a parameter-free gene prioritization approach that measures the interconnectedness (ICN) between genes in a network [136]. ICN measures closeness of each candidate gene to genes possessing the interesting property by considering alternative paths in addition to the direct link and the shortest path distances. The closeness can be efficiently approximated in the case of big networks by using [137].

The eccentricity of a vertex is the length of the longest shortest path starting from it, that is a vertex is central if its farthest vertex is not far. It has been shown that in the metabolic network of *E. coli* the rank order of the vertices based on eccentricity yields very similar rank order to the one based on the closeness close to the central vertices, despite the fact that these measures may disagree significantly in the case of not central vertices [138]; for the protein network of *Yeast*, it has been shown that even if eccentricity is not effective to find essential proteins because not essential proteins can have high eccentricity, the proteins having high eccentricity can be considered not essential [138, 139]. In the following section we will exploit an algorithm to find efficiently all the peripheral and central vertices, according to this notion of centrality.

Shortest path based betweenness depends on the number of shortest paths crossing a vertex. In Protein-Protein Interaction networks, betweenness can be interpreted as the relevance of a protein to be intermediary in the interaction between other proteins, by assuming that this interaction passes through shortest paths [111]. Bottlenecks are vertices with high betweenness centrality and have been found to be key connectors with surprising functional and dynamical properties, often essential [140]. Bottleneck and hub genes were identified in coexpression networks inferred from experimental data, and found to be often essential for virulence in *Salmonella typhimurium* with the role of mediators of transitions between different cellular states or of sentinels that reflect the dynamics of these transitions [141]. Cell cycle checkpoints were found to be bottlenecks in a gene coexpression network of cell cycle regulated genes in the fission *Yeast* [142].

Network metrics in general [143, 144, 145] and betweenness centrality in particular are also used for the rational prediction of drug targets [146]. Essential genes are preferred targets for drug design and central genes are more likely to be essential. Another constraint was imposed in this particular case: the gene must be essential for the pathogen but not for the host, to reduce side effects of the drug.

One problem of shortest path based measures is that communication between biological entities is assumed to pass along those paths, which is often not plausible: from the point of view of Metabolic networks, the shortest path might be defined on the basis of the energy/cofactor requirements instead of the number of hops, while in Gene Regulatory networks and Protein-Protein Interaction networks all active connections will take place and not only the shortest ones. In the former, targets with different shortest paths to a common regulator may exhibit hierarchical gene expression patterns as it is the case for flagellar genes [147].

To overcome the limitation of shortest paths, a vertex can be considered central when it is crossed by many random walks: this is the case of the random walk based betweenness centrality [148]. Some feedback based measures are implicitly based on random walks, like eigenvector [149] and spectral centrality [150]. Eigenvector centrality has been applied to several metabolic networks [151] and has been shown to outperform other metrics for the identification of essential proteins in the Protein-Protein Interaction network of *Yeast* [152], together with subgraph centrality [153].

However since the network express just the potential links and not the real ones, many walks are not feasible, since they traverse edges that are hardly occur together at the same time in the network. For these reasons, very recently, gene expression has been integrated in a centrality measure called Pec [154] which has been used to identify essential genes in *Yeast*. This measure exploits the strength of the connectivity between two adjacent vertices based on an Edge Clustering Coefficient [155], weighted by the co-expression between genes in experimental data.

4.3 COMPUTING THE DIAMETER AND ENUMERATING ALL THE DIAMETRAL VERTICES

Let $G = (V, E)$ be a directed strongly connected graph and let u be any vertex in V. Let $F^F_i(u)$ be the *forward fringe* of u, that is, the set of vertices x such that $d(u, x) = i$. Similarly, let $F^B_i(u)$ be the *backward fringe*, that is, the set of vertices x such that $d(x, u) = i$. In other words, $F^F_i(u)$ (respectively, $F^B_i(u)$) includes all vertices at level i of T^F_u (respectively, T^B_u), where recall that T^F_u (respectively, T^B_u) is the forward (respectively, backward) BFS tree.

Remark 1. *For any two integers* i, j *with* $1 \leqslant i \leqslant ecc_B(u)$ *and* $1 \leqslant j \leqslant ecc_F(u)$, *for any two vertices* x, y *such that* $x \in F^B_i(u)$ *and* $y \in F^F_j(u)$, $d(x, y) \leqslant i + j \leqslant 2\max\{i, j\}$.

Indeed, since $x \in F^B_i(u)$ and $y \in F^F_j(u)$, there exists a path from x to y passing through u that is long $i + j$, so that $i + j$ is an upper bound for $d(x, y)$.

Theorem 4. *For any integer* i *with* $1 < i \leqslant ecc_B(u)$, *for any integer* k *with* $1 \leqslant k < i$, *and for any vertex* $x \in F^B_{i-k}(u)$ *such that* $ecc_F(x) > 2(i-1)$, *there exists* $y \in F^F_j(u)$, *for some* $j \geqslant i$, *such that* $d(x, y) = ecc_F(x)$. *Moreover for any* y *such that* $d(x, y) = ecc_F(x)$, $y \in F^F_j(u)$ *for some* $j \geqslant i$.

Proof. Since $ecc_F(x) > 2(i-1)$, there exists y such that $d(x, y) > 2(i-1)$. For any y such that $d(x, y) > 2(i-1)$, if y was in $F^F_j(u)$ with $j < i$, then from Remark 1 it would follow that $d(x, y) \leqslant 2\max\{i-k, j\} \leqslant 2\max\{i-k, i-1\} = 2(i-1)$, which is a contradiction. Hence, y must be in $F^F_j(u)$ with $j \geqslant i$. □

Similarly to the proof of Theorem 4, we can also prove the following symmetrical result.

Theorem 5. *For any integer* i *with* $1 < i \leqslant \mathrm{ecc}_F(u)$, *for any integer* k *with* $1 \leqslant k < i$, *and for any vertex* $x \in F^F_{i-k}(u)$ *such that* $\mathrm{ecc}_B(x) > 2(i-1)$, *there exists* $y \in F^B_j(u)$, *for some* $j \geqslant i$, *such that* $d(y, x) = \mathrm{ecc}_B(x)$. *Moreover for any* y *such that* $d(y, x) = \mathrm{ecc}_B(x)$, $y \in F^B_j(u)$, *for some* $j \geqslant i$.

In order to describe the DiFUB algorithm, we also need the following definitions. Let

$$B^F_j(u) = \begin{cases} \max_{x \in F^F_j(u)} \mathrm{ecc}_B(x) & \text{if } j \leqslant \mathrm{ecc}_F(u), \\ 0 & \text{otherwise} \end{cases}$$

and

$$B^B_j(u) = \begin{cases} \max_{x \in F^B_j(u)} \mathrm{ecc}_F(x) & \text{if } j \leqslant \mathrm{ecc}_B(u), \\ 0 & \text{otherwise.} \end{cases}$$

By using these two definitions, we are now ready to introduce the DiFUB algorithm, which is shown in Algorithm 15. Intuitively, Theorems 4 and 5 suggest to perform a forward and a backward BFS from a vertex u, and to visit T^F_u and T^B_u in a bottom-up fashion, starting from the vertices in the last fringes. For each level i, we compute the eccentricities of all the vertices in the corresponding fringes: if the maximum eccentricity found lb is greater than $2(i-1)$ then we can conclude that lb is the diameter, since the eccentricities of all the vertices of the remaining levels cannot be greater than lb.

Algorithm 15: DiFUB to compute the diameter

```
Input: A strongly connected di-graph $G$, a vertex $u$, a lower bound $l$ for
       the diameter
Output: The diameter $D$
$i \leftarrow \max\{\mathrm{ecc}_F(u), \mathrm{ecc}_B(u)\}$;
$lb \leftarrow \max\{\mathrm{ecc}_F(u), \mathrm{ecc}_B(u), l\}$;
$ub \leftarrow 2i$;
while $ub - lb > 0$ do
    $lb \leftarrow \max\{lb, B^B_i(u), B^F_i(u)\}$;
    if $lb > 2(i-1)$ then
        return $lb$;
    end
    $ub \leftarrow 2(i-1)$;
    $i \leftarrow i - 1$;
end
return $lb$;
```

Theorem 6. *Algorithm 15 correctly computes the value of the diameter of* G.

Proof. Let D' be the value returned by Algorithm 15. Note that the diameter cannot be smaller than D' since this value is the length of a shortest path. By contradiction assume that there exists a vertex x such that $ecc_F(x) > D'$. Let j be the last value of i for which Algorithm 16 has computed $B_i^B(u)$ and $B_i^F(u)$: thus $D' \geqslant 2(j-1)$. For any vertex v in $F_j^B(u) \cup F_{j+1}^B(u) \cup \ldots \cup F_{ecc_B(u)}^B(u)$, we have computed $ecc_F(v)$, and for any vertex w in $F_j^F(u) \cup F_{j+1}^F(u) \cup \ldots \cup F_{ecc_F(u)}^F(u)$, we have computed $ecc_B(w)$, lb is the maximum eccentricity found. This implies that x have to belong to $F_h^B(u)$ for some $h < j$. Since $ecc_F(x) > D' \geqslant 2(j-1)$, from Theorem 4, there exists $y \in F_k^F(u)$, for some $k \geqslant j$, such that $d(x,y) = ecc_F(x)$. In other words there exists $y \in F_j^F(u) \cup F_{j+1}^F(u) \cup \ldots \cup F_{ecc_F(u)}^F(u)$, such that $ecc_B(y) \geqslant ecc_F(x) > D'$. Since D' is the maximum eccentricity found, this is a contradiction. □

In order to present the algorithm to enumerate all the diametral sources and targets, we define the following quantities, $S_j^F(u)$, that is the set of vertices belonging to $F_j^F(u)$ whose backward eccentricity is $B_j^F(u)$, and the set of their farthest vertices in the transposed graph $T_j^F(u)$.

$$S_j^F(u) = \begin{cases} \{x \in F_j^F(u) : ecc_B(x) = B_j^F(u)\} & \text{if } j \leqslant ecc_F(u), \\ \emptyset & \text{otherwise} \end{cases}$$

$$T_j^F(u) = \bigcup_{x \in S_j^F(u)} \{y : d(y,x) = B_j^F(u)\}$$

Analogously, we define $S_j^B(u)$, that is the set of vertices belonging to $F_j^B(u)$ whose forward eccentricity is $B_j^B(u)$, and the set of their farthest vertices $T_j^B(u)$.

$$S_j^B(u) = \begin{cases} \{x \in F_j^B(u) : ecc_F(x) = B_j^B(u)\} & \text{if } j \leqslant ecc_B(u), \\ \emptyset & \text{otherwise.} \end{cases}$$

$$T_j^B(u) = \bigcup_{x \in S_j^B(u)} \{y : d(x,y) = B_j^B(u)\}$$

With respect to Algorithm 15, every time the lower bound lb is updated, because vertices, whose forward or backward eccentricity is greater than lb are found in the current fringe sets, Algorithm 16 empties and updates also the set of diametral sources DS and the set of diametral targets DT. Every time vertices, whose forward or backward eccentricity is equal to the current value of lb, these vertices are added to the sets DS and DT, respectively. It is worth observing that whenever the guarding condition of the loop is satisfied, because $lb = ub = 2i$, for some i, the eccentricities of the vertices belonging to $F_i^F(u)$ or $F_i^B(u)$ have not been checked, while some of these vertices could have still forward or backward eccentricity equal to $2i$. Thus this check is done in the last part of the algorithm before the returning statement.

Algorithm 16: DiFUB to enumerate all the diametral vertices

```
Input: A strongly connected di-graph G, a vertex $u$, a lower bound $l$ for
       the diameter
Output: The diameter D, DS, that is the set of vertices $x$ such that
        $ecc_F(x) = D$, DT, that is the set of vertices $x$ such that
        $ecc_B(x) = D$.
$i \leftarrow \max\{ecc_F(u), ecc_B(u)\}$;
$lb \leftarrow \max\{ecc_F(u), ecc_B(u), l\}$;
$ub \leftarrow 2i$;
$DS \leftarrow \emptyset$;  $DT \leftarrow \emptyset$;
while $ub - lb > 0$ do
    if $B_i^B(u) > lb$ then
        $lb \leftarrow B_i^B(u)$;
        $DS \leftarrow S_i^B(u)$;  $DT \leftarrow T_i^B(u)$;
    else
        if $B_i^B(u) = lb$ then
            $DS \leftarrow DS \cup S_i^B(u)$;  $DT \leftarrow DT \cup T_i^B(u)$;
        end
    end
    if $B_i^F(u) > lb$ then
        $lb \leftarrow B_i^F(u)$;
        $DS \leftarrow T_i^F(u)$;  $DT \leftarrow S_i^F(u)$;
    else
        if $B_i^F(u) = lb$ then
            $DS \leftarrow DS \cup T_i^F(u)$;  $DT \leftarrow DT \cup S_i^F(u)$;
        end
    end
    if $lb > 2(i-1)$ then
        return $lb, DS, DT$;
    end
    $ub \leftarrow 2(i-1)$;
    $i \leftarrow i-1$;
end
if $B_i^B(u) = lb$ then
    $DS \leftarrow DS \cup S_i^B(u)$;  $DT \leftarrow DT \cup T_i^B(u)$;
end
if $B_i^F(u) = lb$ then
    $DS \leftarrow DS \cup T_i^F(u)$;  $DT \leftarrow DT \cup S_i^F(u)$;
end
return $lb, DS, DT$;
```

Theorem 7. *Algorithm 16 correctly computes all the diametral sources and targets of* G.

Proof. Algorithm 16 performs at least all the visits performed by Algorithm 15 and return the maximum eccentricity found. From Theorem 6,it follows that Algorithm 16 returns the diameter D . The following invariant holds: for any vertex $v \in DS$, $ecc_F(v) \geqslant lb$; indeed $v \in S_i^B(u)$ and $ecc_F(v) = lb$ or $v \in T_i^F(u)$ for some i and $ecc_F(v) \geqslant lb$. Since lb is finally the diameter, all the vertices in DS are diametral sources. Let us prove that all the diametral sources are in DS. By contradiction, assume that there exists a vertex x such that $x \notin DS$ and $ecc_F(x) = D$. Let j be the last value of i for which Algorithm 16 has computed $B_i^B(u)$ and $B_i^F(u)$. Thus for any vertex v in $F_j^B(u) \cup F_{j+1}^B(u) \cup \ldots \cup F_{ecc_B(u)}^B(u)$, we have computed $ecc_F(v)$, and for any vertex w in $F_j^F(u) \cup F_{j+1}^F(u) \cup \ldots \cup F_{ecc_F(u)}^F(u)$, we have computed $ecc_B(w)$. Observe that for any pair of vertices v, w such that $d(v, w) = D$, Algorithm 16 is such that, if v belongs to $F_h^B(u)$ for some $h \geqslant j$, v is added to DS and w is added to DT, if w belongs to $F_k^F(u)$ for some $k \geqslant j$, w is added to DT and v is added to DS. Thus x have to belong to $F_h^B(u)$ for some $h < j$ and any y, such that $d(x, y) = D$, have to belong to $F_k^F(u)$ for some $k < j$. By applying Theorem 4, if $D = ecc_F(x) > 2(j-1)$ then y should belong to $F_z^F(u)$ for some $z \geqslant j$: thus $D \leqslant 2(j-1)$. There are the following two cases.

- Algorithm 16 stops and returns inside the loop. In this case, $B_j^F(u)$ and $B_j^B(u)$ are the last computed and $lb = D > 2(j-1)$, that is a contradiction.
- Algorithm 16 stops and returns outside the loop. In this case $B_j^F(u)$ and $B_j^B(u)$ are the last computed and $lb = ub = D = 2j$, that is a contradiction.

Analogously, it is possible to prove that DT contains all and only the diametral targets. □

Observe that in order to compute $B_j^F(u)$ (respectively, $B_j^B(u)$), we need to compute $ecc_B(x)$ (respectively, $ecc_F(x)$) for any node node x in $F_j^F(u)$ (respectively, $F_j^B(u)$), by performing a visit.

The time complexity of DiFUB can be in the worst case $O(nm)$ where n denotes the number of vertices and m denotes the number of arcs. Indeed, observe that, at each iteration of the **while** loop, $ub - lb$ decreases at least by 2: this implies that, given a starting vertex u, the algorithm executes at most $\max\{\lceil ecc_B(u)/2\rceil, \lceil ecc_F(u)/2\rceil\}$ iterations (note that we have that the number of iterations is bounded by $D/2$); in the worst case, the number of nodes in $F_j^F(u)$ for $j > \lceil ecc_F(u)/2\rceil$ or in $F_i^B(u)$ for $i > \lceil ecc_B(u)/2\rceil$ is linear and for each of these nodes a visit is required (see Section 4.6). In the case of Algorithm 16, one iteration more could be needed.

Since the practical performance of the algorithm depends on the chosen vertex u, the idea behind a good choice of the starting vertex is preferring vertices having a small quantity of vertices at distance greater than or equal to $D/2$. We will consider the following heuristics to choose the starting vertex and to get a corresponding lower bound l.

- *Degree selection.* A simple way of selecting u is choosing a vertex with the highest in-degree or out-degree. We refer to the composition of DiFUB with these two selection strategies as DiFUB*HdOut* and DiFUB*HdIn* respectively.
- *2-Sweep selection.* A more complex way to select u is by using the following heuristic, called 2dSWEEP, which is a natural extension to directed graphs of the 2SWEEP method (in the following, the *middle* vertex between two vertices s and t is defined as the vertex belonging to the shortest path from s to t, whose distance from s is $\lceil d(s,t)/2 \rceil$).

  1. Run a forward BFS from a vertex r: let a_1 be the farthest vertex.
  2. Run a backward BFS from a_1: let b_1 be the farthest vertex.
  3. Run a backward BFS from r: let a_2 be the farthest vertex.
  4. Run a forward BFS from a_2: let b_2 be the farthest vertex.
  5. If $ecc_B(a_1) > ecc_F(a_2)$, then set u equal to the middle vertex between a_1 and b_1 and l equal to $ecc_B(a_1)$. Otherwise, set u equal to the middle vertex between a_2 and b_2 and l equal to $ecc_F(a_2)$.

  We will consider the variants in which r is the vertex with highest out-degree or in-degree, and we will refer to them as 2dSWEEP*HdOut* and 2dSWEEP*HdIn* respectively. Moreover we will refer to DiFUB by applying these two starting strategies as DiFUB+2dSWEEP*HdOut* and DiFUB+2dSWEEP*HdIn*.

4.3.1 *Restricting to Undirected Graphs*

If $G = (V, E)$ is an undirected graph and u is any vertex in V, $F_i^F(u)$, the *forward fringe* of u, coincides with $F_i^B(u)$, the *backward fringe*. By consequence $B_j^B(u) = B_j^F(u)$, and the Algorithm 15 in the case of undirected graph can be simplified as in Algorithm 19, as shown by [156]. Analogously to Theorem 6, it is possible to prove the following.

Theorem 8. *Algorithm 19 correctly computes the value of the diameter of* G.

In order to obtain a good starting vertex u in Algorithm 19, we can simplify 2dSWEEP Algorithm, as shown by Algorithm 18, that is the well known 2SWEEP Algorithm [157, 4].

1. Execute a forward breadth-first search starting from a vertex r: let a_1 be the farthest vertex.

Algorithm 17: 2dSweep

```
Input: A strongly connected graph $G$, a vertex $r$
Output: A vertex and a lower bound for $D$
Run a forward BFS from $r$: let $a_1$ be the farthest vertex;
Run a backward BFS from $a_1$: let $b_1$ be the farthest vertex.
Run a backward BFS from $r$: let $a_2$ be the farthest vertex.
Run a forward BFS from $a_2$: let $b_2$ be the farthest vertex.
if $ecc_B(a_1) > ecc_F(a_2)$ then
    $u \leftarrow$ the middle vertex between $a_1$ and $b_1$;
    $l \leftarrow ecc_B(a_1)$;
else
    $u \leftarrow$ the middle vertex between $a_2$ and $b_2$;
    $l \leftarrow ecc_F(a_2)$;
end
return $u$ and $l$;
```

Algorithm 18: 2Sweep

```
Input: A strongly connected graph $G$, a vertex $r$
Output: A vertex and a lower bound for $D$
Run a forward BFS from $r$: let $a_1$ be the farthest vertex;
Run a forward BFS from $a_1$: let $b_1$ be the farthest vertex.
$u \leftarrow$ the middle vertex between $a_1$ and $b_1$;
$l \leftarrow ecc_F(a_1)$;
return $l$;
```

2. Execute a forward breadth-first search starting from a_1: let b_1 be the farthest vertex.

3. Return the middle vertex between a_1 and b_1.

We will consider the variants called 2Sweep*Hd*, in which r is the vertex with highest degree. Moreover we will refer to iFUB by applying this strategy to select the starting vertex as iFUB+2Sweep*Hd* and to iFUB by starting from the vertex with the highest degree as iFUB*Hd*.

In a similar manner, Algorithm 16 can be simplified in order to deal with undirected graphs.

4.3.2 *Generalizing to Weighted Graphs*

Theorem 4 and 5 can be easily extended to the case of directed weighted graphs. Indeed, let T_u^F (respectively, T_u^B) denote the forward (respectively, backward) lightest path tree rooted at vertex u, computed, for instance, by means

Algorithm 19: iFUB

```
Input: An undirected connected graph $G$, a vertex $u$, a lower bound $l$ for
       the diameter
Output: The diameter $D$
$i \leftarrow ecc_F(u)$;
$lb \leftarrow \max\{ecc_F(u), l\}$;
$ub \leftarrow 2i$;
while $ub - lb > 0$ do
    $lb \leftarrow \max\{lb, B_i^F(u)\}$;
    if $lb > 2(i-1)$ then
        return $lb$;
    else
        $ub \leftarrow 2(i-1)$;
    end
    $i \leftarrow i - 1$;
end
return $lb$;
```

Algorithm 20: DiFUB for weighted directed graphs

```
Input: A weighted directed strongly connected graph $G$, a vertex $u$, a
       lower bound for the diameter $l$
Output: The diameter $D$
Let $d_1 < d_2 < \ldots < d_h$ be the sequence of values $d$ such that $F_d^F(u) \neq \emptyset$
or $F_d^B(u) \neq \emptyset$
$i \leftarrow h$;
$lb \leftarrow \max\{ecc_F(u), ecc_B(u), l\}$;
$ub \leftarrow 2d_i$;
while $ub - lb > 0$ do
    $lb \leftarrow \max\{lb, B_{d_i}^B(u), B_{d_i}^F(u)\}$;
    if $lb > 2d_{i-1}$ then
        return $lb$;
    else
        $ub \leftarrow 2d_{i-1}$;
    end
    $i \leftarrow i - 1$;
end
return $lb$;
```

of the Dijkstra algorithm [158] in G (respectively, in the graph transposed of G). Moreover, let $ecc_F(u)$ (respectively, $ecc_B(u)$) denote the weighted forward (respectively, backward) eccentricity of u, that is the weight of the longest path from (respectively, to) u to (respectively, from) one of the leaves of T_u^F (respectively, T_u^B). Finally, let $F_d^F(u)$ (respectively, $F_d^B(u)$) denote the set of vertices whose weighted distance from (respectively, to) u is equal to d: hence, $F_d^F(u) \neq \emptyset$ if and only if there exists at least one vertex x in T_u^F such that the weight of the path from u to x is equal to d, and $F_d^B(u) \neq \emptyset$ if and only if there exists at least one vertex x in T_u^B such that the weight of the path from x to u is equal to d.

Let $d_1, d_2, \dots, d_h$ be the sequence of distinct values d such that $F_d^F(u) \neq \emptyset$ or $F_d^B(u) \neq \emptyset$ ordered in increasing order, that is, $d_1 < d_2 < \dots < d_h$: note that $d_h = \max\{\mathrm{ecc}_F(u), \mathrm{ecc}_B(u)\}$. We then have the following two results, whose proofs are similar to the proofs of Theorems 4 and 5, respectively.

Theorem 9. *For any integer* i *with* $1 < i \leqslant h$, *for any integer* k *with* $1 \leqslant k < i$, *and for any vertex* $x \in F_{d_{i-k}}^B(u)$ *such that* $\mathrm{ecc}_F(x) > 2d_{i-1}$, *there exists* $y \in F_{d_j}^F(u)$, *for some* $d_j \geqslant d_i$, *such that* $d(x, y) = \mathrm{ecc}_F(x)$. *Moreover for any* y *such that* $d(x, y) = \mathrm{ecc}_F(x)$, $y \in F_{d_j}^F(u)$, *for some* $d_j \geqslant d_i$.

Theorem 10. *For any integer* i *with* $1 < i \leqslant h$, *for any integer* k *with* $1 \leqslant k < i$, *and for any vertex* $x \in F_{d_{i-k}}^F(u)$ *such that* $\mathrm{ecc}_B(x) > 2d_{i-1}$, *there exists* $y \in F_{d_j}^B(u)$, *for some* $d_j \geqslant d_i$, *such that* $d(y, x) = \mathrm{ecc}_B(x)$. *Moreover for any* y *such that* $d(y, x) = \mathrm{ecc}_B(x)$, $y \in F_{d_j}^B(u)$, *for some* $d_j \geqslant d_i$.

We can then appropriately modify the DiFUB algorithm in order to deal with directed weighted graphs. To this aim, we define

$$B_{d_i}^F(u) = \begin{cases} \max_{x \in F_{d_i}^F(u)} \mathrm{ecc}_B(x) & \text{if } F_{d_i}^F(u) \neq \emptyset \text{ and } d_i \leqslant \mathrm{ecc}_F(u), \\ 0 & \text{otherwise} \end{cases}$$

and

$$B_{d_j}^B(u) = \begin{cases} \max_{x \in F_{d_j}^B(u)} \mathrm{ecc}_F(x) & \text{if } F_{d_j}^B(u) \neq \emptyset \text{ and } d_j \leqslant \mathrm{ecc}_B(u), \\ 0 & \text{otherwise.} \end{cases}$$

The DiFUB algorithm for directed weighted graphs is then described in Algorithm 20. Analogously to Theorem 6, it is possible to prove the following.

Theorem 11. *Algorithm 20 correctly computes the value of the diameter of* G.

Observe that, in order to start the execution of the algorithm, we can also modify the 2dSweep algorithm by using single source lightest path algorithm executions instead of BFSes.

4.4 COMPUTING THE RADIUS AND ENUMERATING ALL THE RADIAL VERTICES

In the following, as before, we will assume that G is connected whenever G is undirected, or that G is strongly connected whenever G is directed. Algorithm 21

Algorithm 21: Computing the radius and enumerating all the radial vertices

```
Input: A graph $G$, directed or undirected, a pair of vertices $x, y$
Output: The radius $R$ and $C$, the set of vertices whose forward
        eccentricity is $R$
$\pi \leftarrow$ ordering of the vertices $v \in V$ according to $\max\{d(v,x), d(v,y)\}$;
$C = \emptyset$;
$ub \leftarrow n$;
for $i = 1$ to $n$ do
    $v \leftarrow \pi(i)$;
    if $ecc_F(v) < ub$ then
        $ub \leftarrow ecc_F(v)$;
        $C \leftarrow \{v\}$;
    else
        if $ecc_F(v) = ub$ then
            $C \leftarrow C \cup \{v\}$;
        end
    end
    if $i \neq n$ then
        $u \leftarrow \pi(i+1)$;
        if $ub < \max\{d(u,x), d(u,y)\}$ then
            return $ub$ and $C$;
        end
    end
end
return $ub$ and $C$;
```

computes all the vertices whose eccentricity is equal to the radius. In particular, given in input a pair of vertices x, y, Algorithm 21 orders the vertices v according to $\max\{d(v,x), d(v,y)\}$ and scans their eccentricity. At each step, a lower bound on the eccentricities of the vertices still to process can be easily retrieved.

Remark 2. *For any* i*, let* u *be* $\pi(i+1)$*, then*

$$ecc_F(z) \geqslant \max\{d(z,x), d(z,y)\} \geqslant \max\{d(u,x), d(u,y)\}$$

for any z such that $z = \pi(j)$*, with* $j \geqslant i+1$.

For increasing values of i, we can compute the eccentricity of the vertex $v = \pi(i)$, and maintain the minimum eccentricity found, that is an upper bound ub for the radius. Remark 2 implies that $\max\{d(u,x), d(u,y)\}$ is a lower bound of the eccentricities of the vertices to be processed. Thus if ub is less than this lower bound, we can stop the computation because it is not possible to decrease

ub. In particular this implies that all the vertices, whose eccentricity has not yet been computed, have eccentricity strictly greater than R. Then the following result holds.

Lemma 4. *Algorithm 21 returns all and only the radial vertices.*

While scanning the eccentricities of the vertices, a list C, of the examined vertices whose eccentricity is equal to the current value of the upper bound, is maintained.

The performances of Algorithm 21 are strongly affected by the choice of the starting pair of vertices x, y. A good strategy is applying the 2dSWEEP algorithm and, referring to Algorithm 17, taking a_1 and b_2. In particular in the following we will consider the 2dSWEEP*HdOut* and 2dSWEEP*HdIn*. We will refer to Algorithm 21 with starting strategies 2dSWEEP*HdOut* and 2dSWEEP*HdIn* as rad+2dSWEEP*HdIn* and rad+2dSWEEP*HdIn* respectively.

Observe that Algorithm 21 can be applied also in the case of undirected graphs. In this case, by applying 2SWEEP*Hd* Algorithm, referring to Algorithm 17, the vertices a_1 and b_1 can be used as starting vertices for Algorithm 21. In the following, we will refer to this Algorithm with this starting choice as rad+2dSWEEP*Hd*. Moreover, by using Dijkstra's Algorithm, instead of using the BFS Algorithm, the algorithm can be applied also in the case of weighted graphs.

4.5 ENUMERATING DIAMETRAL AND RADIAL VERTICES: AN EXAMPLE

Let us consider the graph shown in the top part of Figure 9, whose all pairwise distances, with the forward and backward eccentricities of all its vertices are shown. If we choose $u = v_1$, the corresponding two breadth-first search trees T^F_u and T^B_u are shown in the bottom part of the figure. From these two trees we can easily derive the forward and backward fringe sets, which are shown in the bottom part of the figure, together with $B^F_i(v_1)$, $B^B_i(v_1)$, $S^F_i(v_1)$, $T^F_i(v_1)$, $S^B_i(v_1)$, and $T^B_i(v_1)$.

If we choose $i = 2$, $j = 3$, $x = v_6$, and $y = v_8$, then it is easy to verify, by inspecting the two BFSes trees, that we can go from v_6 to v_8 by first going up in $T^B_{v_1}$ (by means of two arcs) and then by going down in $T^F_{v_1}$ (by means of three arcs). Hence, as observed in Remark 1, $d(v_6, v_8) \leqslant 5$: indeed, $d(v_6, v_8) = 3$ (passing through v_4 and v_7). Moreover, if we choose $i = 2$, $k = 1$, and $x = v_4 \in F^B_1(v_1)$, then we have that $ecc_F(v_4) = 4 > 2 = 2(i-1)$: Theorem 4 is in this case witnessed by vertex $y = v_2 \in F^F_2(v_1)$ (indeed, $d(v_4, v_2) = 3$).

Suppose we invoke Algorithm 16 with $u = v_1$ and $l = 0$. Before the execution of the **while** loop starts, the two variables i and lb are both set equal to $\max\{ecc_F(v_1), ecc_B(v_1)\} = 5$, while variable ub is set equal to $2i = 10$ and the sets DS and DT are both empty. Since $ub - lb = 5 > 0$, the algorithm enters the **while** loop with $i = 5$. Since, $B^B_5(v_1) = 7 > lb$, lb is set to 7 and DS and

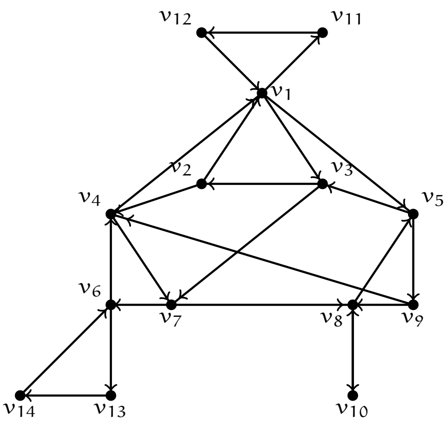

	v_1	v_2	v_3	v_4	v_5	v_6	v_7	v_8	v_9	v_{10}	v_{11}	v_{12}	v_{13}	v_{14}	ecc_F
v_1	0	2	1	3	1	3	2	3	2	4	1	2	4	5	5
v_2	1	0	2	1	2	3	2	3	3	4	2	3	4	5	5
v_3	2	1	0	2	3	2	1	2	4	3	3	4	3	4	4
v_4	1	3	2	0	2	2	1	2	3	3	2	3	3	4	4
v_5	3	2	1	2	0	3	2	2	1	3	4	5	4	5	5
v_6	2	4	3	1	3	0	2	3	4	4	3	4	1	2	4
v_7	3	4	3	2	2	1	0	1	3	2	4	5	2	3	5
v_8	4	3	2	3	1	4	3	0	2	1	5	6	5	6	6
v_9	2	4	3	1	2	3	2	1	0	2	3	4	4	5	5
v_{10}	5	4	3	4	2	5	4	1	3	0	6	7	6	7	7
v_{11}	2	4	3	5	3	5	4	5	4	6	0	1	6	7	7
v_{12}	1	3	2	4	2	4	3	4	3	5	2	0	5	6	6
v_{13}	4	6	5	3	5	2	4	5	6	6	5	6	0	1	6
v_{14}	3	5	4	2	4	1	3	4	5	5	4	5	2	0	5
ecc_B	5	6	5	5	5	5	4	5	6	6	6	7	6	7	

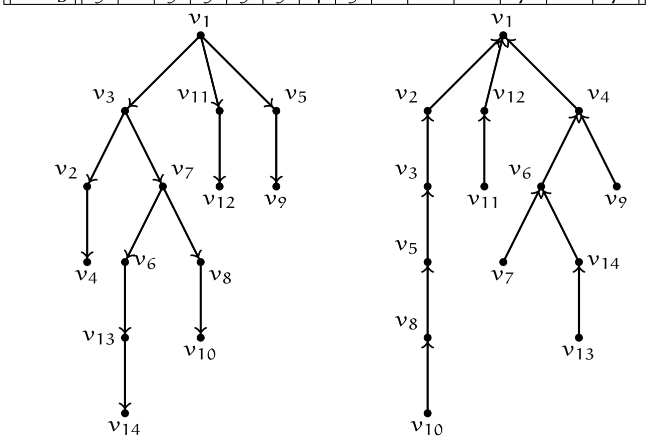

i	$F_i^F(v_1)$	$F_i^B(v_1)$	$B_i^F(v_1)$	$B_i^B(v_1)$	$S_i^F(v_1)$	$T_i^F(v_1)$	$S_i^B(v_1)$	$T_i^B(v_1)$
1	v_3, v_5, v_{11}	v_2, v_4, v_{12}	6	6	v_{11}	v_{10}	v_{12}	v_{14}
2	v_2, v_7, v_9, v_{12}	v_3, v_6, v_9, v_{11}	7	7	v_{12}	v_{10}	v_{11}	v_{14}
3	v_4, v_6, v_8	v_5, v_7, v_{14}	5	5	v_4, v_6, v_8	v_{10}, v_{11}, v_{13}	v_5, v_7, v_{14}	$v_2, v_9, v_{10}, v_{12}, v_{14}$
4	v_{10}, v_{13}	v_8, v_{13}	6	6	v_{10}, v_{13}	v_{10}, v_{11}, v_{13}	v_8, v_{13}	$v_2, v_9, v_{10}, v_{12}, v_{14}$
5	v_{14}	v_{10}	7	7	v_{14}	v_{10}, v_{11}	v_{10}	v_{12}, v_{14}

Figure 9: A strongly connected graph with the corresponding all pairwise distances, forward and backward eccentricities and BFSes trees rooted at v_1, and the fringe set properties.

DT are respectively set to $\{v_{10}\}$ and $\{v_{12}, v_{14}\}$. Then since $B_5^F(v_1) = 7$ is equal to lb, $DS = \{v_{10}\} \cup \{v_{10}, v_{11}\}$ (v_{11} is added to DS) and $DT = \{v_{12}, v_{14}\} \cup \{v_{14}\}$ (DT does not change). Since $lb = 7 < 8 = 2(i-1)$, the algorithm sets ub equal to 8 and performs another iteration with $i = 4$. Since $B_4^F(v_1) = B_4^B(v_1) = 6$ and $6 < 7 = lb$ the lower bound lb is not improved and the sets DS and DT are not modified. Since $lb = 7 > 2(i-1) = 6$ the algorithm returns: $lb = 7$ is the diameter of the graph, $DS = \{v_{10}, v_{11}\}$ is the set of all the diametral sources (indeed $ecc_F(v_{10}) = ecc_F(v_{11}) = 7$), and $\{v_{12}, v_{14}\}$ is the set of all the diametral targets (indeed $ecc_B(v_{12}) = ecc_B(v_{14}) = 7$).

Finally suppose we invoke Algorithm 21, with input the pair of vertices v_1, v_{10}. We define the sets C_i as $\{u : \max\{d(u, v_1), d(u, v_{10})\} = i\}$ and for any i we show the corresponding C_i in the following.

i	$C_i = \{u : \max\{d(u, v_1), d(u, v_{10})\} = i\}$
1	$\emptyset$
2	v_9
3	v_3, v_4, v_5, v_7
4	v_1, v_2, v_6, v_8
5	v_{10}, v_{12}, v_{14}
6	v_{11}, v_{13}

Thus Algorithm 21 order the vertices as follows

$$\langle v_9, v_3, v_4, v_5, v_7, v_1, v_2, v_6, v_8, v_{10}, v_{12}, v_{14}, v_{11}, v_{13} \rangle.$$

ub is set to n and C is empty. In the first iteration we have $v = v_9$ and since $ecc_F(v_9) = 5$, ub is set to 5 and $C = \{v_9\}$. Since $ub = 5 > \max\{d(v_3, v_1), d(v_3, v_{10})\} = 3$, where v_3 is the successor of v_9 in the order, the algorithm performs a new iteration. In this latter iteration $v = v_3$, ub is improved and set to $ecc_F(v_3) = 4$ and $C = \{v_3\}$. Since $ub = 4 > \max\{d(v_4, v_1), d(v_4, v_{10})\} = 3$, the algorithm does not stop and considers as new v the vertex v_4. Since $ecc_F(v_4) = 4$, v_4 is added to C, so that $C = \{v_3, v_4\}$. Since $ub = 4 > \max\{d(v_5, v_1), d(v_5, v_{10})\} = 3$, the algorithm performs an iteration by using v_5 as v: in this case ub is not improved and C does not change. The same happens by considering as v the vertices v_7, v_1, and v_2. When considering as v the vertex v_6, since $ecc_F(v_6) = 4 = ub$, ub is not improved and v_6 is added to C. Since $ub = 4 = \max\{d(v_8, v_1), d(v_8, v_{10})\} = 4$, a new iteration is performed, where $v = v_8$. At the end of this latter iteration, since $ecc_F(v_8) = 6 > ub$, ub is not improved and C is not changed; since $ub = 4 < \max\{d(v_{10}, v_1), d(v_{10}, v_{10})\} = 5$, the algorithm stops. Indeed all the vertices after v_{10} have ecc_F at least $\max\{d(v_{10}, v_1), d(v_{10}, v_{10})\} = 5$. Thus $ub = 4$ is the radius of the graph, and $C = \{v_3, v_4, v_6\}$ is the set of radial vertices, since $ecc_F(v_3) = ecc_F(v_4) = ecc_F(v_6) = 4$.

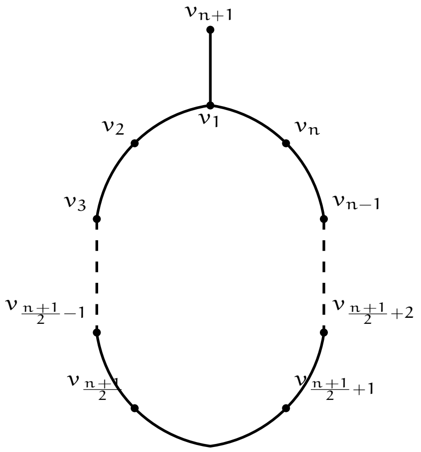

Figure 10: A bad network for Algorithm 16. By replacing each edge with two opposite arcs, this graph becomes a bad network for DIFUB algorithm.

4.6 *ad hoc* BAD CASES

There exist graphs, such as the graph shown in Figure 10 and other graphs available at [159], where our algorithms use $\Theta(n)$ BFSes. These graphs are characterized by an extreme regularity: the BFS trees at their vertices are very similar, with the radius and the diameter values very close, namely, $R \approx D$, and all vertices have close eccentricity. Figure 10 show an example in which IFUB perform $\Theta(n)$ BFSes even if the number of diametral vertices is constant, while Figure 12 show an example in which Algorithm 21 performs $\Theta(n)$ BFSes even if the number of radial vertices is constant.

Whenever R is close to D, about $D/2$ iterations will always be executed in the IFUB algorithm, so that the number of visits performed by IFUB is more likely also close to n, even if the number of diametral vertices is constant. Thus in the case of these graphs, the complexity of IFUB is $\Theta(nm)$. For instance, a cycle with n vertices (n odd), $v_1, \ldots, v_n$, connected to a vertex v_{n+1} by the edge (v_1, v_{n+1}) has diameter $\frac{n+1}{2}$. Any of its vertices has the same BFS tree, whose height is $\frac{n-1}{2}$, except for v_{n+1}, $v_{\frac{n+1}{2}}$, and $v_{\frac{n+1}{2}+1}$ whose eccentricity is $\frac{n+1}{2}$, (see Figure 10). Thus, referring to Algorithm 15 and Algorithm 16, by starting from any vertex with eccentricity $\frac{n-1}{2}$, IFUB repeats its loop until $2(i-1) \geqslant \frac{n-1}{2} + 1$, that is $i \geqslant \frac{n+5}{4}$, and stops the first time that $2(i-1) < \frac{n-1}{2} + 1$, for a total number of iterations equal to $\frac{n-1}{2} - \frac{n+5}{4} + 2 = \frac{n+1}{4}$. Since each level has at least two vertices, the number of BFSes performed by IFUB is thus linear and greater than $\frac{n+3}{2}$. Similar result can be found if Algorithm 15 and Algorithm 16 start from v_{n+1}, $v_{\frac{n+1}{2}}$, or $v_{\frac{n+1}{2}+1}$. These bad undirected graphs for IFUB can be easily adapted to build bad directed graphs for DIFUB, by replacing each edge by two opposite arcs.

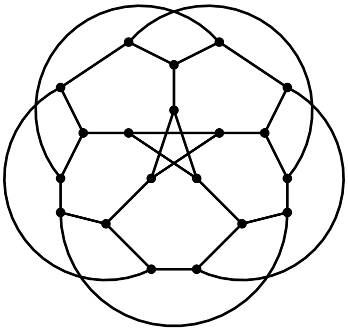

Figure 11: A bad network for Algorithm 15 and 21 with small diameter. By replacing each edge with two opposite arcs, this graph becomes a bad network for the directed versions of the algorithms.

Observe that this graph has linear diameter. However there are graphs, like the one shown in Figure 11 and their generalizations in [159], whose diameter is small, and for which Algorithm 15 uses a linear number of visits.

In the graph shown in Figure 12, that is composed by two cycles $v_1, \dots, v_n$ and $v_1, u_2, \dots u_n$, such that for any i, with $2 \leqslant i \leqslant n$, there is an edge between u_i and v_i, every vertex have eccentricity equal to the diameter $D = \frac{n+1}{2}$, except for v_1, whose eccentricity is equal to the radius $R = D - 1$. If the starting pair of vertices for Algorithm 21 is $u_2, v_{\frac{n+1}{2}+1}$, then v_1 can be one of the last vertex to be processed, so that the number of visits performed by Algorithm 21 is linear. Once again, this bad undirected graph can be easily adapted to build an example of bad directed graph, by replacing each edge by two opposite arcs.

4.7 experiments

We collected several real-world directed or undirected graphs, which have been chosen in order to cover the largest possible set of network typologies. An important feature is that almost all graphs in our dataset are sparse (that is, $m = O(n)$). Note that, in the case of several of these graphs, the diameter value was still unknown.

Our computing platform is a machine with a Pentium Quad-Core CPU (Intel(R) Xeon(R) E5405 @ 2.00GHz), with a 10GB shared memory. The operating system is a Ubuntu GNU/Linux 12.04.1, with a Linux version 3.2.0-34 and gcc version 4.6.3. For each network we report number of vertices and arcs/edges in the original graph and in the biggest (strongly) connected component. For this latter we have computed the diameter D and the radius R, together with the diametral sources, the diametral targets, and the radial vertices.

The code and the data set are available at `amici.dsi.unifi.it/lasagne/`.

In Sections 4.7.1 and 4.7.2 we will report all the details of our dataset and experiments for directed and undirected graphs, respectively. In Section 4.7.3 we will summarize our results, in Section 4.7.4 we will show the effectiveness in our dataset of 2dSweep and 2Sweep in finding a tight lower bound for the diameter. Finally in Section 4.7.5 we will compare the performance of iFub with other methods in the literature to compute the diameter of undirected graphs.

4.7.1 *Directed Graphs*

In the case of directed graphs, we have experimented Algorithm 16 by using several ways of choosing the starting vertex.

- DiFub*HdOut*. DiFub by starting from the vertex with highest out-degree.
- DiFub*HdIn*. DiFub by starting from the vertex with highest in-degree.
- DiFub+2dSweep*HdOut*. Apply 2dSweep*HdOut*, Algorithm 17 by starting from the vertex with highest out-degree, and obtain the vertex u; apply DiFub by starting from u.
- DiFub+2dSweep*HdIn*. Apply 2dSweep*HdIn*, Algorithm 17 by starting from the vertex with highest in-degree, and obtain the vertex u; apply DiFub by starting from u.

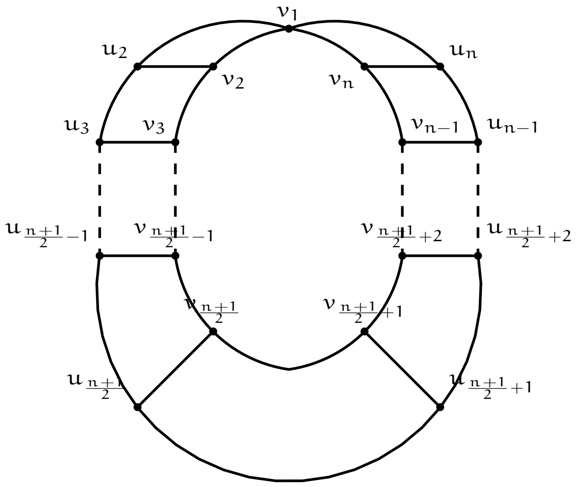

Figure 12: A bad network for Algorithm 21. By replacing each edge with two opposite arcs, this graph becomes a bad network for the directed version of the algorithm.

Observe that each experiment is deterministic, since ties between vertices are broken by considering the vertex whose index is minimum.[1]

Moreover we have experimented Algorithm 21 by considering two ways of selecting the starting pair of vertices.

- rad+2dSweep*HdOut*. Apply 2dSweep*HdOut*, Algorithm 17 by starting from the vertex with highest out-degree, and obtain the vertex u; apply Algorithm 21 by starting from u.

- rad+2dSweep*HdIn*. Apply 2dSweep*HdIn*, Algorithm 17 by starting from the vertex with highest in-degree, and obtain the vertex u; apply Algorithm 21 by starting from u.

We have reported the number of visits performed by each approach.

In the following we report the results of our experiments for metabolic networks, in particular bipartite networks, compound networks, and reaction networks, taken from [160, 24] . In particular we have considered only the biological sources, whose number of nodes of the strongly connected component of the bipartite network is greater than 500. In order to facilitate the correspondence between the names of the networks in the following tables and their real names, reported in Table 1 as they appear in [160, 24] , the networks have been listed in alphabetical order.

[1] Ties are not frequent and no substantial differences have been observed by breaking ties in different way.

BIPARTITE METABOLIC NETWORKS.

	Original Graph		Biggest SCC		Diameter							Radius			
								visits						visits	
Network	n	m	n	m	D	# Diam. Source Nodes	# Diam. Target Nodes	DiFUB *HdOut*	DiFUB *HdIn*	DiFUB 2Sweep *HdOut*	DiFUB 2Sweep *HdIn*	R	# Rad. Nodes	rad 2Sweep *HdOut*	rad 2Sweep *HdIn*
Acyro	2272	3515	1098	2168	28	2	3	12	7	11	11	12	1	26	26
Agroo	2304	3600	988	2082	21	1	1	4	7	8	11	11	5	10	75
Arabo	2793	3121	540	765	69	1	1	43	212	46	85	35	1	26	275
Bacio	1580	2440	701	1405	24	3	1	6	6	10	10	11	1	21	21
Baci2	1763	2765	824	1665	24	1	1	4	8	8	8	12	2	26	26
Chla1	3825	10046	3076	8820	28	1	1	7	6	13	11	13	3	304	37
Cupro	2277	3602	1046	2169	20	3	4	10	18	14	14	10	1	8	17
Escho	4058	9853	3029	8635	18	2	6	24	17	58	62	10	4	95	45
Esch1	2826	4549	1394	2870	23	1	3	5	8	9	9	11	2	22	22
Esch2	2788	3133	569	805	73	1	1	24	17	19	7	32	3	79	79
Esch3	2749	3086	567	806	75	1	1	23	18	19	7	32	2	64	64
Esch4	2802	3154	558	791	73	1	1	24	17	19	7	32	3	79	79
Esch5	2835	3185	565	800	73	1	1	24	17	19	7	32	3	79	79
Esch6	2750	3091	563	801	75	1	1	23	18	19	7	32	2	64	64
Esch7	2821	3177	565	801	73	1	1	24	17	19	7	32	3	79	79
Esch8	2799	3147	563	799	75	1	1	23	18	19	7	32	2	64	64
Esch9	2779	3117	578	821	61	1	1	50	5	9	15	30	5	96	12
Esch10	2816	3168	594	839	81	1	1	43	8	7	7	32	3	79	79
Esch11	2394	2654	543	755	62	3	2	75	77	51	51	28	2	84	84
Esch12	2791	3131	574	819	75	1	1	23	18	19	7	32	2	64	64
Esch13	3074	3507	810	1166	78	1	2	5	44	9	9	35	2	119	119
Esch14	2795	3131	568	804	73	1	1	24	17	19	7	32	3	79	79
Esch15	2838	3197	570	808	73	1	1	24	17	19	7	32	3	79	79
Esch16	2827	3185	606	859	69	2	1	33	20	8	9	32	3	79	79
Esch17	2778	3121	567	809	75	1	1	22	18	19	7	32	2	60	60
Esch18	2810	3196	620	882	84	1	1	36	29	8	8	34	2	61	61
Esch19	2830	4545	1390	2861	23	1	4	9	9	9	9	11	2	22	22
Esch20	4354	9535	2752	7741	18	8	13	27	22	72	104	10	4	90	9
Esch21	4354	9535	2752	7741	18	8	13	27	22	72	104	10	4	90	9
Esch22	2819	3164	568	805	73	1	1	24	17	19	7	32	3	79	79
Esch23	2801	3158	608	862	69	2	1	33	20	8	9	32	3	79	79
Esch24	2884	4648	1430	2948	23	1	3	5	8	9	9	11	2	22	22
Esch25	2707	3070	590	831	75	1	1	26	17	7	9	32	1	79	79
Esch26	2689	3059	590	831	75	1	1	26	17	7	9	32	1	79	79
Esch27	2823	3189	606	851	75	1	1	26	17	7	9	32	1	79	79
Esch28	2711	3138	722	1023	79	1	1	4	25	7	7	31	2	70	70
Esch29	2864	4639	1452	2983	27	1	1	5	3	15	15	13	7	23	23
Esch30	2729	3072	580	823	77	2	1	21	17	9	9	32	2	64	64
Esch31	2716	3079	566	805	73	1	1	24	17	15	7	32	3	79	79
Esch32	2687	3039	562	798	73	1	1	24	17	15	7	32	3	79	79
Esch33	2731	3068	568	808	75	1	1	23	18	19	7	32	2	64	64
Esch34	2805	3147	569	803	79	1	1	16	11	7	7	32	3	78	78
Esch35	2789	3131	569	803	79	1	1	16	11	7	7	32	3	78	78
Esch36	2777	3120	569	803	79	1	1	16	11	7	7	32	3	78	78
Esch37	2797	3139	569	803	79	1	1	16	11	7	7	32	3	78	78
Esch38	2788	3132	572	810	73	1	1	24	17	19	7	32	3	78	78
Esch39	2781	3128	572	810	73	1	1	24	17	19	7	32	3	78	78
Esch40	2793	3137	572	810	73	1	1	24	17	19	7	32	3	78	78
Esch41	2679	3041	553	787	75	1	1	23	18	15	7	32	2	64	64
Esch42	2768	3106	562	799	75	1	1	23	18	19	7	32	2	64	64
Esch43	2841	3201	578	819	76	1	1	23	19	26	8	32	2	63	63
Esch45	2850	3208	575	817	73	1	1	24	17	19	7	32	3	79	79
Esch46	2827	3186	576	817	73	1	1	24	17	19	7	32	3	79	79
Esch47	2787	3126	564	803	75	1	1	23	18	19	7	32	2	64	64
Homoo	2840	3358	780	1073	132	2	2	68	68	683	683	69	1	37	37
Klebo	2657	2975	680	940	72	2	2	45	52	47	47	37	2	120	120
Kleb1	2659	2982	660	912	66	1	1	57	16	50	50	35	2	23	23
Kleb2	2682	3000	684	946	65	1	1	46	11	75	75	32	1	55	14
Leiso	2277	4375	1333	3114	32	1	3	43	31	109	109	11	1	21	182
Metao	10592	19821	6933	15397	28	3	1	25	15	67	67	16	2	22	22
Meth4	2096	3291	952	1988	21	1	1	5	10	15	15	11	1	18	18
Muso	2275	2546	526	715	104	1	1	66	66	302	302	59	8	33	33
Plano	3514	5144	1719	3171	32	1	1	18	6	8	8	15	2	28	28
Pseu1	2275	2470	557	742	57	1	1	208	35	72	79	27	1	7	7
Pseu2	2282	2501	574	769	60	2	1	164	27	60	60	27	1	8	8
Ralso	2325	2527	515	693	65	1	1	54	7	140	101	23	1	20	20
Rhizo	2377	2582	529	716	104	1	1	20	35	13	13	43	1	52	6
Sacco	2969	6681	1976	5381	22	7	2	29	14	18	18	11	4	42	42
Salmo	2253	2520	582	784	95	1	1	21	59	10	11	44	1	69	74
Shigo	2621	2939	518	731	64	1	1	35	8	38	45	31	2	90	90
Shig2	2699	3028	537	757	62	1	2	51	11	47	155	31	3	114	114
Shig3	2705	3035	540	761	62	1	2	51	11	47	155	31	3	114	114
Shig4	2707	3038	531	750	64	1	2	38	11	42	50	31	2	93	93
Shig5	2708	3049	521	731	70	1	2	17	6	10	10	31	2	93	93
Yerso	2071	3245	1008	2039	24	2	1	13	7	19	19	13	16	38	117
Yers1	2184	2389	506	683	98	1	1	33	20	8	8	34	2	58	58

COMPOUND METABOLIC NETWORKS.

Network	Original Graph		Biggest SCC		Diameter							Radius			
						# Diam. Source Nodes	# Diam. Target Nodes	visits					# Rad. Nodes	visits	
	n	m	n	m	D			DiFUB *HdOut*	DiFUB *HdIn*	DiFUB 2SWEEP *HdOut*	DiFUB 2SWEEP *HdIn*	R		rad 2SWEEP *HdOut*	rad 2SWEEP *HdIn*
Acyro	1232	2444	383	1157	14	2	3	7	7	11	11	6	1	17	17
Agroo	1269	2505	329	1067	10	5	1	10	9	14	14	5	1	10	12
Arabo	1464	1772	207	383	34	1	1	26	101	27	41	17	1	16	104
Bacio	866	1732	249	779	12	3	1	6	5	10	10	6	3	17	17
Baci2	966	1991	295	932	12	1	1	4	6	8	8	6	3	17	17
Chla1	1706	7536	1148	5949	14	1	1	6	5	10	10	6	1	6	20
Cupro	1242	2536	362	1148	10	3	4	10	15	14	14	5	1	7	12
Escho	1805	7261	1120	5854	9	2	6	12	9	17	51	5	4	73	29
Esch1	1501	3166	497	1642	11	2	3	4	7	58	58	6	7	19	19
Esch2	1493	1801	232	438	36	1	1	13	9	22	22	16	3	36	36
Esch3	1475	1779	230	439	37	1	1	11	9	13	7	16	2	29	29
Esch4	1499	1815	227	430	36	1	1	13	9	22	22	16	3	36	36
Esch5	1518	1829	230	436	36	1	1	13	9	22	22	16	3	36	36
Esch6	1475	1781	228	435	37	1	1	11	9	13	7	16	2	29	29
Esch7	1505	1823	230	436	36	1	1	13	9	22	22	16	3	36	36
Esch8	1494	1804	229	436	37	1	1	11	9	13	7	16	2	29	29
Esch9	1482	1783	234	447	30	1	1	30	6	13	13	15	5	45	11
Esch10	1503	1822	242	455	40	1	1	21	7	8	8	16	3	36	36
Esch11	1292	1544	214	390	30	3	2	35	33	35	35	14	5	37	37
Esch12	1499	1806	233	448	37	1	1	11	9	13	7	16	2	29	29
Esch13	1631	2014	325	631	38	2	2	6	21	10	13	18	9	64	64
Esch14	1500	1798	231	438	36	1	1	13	9	22	22	16	3	36	36
Esch15	1516	1839	232	440	36	1	1	13	9	22	22	16	3	36	36
Esch16	1510	1830	247	469	34	2	1	18	10	11	11	16	3	36	36
Esch17	1490	1800	231	443	37	1	1	11	9	13	7	16	2	28	28
Esch18	1494	1839	247	472	41	1	1	18	14	7	7	17	3	32	32
Esch19	1509	3171	494	1629	11	5	4	8	8	63	63	6	6	19	19
Esch20	1972	6812	1005	5117	9	8	13	13	10	19	17	5	4	68	9
Esch21	1972	6812	1005	5117	9	8	13	13	10	19	17	5	4	68	9
Esch22	1509	1818	231	438	36	1	1	13	9	22	22	16	3	36	36
Esch23	1496	1818	248	471	34	2	1	18	10	11	11	16	3	36	36
Esch24	1534	3235	506	1669	11	2	3	4	7	59	59	6	7	19	19
Esch25	1442	1775	241	451	37	1	1	13	9	10	8	16	1	36	36
Esch26	1431	1770	241	451	37	1	1	13	9	10	8	16	1	36	36
Esch27	1503	1830	248	461	37	1	1	13	9	9	8	16	1	36	36
Esch28	1429	1843	296	589	39	1	1	3	13	7	7	15	2	32	32
Esch29	1513	3221	518	1698	13	2	1	4	3	28	28	7	10	17	17
Esch30	1462	1771	235	446	38	1	1	11	9	10	10	16	2	29	29
Esch31	1448	1780	229	437	36	1	1	13	9	19	19	16	3	36	36
Esch32	1433	1754	228	434	36	1	1	13	9	19	19	16	3	36	36
Esch33	1465	1772	230	439	37	1	1	11	9	13	7	16	2	29	29
Esch34	1506	1813	232	437	39	1	1	8	7	8	7	16	3	36	36
Esch35	1495	1801	232	437	39	1	1	8	7	8	7	16	3	36	36
Esch36	1488	1796	232	437	39	1	1	8	7	8	7	16	3	36	36
Esch37	1499	1803	232	437	39	1	1	8	7	8	7	16	3	36	36
Esch38	1495	1803	233	442	36	1	1	13	9	22	22	16	3	36	36
Esch39	1490	1801	233	442	36	1	1	13	9	22	22	16	3	36	36
Esch40	1497	1805	233	442	36	1	1	13	9	22	22	16	3	36	36
Esch41	1425	1755	224	429	37	1	1	11	9	11	7	16	2	29	29
Esch42	1487	1789	228	435	37	1	1	11	9	13	7	16	2	29	29
Esch43	1515	1837	235	446	37	1	1	11	9	13	7	16	2	33	33
Esch45	1527	1849	233	443	36	1	1	13	9	22	22	16	3	36	36
Esch46	1510	1832	234	445	36	1	1	13	9	22	22	16	3	36	36
Esch47	1496	1800	228	436	37	1	1	11	9	13	7	16	2	29	29
Homoo	1482	1945	310	583	65	2	2	28	29	278	278	34	1	20	20
Klebo	1417	1733	276	507	35	2	2	21	24	25	25	18	2	53	53
Kleb1	1415	1734	268	489	32	1	1	32	10	29	29	17	2	15	15
Kleb2	1435	1755	276	505	32	1	1	24	8	47	47	16	2	33	15
Leiso	1165	3582	515	2045	15	1	6	23	17	43	43	5	1	21	85
Metao	5131	13313	2423	8590	13	10	1	16	11	35	35	8	6	15	15
Meth4	1151	2339	331	1073	10	1	2	9	11	13	13	5	1	9	12
Muso	1201	1442	212	364	51	1	1	18	16	133	133	29	5	20	20
Plano	1791	3354	648	1761	16	1	1	5	5	8	8	8	12	20	20
Pseu1	1249	1438	234	394	28	1	1	112	26	48	48	13	1	7	7
Pseu2	1246	1452	239	405	29	1	1	77	12	27	28	13	1	8	8
Ralso	1271	1474	215	375	32	1	1	36	6	76	14	11	1	13	8
Rhizo	1292	1482	219	382	51	1	1	11	18	10	9	21	1	28	6
Sacco	1392	5209	733	3746	10	10	13	36	23	27	62	5	4	27	27
Salmo	1212	1496	241	422	47	1	1	11	27	9	9	22	1	35	37
Shigo	1407	1693	212	396	31	1	1	17	5	18	23	16	6	44	44
Shig2	1448	1741	219	408	30	1	2	29	9	32	32	15	1	49	49
Shig3	1451	1745	220	410	30	1	2	29	9	32	32	15	1	49	49
Shig4	1451	1746	216	405	31	1	2	18	6	20	24	16	6	45	45
Shig5	1450	1756	212	392	34	1	2	11	6	10	10	16	6	45	45
Yerso	1119	2296	371	1179	11	3	4	8	6	25	25	6	5	14	19
Yers1	1194	1398	209	365	48	1	1	19	11	8	8	17	3	28	28

REACTION METABOLIC NETWORKS.

	Original Graph		Biggest SCC		Diameter							Radius			
						#	#	visits						visits	
Network	n	m	n	m	D	Diam. Source Nodes	Diam. Target Nodes	DiFUB *HdOut*	DiFUB *HdIn*	DiFUB 2Sweep *HdOut*	DiFUB 2Sweep *HdIn*	R	# Rad. Nodes	rad 2Sweep *HdOut*	rad 2Sweep *HdIn*
Acyro	1040	53173	715	37171	13	5	13	7	33	11	11	6	80	170	170
Agroo	1035	69831	659	41591	10	1	4	18	201	15	15	5	4	68	68
Arabo	1328	2385	333	832	34	1	6	61	317	30	77	18	8	25	291
Bacio	714	33624	452	20097	11	3	1	6	38	11	11	5	1	14	14
Baci2	797	39245	529	26963	11	1	2	6	47	11	11	6	52	80	80
Chla1	2119	137620	1928	133598	13	5	3	11	6	11	11	6	2	20	20
Cupro	1035	73018	684	49080	9	11	5	25	29	232	232	5	73	83	83
Escho	2253	313224	1909	309348	8	14	7	34	254	96	104	5	280	337	337
Esch1	1325	74764	897	50618	11	1	5	44	4	8	8	5	2	15	9
Esch2	1295	2256	337	841	36	1	3	31	35	11	11	16	7	19	55
Esch3	1274	2203	337	847	37	1	3	19	28	7	7	16	6	16	46
Esch4	1303	2310	331	825	36	1	3	30	35	11	11	16	7	19	55
Esch5	1317	2306	335	836	36	1	3	30	35	11	11	16	7	19	55
Esch6	1275	2202	335	845	37	1	3	19	28	7	7	16	6	16	46
Esch7	1316	2330	335	838	36	1	3	31	35	11	11	16	7	19	55
Esch8	1305	2295	334	839	37	1	3	19	28	7	7	16	6	16	46
Esch9	1297	2333	344	882	30	1	3	97	37	17	17	15	30	37	37
Esch10	1313	2304	352	884	40	1	3	27	17	12	12	16	7	19	55
Esch11	1101	2025	329	765	31	3	2	44	92	36	36	14	2	54	54
Esch12	1292	2258	341	862	37	1	3	19	28	7	7	16	6	16	46
Esch13	1443	2768	485	1265	39	1	2	4	53	7	8	17	2	72	72
Esch14	1295	2266	337	841	36	1	3	30	35	11	11	16	7	19	55
Esch15	1322	2365	338	845	36	1	3	30	35	11	11	16	7	19	55
Esch16	1317	2312	359	902	34	2	3	53	45	15	15	16	7	19	55
Esch17	1288	2256	336	849	37	1	3	19	25	7	7	16	6	16	43
Esch18	1316	2428	373	889	42	1	1	8	39	8	8	17	2	36	36
Esch19	1321	75334	896	51048	11	1	6	49	4	8	8	5	2	15	15
Esch20	2382	233925	1747	227170	8	23	25	47	429	596	596	5	236	299	299
Esch21	2382	233925	1747	227170	8	23	25	47	429	596	596	5	236	299	299
Esch22	1310	2306	337	843	36	1	3	31	35	11	11	16	7	19	55
Esch23	1305	2337	360	904	34	2	3	52	45	15	15	16	7	19	55
Esch24	1350	80306	924	54488	11	1	5	47	4	8	8	5	2	15	9
Esch25	1265	2245	349	851	37	1	3	28	26	7	7	16	2	12	55
Esch26	1258	2230	349	847	37	1	3	28	26	7	7	16	2	12	55
Esch27	1320	2325	358	874	37	1	3	29	26	7	7	16	2	12	55
Esch28	1282	2456	426	1117	39	1	2	4	53	7	7	16	10	48	48
Esch29	1351	77894	934	54047	13	1	1	11	10	12	12	6	7	14	14
Esch30	1267	2214	345	861	38	2	3	27	28	11	11	16	6	16	46
Esch31	1268	2294	337	850	36	1	3	28	35	11	11	16	7	19	55
Esch32	1254	2254	334	839	36	1	3	28	35	11	11	16	7	19	55
Esch33	1266	2222	338	848	37	1	3	19	28	7	7	16	6	16	46
Esch34	1299	2261	337	831	39	1	3	31	17	7	7	16	7	19	54
Esch35	1294	2252	337	831	39	1	3	31	17	7	7	16	7	19	54
Esch36	1289	2250	337	831	39	1	3	31	17	7	7	16	7	19	54
Esch37	1298	2258	337	831	39	1	3	31	17	7	7	16	7	19	54
Esch38	1293	2267	339	847	36	1	3	30	35	11	11	16	7	19	54
Esch39	1291	2271	339	847	36	1	3	30	35	11	11	16	7	19	54
Esch40	1296	2272	339	847	36	1	3	30	35	11	11	16	7	19	54
Esch41	1254	2262	329	830	37	1	3	18	28	7	7	16	6	16	46
Esch42	1281	2224	334	840	37	1	3	19	28	7	7	16	6	16	46
Esch43	1326	2357	343	856	38	1	1	19	22	8	8	16	5	17	40
Esch45	1323	2321	342	859	36	1	3	30	35	11	11	16	7	19	55
Esch46	1317	2333	342	854	36	1	3	30	35	11	11	16	7	19	55
Esch47	1291	2232	336	847	37	1	3	19	28	7	7	16	6	16	46
Homoo	1358	3023	470	1159	66	2	2	33	32	412	412	35	1	26	26
Klebo	1240	2311	404	1035	36	2	2	29	57	32	32	19	3	76	57
Kleb1	1244	2382	392	1009	33	1	1	7	35	30	30	18	3	17	54
Kleb2	1247	2343	408	1024	32	1	1	54	45	39	71	16	1	44	13
Leiso	1112	25523	818	23722	16	1	3	36	22	73	73	6	192	231	344
Metao	5461	2646308	4510	2193013	14	3	1	15	29	48	48	8	3	14	14
Meth4	945	61460	621	40985	10	9	1	30	70	32	32	6	83	89	89
Muso	1074	1837	314	735	52	1	1	25	39	192	192	29	3	18	18
Plano	1723	75296	1071	61858	15	2	7	13	9	139	11	7	2	7	7
Pseu1	1026	1678	323	699	28	2	1	281	101	168	67	14	1	11	11
Pseu2	1036	1783	335	747	30	2	1	247	79	43	43	14	1	11	11
Ralso	1053	1860	300	672	32	1	2	48	49	101	101	12	1	14	33
Rhizo	1084	1843	310	685	52	1	1	12	20	11	11	22	1	30	7
Sacco	1577	97334	1243	93080	11	7	2	253	13	16	16	6	416	457	457
Salmo	1041	1790	341	750	47	1	2	14	38	9	9	22	1	41	44
Shigo	1214	2099	306	754	32	1	1	75	31	32	32	15	2	13	56
Shig2	1251	2101	318	782	31	1	2	78	38	34	34	15	2	14	70
Shig3	1254	2108	320	789	31	1	2	78	38	34	34	15	2	14	70
Shig4	1256	2102	315	780	32	1	2	78	36	36	36	15	2	13	58
Shig5	1258	2173	309	749	35	1	2	49	23	24	24	15	2	13	58
Yerso	952	52572	637	35195	12	2	1	13	9	15	15	6	11	16	16
Yers1	990	1733	297	678	49	1	1	20	20	7	7	17	5	36	36

Name	Acronym
Acyrthosiphon pisum + Buchnera BaobabCyc	Acyr0
Agrobacterium tumefaciens Strain C58 MicroCyc	Agro0
Arabidopsis thaliana Strain col AraCyc	Arab0
Bacillus amyloliquefaciens Strain FZB42 MicroCyc	Baci0
Bacillus subtilis Strain 168 MicroCyc	Baci2
Chlamydomonas reinhardtii iRC1080	Chla1
Cupriavidus taiwanensis Strain LMG19424 MicroCyc	Cupr0
Escherichia coli iJO1366	Esch0
Escherichia coli Strain 042 MicroCyc	Esch1
Escherichia coli Strain 101-1 MicroCyc	Esch2
Escherichia coli Strain 536 MicroCyc	Esch3
Escherichia coli Strain 53638 MicroCyc	Esch4
Escherichia coli Strain 55989 MicroCyc	Esch5
Escherichia coli Strain APEC O1 MicroCyc	Esch6
Escherichia coli Strain ATCC 8739 MicroCyc	Esch7
Escherichia coli Strain B str REL606 MicroCyc	Esch8
Escherichia coli Strain B171 MicroCyc	Esch9
Escherichia coli Strain B7A MicroCyc	Esch10
Escherichia coli Strain BL21-GoldDE3pLysS AG MicroCyc	Esch11
Escherichia coli Strain CFT073 MicroCyc	Esch12
Escherichia coli Strain DH1 MicroCyc	Esch13
Escherichia coli Strain E110019 MicroCyc	Esch14
Escherichia coli Strain E22 MicroCyc	Esch15
Escherichia coli Strain E24377A MicroCyc	Esch16
Escherichia coli Strain ED1a MicroCyc	Esch17
Escherichia coli Strain ETEC H10407 MicroCyc	Esch18
Escherichia coli Strain F11 MicroCyc	Esch19
Escherichia coli Strain flux1 Ec iAF1260	Esch20
Escherichia coli Strain flux2 Ec iAF1260	Esch21
Escherichia coli Strain HS MicroCyc	Esch22
Escherichia coli Strain IAI1 MicroCyc	Esch23
Escherichia coli Strain IAI39 MicroCyc	Esch24
Escherichia coli Strain K-12 BW2952 MicroCyc	Esch25
Escherichia coli Strain K-12 DH10B MicroCyc	Esch26
Escherichia coli Strain K-12 substr W3110 MicroCyc	Esch27
Escherichia coli Strain K12 BioCyc	Esch28
Escherichia coli Strain K12 MicroCyc	Esch29
Escherichia coli Strain LF82 MicroCyc	Esch30
Escherichia coli Strain O103H2 str 12009 MicroCyc	Esch31
Escherichia coli Strain O111H- str 11128 MicroCyc	Esch32
Escherichia coli Strain O127H6 E2348-69 MicroCyc	Esch33
Escherichia coli Strain O157H7 EC4042 MicroCyc	Esch34
Escherichia coli Strain O157H7 EC4045 MicroCyc	Esch35
Escherichia coli Strain O157H7 EC4115 MicroCyc	Esch36
Escherichia coli Strain O157H7 EC4206 MicroCyc	Esch37
Escherichia coli Strain O157H7 EDL933 MicroCyc	Esch38
Escherichia coli Strain O157H7 MicroCyc	Esch39
Escherichia coli Strain O157H7 TW14588 MicroCyc	Esch40
Escherichia coli Strain O26H11 str 11368 MicroCyc	Esch41
Escherichia coli Strain S88 MicroCyc	Esch42
Escherichia coli Strain SE11 MicroCyc	Esch43
Escherichia coli Strain SE15 MicroCyc	Esch44
Escherichia coli Strain SMS-3-5 MicroCyc	Esch45
Escherichia coli Strain UMN026 MicroCyc	Esch46
Escherichia coli Strain UTI89 MicroCyc	Esch47
Homo sapiens BioCyc	Homo0
Klebsiella pneumoniae Strain 342 MicroCyc	Kleb0
Klebsiella pneumoniae Strain NTUH-K2044 MicroCyc	Kleb1
Klebsiella pneumoniae Strain subsp pneumoniae MGH 78578 MicroCyc	Kleb2
Leishmania major iAC560	Leis0
MetaCyc	Meta0
Methylobacterium radiotolerans Strain JCM 2831 MicroCyc	Meth4
Mus musculus MouseCyc	Mus0
PlantCyc	Plan0
Pseudomonas aeruginosa Strain PAO1 MicroCyc	Pseu1
Pseudomonas aeruginosa Strain UCBPP-PA14 MicroCyc	Pseu2
Ralstonia eutropha Strain H16 MicroCyc	Rals0
Rhizobium etli Strain CFN 42 MicroCyc	Rhiz0
Saccharomyces cerevisiae iMM904	Sacc0
Salmonella enterica Strain serovar Typhi MicroCyc	Salm0
Shigella boydii Strain Sb227 MicroCyc	Shig0
Shigella flexneri Strain 2a 2457T MicroCyc	Shig2
Shigella flexneri Strain 2a 301 MicroCyc	Shig3
Shigella flexneri Strain 5 8401 MicroCyc	Shig4
Shigella sonnei Strain Ss046 MicroCyc	Shig5
Yersinia pestis Strain CO92 MicroCyc	Yers0
Yersinia pseudotuberculosis Strain YPIII MicroCyc	Yers1

Table 1: Biosources from [160, 24] and their acronyms

In Bipartite Metabolic Networks, DiFUB*HdOut*, DiFUB*HdIn*, DiFUB+2dSweep*HdOut*, and DiFUB+2dSweep*HdIn* use a number of visits less than 10%n for 71, 72, 70, 67 networks respectively. rad+2dSweep*HdOut* and rad+2dSweep*HdOut* use a number of visits less than 15%n for 68 networks.

In Compound Metabolic Networks, DiFUB*HdOut*, DiFUB*HdIn*, DiFUB+2dSweep*HdOut*, and DiFUB+2dSweep*HdIn* use a number of visits less than 10%n for 67, 72, 62, 61 networks respectively. rad+2dSweep*HdOut* and rad+2dSweep*HdOut* use a number of visits less than 16%n for 67 and 66 networks respectively.

In Reaction Metabolic Networks, DiFUB*HdOut*, DiFUB*HdIn*, DiFUB+2dSweep*HdOut*, and DiFUB+2dSweep*HdIn* use a number of visits less than 10%n for 61, 38, 62, 61 networks respectively. rad+2dSweep*HdOut* and rad+2dSweep*HdOut* use a number of visits less than 15%n for 67 and 38 networks respectively.

DIRECTED SOCIAL NETWORKS. This class of networks includes for instance a *who-trust-whom* online social network of the general consumer review site

`Epinions.com`, the social network of `LiveJournal`, that is a free on-line community allowing members to maintain journals, individual and group blogs, and allowing people to declare which other members are their friends, and the social network of `Slashdot`, that is a technology-related news website that allows users to tag each other as friends or foes. Moreover there is the *who-votes-on-whom network* Wikipedia network: indeed Wikipedia is a free encyclopedia written collaboratively by volunteers and in order for a user to become an administrator a request for adminship is issued and the Wikipedia community via a public discussion or a vote decides who to promote to adminship [161].

Network	Original		Biggest SCC		Source
	n	m	n	m	
ljournal-2008	5363260	79023142	4185423	74928066	[162]
soc-Epinions1	75888	508837	32223	443506	[161]
soc-LiveJournal1	4847571	68993773	3828682	65825429	[161]
soc-sign-epinions	131828	841372	41441	693737	[161]
soc-sign-Slashdot081106	77357	516575	26996	337351	[161]
soc-sign-Slashdot090216	81871	545671	27222	342747	[161]
soc-sign-Slashdot090221	82144	549202	27382	346652	[161]
soc-Slashdot0811	77360	905468	70355	888662	[161]
soc-Slashdot0902	82168	948464	71307	912381	[161]
wiki-Vote	8298	103689	1300	39456	[161]

Observe that in this class all the DiFUB algorithms uses always less visits than 0.1% of the number of vertices of the largest strongly connected component, n, except for `soc-Slashdot0811` and `WikiVote` in which DiFUB uses respectively less than 1%n and 2%n. The computation of radial vertices has used always a number of visits less than 1%n except for `soc-Slashdot0902`, `soc-Slashdot0811`, and `wiki-Vote`, in which the number of visits is less than 25%n.

Network	Diameter							Radius			
				visits						visits	
	D	# Diametral Source Vertices	# Diametral Target vertices	DiFUB *HdOut*	DiFUB *HdIn*	DiFUB 2dSWEEP *HdOut*	DiFUB 2dSWEEP *HdIn*	R	# Radial Vertices	rad 2dSWEEP *HdOut*	rad 2SWEEP *HdIn*
ljournal-2008	49	4	2	51	49	73	73	-	-	-	-
soc-Epinions1	16	1	1	8	11	14	14	8	99	173	173
soc-LiveJournal1	21	16	4	159	286	145	423	11	1	3638	3638
soc-sign-epinions	16	1	1	34	8	10	10	7	1	28	28
soc-sign-Slashdot081106	15	1	1	9	11	22	22	7	62	237	237
soc-sign-Slashdot090216	15	1	1	9	11	21	21	7	35	103	103
soc-sign-Slashdot090221	15	1	1	9	11	22	22	7	35	103	103
soc-Slashdot0811	12	8	26	110	110	442	442	7	7790	17331	17331
soc-Slashdot0902	13	1	1	10	10	19	19	7	7685	12732	12732
wiki-Vote	9	1	148	9	9	17	17	3	10	293	242

For the graph `ljournal-2008` we were not able to complete our experiments in the case of rad+2dSWEEP*HdOut* and rad+2dSWEEP*HdIn*(see Section 4.7.3).

WEB NETWORKS. Vertices represent pages and an arc represent hyperlinks between them. The pages considered are restricted to the one belonging to `berkely.edu`, and `stanford.edu` domains, the `nd.edu` domain, that is University of Notre Dame (released by Albert Barabási), the pages considered in 2002 by Google as a part of a Google Programming Contest, the .it domain, the Italian CNR domain, the `.in` and `.indochina` domains (crawled by the Nagaoka University of Technology), the `.eu` domain (collected for the DELIS project, a collection of web graphs by taking snapshots at a monthly rate focussing on the `.uk` domain). Moreover there are the snapshots performed by UbiCrawler of the

`.uk` domain in 2002 and 2005, of the the `.sk` domain in 2005, and one aimed at countries whose web sites could contain pages written in Arabic in 2005. Finally we have considered the snapshot obtained by the WebBase crawler in 2001.

	Original		Biggest SCC		
Network	n	m	n	m	Source
arabic-2005	22744080	639999458	15177163	473619298	[162]
as-caida20071105	65536	106762	26475	106762	[161]
cnr-2000	325557	3216152	112023	1646332	[162]
eu-2005	862664	19235140	752725	17933415	[162]
in-2004	1382908	16917053	593687	7827263	[162]
indochina-2004	7414866	194109311	3806327	98815195	[162]
it-2004	41291594	1150725436	29855421	938694394	[162]
uk-2002	18520486	298113762	12090163	232137936	[162]
uk-2005	39459925	936364282	25711307	704151756	[162]
uk-2007-05@100000	100000	3050615	53856	1683102	[162]
uk-2007-05@1000000	1000000	41247159	480913	22057738	[162]
web-BerkStan	685231	7600595	334857	4523232	[161]
web-Google	916428	5105039	434818	3419124	[161]
web-NotreDame	325729	1497134	53968	304685	[161]
web-Stanford	281904	2312497	150532	1576314	[161]
webbase-2001	118142155	1019903190	53891939	630006857	[162]

In this class of networks DIFUB has used a number of visits always less than 0.1%n, except when DIFUB*HdOut* and DIFUB*HdIn* are applied to: `in-2004`, in which the number of visits is less than 4%n, `uk-2007-05@100000`, in which the number of visits is about 75%n, and `uk-2007-05@1000000`, in which the number of visits is less than 0.5%n. In order to compute all the radial vertices, our algorithm takes always less than 1%n number of visits, except for the graph `web-Stanford`, in which it has used about than 10%n visits. For the biggest graphs, i.e. the ones with more than 3.5 million of vertices, we were not able to complete our experiments concerning the radius: indeed the time needed on our platform for each BFS is greater than 13 seconds (as for `indochina-2004`), so that, even by performing just 3%n visits, more than two weeks are needed in order to complete one single experiment (see Section 4.7.3).

	Diameter							Radius			
				visits						visits	
Network	D	# Diametral Source Vertices	# Diametral Target Vertices	DIFUB *HdOut*	DIFUB *HdIn*	DIFUB 2dSWEEP *HdOut*	DIFUB 2dSWEEP *HdIn*	R	# Radial Vertices	rad 2dSWEEP *HdOut*	rad 2SWEEP *HdIn*
arabic-2005	133	1	1	81	54	58	58	-	-	-	-
as-caida20071105	17	45	45	10	10	8	8	9	2	7	7
cnr-2000	81	1	1	122	101	17	17	25	3	551	551
eu-2005	82	1	2	18	8	9	9	31	161	6641	6641
in-2004	56	1	2	18325	1539	93	93	28	8	4713	39
indochina-2004	235	2	1	93	87	8	8	-	-	-	-
it-2004	873	7	2	780	772	87	87	-	-	-	-
uk-2002	218	1	11	163	151	18	18	-	-	-	-
uk-2005	166	1	6	200	174	184	184	-	-	-	-
uk-2007-05@100000	7	8	6991	39220	39654	14	14	3	1	401	401
uk-2007-05@1000000	40	5	30	1997	1779	41	41	7	1	4573	4573
web-BerkStan	679	1	1	244	235	7	7	249	2	255	255
web-Google	51	1	3	51	12	9	9	24	3	248	248
web-NotreDame	93	1	1	6	5	7	7	44	45	50	50
web-Stanford	210	2	1	43	5	9	9	97	16	13946	13946
webbase-2001	1342	2	1	85	76	16	16	-	-	-	-

CITATION NETWORKS. Arxiv Hep-Ph (high energy physics phenomenology) and Hep-Th (high energy physics theory) citation graphs are from the e-print arXiv and covers all the citations from January 1993 to April 2003 in their respective categories. If a paper i cites paper j, the graph contains an arc from i to j.

Network	Original		Biggest SCC		Source
	n	m	n	m	
cit-HepPh	9912554	421578	12711	139981	[161]
cit-HepTh	9912294	352807	7464	116268	[161]

In both the graphs, both DiFUB+2dSweep*HdOut* and DiFUB+2dSweep*HdIn* have always used a number of visits less than 1%n. DiFUB*HdOut* and DiFUB*HdIn* have used a number of visits respectively about 15%n and 75%n for cit-HepPh, and both less than 5%n for `cit-HepTh`. The computation of radial vertices instead has required always less than 1.5%n number of visits.

Network	Diameter							Radius			
	D	# Diametral Source Vertices	# Diametral Target Vertices	visits				R	# Radial Vertices	visits	
				DiFUB *HdOut*	DiFUB *HdIn*	DiFUB 2dSweep *HdOut*	DiFUB 2dSweep *HdIn*			rad 2dSweep *HdOut*	rad 2Sweep *HdIn*
cit-HepPh	49	3	1	1719	9604	9	9	15	2	7	75
cit-HepTh	35	1	1	13	361	7	7	13	1	101	101

COMMUNICATION NETWORKS. In this class of networks, given a set of email messages, each vertex corresponds to an email address, and there is an arc between vertices i and j, if i sent at least one message to j. This class of networks include a network generated using email data from a large European research institution, Enron email communication network covering all the email communication within a dataset of around half million emails (this data was originally made public, and posted to the web, by the Federal Energy Regulatory Commission during its investigation). Moreover in the `wiki-Talk` network, the vertices represent Wikipedia users and an arc from vertex i to vertex j represents that user i at least once edited a talk page of user j.

Network	Original		Biggest SCC		Source
	n	m	n	m	
email-EuAll	265214	420045	34203	151930	[161]
enron	69244	276143	8271	147353	[162]
wiki-Talk	2394385	5021410	111881	1477893	[161]

In all these graphs DiFUB has used less than or about 1%n visits to list all the diametral vertices. The computation of all the radial vertices has required always a number of visits between 10%n and 15%n, except for `wiki-Talk`.

Network	Diameter							Radius			
	D	# Diametral Source Vertices	# Diametral Target Vertices	visits				R	# Radial Vertices	visits	
				DiFUB *HdOut*	DiFUB *HdIn*	DiFUB 2dSweep *HdOut*	DiFUB 2dSweep *HdIn*			rad 2dSweep *HdOut*	rad 2Sweep *HdIn*
email-EuAll	10	7	3	183	183	143	143	5	490	3752	3752
enron	10	7	18	93	58	60	97	6	203	1245	1057
wiki-Talk	10	1	19	834	159	189	311	5	6701	27051	50867

P2P NETWORKS. A sequence of snapshots of the `Gnutella` peer-to-peer file sharing network from August 2002. Vertices represent hosts in the `Gnutella` network topology and edges represent connections between the `Gnutella` hosts.

Network	Original		Biggest SCC		Source
	n	m	n	m	
p2p-Gnutella04	10879	39994	4317	18742	[161]
p2p-Gnutella05	8846	31839	3234	13453	[161]
p2p-Gnutella06	8717	31525	3226	13589	[161]
p2p-Gnutella08	6301	20777	2068	9313	[161]
p2p-Gnutella09	8114	26013	2624	10776	[161]
p2p-Gnutella24	26518	65369	6352	22928	[161]
p2p-Gnutella25	22687	54705	5153	17695	[161]
p2p-Gnutella30	36682	88328	8490	31706	[161]
p2p-Gnutella31	62586	147892	14149	50916	[161]

In these networks DiFUB uses less than 5%n visits, except for `p2p-Gnutella09` (in which a number of visits between 5%n and 12%n are used) `p2p-Gnutella30` (in which a number of visits between 3%n and 15%n are used), `p2p-Gnutella08` (in which DiFUB*HdOut* uses about 24%n visits), and `p2p-Gnutella25`, (in which DiFUB*HdIn* uses about 19%n visits). The number of visits required for the computation of the radial vertices ranges between 0.4%n and about 5%n, except when rad+2dSweep*HdIn* is applied to `p2p-Gnutella08` and `p2p-Gnutella30`, requiring about 12%n visits.

Network	Diameter							Radius			
				visits						visits	
	D	# Diametral Source Vertices	# Diametral Target Vertices	DiFUB *HdOut*	DiFUB *HdIn*	DiFUB 2dSweep *HdOut*	DiFUB 2dSweep *HdIn*	R	# Radial Vertices	rad 2dSweep *HdOut*	rad 2Sweep *HdIn*
p2p-Gnutella04	25	1	2	44	117	38	38	15	3	43	43
p2p-Gnutella05	22	3	1	79	104	69	69	14	18	131	45
p2p-Gnutella06	19	3	2	113	117	172	172	12	4	172	172
p2p-Gnutella08	19	1	2	499	51	39	58	12	16	23	242
p2p-Gnutella09	19	3	2	137	187	307	307	13	3	33	33
p2p-Gnutella24	28	1	1	18	51	27	27	15	1	25	25
p2p-Gnutella25	21	1	2	88	1003	64	64	13	10	258	160
p2p-Gnutella30	23	1	1	1281	306	516	288	15	3	438	945
p2p-Gnutella31	30	2	2	215	324	397	194	19	3	311	311

PRODUCT CO-PURCHASING NETWORKS. These networks were collected by crawling Amazon website and are based on *Customers Who Bought This Item Also Bought* feature of the Amazon website, so that if a product i is frequently co-purchased with product j, the graph contains an arc from i to j.

Network	Original		Biggest SCC		Source
	n	m	n	m	
amazon-2008	735323	5158388	627646	4706251	[162]
amazon0302	262111	1234877	241761	1131217	[161]
amazon0312	400727	3200440	380167	3069889	[161]
amazon0505	410236	3356824	390304	3255816	[161]
amazon0601	403394	3387388	395234	3301092	[161]

For these networks DiFUB has used almost always less than 0.05%n visits, except for `amazon0312` and `amazon0302` in which the number of visits used ranges between 0.06%n and 1.32%n. The computation of the radial vertices requires instead a number of visits in between 0.01%n and 0.72%n.

Network	Diameter							Radius			
				visits						visits	
	D	# Diametral Source Vertices	# Diametral Target Vertices	DiFUB *HdOut*	DiFUB *HdIn*	DiFUB 2dSweep *HdOut*	DiFUB 2dSweep *HdIn*	R	# Radial Vertices	rad 2dSweep *HdOut*	rad 2Sweep *HdIn*
amazon-2008	47	3	5	623	243	85	85	23	2	474	56
amazon0302	88	10	1	293	157	705	705	48	1	289	289
amazon0312	52	5	2	4093	5002	381	381	26	1	247	247
amazon0505	55	12	1	173	194	41	24	27	8	2825	2825
amazon0601	52	1	4	1118	115	82	82	25	8	1026	1026

WORD ASSOCIATION NETWORKS. The Free Word Association Norms Network is a directed graph describing the results of an experiment of free word association performed by more than 6000 participants in the United States: its vertices correspond to words and arcs represent a cue-target pair and an arc from x to y means that the word y was output by some of the participants based on the stimulus x [162].

	Original		Biggest SCC		
Network	n	m	n	m	Source
wordassociation-2011	10617	72172	4845	61567	[162]

The word association network seems to be a real world negative example for our algorithms: DiFUB uses between $20\%n$ and $70\%n$ visits in all the strategies while the computation of the radial vertices requires about $45\%n$ visits.

	Diameter							Radius			
				visits						visits	
		# Diametral	# Diametral			DiFUB	DiFUB			rad	rad
Network		Source	Target	DiFUB	DiFUB	2dSweep	2dSweep		# Radial	2dSweep	2Sweep
	D	Vertices	Vertices	*HdOut*	*HdIn*	*HdOut*	*HdIn*	R	Vertices	*HdOut*	*HdIn*
wordassociation-2011	10	1	6	1055	1481	3371	3371	7	107	2050	2269

4.7.2 *Undirected Graphs*

The effectiveness of Algorithm 19 has been experimentally proved in [5, 6, 156] by using several ways of choosing the starting vertex.

- *Random selection.* By picking it uniformly at random.
- *Degree selection.* By choosing a vertex with the highest degree.
- *4-Sweep selection.* By using the 4Sweep method, that is an evolution of 2Sweep method using four BFSes. Let r_1 be a vertex in V, let a_1 be one of the farthest vertices from r_1, and let b_1 be one of the farthest vertices from a_1. If r_2 is the vertex halfway between a_1 and b_1, then we define analogously a_2 and b_2. The vertex u is then defined as the middle vertex of the path between a_2 and b_2. In particular, two different ways of selecting vertex r_1 have been considered: one method chooses r_1 uniformly at random, while the other method chooses r_1 as a vertex with the highest degree.

By using these latter two selection strategies, it has been shown that in almost any graph with more than 10000 vertices of the considered dataset, the number of visits is always much less than 0.1% of the number of all vertices in the largest connected component, except for the road networks (in which the number of executions of the shortest path algorithm performed is less than 10%) and Erdős-Rényi graphs. Instead it has been shown that it is not convenient to run iFUB by starting from random vertices, since sometimes the number of performed visits is high with respect to the number of vertices.

In the following we will report the experimental evaluation of the performances of iFUB*Hd* and iFUB+2Sweep*Hd* when used not just to compute the diameter but also to enumerate the diametral vertices.

Thus we have experimented Algorithm 16, simplified as shown by Algorithm 19 for undirected graphs, by using the following ways of choosing the starting vertex.

- iFUB*Hd*. iFUB by starting from the vertex with highest degree.

- iFUB+2Sweep*Hd*. Apply 2Sweep*Hd*, Algorithm 18 by starting from the vertex with highest degree, and obtain the vertex u; apply iFUB by starting from u.

Moreover we have experimented Algorithm 21 by using:

- rad+2dSweep*Hd*. Apply 2Sweep*Hd*, Algorithm 18, by starting from the vertex with highest degree, and obtain the vertex u; apply Algorithm 21 by starting from u.

Once again, we have reported the number of visit performed by each approach.

Observe that several networks that we will report are not really naturally undirected since the relationship that they represent is implicitly not symmetrical. However since they are released by the owner companies or the owner universities in undirected format, we have catalogued them in this section.

PROTEIN-PROTEIN INTERACTION NETWORKS.

	Original		Biggest CC		
Network	n	m	n	m	Source
dip20090126_MAX	19928	82404	19928	82404	[163]
HC-BIOGRID	4039	20642	4039	20642	[163]
hprd_pp	9617	74078	9219	73800	[164]
interdom	1760	157966	1654	157832	[165]
iPfam	1541	24004	513	18740	[166]
Mus_musculus	4696	11494	3745	10340	[167]
ppi_dip_swiss	3839	23916	3766	23844	[168]
ppi_gcc	37333	271236	37333	271236	[168]
psimap	1178	23230	526	19048	[169]
Rattus_norvegicus	1970	4220	1415	3570	[167]
string	2658	53610	2575	53514	[168]

In these networks iFUB has almost always used a number of visits in between 0.1%n and 1%n. In the graph `iPfam` it has used about 6%n visits. For the computation of the radial vertices the number of visits has been always less than 3%n except for `psimap` (6%n), `string` (35%n), `interdom` (43%n).

	Diameter				Radius		
			visits				visits
Network	D	# Diametral Vertices	iFUB *Hd*	iFUB 2Sweep *Hd*	R	# Radial Vertices	rad 2Sweep *Hd*
dip20090126_MAX	30	2	56	19	15	1	7
HC-BIOGRID	23	3	5	12	12	17	81
hprd_pp	14	4	7	10	8	133	266
interdom	8	4	12	16	4	33	713
iPfam	12	22	34	27	6	1	4
Mus_musculus	20	2	17	21	10	2	31
ppi_dip_swiss	12	4	6	32	6	2	15
ppi_gcc	27	4	24	7	14	8	11
psimap	11	7	13	8	6	27	32
Rattus_norvegicus	19	5	17	8	10	7	14
string	9	7	20	43	5	54	898

COLLABORATION NETWORKS. This class includes the graph of movie actors using data from IMDB (Internet Movies DataBase), whose vertices are actors, and two actors are linked by an edge whenever they collaborated in a movie. Moreover there are the graphs of co-authorship (if an author i co-authored a paper with author j, the graph contains an edge from i to j), based on DBLP, MathSciNet [170], Arxiv Astro Physics, Arxiv Condensed Matter, Arxiv General

Relativity, Arxiv High Energy Physics, Arxiv High Energy Physics Theory e-print categories arXiv, and the original Condensed Matter section of arXiv E-Print Archive between 1995 and 1999 used by Newman in [88]. More peculiar are the networks Eva, in which there is an edge (x, y) from company x to company y whether the company x is an owner of company y or vice versa [171], Advogato, a research testbed for testing attack-resistant trust metrics [172], the network of the collaborations among Jazz musicians [173], and the network of users of the *Pretty-Good-Privacy* algorithm for secure information interchange [174]. Observe that if the collaboration involves k collaborators, this generates a completely connected subgraph on k vertices.

	Original		Biggest CC		
Network	n	m	n	m	Source
advogato	7418	90929	5272	88719	[172]
alr20–wCoAuNw–MathSciNet	391529	1747550	332689	1641288	[175]
ca-AstroPh	18771	396100	17903	393944	[161]
ca-CondMat	23133	186878	21363	182572	[161]
ca-GrQc	5241	28968	4158	26844	[161]
ca-HepPh	12006	236978	11204	235238	[161]
ca-HepTh	9875	51946	8638	49612	[161]
dblp20080824_MAX	511163	3742140	511163	3742140	[163]
eva	7253	13422	4475	9304	[176]
geom	6158	23796	3621	18922	[176]
jazz	198	5484	198	5484	[177]
imdb	908830	75177226	880455	74989272	[168]
Newman-Cond_mat_95-99-two_mode	22016	117156	22015	117156	[178]
PGPgiantcompo	10680	48632	10680	48632	[177]

In these networks iFUB has used less than or about $1\%n$ visits except for the smallest networks, jazz, eva, geom, Newman-Cond_mat, and PGPgiantcompo. The number of visits required for the computation of the radial vertices is always less tha $5\%n$, except for jazz, advogato, and Newman-Cond_mat.

	Diameter				Radius		
			visits				visits
				iFUB			rad
Network		# Diametral	iFUB	2Sweep		# Radial	2Sweep
	D	Vertices	*Hd*	*Hd*	R	Vertices	*Hd*
advogato	9	2	2	6	5	488	491
alr20–wCoAuNw–MathSciNet	24	9	23	56	13	317	972
ca-AstroPh	14	12	32	57	8	139	445
ca-CondMat	15	11	6	14	8	6	24
ca-GrQc	17	8	11	56	9	13	71
ca-HepPh	13	17	10	51	7	12	101
ca-HepTh	18	4	30	29	10	74	340
dblp20080824_MAX	22	9	42	43	12	72	1554
eva	18	22	807	257	10	15	72
geom	14	20	50	48	7	1	7
jazz	6	9	9	27	4	56	70
imdb	14	24	104	272	8	19751	40929
Newman-Cond_mat_95-99-two_mode	12	4	2405	5126	8	1306	10078
PGPgiantcompo	24	3	8	23	12	2	8

UNDIRECTED SOCIAL NETWORKS. These networks include *MySpace* and *Flickr* friendship, the membership of *Yahoo!* users to *Yahoo!* groups, and one network used to test trust metrics.

	Original		Biggest CC		
Network	n	m	n	m	Source
flickr	62572	491276	52295	479008	[168]
myspace	13746	131958	13723	131930	[168]
trust	49288	762253	49288	762253	[172]
ydata-ygroups-user-group-membership-graph-v1_0	1637868	30410032	1637868	30410032	[179]

The number of visits required to compute all the diametral and radial vertices is less than 0.06%n, except for `myspace` in which the diametral and radial vertices are computed with less than 2.2%n visits.

	Diameter				Radius		
			visits				visits
Network	D	# Diametral Vertices	iFUB *Hd*	iFUB 2SWEEP *Hd*	R	# Radial Vertices	rad 2SWEEP *Hd*
flickr	20	2	7	10	10	1	7
myspace	11	11	22	282	6	2	298
trust	14	2	4	7	7	1	4
ydata-ygroups-user-group-membership-graph-v1_0	22	9	33	100	12	342	1008

UNDIRECTED COMMUNICATION NETWORKS. These networks are mainly provided by [179] and [180] . There is an edge between two vertices whether there has been a communication between them.

	Original		Biggest CC		
Network	n	m	n	m	Source
allB	1014336	6674992	983526	6634502	[180]
d00.txt	50576	159256	27517	85992	[179]
d01.txt	52015	164380	29388	91843	[179]
d02.txt	52120	164281	27373	82736	[179]
d03.txt	51913	162590	29231	89401	[179]
d04.txt	50547	157249	29278	90459	[179]
d05.txt	34042	90984	22975	69791	[179]
d06.txt	36379	101726	25930	80616	[179]
d07.txt	60088	197153	40156	129336	[179]
d08.txt	100000	362595	84914	293123	[179]
d09.txt	60928	198589	37548	116889	[179]
d10.txt	56526	179382	34538	107276	[179]
d11.txt	52249	161357	28001	84907	[179]
d12.txt	34583	90569	23425	69552	[179]
d13.txt	35375	97124	24837	76824	[179]
d14.txt	52201	161734	27820	83308	[179]
d15.txt	51811	161589	30091	93435	[179]
d16.txt	50419	155664	25727	76774	[179]
d17.txt	49610	151714	25111	73562	[179]
d18.txt	46765	136773	22466	64497	[179]
d19.txt	30380	75887	19299	55890	[179]
d20.txt	31499	78802	19769	56699	[179]
d21.txt	48992	148154	27375	82304	[179]
d22.txt	49437	150464	26604	78063	[179]
d23.txt	48087	146933	23283	68218	[179]
d24.txt	47394	143962	25411	77817	[179]
d25.txt	44485	130120	23097	68649	[179]
d26.txt	28938	70833	17926	51006	[179]
d27.txt	29760	75428	19133	56466	[179]
halfyearA	936445	5293466	906148	5256018	[180]
halfyearB	840485	4884628	805787	4838434	[180]
onemonthA	430149	1401384	379500	1338248	[180]
onemonthB	450264	1588592	401050	1524102	[180]
oneyearA	1160625	8837202	1138557	8809978	[180]
oneyearB	967896	6470798	936831	6429882	[180]

In these networks iFUB+2SWEEP*Hd* uses always less than 1%n visits, while iFUB*Hd* uses almost always less than 5%n visits, except for `d21.txt` and `d02.txt`. The computation of the radial vertices has required always less than 1%n visits except for `halfyearA` and `oneyearA` (at most 7%n visits).

Network	Diameter				Radius		
	D	# Diametral Vertices	visits		R	# Radial Vertices	visits
			iFUB *Hd*	iFUB 2Sweep *Hd*			rad 2Sweep *Hd*
allB	22	3	54	47	12	1432	1573
d00.txt	69	4	1362	6	35	2	5
d01.txt	60	23	91	36	31	9	33
d02.txt	43	10	110	72	22	3	8
d03.txt	65	19	757	191	35	1	33
d04.txt	54	3	1127	8	27	1	4
d05.txt	39	10	94	20	20	9	31
d06.txt	52	3	60	10	27	15	18
d07.txt	57	4	1737	85	32	3	414
d08.txt	48	17	1517	593	26	2	370
d09.txt	42	3	36	49	22	57	440
d10.txt	61	4	2235	6	31	3	6
d11.txt	43	5	132	15	22	1	6
d12.txt	44	4	12	9	22	1	4
d13.txt	38	11	181	20	20	8	73
d14.txt	47	7	92	16	24	8	18
d15.txt	60	8	591	102	31	100	151
d16.txt	46	4	46	12	24	3	41
d17.txt	44	13	63	50	23	19	67
d18.txt	39	8	23	84	21	27	137
d19.txt	46	3	69	12	23	3	6
d20.txt	46	2	42	7	23	2	5
d21.txt	74	2	2333	7	37	1	4
d22.txt	50	6	1352	11	25	5	8
d23.txt	64	4	98	9	32	1	4
d24.txt	57	2	561	6	29	5	9
d25.txt	75	2	591	6	38	3	6
d26.txt	38	9	248	115	20	1	18
d27.txt	42	6	67	21	22	2	32
halfyearA	19	24	51	67	11	4470	65991
halfyearB	23	3	9	53	12	3	46
onemonthA	24	2	30	322	13	317	2365
onemonthB	28	9	30	83	14	1	17
oneyearA	18	15	66	141	10	600	23709
oneyearB	22	3	47	79	12	1153	1266

AUTONOMOUS SYSTEMS NETWORKS. `itdk0304_rlinks_undirected` and `as-skitter` are Internet topology graphs from traceroutes run respectively in 2004 and in 2005.

Network	Original		Biggest CC		Source
	n	m	n	m	
as-skitter	1696415	22190596	1694616	22188418	[161]
itdk0304_rlinks_undirected	192244	1218132	190914	1215220	[163]

The number of visits required by iFUB is always less than 0.02%n, while the radial vertices can be computed with at most 0.36%n visits.

Network	Diameter				Radius		
	D	# Diametral Vertices	visits		R	# Radial Vertices	visits
			iFUB *Hd*	iFUB 2Sweep *Hd*			rad 2Sweep *Hd*
as-skitter	31	2	12	7	16	5	26
itdk0304_rlinks_undirected	26	7	32	16	14	155	689

ROAD NETWORKS. These graphs are the road networks of California, Pennsylvania, and Texas. Intersections and endpoints are represented by vertices and the roads connecting these intersections or road endpoints are represented by edges [161].

Network	Original		Biggest CC		Source
	n	m	n	m	
roadNet-CA	1965206	5533214	1957027	5520776	[161]
roadNet-PA	1088092	3083796	1087562	3083028	[161]
roadNet-TX	1379917	3843320	1351137	3758402	[161]

The completed experiments are about rad+2dSWEEP*Hd*: for `roadNet-PA` and `roadNet-TX` the number of visits has been less than 0.2%n, while for `roadNet-CA` the number of visits has been less than 15%n. The values of the diameters have been computed by applying Algorithm 15 (see [6]).

Network	Diameter				Radius		
			visits				visits
	D	# Diametral Vertices	iFUB *Hd*	iFUB 2SWEEP *Hd*	R	# Radial Vertices	rad 2SWEEP *Hd*
roadNet-CA	865	-	-	-	494	2	219765
roadNet-PA	794	-	-	-	402	2	2070
roadNet-TX	1064	-	-	-	540	3	988

WORD ADJACENCY NETWORKS. In these networks, the vertices are words and there is an edge between x and y whether x appears close to y in at least one phrase of the considered book or web pages.

Network	Original		Biggest CC		Source
	n	m	n	m	
darwinBookInter_st	7381	88414	7377	88410	[181]
eatRS	23219	609874	23219	609874	[176]
eatSR	23218	609868	23218	609868	[176]
frenchBookInter_st	8325	47682	8308	47664	[181]
japaneseBookInter_st	2704	15996	2698	15990	[181]
spanishBookInter_st	11586	86130	11558	86100	[181]
ydata-ysm-advertiser-phrase-graph-v1_0	653260	4556896	653260	4556896	[179]

The computation of the diametral and radial vertices requires almost always at most 1.5%n, except for the networks `eatRS` and `eatSR`, and when rad+2dSWEEP*Hd* is applied to `japaneseBookInter_st`.

Network	Diameter				Radius		
			visits				visits
	D	# Diametral Vertices	iFUB *Hd*	iFUB 2SWEEP *Hd*	R	# Radial Vertices	rad 2SWEEP *Hd*
darwinBookInter_st	8	16	26	248	4	1	15
eatRS	6	280	9670	18244	4	7446	20610
eatSR	6	280	9669	15171	4	7446	17285
frenchBookInter_st	9	25	6	24	5	19	57
japaneseBookInter_st	8	9	24	38	5	569	786
spanishBookInter_st	10	8	4	13	5	1	4
ydata-ysm-advertiser-phrase-graph-v1_0	24	3	14	43	12	4	31

4.7.3 *Overall results*

In the following we resume the results of our experiments, grouping them by number of visits v, and showing for any method the number of networks in which it has performed v visits.

In the case of directed graphs, DiFUB+2dSWEEP*HdOut* and DiFUB+2dSWEEP*HdIn* seems to be the more promising strategies in order to compute the diametral vertices. No substantial differences have been observed between the methods rad+2dSWEEP*HdOut* and rad+2dSWEEP*HdIn*.

	# Networks in which the method performs v visits					
	Methods					
	Diameter				Radius	
v	DiFUB *HdOut*	DiFUB *HdIn*	DiFUB 2dSweep *HdOut*	DiFUB 2dSweep *HdIn*	rad 2dSweep *HdOut*	rad 2dSweep *HdIn*
$v \leqslant 0.01\%n$	10	13	14	14	1	3
$0.01\%n < v \leqslant 0.1\%n$	13	13	16	16	9	7
$0.1\%n < v \leqslant 1\%n$	10	8	8	7	14	14
$1\%n < v \leqslant 10\%n$	9	9	7	8	9	7
$10\%n < v$	5	4	2	2	6	8

In Figure 13 we report the number of visits performed by DiFUB*HdOut*, DiFUB*HdIn*, DiFUB+2dSweep*HdOut*, DiFUB+2dSweep*HdIn* to compute the diameter and the diametral vertices, as a function of the number of vertices. Analogously in Figure 14 we report the number of visits performed by rad+2dSweep*HdOut*, rad+2dSweep*HdIn* to compute the radius and the radial vertices, as a function of the number of vertices. In particular for each one of the directed graphs presented, having x vertices, in which a method performs y visits, we draw in position (x, y) the symbol corresponding to the method.

Observe that in the case of Figure 13, when the number of vertices increases, no increase can be detected in the number of visits. We argue that our methods perform a constant number of visits in practice. It is worth observing that the maximum number of visits correspond to the application of DiFUB*HdOut* and DiFUB*HdIn* to `uk-2007-05@100000`: we argue that the in-degree and the out-degree are not good centrality measures for this graph: indeed for the same graph, DiFUB is effective by starting from other vertices.

In the case of Figure 14, when the number of vertices increases, the number of visits slightly increases, so that whenever a graph have more than 3.5 millions of vertices, it seems that 100 thousands of visits (i.e. 2.8%n) are required and if each visit takes more than 13 seconds, at least 15 days are required to conclude one experiment. This is the case of the following 7 Networks: `uk-2002`, `indochina-2004`, `it-2004`, `arabic-2005`, `uk-2005`, `webbase-2001`, and `ljournal-2008`, for which we were not able to conclude our experiments concerning radius and radial vertices. Observe that according to our statistics, whenever the exhaustive method would be applied, for these graphs at least 526 days would be required to conclude one experiment. In these cases, the methods using external memory seem to be a promising alternative [182, 183].

In the case of undirected graphs, iFUB+2Sweep*Hd* seems to be more stable than iFUB*Hd* in order to compute the diametral vertices. Indeed even if there are some networks in which iFUB*Hd* performs less than $0.01\%n$ visits and iFUB+2Sweep*Hd* performs slightly more than $0.01\%n$ visits, there are networks in which iFUB*Hd* performs more than $1\%n$ visits and iFUB+2Sweep*Hd* performs much less visits.

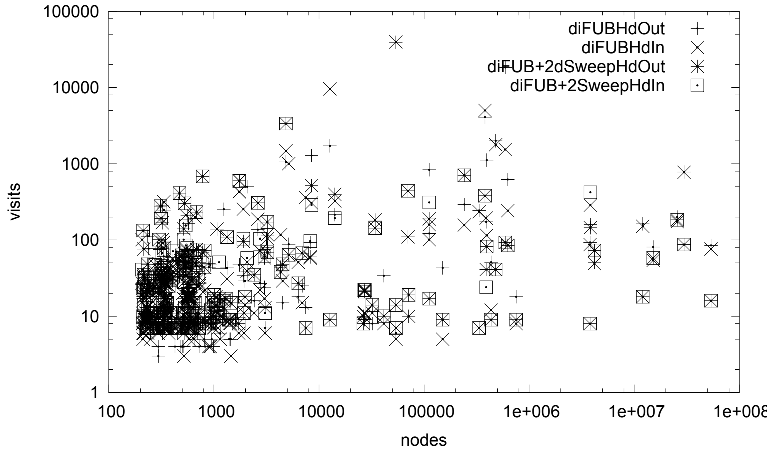

Figure 13: Visits performed by difub*HdOut*, difub*HdIn*, difub+2dSweep*HdOut*, difub+2dSweep*HdIn* to compute the diameter and the diametral vertices, as a function of the number of vertices. For each one of the directed graphs presented, with x vertices, in which a method performs y visits, we draw in position (x, y) the symbol corresponding to the method.

	# Networks in which the method performs v visits		
	Methods		
	Diameter		Radius
v	ifub *Hd*	ifub 2Sweep *Hd*	rad 2Sweep *Hd*
$v \leqslant 0.01\%n$	13	9	5
$0.01\%n < v \leqslant 0.1\%n$	13	27	21
$0.1\%n < v \leqslant 1\%n$	26	24	26
$1\%n < v \leqslant 10\%n$	17	9	14
$10\%n < v$	4	4	7

In Figure 15 we report the number of visits performed by ifub*Hd* and ifub+2Sweep*Hd* to compute the diameter and the diametral vertices, as a function of the number of vertices. Analogously in Figure 16 we report the number of visits performed by rad+2dSweep*Hd* to compute the radius and the radial vertices, as a function of the number of vertices. In particular for each one of the undirected graphs presented, having x vertices, in which a method performs y visits, we draw in position (x, y) the symbol corresponding to the method.

Observe that once again in the case of Figure 15, when the number of vertices increases, no increase can be detected in the number of visits. We argue that our methods perform a constant number of visits in practice. We conjecture that the impossibility of concluding our experiments in the case of ifub for `roadNet-CA`, `roadNet-PA` and `roadNet-TX` is due to unidentified special topological properties of these graphs.

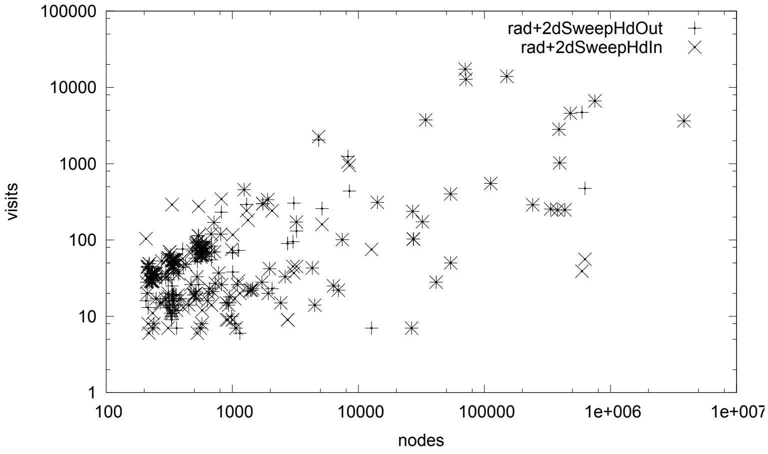

Figure 14: Visits performed by rad+2dSWEEP*HdOut*, rad+2dSWEEP*HdIn* to compute the radius and the radial vertices, as a function of the number of vertices. For each one of the directed graphs presented, with x vertices, in which a method performs y visits, we draw in position (x, y) the symbol corresponding to the method.

Once again in the case of Figure 16, when the number of vertices increases, the number of visits very slightly increases, but in this case this does not hinder the central vertex computations.

4.7.4 *Computing tight lower bounds of the diameter by* 2dSWEEP *or* 2SWEEP

In the following we show for the directed graphs of our dataset the effectiveness of 2dSWEEP*HdOut*, that is the 2dSWEEP by starting from the highest out-degree vertex, and 2dSWEEP*HdIn*, that is the 2dSWEEP by starting from the highest in-degree vertex, in order to find tight lower bounds of the diameter. In the following table we report for each category of networks, the number of networks in which 2dSWEEP*HdOut* and 2dSWEEP*HdIn* return a tight lower bound, and the maximum absolute error achieved among all the networks belonging to that category.

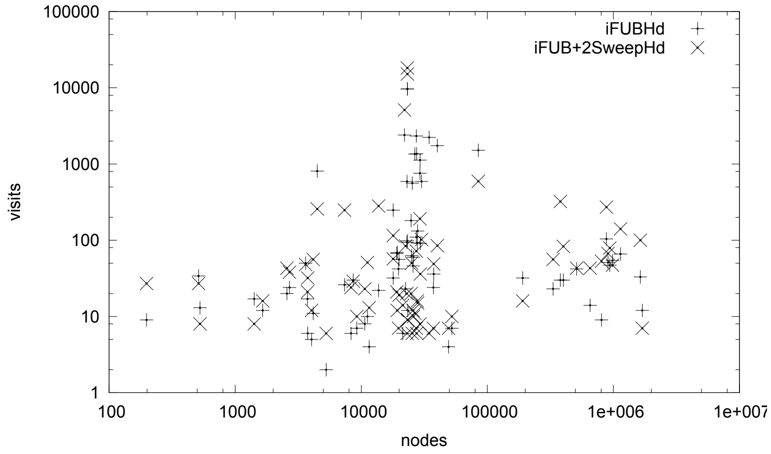

Figure 15: Visits performed by iFUB*Hd* and iFUB+2Sweep*Hd* to compute the diameter and the diametral vertices, as a function of the number of vertices. For each one of the directed graphs presented, with x vertices, in which a method performs y visits, we draw in position (x, y) the symbol corresponding to the method.

Category	# of Networks	2dSweep*HdOut*		2dSweep*HdIn*	
		# of Networks in which lb is tight	Maximum error	# of Networks in which lb is tight	Maximum error
Metabolic Bipartite	76	73	19	75	19
Metabolic Compound	76	73	9	75	9
Metabolic Reaction	76	73	10	75	10
Directed Social	10	10	0	10	0
Web	16	16	0	16	0
Citation	2	2	0	2	0
Communication	3	3	0	2	1
P2P	9	8	1	7	1
Product co-Purchasing	5	5	0	5	0
Word-association	1	1	0	1	0

In almost all the networks we have considered the lower bound achieved by 2dSweep is tight. In the cases in which this lower bound is not tight, the maximum absolute error achieved is 1, except for the Metabolic Bipartite, Compound, and Reaction networks of the bio-sources `arab0` (where the maximum error is 13), of `homo0` (where the maximum error is 19), and of `kleb2` (where the maximum error is 3).

In the case of the undirected graphs, we show the effectiveness of 2Sweep*Hd*, that is the 2Sweep by starting from the highest degree vertex. In the following table we report for each category of networks, the number of networks in which 2Sweep*Hd* returns a tight lower bound, and the maximum absolute error achieved among all the networks belonging to that category.

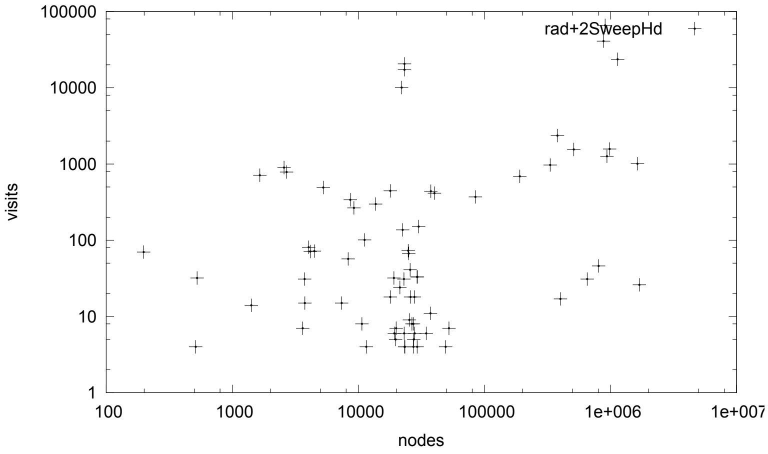

Figure 16: Visits performed by rad+2dSweep*Hd* to compute the radius and the radial vertices, as a function of the number of vertices. For each one of the directed graphs presented, with x vertices, in which a rad+2dSweep*Hd* performs y visits, we draw in position (x, y) the symbol corresponding to rad+2dSweep*Hd*.

Category	# of Networks	2Sweep*Hd*	
		# of Networks in which lb is tight	Maximum error
Protein-Protein Interaction	14	11	1
Collaboration	14	12	1
Undirected Social	4	4	0
Undirected Communication	36	34	2
Autonomous System	2	1	1
Road	3	1	14
Word Adjacency	7	4	1

In almost every undirected network we considered, the lower bound computed by 2Sweep*Hd* is tight. Whenever this lower bound is not tight, the maximum absolute error is 1, except for the communication network `d09.txt`, where the absolute error is 2.

See [6, 156] for the effectiveness of the natural generalization of 2Sweep, 4Sweep, in the case of undirected graphs.

4.7.5 *Comparing ifub with other methods to compute the diameter*

In the following we will focus our attention on the subset of naturally undirected real-world networks included in our dataset, in order to run a fair comparison with other algorithms. Indeed these other algorithms have been designed to be applied just to undirected networks and just to compute the diameter. The categories involved are biological networks (in particular, protein interaction networks), collaboration networks, words adjacency networks, and autonomous systems graphs. We have chosen to use in the experiments the IFUB*Hd* strategy. Observe that all the networks included in this restricted dataset have one vertex of maximum degree, apart from `iPfam` (with 5 vertices of maximum degree) and `interdom` (with 8 vertices of maximum degree): in the case of these two networks, we have experimentally verified that the performances of IFUB*Hd* are independent of the choice of the starting vertex.

COMPARING IFUB WITH UPPER BOUND COMPUTATION METHODS. The lower bounds provided by the 2SWEEP or the 4SWEEP methods turn out to be, in practice, almost always tight: however, there is, in theory, no guarantee about the quality of the approximation. For this reason, some methods have been proposed in [4, 157] in order to find an upper bound on the diameter which bounds the absolute error or even validates the tightness of the lower bound. All these methods return the diameter of the BFS tree of a vertex r, i.e. T_r. In particular, two methods, called RTUB and HTUB respectively, have been presented in [157]: RTUB selects r as a random vertex, while HTUB chooses r as one vertex with the highest degree. Thus, both RTUB and HTUB execute two BFSes: one BFS from r is used to create T_r and one BFS is used to compute the diameter of T_r. The other two methods, called MTUB and MTUBHD respectively, are evolutions of a method proposed in [4]: in the case of MTUB, r is the vertex returned by 4SWEEP starting from a random vertex, while in the case of MTUBHD , r is the vertex returned by 4SWEEP from the vertex with highest degree. Hence, both MTUB and MTUBHD execute six BFSes: four BFSes are used to execute 4SWEEP and to select r, one BFS from r is used to create T_r, and one BFS is used to compute the diameter of T_r.

Table 2 shows the upper bounds found by using HTUB and MTUBHD, and the randomized methods MTUB and RTUB: in order to run a fair comparison, we have applied the following schema in the case of the randomized methods. Let ν be the number of BFSes performed by IFUB in order to calculate the diameter: in each experiment, we have repeated at least $\lceil \nu/6 \rceil$ times the MTUB and RTUB methods. Specifically, we have executed ten experiments: we report the best upper bound over all these experiments in Table 2, along with the number of runs out of ten in which the returned upper bound is tight. Consistently with [4], MTUB and MTUBHD seem to be more effective in finding better upper bounds rather than RTUB and HTUB. However in the great majority of the networks, all these methods are not able to find a tight upper bound (see the rightmost part of Table 2). Finally, it is worth observing that the 2SWEEP or 4SWEEP methods return the height of a BFS tree and that, in any graph, there is always at least one vertex such that the height of its BFS tree is equal to the diameter. On the other hand, the upper bound based methods return the diameter of a BFS tree, and there are infinite graphs such that no vertex have a BFS tree whose diameter is equal to the diameter of the graph (note that this is the case of the graph shown in Figure 10).

		Exact Algorithms		Upper Bound Algorithms					
		iFUB*Hd*	TK	MTUB		MTUBHD	RTUB		HTUB
Name	D	BFSes	BFSes	Best UB	# Runs (out of 10) s.t. UB=D	Best UB	Best UB	# Runs (out of 10) s.t. UB=D	Best UB
jazz	6	**3**	7	7	0	7	8	0	8
iPfam	12	**4**	**4**	12	10	12	12	3	13
psimap	11	13	**6**	12	0	12	12	0	12
Rattus_norvegicus	19	17	**4**	20	0	20	20	0	23
interdom	8	**3**	7	8	6	9	8	1	8
string	9	20	**15**	10	0	12	11	0	10
japaneseBookInter_st	8	**4**	13	9	0	10	10	0	9
geom	14	7	**6**	14	1	15	14	1	16
Mus_musculus	20	**3**	6	20	4	21	21	0	22
ppi_dip_swiss	12	**3**	4	13	0	13	13	0	14
HC-BIOGRID	23	**5**	**5**	24	0	25	23	1	25
ca-GrQc	17	**11**	14	20	0	20	19	0	19
darwinBookInter_st	8	**3**	4	9	0	8	9	0	8
frenchBookInter_st	9	**6**	12	10	0	11	10	0	11
ca-HepTh	18	**9**	17	20	0	20	20	0	21
hprd_pp	14	**3**	8	16	0	16	16	0	16
ca-HepPh	13	**10**	20	15	0	15	15	0	15
spanishBookInter_st	10	**2**	4	10	10	10	11	0	11
ca-AstroPh	14	**12**	19	15	0	15	17	0	16
dip20090126_MAX	30	33	**7**	30	10	31	30	3	34
ca-CondMat	15	**6**	14	16	0	18	17	0	17
Cond_mat_95-99	12	**78**	577	15	0	16	15	0	15
ppi_gcc	27	24	**7**	27	10	27	28	0	30
itdk0304_rlinks	26	**11**	**11**	28	0	28	28	0	29
dblp20080824_MAX	22	**13**	30	25	0	26	24	0	25
imdb	14	**19**	33	16	0	16	16	0	16
as-skitter	31	12	**5**	32	0	32	34	0	40

Table 2: Comparing iFUB with other methods.

COMPARING IFUB WITH TAKES-KOSTERS ALGORITHM. Recently and independently from this work, a new algorithm to compute the diameter of large real-world networks has been proposed in [103]. The algorithm, which we refer to as TK, maintains a lower bound Δ_L and an upper bound Δ_U of the diameter D and, for each vertex w, it maintains a lower bound $\varepsilon_L[w]$ and an upper bound $\varepsilon_U[w]$ of its eccentricity $\mathrm{ecc}(w)$. Moreover, it maintains a set W of vertices, at the beginning initialized with V, that are candidate extremes of a path whose length is the diameter. At the beginning all the lower and upper bounds are respectively initialized with 0 and n. At each step the vertex u, with minimum lower bound or with maximum upper bound, is selected from set W: Δ_L is updated with $\max\{\Delta_L, \mathrm{ecc}(v)\}$, Δ_U is updated with $\min\{\Delta_U, 2\mathrm{ecc}(v)\}$, and, for any vertex w, $\varepsilon_L[w]$ is updated with $\max\{\varepsilon_L[w], \mathrm{ecc}(v) - d(v,w), d(v,w)\}$ and $\varepsilon_U[w]$ is updated with $\min\{\varepsilon_U[w], \mathrm{ecc}(v) + d(v,w)\}$. Then, the vertices $v \in W$ such that $\varepsilon_U[v] \leqslant \Delta_L$ and $\varepsilon_L[v] \geqslant \Delta_U/2$ are removed from W, since a selection of v cannot improve the bounds Δ_L and Δ_U. The algorithm terminates and returns Δ_L when Δ_L is equal to Δ_U or the set W is empty. In Table 2, we report for each network the number of BFSes performed by TK to compute the diameter, by applying the implementation given by the authors. In the case of the 27 networks in our dataset, the more effective approach is iFUB*Hd*: it requires less BFSes than TK in the case of 17 networks, and more BFSes than TK in the case of just 7 networks (while the two methods require the same number of BFSes in the remaining 3 networks).[2]

4.8 conclusion and open problems

In the previous sections we have described and experimented new algorithms for computing the diameter and radius of directed and undirected (weighted) graphs, together with all the diametral and radial vertices. Even though these algorithms have $O(nm)$ time complexity in the worst case, our experiments suggest that their execution for real-world networks requires time $O(m)$ in the case of the diameter and almost $O(m)$ in the case of the radius.

The computation of the radius with our algorithm is affected by the choice of the starting vertices x, y so that the best performances are achieved whenever x and y are both diametral targets. The performance of DiFUB depends on the choice of the starting vertex u (indeed, it could be interesting to experimentally analyse its behaviour depending on this choice). Ideally, u should be such that the maximum between the forward and the backward eccentricity of u should be close to the $\min_{v \in V}\{\max\{ecc_F(v), ecc_B(v)\}\}$. Surprisingly, we have observed that in the case of real-world graphs, this value is close to the minimum possible, that is $D/2$. This peculiar structural property affects the performance of our algorithm: in these cases, the upper bound on the iterations is minimum and equal to $R - D/2 + 1$.

The main fundamental questions are now the following. Why the double sweep, both in the directed and in the undirected version, is so effective in finding tight lower bounds for the diameter and vertices with low eccentricity? Which one is the topological underlying property that can lead us to these results? Why real world graphs exhibit this property? Some progress has been done by [184], but still a lot has to be done. Finally, it could be interesting to analyse a parallel implementation of the DiFUB algorithm. Indeed, the eccentricities of the vertices belonging to the same fringe set can be computed in parallel. Moreover, a variety of parallel BFS algorithms have been explored in the literature and can be integrated in the implementation of our algorithm.

[2] A comment is in order on the parallelization of iFUB and of TK to speed up the computation: indeed, while the selection process in TK seems to be inherently sequential, the BFSes of the vertices at the same level i required by iFUB to compute $B_i(u)$ can be performed in parallel.

4.9 MORE ABOUT DISTANCE ANALYSIS

In other works, the diameter is also referred to as the average distance among all the pairs of vertices, as in [185, 186], but as shown by [187], diameter and average distance can provide together an overall indication of the structure of a network, in particular showing how much the network is cohesive. For instance, a network with large diameter and small average distance may indicate that there are branches or spurs to the network that are mostly inaccessible to other vertices.

The small average distance commonly observed in biological networks pertains to the so called small-world effect [188]. The average distance ranged between 3 and 5 in 43 metabolic networks of 200 to 800 vertices [189], showing that all vertices are quite close to each other. Although several groups confirmed the small-world property of the MN in different organisms [190, 191, 192, 193, 194], Arita [195] heavily criticized the way the pathways are computed in those works, since they do not conserve their structural moieties. When this problem is accounted for correctly, the analysis revealed that the average shortest path length of the *E. coli* metabolism is much longer than previously thought [195, 196]. In [197] it has been shown that with respect to some models, the average shortest path length of biological networks is bigger than the expected one, whenever the degree distribution or the modularity is fixed.

Moreover it is important to underline that the small world phenomenon is based on shortest paths. Most of those in metabolic networks are irrelevant short-cuts that use the so called pool metabolites, so that for instance water can be transformed directly into ethanol violating the mass conservation law: in such a context these irrelevant short-cuts induce artificially the small world effect. In gene regulatory networks, a shortest path in the potential network may not correspond to a real path, that is a path included in at least one realization, i.e. the genes in the considered paths could be not expressed at the same time. Notice that such observations are valid also for interpreting the results of the centrality analysis according to the different definitions. The robustness of some of the centrality measures described before with respect to the sampling has been shown in [38]. Even if the realization of a network is not a random subgraph, this work shows that in general the role of a vertex inferred in the potential graph not necessarily coincides with his role in a subgraph of the network, i.e. a realization. Indeed for instance a gene can be essential in one or more growth conditions but possibly not in all. In such a context, it is interesting to distinguish between the static and dynamic hubs, like was done in the case of the protein-protein interaction network of *Saccharomyces cerevisiae* in [124] and integrating more biological information in these measurements in order to to improve our ability to predict biologically important vertices in a network.

Other variants of diameter have been proposed: the *effective diameter* is defined as the 90-th percentile of the cumulative distribution of the shortest path lengths and can be computed by using [92, 93]. Even if this measure may appear more robust, it is known that the diameter and the effective diameter tend to exhibit qualitatively similar behavior [198].

However in general a high diameter does not necessarily imply a low compactness (the great majority of the vertices could be still close). In such a context, it could be interesting to inspect the distance distribution, also called *distance histogram*. The distribution of distances may be more informative than the average distance and the diameter about the global properties of a network [197]. To this aim, several tools have been proposed [93, 92, 95, 96, 97, 98, 99, 100].

If G is directed and strongly connected or undirected and connected, the distance distribution is defined as the set of values N_h $(1 \leqslant h < n)$, where N_h is the normalized number of ordered pairs of vertices having distance h, that is $N_h = |\{(u, v) \in V \times V : d(u, v) = h\}|/(n(n-1))$. For example, if G is an undirected path with n vertices then, for any $1 \leqslant h < n$, there are $2(n-h)$ ordered pairs of vertices at distance h: hence, in this case, $N_h = \frac{2(n-h)}{n(n-1)}$. (Note that, as expected, $\sum_{h=1}^{n-1} N_h = 1$). For any G, observe that $N_h = 0$ for $D < h < n$. On the other hand, N_1 is related to the number of edges: namely, $N_1 = \frac{2m}{n(n-1)}$ when G is undirected and $N_1 = \frac{m}{n(n-1)}$ when G is directed.

Whenever the network is strongly connected or undirected, like for PPNs, a logarithmic amount of vertices can be sampled and the distribution of distances of all the vertices from the vertices in the sample can provide a good approximation for the exact distribution or for the average distance, as we have shown in

[105] P. Crescenzi, R. Grossi, L. Lanzi, and A. Marino. A Comparison of Three Algorithms for Approximating the Distance Distribution in Real-World Graphs. In *Proceedings of the 1st International ICST Conference on Theory and Practice of Algorithms in (Computer) Systems, TAPAS 2011*, volume 6595 of *Lecture Notes in Computer Science*, 2011.

Let us define the quantity $N_h(U) = |\{(u, v) \in U \times V : d(u, v) = h\}|/(|U|\,(n-1))$, where $U \subseteq V$. By performing a random sample of k vertices from V obtaining the multiset $U = \{u_1, u_2, \ldots, u_k\} \subseteq V$ and by executing a BFS of G starting from vertex u_i, $N_h(U)$ is an approximation of N_h whose effectiveness, whenever $k = \Theta(\epsilon^{-2} \log n)$, is given by the following theorem, whose proof follows from the Hoeffding Bound [199].

Theorem 12. *Let G be a (strongly) connected graph with n vertices and m edges. For any arbitrarily small $\epsilon > 0$, the algorithm with $k = \Theta(\epsilon^{-2} \log n)$ computes in time $O(k\,m)$ an approximation of the distance distribution N_h of G whose absolute error is bounded by ϵ, with high probability.*

In the case of directed networks not strongly connected, the effectiveness of the sampling method, i.e. the size of the sample, depends on the fraction of pairs of vertices (x, y), such that there is no path from x to y.

Let r be the number of reachable pairs, that is $n(n-1)(1-N_\infty)$

$$R_h = \frac{|\{(u,v) \in V \times V : d(u,v) = h\}|}{r} = \frac{N_h}{1-N_\infty} \qquad R_h(U) = \frac{N_h(U)}{1-N_\infty}.$$

$$N_h(U) = N_h + \epsilon \Longrightarrow |R_h(U) - R_h| = \left| \frac{N_h(U)}{1-N_\infty} - \frac{N_h}{1-N_\infty} \right| \leqslant \frac{|\epsilon|}{1-N_\infty}$$

Thus the error is big whenever N_∞ is close to 1, which means that in order to capture the very few pairs of connected vertices we have to increase the size of the sample. By applying the Hoeffding bound, we have that if the size of the sample is $\Theta\left(\frac{\log n}{\gamma^2(1-N_\infty)^2}\right)$, then the error is such that $|R_h(U) - R_h| \leqslant \gamma$ with high probability. It is worth observing that $1 - N_\infty$ could be estimated a priori by using sampling again.

Anyway, in both directed and undirected cases the HyperANF tools, seems to be a promising alternative to approximate the distance distribution [93].

5

TELLING STORIES: ENUMERATING MAXIMAL DIRECTED ACYCLIC GRAPHS WITH CONSTRAINED SET OF SOURCES AND TARGETS

In this chapter we propose an example of enumeration problem with a potentially exponential number of solutions that we solve by using a non-trivial brute force approach. The problem is a constrained version of the problem of enumerating all maximal directed acyclic subgraphs (DAG) of a graph G*. In this version, we enumerate maximal DAGs whose sources and targets belong to a predefined subset of the vertices. We call such DAGs* stories*. Given a Metabolic network, each individual story should explain how some interesting metabolites are derived from some other through a chain of reactions, by keeping alternative pathways. We first show how to compute one story in polynomial-time, and then describe two different algorithms to "tell" all possible stories.*

5.1 INTRODUCTION

A classical goal of metabolic studies is to try to understand which are the metabolic processes involved in the adaptation to an environmental change. Although it is possible to keep track of some monitored metabolites, the internal mechanisms that lead to the observed variation are not clear. For "genome scale" networks, the metabolism of a whole organism is taken into account, while a metabolic perturbation may impact only a small portion of this complex network.

Recently, metabolomic techniques gained the spotlight by providing a way to monitor metabolism by measuring the concentration of metabolites in different conditions or time points. Typical results from these experiments are lists of metabolites whose concentrations significantly changed when the cell was exposed to stress. How to interpret this list of metabolites became then a new research topic, consisting in identifying the metabolic processes that link the metabolites of interest, possibly explaining the observed variations in their concentrations. Some examples of approaches to deal with this kind of data may be found in [200, 201, 51].

Informally, we call a set of metabolic reactions linking all the metabolites of interest a *metabolic story*. For instance, a metabolomics study analysis compared a *Yeast* cell under two conditions, with and without exposition to cadmium [9]. The Metabolic network reconstruction of *Yeast* has about 1300 metabolites and

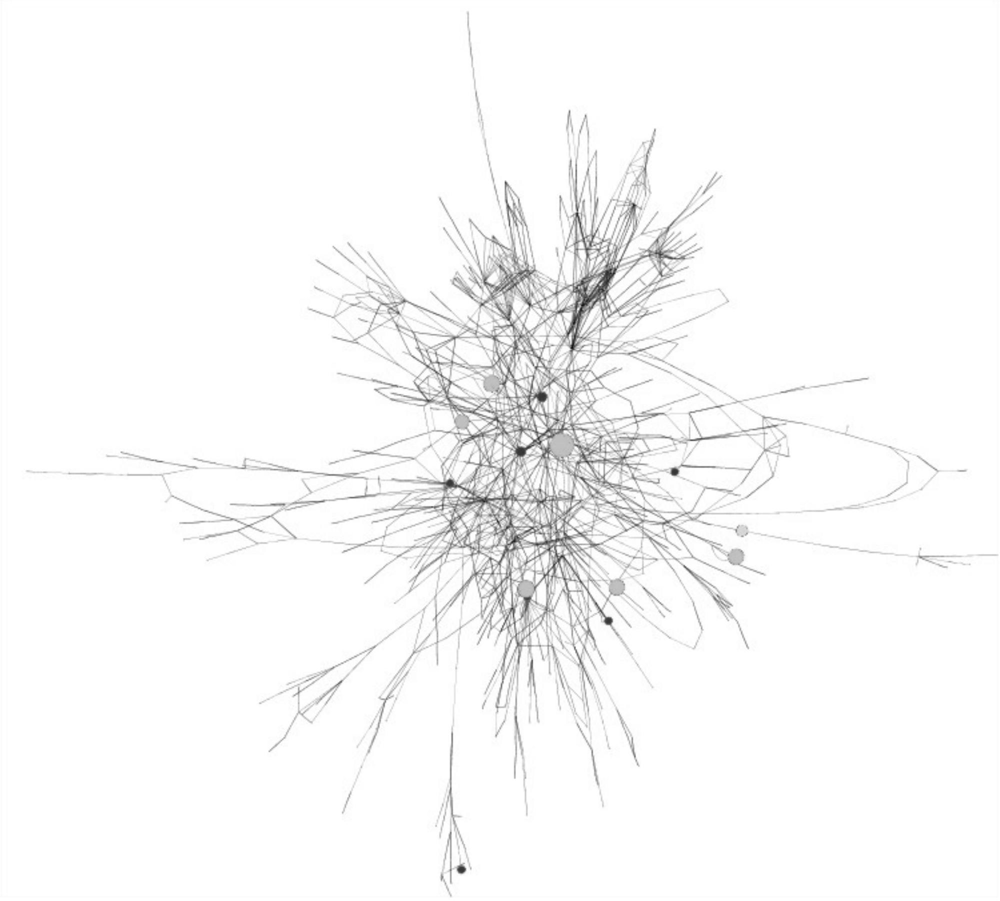

Figure 17: Compound Metabolic Network of *Yeast*

the experiment identified a list of 22 metabolites whose concentrations changed. Figure 17 presents the *Yeast* network, and the highlight vertices, i.e. the light grey and the dark grey vertices, correspond to the metabolites identified in the experiment. The light grey vertices are those whose concentrations increased while the dark grey ones are the ones whose concentrations decreased. The concentrations of the other metabolites did not change significantly. Figure 18 presents a metabolic story that gives one possible explanation for the change in the concentration of the metabolites in the network. This particular story was found as one of the top scores using a score function that assigns a value to a story, after the enumeration process, based on the concentration data from the metabolomic experiment. The chain of reactions present in this story is very close to the conclusions found in [9], since the order in which metabolites are transformed is almost the same. There are several other possible scenarios with a score close to the one of this story that could be considered and could provide new insights on the biology of the underlying metabolic process. Finding and enumerating all those alternatives is the metabolic stories problem.

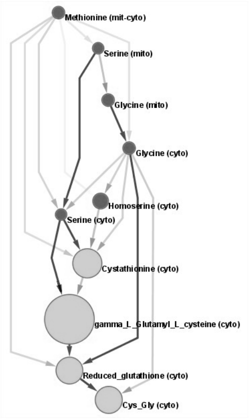

Figure 18: A story of the Compound Metabolic Network of *Yeast*

Hence, a metabolic story should capture the relationship between the vertices of interest. Each individual story should explain how some metabolites are derived from others through a chain of reactions. In this sense, only light grey and dark grey vertices are allowed to be sources and targets in a story, even if they can appear as intermediate vertices in some stories. In order to enumerate all scenarios in which only dark grey or light grey vertices play the role of sources and/or targets, we introduce the acyclicity constraint. On the other hand, alternative pathways between these vertices that do not create cycles should always be included since they give additional explanations on the interconnection between them, and for this reason we introduce a maximality condition.

contribution. In this chapter we define the new problem of enumerating stories, that is a constrained version of the problem of enumerating all maximal directed acyclic subgraphs (DAG) of a graph G [12]. In our version, only a given subset $\mathbb{B}$ of the vertices are allowed to be sources or targets of the DAGs to be enumerated. For the computational problem, we will not distinguish dark and light grey metabolites, modelling them in the same way as black vertices.

The problem seems to be related to a Steiner tree/network problem, since the goal is to connect a distinguished set of vertices. Although the problem was originally motivated by biology where Steiner tree approaches have been widely explored[202], it is surprising that, as far as we know, such a constraint on sources and targets was never considered before. In this chapter, we show that introducing this constraint is enough to change the nature of the enumeration problem. Enumerating DAGs without the constraint is equivalent to enumerating feedback arc sets (FASs). A feedback arc set is a set of arcs that break all the cycles, i.e. it is the *complement* of a DAG. In this sense enumerating stories is a generalisation of enumerating minimal FASs, since the complement of a story is a minimal set of arcs that breaks all the cycles and also avoids sources or targets that are not in $\mathbb{B}$. A sets of arcs that breaks all the cycles and also avoids sources or targets that are not in $\mathbb{B}$ is called *story arc sets* (SASs). Hence every SAS is a FAS. We show that not every minimal FAS is a minimal SAS, and give evidence that telling stories is possibly harder than enumerating minimal feedback arc sets.

In this chapter we will show a polynomial algorithm to compute one story, and then describe two different algorithms to enumerate all possible stories.

The contents of this chapter appeared in [10, 11, 203]. Moreover, the open problems we propose appeared in [13].

STRUCTURE OF THE CHAPTER. The chapter is organised in the following way. After introducing the main definitions and notations in Section 5.2, Section 5.3 presents some operations to simplify the graph without losing solutions. Section 5.4 shows a polynomial time algorithm for finding one story and also a proof that the problem of finding stories with a specific set of sources and targets is NP-complete. Sections 5.5.1 and 5.5.2 propose two different approaches to enumerate stories: the first one makes use of a minimal feedback-arc-set enumerator but can only be applied to a specific class of graphs while the second one is an extension of our algorithm to enumerate one story based on an initial permutation of the vertices and can be used for any graph; the example in Section 5.6 shows how this latter enumerator works. Section 5.7 provides complexity results for an alternative definition of stories and, finally, Section 5.8 conclude with some open problems.

5.2 PRELIMINARIES

Let $G = (\mathbb{B} \cup \mathbb{W}, E)$ be a directed graph such that $\mathbb{B} \cap \mathbb{W} = \emptyset$. We write $V = \mathbb{B} \cup \mathbb{W}$. Vertices in $\mathbb{B}$ are said to be *black* while those in $\mathbb{W}$ are said to be *white*.

A *pitch* of G is an acyclic subgraph $G' = (\mathbb{B} \cup \mathbb{W}', E')$ of G with $\mathbb{W}' \subseteq \mathbb{W}$ and $E' \subseteq E$ and, for each vertex $w \in \mathbb{W}'$, $d^+(w) > 0$ and $d^-(w) > 0$. A trivial pitch is $G' = (\mathbb{B} \cup \emptyset, \emptyset)$: the subgraph containing all the black vertices and no arc. We define a *story* as a maximal pitch. We denote by $\Sigma(G)$ the set of stories of G. Thus, given $G = (\mathbb{B} \cup \mathbb{W}, E)$, we want to enumerate $\Sigma(G)$.

For independent reading, we define a *feedback arc set* (FAS) of a directed graph $G = (V, E)$, which is a subset F of E such that $G - F = (V, E \setminus F)$ is acyclic. A FAS is said to be *minimal* if there exists no $f \in F$ such that $F \setminus \{f\}$ is a FAS. We notice that, if $V = \mathbb{B} \cup \mathbb{W}$, the complement of a FAS is not always a story since $G - F$ may contain white sources or targets. Indeed, the FAS enumeration problem is a particular instance of our problem in which every vertex is black, i.e., $\mathbb{W} = \emptyset$. We define a *story arc set* (SAS) as a FAS S with the extra property that no white vertex in $G - S$ is a source or a target. A SAS is said to be *minimal* if there exists

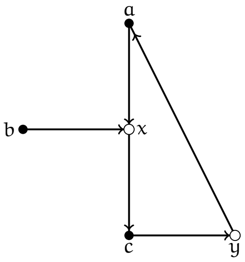

Figure 19: In this case, $\mathbb{B} = \{a, b, c\}$ and $\mathbb{W} = \{x, y\}$. There are 4 possible minimal FASs: $\{(a, x)\}$, $\{(x, c)\}$, $\{(c, y)\}$, and $\{(y, a)\}$. Only one of these minimal FASs (that is, the first one) is also a minimal SAS. For example, the second one is not a SAS since $G - (x, c)$ contains a white target (that is, vertex x). On the other hand, another minimal SAS is $\{(c, y), (y, a)\}$, which is not a minimal FAS (even though it is a FAS).

no subset S' of S such that $S \setminus S'$ is a SAS. This implies that if S is minimal, then for every $s \in S$, the graph $G = (\mathbb{B} \cup \mathbb{W}, (E \setminus S) \cup \{s\})$ either contains a cycle or contains a white source or target. If S is a minimal SAS, then $G - S$ is a story. A SAS is also a FAS. However, the example in Figure 19 shows that, as expected, not every minimal FAS is a minimal SAS and, more surprisingly, that not every minimal SAS is a minimal FAS. For this reason, the use of a polynomial-time-delay enumeration algorithm for minimal FAS as the one proposed in [12] to enumerate stories is limited, since some minimal SASs may not be detected. We shall see in a later section that this is not the case when we restrict ourselves to a particular class of graphs.

5.3 PREPROCESSING THE GRAPH

In this section, we show how a graph may be simplified without essentially changing the set of its stories. The simplifications allow shorter proofs of our results.

The simplified graphs turn out to be interesting from a biological point of view since they correspond to a more compact representation of graphs that is equivalent in terms of story sets. We applied the preprocessing steps described in this section on a collection of 107 Metabolic networks obtained from MetExplore[160, 24], randomly choosing sets of black vertices with sizes varying from 5% to 15%. The compression ratio on the number of vertices goes from 65% to 98% with an average reduction of 83%, while the compression ratio on the number of arcs goes from 56% to 99% with an average reduction of 77%. This more compact representation of the interaction between the black vertices greatly facilitates the visualisation and analysis of the input data.

We now define the following four simplification operations:

- A *white source and target removal* consists in removing iteratively a white vertex from the graph that is either a source or a target. Clearly such vertices cannot appear in any story. Let $\mathtt{de}(G)$ be the graph resulting of such removals.

- A *self-loop removal* consists in removing all arcs of the form (u, u). Since stories are acyclic, such arcs do not appear in any story. Let $\mathtt{sl}(G)$ be the resulting graph of such removals.

- A *forward bottleneck removal* consists in removing a white vertex v whose out-degree is equal to 1, and directly connecting any predecessor of v to the unique successor of v (without creating multi-arcs). Let $\mathtt{fb}(G, v)$ be the resulting graph.

- A *backward bottleneck removal* consists in removing a white vertex whose in-degree is equal to 1, and directly connecting the unique predecessor of v to the successors of v (without creating multi-arcs). Let $\mathtt{bb}(G, v)$ be the resulting graph.

We prove that the last two operations leave the set of stories essentially unaltered. First an observation:

Observation 1. *Let v, p, and s be three vertices such that $(p, v), (v, s), (p, s) \in E$ and v is a (white) bottleneck. Then, for any story S, $(p, v), (v, s) \in S$ if and only if $(p, s) \in S$.*

Given three vertices $v, p, s \in V$ with $(p, v), (v, s) \in E$ and $(p, s) \notin E$, let $\mathtt{ab}(G, v, p, s)$ denote the graph obtained by adding to G the arc (p, s).

Lemma 5. *Let $v \in W$ be a forward bottleneck and let $p, s \in V$ be such that $(p, v), (v, s) \in E$ and $(p, s) \notin E$. Then there exists a bijection from $\Sigma(G)$ to $\Sigma(\mathtt{ab}(G, v, p, s))$.*

Proof. For any story $S \in \Sigma(G)$, we define $f(S) = S \cup \{(p, s)\}$ if $(p, v) \in S$ (and hence, $(v, s) \in S$ since v is a forward bottleneck), otherwise $f(S) = S$. To prove that $f(S) \in \Sigma(\mathtt{ab}(G, v, p, s))$, we use Observation 1 to show that $f(S)$ is acyclic if and only if S is acyclic. We now show that $f(S)$ is maximal. Indeed, if $(p, s) \in f(S)$, then no set of arcs could be added to $f(S)$ since otherwise it could also be added to S. Otherwise, if (p, s) could be added to $f(S)$, then, from Observation 1 also (p, v) and (v, s) could be added to $f(S)$ and, hence, these two arcs could be added to S.

Let us now prove that, if S_1 and S_2 are two stories such that $S_1 \neq S_2$, then $f(S_1) \neq f(S_2)$. If $(p, v) \notin S_1 \cup S_2$, then $f(S_1) = S_1 \neq S_2 = f(S_2)$. Otherwise, if $(p, v) \in S_1 \cap S_2$, then $f(S_1) = S_1 \cup \{(p, s)\} \neq S_2 \cup \{(p, s)\} = f(S_2)$. Finally, if $(p, v) \in S_1 \setminus S_2$ (the other case can be dealt with similarly), then $(p, s) \in f(S_1)$ while $(p, s) \notin f(S_2)$ and, hence, $f(S_1) \neq f(S_2)$.

It remains to show that, for any $S' \in \Sigma(\mathtt{ab}(G, \nu, p, s))$, there exists a $S \in \Sigma(G)$ such that $f(S) = S'$. Define $S = S' \setminus \{(p, s)\}$. Since S' is acyclic, so is S. If $(p, s) \notin S'$, then $S = S'$ and $S \in \Sigma(G)$, since the only difference between G and $\mathtt{ab}(G, \nu, p, s)$ is the arc (p, s). Otherwise, from Observation 1, it follows that $(p, \nu), (\nu, s) \in S'$ and, hence, $(p, \nu), (\nu, s) \in S$: the maximality of S then follows from the maximality of S', since any set of arcs that could be added to S could also be added to S'. □

By this lemma we may assume that, for any forward bottleneck $\nu \in \mathbb{W}$ whose unique successor is s, and for any predecessor p of ν, the graph contains the arc (p, s). To complete the forward bottleneck removal operation, we then need to delete the vertex ν without changing the stories set of the graph. Consider now the following operation: given a graph G with a forward bottleneck ν, $\mathtt{dp}(G, \nu)$ denote the graph obtained by deleting from G the vertex ν and all incident arcs.

Lemma 6. *Let $\nu \in \mathbb{W}$ be a forward bottleneck and s its unique successor. Suppose that for any predecessor p of ν, the graph contains the arc (p, s). Then there is a bijection from $\Sigma(G)$ to $\Sigma(\mathtt{dp}(G, \nu))$.*

Proof. For any $S \in \Sigma(G)$, we define $f(S) = S \setminus \{\nu\}$, that is the subgraph obtained by removing ν and all incident arcs from S if $\nu \in S$. Since S is acyclic, so is $f(S)$. Moreover, from Observation 1, it follows that if $(p, \nu), (\nu, s) \in S$, then $(p, s) \in S$ and, hence, $(p, s) \in f(S)$. The maximality of $f(S)$ then follows from the maximality of S, since any set of arcs that could be added to $f(S)$ could also be added to S.

Let us now prove that, if S_1 and S_2 are two stories such that $S_1 \neq S_2$, then $f(S_1) \neq f(S_2)$. If $(p, s) \notin S_1 \cup S_2$, then $(p, \nu), (\nu, s) \notin S_1 \cup S_2$ and $f(S_1) = S_1 \neq S_2 = f(S_2)$. Otherwise, if $(p, s) \in S_1 \cap S_2$, then $(p, \nu), (\nu, s) \in S_1 \cap S_2$ and $f(S_1) = S_1 \setminus \{(p, \nu), (\nu, s)\} \neq S_2 \setminus \{(p, \nu), (\nu, s)\} = f(S_2)$. Finally, if $(p, s) \in S_1 \setminus S_2$ (the other case can be dealt with similarly), then $(p, s) \in f(S_1)$ while $(p, s) \notin f(S_2)$ and, hence, $f(S_1) \neq f(S_2)$.

Finally, let S' be a story of $\mathtt{dp}(G, \nu)$. Then S obtained by adding to S' the path $(p, \nu), (\nu, s)$ for every predecessor p of ν such that $(p, s) \in S'$ is clearly a story and $f(S) = S'$. □

Using the two previous lemmas, we obtain a justification for the third simplification operation.

Theorem 13. *For any forward bottleneck $\nu \in \mathbb{W}$, $\Sigma(G) = \Sigma(\mathtt{fb}(G, \nu))$.*

Analogously, we can justify the fourth operation.

Theorem 14. *For any backward bottleneck $\nu \in \mathbb{W}$, $\Sigma(G) = \Sigma(\mathtt{bb}(G, \nu))$.*

For any graph G, let $\mathtt{fb}(G)$ (respectively $\mathtt{bb}(G)$) denote the graph obtained by applying as many times as possible the forward (respectively backward) bottleneck removal operation. Notice that, even if G does not contain self-loops, it might happen that $\mathtt{fb}(G)$ (respectively $\mathtt{bb}(G)$) contains self-loops created by one bottleneck removal. Remember also that $\mathtt{sl}(G)$ denotes the graph obtained by the removal of all self-loops from G and $\mathtt{de}(G)$ denotes the graph obtained by the iterative removal of all white sources and targets from G. Our simplification procedure can now be described as follows.

(1) Let $G_0 = \mathtt{sl}(\mathtt{de}(G))$ and let $i = 0$.

(2) Let $G_{i+1} = \mathtt{sl}(\mathtt{bb}(\mathtt{sl}(\mathtt{fb}(G_i))))$.

(3) If $G_{i+1} = G_i$ then return G_i, otherwise let $i = i + 1$ and go to Step 2.

As a consequence of the previous results, we have that if H is the graph returned by this procedure, then there is a bijection between $\Sigma(G)$ and $\Sigma(H)$, and we may enumerate $\Sigma(H)$ instead. Hence from now on, we assume that any $v \in \mathbb{W}$ has $d^+(v) > 1$ and $d^-(v) > 1$. Notice that this avoids graphs like the one shown in Figure 19. Indeed, in this case, the two arcs (c, y) and (y, a) would disappear and the arc (c, a) would be inserted. Furthermore, also x will disappear and we get arcs (b, c) and (a, c). Observe also that this simplification procedure does not guarantee that a minimal FAS enumerator would produce all possible minimal SAS as we shall see in the next section.

5.4 FINDING SINGLE STORIES

Let us first consider the case of finding some story. We show that this can be done in polynomial time. Our algorithm basically starts with a pitch and grows it into a story by adding paths between black vertices while avoiding cycles. We can start with a trivial pitch such as the subgraph containing all the black vertices and no arcs.

Theorem 15. *A story can be determined in polynomial time.*

Proof. The algorithm COMPLETE_PITCH determines a story by completing a starting pitch P. It chooses a topological order π of the vertices consistent with the pitch. Starting in u, which can be any of the first vertices in this order that has not been scanned yet, a breadth-first search (BFS) is performed using only arcs not in $E(P)$. Any branch of the BFS tree is pruned as soon as it hits a vertex $v \in V(P)$. If v has $\pi(u) < \pi(v)$ or u and v are incomparable, then the path $u \rightsquigarrow v$ is added to P and the topological order is updated. This addition creates no cycle since there was no path $v \rightsquigarrow u$ in P due to the fact that $\pi(u) < \pi(v)$ or u and v were incomparable, which can be checked in polynomial time. Moreover, since P contained no white source nor target before the addition of the path, then it does not contain any after adding the path because u and v, which are the only

Algorithm 22: COMPLETE_PITCH(G, P)

```
Input: A graph $G = (\mathbb{B} \cup \mathbb{W}, E))$ with $\mathbb{B} \cap \mathbb{W} = \emptyset$ and an initial pitch $P$;
Output: A story completing $P$
$i \leftarrow 1$;
$\pi \leftarrow$ any topological order of $P$;
while $i \leqslant |V(P)|$) do
    $u \leftarrow i$-th element according to $\pi$ with $u \in V(P)$;
    Apply $\mathrm{BFS}(u, G \setminus E(P))$ until reach a vertex $v \in V(P)$;
    if $\pi(u) < \pi(v) \vee (u$ and $v$ are incomparable$)$ then
        include the path $u \rightsquigarrow v$ in $P$ and update $\pi$;
        $i \leftarrow 1$;
    else
        if no such vertex $v$ exists then
            $i \leftarrow i + 1$;
        end
    end
end
return $P$;
```

candidates to become source or target, were already present in P. Hence, the addition of $u \rightsquigarrow v$ to P creates a new pitch.

This procedure is repeated until no new path starting from u can be found. At this point, we continue with the next vertex in the updated order π. Every time a new path is found, π is updated and the procedure is started from the minimum vertex according to the new order. Since at each updating of the topological order, we add at least one arc, the algorithm terminates in polynomial time. The final pitch produced by this procedure is maximal and, therefore, a story. □

We proceed by showing that the problem becomes NP-complete if we wish to identify a specific single story, i.e., one having a particular set of sources and/or targets.

Theorem 16. *Deciding whether there exists a story with a given set of sources and targets is NP-complete.*

Proof. In order to prove this theorem, we show how the 3-SAT problem[204] is reducible to the problem of deciding whether, given a directed graph $G = (V, E)$ and two subsets S and T of V, G contains a maximal DAG with its set of sources equal to S, and its set of targets equal to T. If this is true for maximal DAGs, it is also true for stories since any story is also a maximal DAG.

Consider a 3-CNF Boolean formula φ with clauses C_i, $i = 1, \dots, m$, over a set Boolean variables x_j, $j = 1, \dots, n$. We define a directed graph G as follows (see also Figure 20).

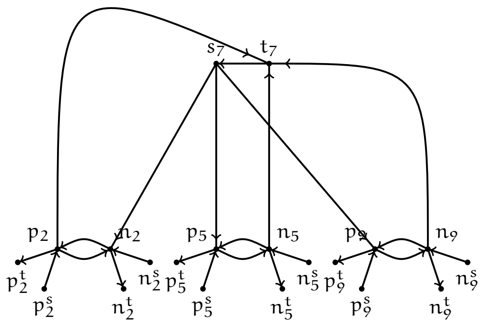

Figure 20: The subgraph corresponding to the clause $C_7 = \neg x_2 \vee x_5 \vee x_9$

- For each variable x_j, we create a set of six vertices, $p_j, p_j^s, p_j^t, n_j, n_j^s, n_j^t$, and for each clause C_i, two vertices s_i and t_i. We define the set $S = \{p_j^s, n_j^s \mid j = 1, \ldots, n\} \cup \{s_i \mid i = 1, \ldots, m\}$ and the set $T = \{p_j^t, n_j^t \mid j = 1, \ldots, n\} \cup \{t_i \mid i = 1, \ldots, m\}$.
- The set of arcs of G includes the six arcs

  $$(p_j^s, p_j), (p_j, p_j^t), (p_j, n_j), (n_j, p_j), (n_j^s, n_j), (n_j, n_j^t)$$

  related to each variable x_j and the arc (t_i, s_i) for each clause C_i.
- For each clause $C_i = l_i^1 \vee l_i^2 \vee l_i^3$, we introduce for each literal two arcs: if $l_i^h = x_j$ then we create the arcs (s_i, p_j) and (n_j, t_i), and if $l_i^h = \neg x_j$ the arcs (s_i, n_j) and (p_j, t_i), $h = 1, 2, 3$.

We prove that φ is satisfiable if and only if G includes a maximal DAG whose sets of sources and targets are, respectively, S and T.

Suppose φ is satisfiable and let τ be a satisfying truth-assignment. In the FAS F we include the arc (n_j, p_j) if $\tau(x_j) = \texttt{true}$ and the arc (p_j, n_j) if $\tau(x_j) = \texttt{false}$. Moreover, for each clause C_i, we include in F the arc (t_i, s_i) (see Figure 21). Clearly, the resulting subgraph $G - F$ is a DAG whose set of sources (respectively, targets) is equal to S (respectively, T). Moreover, $G - F$ is maximal since removing any arc from F would create either a two-vertex variable cycle or, for some clause C_i, at least one six-vertex cycle corresponding to a true literal in C_i.

Now suppose that G' is a maximal DAG with sources S and targets T. Clearly, for each clause C_i, the arc (t_i, s_i) is not in G'. Maximality of G' implies that for each variable x_j, exactly one of (p_j, n_j) and (n_j, p_j) is in G'. All other arcs are included in G'. Let τ be a truth-assignment defined as follows: for each variable x_j, $\tau(x_j) = \texttt{true}$ if and only if (p_j, n_j) is in G'. We prove that this assignment satisfies φ. Suppose, to the contrary, that there exists an unsatisfied clause C_i. Wlog we may assume that $C_i = x_1 \vee x_2 \vee x_3$ (see Figure 22). Then the three

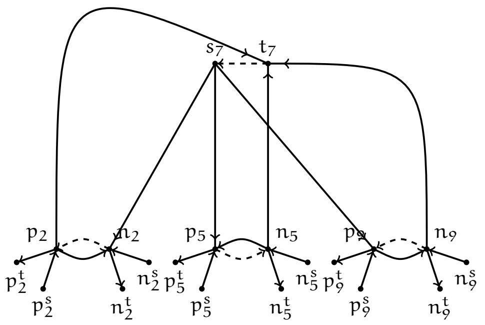

Figure 21: The directed acyclic subgraph corresponding to the truth assignment $\tau(x_2) =$ `true`, $\tau(x_5) =$ `false`, and $\tau(x_9) =$ `true` that satisfies the clause $C_7 = \neg x_2 \vee x_5 \vee x_9$: the dashed arcs are in the FAS

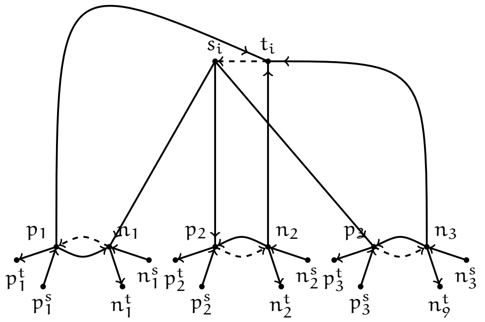

Figure 22: A directed acyclic subgraph (the dashed arcs are in the FAS) corresponding to the truth assignment $\tau(x_2) =$ `true`, $\tau(x_5) =$ `false`, and $\tau(x_9) =$ `false` that does not satisfy the clause $C_7 = \neg x_2 \vee x_5 \vee x_9$: the DAG is not maximal since the arc (t_7, s_7) can be taken out from the FAS.

cycles containing the arc (t_i, s_i) are broken both by this arc and by the three arcs (n_j, p_j), $j = 1, 2, 3$ not in G'. Hence, G' is not maximal since the arc (t_i, s_i) can be added to G' without creating any new cycle. This contradicts the hypothesis on G'. □

It is easy to modify the previous reduction in order to prove that the same result holds even if we specify only the set of sources *or* only the set of targets.

5.5 ENUMERATING STORIES

5.5.1 *Enumerating stories by enumerating* FASs

We already noticed that there exist graphs for which the set $\mathcal{S}(G)$ of minimal SASs and the set $\mathcal{F}(G)$ of minimal FASs are not comparable in terms of the inclusion relation. In this section, we show that, for some particular cases, $\mathcal{S}(G)$ is contained in $\mathcal{F}(G)$.

A white vertex $v \in \mathbb{W}$ is called *bad* if, for any predecessor p of v and for any successor s of v, there exists a cycle containing the arcs (p, v) and (v, s) (see Figure 23).

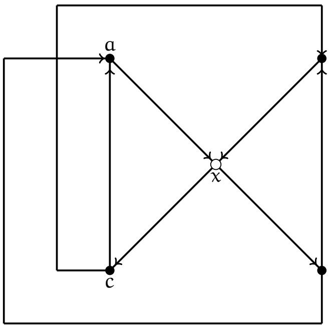

Figure 23: Example of a bad vertex. The minimal SAS $\{(a,x),(b,x),(x,c),(x,d)\}$ is not a minimal FAS.

Proposition 1. *Any $v \in \mathbb{W}$, which is not bad, belongs to every story.*

Proof. Consider a pitch P not containing v. As v is not bad, it has a predecessor p and a successor s such that there exists no cycle containing the arcs (p, v) and (v, s). By simplification rule 2, there exists a path $p_k, p_{k-1}, \ldots, p_1 = p$ with $k \geqslant 1$ such that $p_k \in \mathbb{B}$ and $p_i \in \mathbb{W}$, for any i with $i < k$. Let j be the minimum $i < k$ such that $p_i \in P$: if no such j exists, then we define $j = k$. Similarly a path $s = s_1, \ldots, s_{\ell-1}, s_\ell$ ending in a black vertex exists, and let $s_{j'}$ be the first vertex on that path belonging to P, or $s_{j'} = s_\ell$ if no such vertex exists.

Then $P' = P \cup \{(p_j, p_{j-1}), \ldots, (p, v), (v, s), \ldots, (s_{j'-1}, s_{j'})\}$ has no white source nor target as p_j and $s_{j'}$ are not white sources or targets in P. Moreover, P' is acyclic as P is acyclic and any cycle containing the additional path would contradict the fact that v is not a bad vertex. Thus any pitch not containing v is not maximal, hence not a story. □

Corollary 1. *If* G *does not include any bad vertex, then any minimal* SAS *is a minimal* FAS.

Proof. By absurdum, assume that A is a minimal SAS which is not a minimal FAS. Then, there exists an arc $e = (u, v) \in A$ such that $A \setminus \{e\}$ is a FAS but not a

SAS. This implies that in $G - (A \setminus \{e\})$, either u is a white target or v is a white source. We restrict ourselves to consider the latter case, since the former one can be dealt with similarly. Since v is a white source in $G - (A \setminus \{e\})$, and it is not in $G - A$, all arcs incident to v are in A. In other words, the story corresponding to A does not contain v, which contradicts Proposition 1. □

The previous proposition and its corollary state that, in a graph with no bad vertices, each story corresponds to a minimal FAS. This suggests that for such graphs, we could enumerate all stories by enumerating all the minimal FASs and by checking for each of them whether the resulting graph is a story (which can be done by checking that no white vertex is source or target). Unfortunately, there are graphs with no bad vertices in which the number of minimal FASs is exponentially larger than the number of minimal SASs. An example is given in Figure 24.

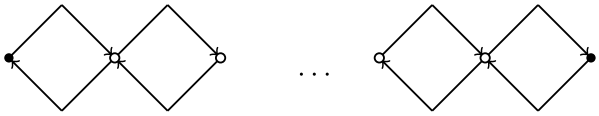

Figure 24: Graph with no bad vertex and in which the number of minimal FASs is 2^n and the number of minimal SASs is 2.

5.5.2 *Enumerating stories by enumerating permutations*

In the previous section, we suggested a method for enumerating all stories in the case of graphs with no bad vertices. Unfortunately, many graphs arising from the biological application briefly described in Section 5.1 contain a huge number of bad vertices. We thus need a method for enumerating stories which is able to deal with these cases.

Remember how we can find a single story as explained in the proof of Theorem 15. Consider the following two simple operations, CLEAN and CONSISTENT_ARCS. For any graph $G(\mathbb{B} \cup \mathbb{W}, E)$, and for any total order π of the vertices:

> $G'(\mathbb{B} \cup \mathbb{W}, E') \equiv \textsc{consistent\_arcs}(G, \pi)$: for each arc $(u, v) \in E$, $(u, v) \in E'$ if $\pi(u) < \pi(v)$;
>
> $G'(\mathbb{B} \cup \mathbb{W}', E') \equiv \textsc{clean}(G)$: recursively remove white vertices that are sources, targets or isolated in G.

We can thus define the composed operation

$$\textsc{pitch}(G, \pi) = \textsc{clean}(\textsc{consistent\_arcs}(G, \pi)).$$

PITCH produces a pitch since the resulting graph G' contains only arcs that respect the order π and therefore is acyclic. Moreover, due to the cleaning step, G' is guaranteed to have neither white sources nor white targets.

Theorem 17. *For any story S, there exists a permutation π such that* PITCH(G, π) $= S$.

Proof. It is enough to show that, for any story S of $G = (\mathbb{B} \cup \mathbb{W}, E)$ and for any topological order π of $V(S)$, PITCH$(G, \pi) = S$. Because of the maximality of a story, it suffices to show that $S \subseteq$ PITCH(G, π). Given an arc (u, v) of S, we have $\pi(u) < \pi(v)$. Therefore (u, v) is in CONSISTENT_ARCS(G, π). Since (u, v) is an arc of S, there exists a path p in S between two black vertices containing u and v. Then p is also in CONSISTENT_ARCS(G, π), and thus u and v are both black or, if one or both of them is white, then they are neither source nor target in CONSISTENT_ARCS(G, π). Since CLEAN(CONSISTENT_ARCS(G, π)) removes neither black nor white vertices that are neither source nor target, we conclude that (u, v) is also in CLEAN(CONSISTENT_ARCS(G, π)) $=$ PITCH(G, π). □

This theorem together with Theorem 15 suggest an approach to enumerate stories which simply consists in generating all permutations π of the vertices of G and computing $P =$ PITCH(G, π): if P is not a story, then we use COMPLETE_PITCH to grow it into a story.

In order to avoid to output several times the same story, we store in memory the previous solutions and every time we check whether the current story has been already generated.

It is worth observing that, in order to enumerate all the stories, all the possible permutations should be inspected. Thus the resulting total complexity is $\Omega(n!)$, even in the case of a graph with a constant number of stories, like the one shown in Figure 24.

5.6 ENUMERATING STORIES: AN EXAMPLE

Referring to the graph $G = (\mathbb{B} \cup \mathbb{W}, E)$ shown in Figure 25a, the subgraph of G, $G' = (\mathbb{B} \cup \mathbb{W}, \{(a, b), (c, d), (e, f), (f, c)\})$ is a pitch. Let $\pi = \langle a, b, e, f, c, d \rangle$ be an ordering of its vertices. In order to complete this pitch in a story, Algorithm 22 consider in the first iteration the vertex b and a BFS from b until the vertices belonging to the pitch c and f are reached: the corresponding paths are simply the arcs out-going from b, (b, c) and (b, f); since b is not comparable with c and f, both the arcs are added. The next vertex to be considered is f: the BFS from f gives the arcs (f, a) and (f, d); the arc (f, a) cannot be added since $a > f$, while the arc (f, d) is added since $f < d$. The next vertex considered is thus d, and the BFS from d until the vertices belonging to the pitch are reached: the corresponding path is the arc (d, e) and, since $d > e$, this arc is not added to the pitch. The subgraph of G, shown in Figure 25b, $G'' = (\mathbb{B} \cup \mathbb{W}, E'')$, where $E'' = \{(a,b),(b,c),(b,f),(c,d),(e,f),(f,c),(f,d)\}$, is thus a story.

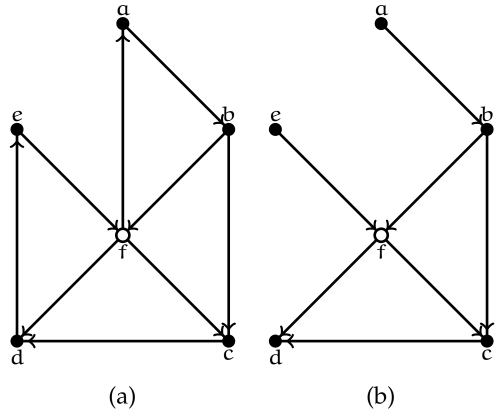

Figure 25: An example of network and story

Given a new ordering of the vertices $\pi = \langle f,d,e,a,b,c \rangle$, the operation CONSISTENT_ARCS activates the following set of arcs:

$$\{(a,b),(b,c),(d,e),(f,a),(f,c),(f,d)\}$$

that are the arcs compatible with the given order. Indeed the arcs (b,f), (c,d), (e,f) are not compatible with π. Since f is a white source, the operation CLEAN deletes the arcs (f,a), (f,c), (f,d). The resulting set of arcs $\{(a,b),(b,c),(d,e)\}$ induces a pitch. By applying Algorithm 22, it is thus possible to complete the pitch in order to get a story.

Observe that in the graph shown in Figure 25a, it is possible to verify the Theorem 17: for any story S there exists an order π of its vertices such that $\text{PITCH}(G,\pi) = S$. Considering the story G'', shown in Figure 25b, the ordering of the vertices $\pi = \langle a,b,e,f,c,d \rangle$ is such that $\text{PITCH}(G,\pi) = G''$. Indeed by starting from this order, the operation CONSISTENT_ARCS activates all the arcs in E'', that are the arcs compatible with the given order. The arcs (d,e) and (f,a) are indeed not compatible with π. The operation CLEAN does not affect the solution, since no white source or target is present. Thus E'' induces a pitch that is also a story.

5.7 ALTERNATIVE DEFINITION OF A STORY

It is clear that, according to our definition of a story, no white vertex can be either source or target in the original graph, since otherwise such a white vertex would not belong to any story. This implies that the original graph can be seen as the union of a finite set $\mathcal{P}$ of directed paths between black vertices: in particular, if $\mathcal{P}$ includes all paths between every pair of black vertices, then it is

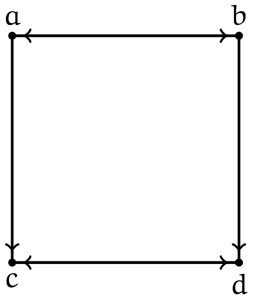

Figure 26: Graph obtained by two paths (a, b, d, c) and (b, a, c, d). According to the alternative definition, this graph clearly contains only two stories, which correspond to the two paths. According to the original definition, instead, the graph contains the following four minimal SAS: $\{(a, b), (c, d)\}$, $\{(a, b), (d, c)\}$, $\{(b, a), (c, d)\}$, and $\{(b, a), (d, c)\}$. Note that these four minimal SAS originated four stories which are all different from the two stories obtained according to the second definition.

easy to verify that a story is a maximal subset $\mathcal{S}$ of $\mathcal{P}$ such that the graph defined as the union of the paths in $\mathcal{S}$ is acyclic and there exists no path p in $\mathcal{P} - \mathcal{S}$ that can be added to $\mathcal{S}$ without disturbing the acyclicity. Let us call this alternative definition of story a *path-story*. A minimal number of paths to be removed from $\mathcal{P}$ such that the union of the remaining paths is a path-story is called a *feedback path set*.

A natural question is whether the problem changes when a set $\mathcal{P}$ is given as input, and the graph $G_{\mathcal{P}}$ is defined by the union of the paths of $\mathcal{P}$, where the endpoints of the paths in $\mathcal{P}$ form the set of black vertices of $G_{\mathcal{P}}$. Clearly, since $\mathcal{P}$ may not contain all paths between every pair of the black vertices in $G_{\mathcal{P}}$, the set of path-stories of $G_{\mathcal{P}}$ is different from the set of stories of $G_{\mathcal{P}}$ (see for an example Figure 26). We will prove that enumerating path-stories is at least as hard as enumerating hitting sets, which is a well-known enumeration problem (for a survey, we refer to [205]) with its computational complexity still open, after more than 28 years.

Theorem 18. *Enumerating path-stories is at least as hard as enumerating minimal hitting sets.*

Proof. Let $\mathcal{C}$ be a collection of subsets of a domain set X. $H \subset X$ is a *hitting set* of $\mathcal{C}$ if for any $C \in \mathcal{C}$, $H \cap C \neq \emptyset$.

We reduce $\mathcal{C}$ to a collection $\mathcal{P}$ of paths, such that there is a bijective correspondence between (minimal) hitting sets of $\mathcal{C}$ and (minimal) feedback path sets of $\mathcal{P}$ and, hence, between hitting sets of $\mathcal{C}$ and path-stories of $\mathcal{P}$.

We order all sets of $\mathcal{C}$ and all elements of X. Within any set of $\mathcal{C}$ the elements are ordered. For each element in each set we create a vertex of the graph $G_{\mathcal{P}}$.

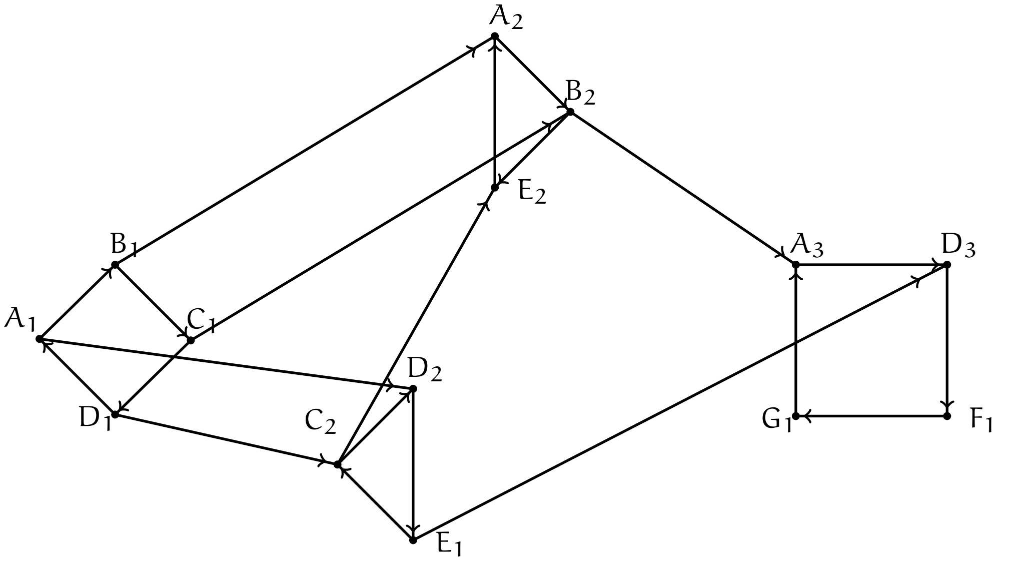

Figure 27: An example of reduction: $C_1 = \{A, B, C, D\}$, $C_2 = \{C, D, E\}$, $C_3 = \{A, B, E\}$, and $C_4 = \{A, D, F, G\}$.

For each set $C_i \in \mathcal{C}$ with $C_i = \{x_{i_1}, \dots, x_{i_{k_i}}\}$, create a cycle by introducing the arcs $(x_{i_\ell}, x_{i_{\ell+1}})$, $\ell = 1, \dots, k_i$ and $(x_{i_{k_i}}, x_{i_1})$. We call this cycle also C_i. Moreover, suppose that $x_{i_\ell} = x_j$ is the h-th occurrence of x_j and x_{r_t} the next occurrence, then we introduce an arc $(x_{i_{\ell+1}}, x_{r_t})$, i.e., there is a path of two arcs between any two consecutive occurrences of the same element. Let us call the latter set of arcs the *element-arcs* and the set of arcs on the cycles the *set-arcs*. Notice that the element arcs are not in any cycle.

Now for each element x_j we define a path $P_j \in \mathcal{P}$, by starting in the vertex of the first occurrence of x_j, and every time selecting the two arcs connecting it to the next occurrence vertex, until we arrive at the last occurrence vertex.

The graph induced by $\mathcal{P}$ contains all the arcs just introduced. In particular it contains all the cycles corresponding to the sets in $\mathcal{C}$. An example of the reduction is shown in Figure 27.

It is easy to see that a path P_j cuts cycle C_i if and only if x_j hits the set C_i. Hence there is a one-to-one correspondence between a minimal path set of $\mathcal{P}$ and a minimal hitting set of $\mathcal{C}$. This proves the theorem. □

In this chapter we have mainly focused our attention on the first definition of stories, since this definition seems to fit better with the informal subnetwork definition the biologists are looking for.

5.8 CONCLUSION AND OPEN PROBLEMS

In this chapter, we have introduced the new notion of a story, which is a maximal acyclic subgraph of a directed graph in which only specified vertices can be sources or targets. We have proved some complexity results and designed some algorithms for enumerating all possible stories of a graph. From a theoretical point of view, the main question left open is to establish the complexity of the enumeration problem. Indeed the enumeration algorithm presented, even if it works well in practice, as shown by [203], gives no guarantee on the delay between the output of two consecutive solutions. Notice that any changes in the definition will imply a revision of the formal results, and may even imply that finding one story can not be polynomial-solvable. We address as a future work, exploiting the relationship between stories and subset feedback vertex sets, that has been studied in [206] by applying a *Measure and Conquer* approach [207].

From a practical point of view, for some graphs the number of solutions found is extremely large and therefore the analysis of the results is compromised. Adding more constraints to the model could be a way to filter a priori the set of solutions.

This observation on the size of the output leads us to consider the problem from a modeling point of view. For instance, the acyclicity constraint could be relaxed allowing cycles between white vertices. Moreover, the model could be enriched by exploring the information on the concentrations given by the metabolomics experiment. Notice that in this case the nature of the problem changes into an optimization problem. Another alternative is to consider integrated models, adding to the Metabolic network other layers of information such as regulation, or taking the stoichiometry of the reactions into account. Finally, in metabolomics a current challenge is to correctly predict which are the metabolites corresponding to the peaks in the spectrum and whether the changes in concentration are actually significant, which suggests that the model should also account for noisy data corresponding to on incertitude on the *interesting* or *not interesting* labels assigned to the vertices.

6 ENUMERATING CYCLES AND (S,T)-PATHS IN UNDIRECTED GRAPHS

We present the first optimal solution to list all the simple cycles in an undirected graph G *with* n *vertices and* m *edges. Specifically, let* $\mathcal{C}(G)$ *denote the set of all these cycles. For a cycle* $c \in \mathcal{C}(G)$*, let* $|c|$ *denote the number of edges in* c*. Our algorithm requires* $O(m + \sum_{c \in \mathcal{C}(G)} |c|)$ *time and is asymptotically optimal:* $\Omega(m)$ *time is necessarily required to read* G *as input, and* $\Omega(\sum_{c \in \mathcal{C}(G)} |c|)$ *time is required to list the output.*

We also present the first optimal solution to list all the simple paths from s *to* t *(shortly,* (s,t)*-paths) in an undirected graph* G*. Let* $\mathcal{P}_{st}(G)$ *denote the set of* (s,t)*-paths in* G *and, for an* (s,t)*-path* $\pi \in \mathcal{P}_{st}(G)$*, let* $|\pi|$ *be the number of edges in* π*. Our algorithm lists all the* (s,t)*-paths in* G *optimally in* $O(m + \sum_{\pi \in \mathcal{P}_{st}(G)} |\pi|)$ *time.*

This result can be useful for undirected Protein-Protein Interaction networks. The main question arising from our work, is whether it is possible to extend our result to directed graphs in order to efficiently deal also with interaction networks in general, as signalling and gene regulatory networks.

6.1 INTRODUCTION

Listing all the simple cycles (hereafter just called cycles) in a graph is a classical problem whose efficient solutions date back to the early 70s. For a graph with n vertices and m edges, containing η cycles, the best known solution in the literature is given by Johnson's algorithm [18] and takes $O((\eta + 1)(m + n))$ time. In the case of biological networks, studying paths or cycles can be useful for several purposes. In the case of interaction graphs, such as gene regulatory networks, the importance of enumeration has been shown in [14], and two algorithms for this problem have been proposed in [28, 14]. As shown in Chapter 2, these networks are directed and their arcs are signed, where the sign or weight of the arcs indicates the causal relationship between the vertices, such as activation or inhibition. In particular, as summarized by [14], cycles and paths can be useful for studying:

- dependencies among vertices: a vertex x activates another vertex y when at least one positive path from x to y exists but no negative one [28].
- the steady state and multistationarity of dynamic models [208, 15, 16].

- monotonicity with respect to changes in the initial conditions [209].

In particular the enumeration of cycles and paths can be useful for investigating:

- feedback loops, that are claimed to be sources of complex dynamics [15, 16]. Moreover feedback loops are related to robustness in cell signalling networks [17].
- signalling paths, by analysing the different positive and negative routes along which a molecule can affect another.
- (Minimal) cut sets: for a given set of feedback loops or signalling paths one may compute a set of interventions interrupting the signal flow in them [28].

In the following we will consider the problem of enumerating paths and cycles in the case of undirected graphs. Our contribution is not just restricted to biological networks, but extends also to arbitrary graph. This result can be useful for undirected Protein-Protein Interaction networks, but in the case of interaction networks in general, our approach neglects the effects of the controls, i.e. the sign and direction of the arcs. In this latter case, the cycles can be enumerated in the underlying undirected graph and *a posteriori* filtered or *ad hoc* algorithms can be applied. The main question arising from our work, is whether it is possible to extend it to directed graphs in order to efficiently deal also with this kind of networks.

PREVIOUS WORK. The classical problem of listing all the cycles of a graph has been extensively studied for its many applications in several fields, ranging from the mechanical analysis of chemical structures [210] to the design and analysis of reliable communication networks, and the graph isomorphism problem [211]. In particular, at the turn of the seventies several algorithms for enumerating all cycles of an undirected graph have been proposed. There is a vast body of work, and the majority of the algorithms listing all the cycles can be divided into the following three classes (see [212, 213] for excellent surveys).

1. *Search space algorithms.* According to this approach, cycles are looked for in an appropriate search space. In the case of undirected graphs, the *cycle vector space* [214] turned out to be the most promising choice: from a basis for this space, all vectors are computed and it is tested whether they are a cycle. Since the algorithm introduced in [211], many algorithms have been proposed: however, the complexity of these algorithms turns out to be exponential in the dimension of the vector space, and thus in n. For planar graphs, an algorithm listing cycles in $O((\eta + 1)n)$ time was presented in [215].

2. *Backtrack algorithms.* By this approach, all paths are generated by backtrack and, for each path, it is tested whether it is a cycle. One of the first algorithms is the one proposed in [21], which is however exponential in η. By adding a simple pruning strategy, this algorithm has been successively modified in [60]: it lists all the cycles in $O(nm(\eta+1))$ time. Further improvements were proposed in [18, 216, 61], leading to $O((\eta+1)(m+n))$-time algorithms that work for both directed and undirected graphs.

3. *Using the powers of the adjacency matrix.* This approach uses the so-called *variable adjacency matrix*, that is, the formal sum of edges joining two vertices. A non-zero element of the p-th power of this matrix is the sum of all walks of length p: hence, to compute all cycles, we compute the nth power of the variable adjacency matrix. This approach is not very efficient because of the non-simple walks. Algorithms based on this approach (e.g. [217, 218]) basically differ only on the way they avoid to consider walks that are neither paths nor cycles.

Almost 40 years after Johnson's algorithm [18], the problem of efficiently listing all cycles of a graph is still an active area of research (e.g. [22, 219, 220, 221, 222, 223, 224]). Nevertheless, no significant improvement has been obtained from the theory standpoint: in particular, Johnson's algorithm is still the theoretically most efficient. His $O((\eta+1)(m+n))$-time solution and its linear delay guarantee is surprisingly not optimal for undirected graphs as we show in this chapter.

CONTRIBUTION. We present the first optimal solution to list all the cycles in an undirected graph G. Specifically, let $\mathcal{C}(G)$ denote the set of all these cycles ($|\mathcal{C}(G)| = \eta$). Our algorithm requires $O(m + \sum_{c\in\mathcal{C}(G)} |c|)$ time and is asymptotically optimal: indeed, $\Omega(m)$ time is necessarily required to read G as input, and $\Omega(\sum_{c\in\mathcal{C}(G)} |c|)$ time is necessarily required to list the output. Since the length of a cycle $|c| \leqslant n$, the cost of our algorithm never exceeds $O(m + (\eta+1)n)$ time.

Along the same lines, we also present the first optimal solution to list all the simple paths from s to t (shortly, (s,t)-paths) in an undirected graph G. Let $\mathcal{P}_{st}(G)$ denote the set of (s,t)-paths in G. Our algorithm lists all the (s,t)-paths in G optimally in $O(m + \sum_{\pi\in\mathcal{P}_{st}(G)} |\pi|)$ time, observing that $\Omega(\sum_{\pi\in\mathcal{P}_{st}(G)} |\pi|)$ time is necessarily required to list the output.

We prove the following reduction to relate $\mathcal{C}(G)$ and $\mathcal{P}_{st}(G)$ for some suitable choices of vertices s, t: if there exists an optimal algorithm to list the (s,t)-paths in G, then there exists an optimal algorithm to list the cycles in G. Hence, we can focus on listing (s,t)-paths.

Our work appeared in [19].

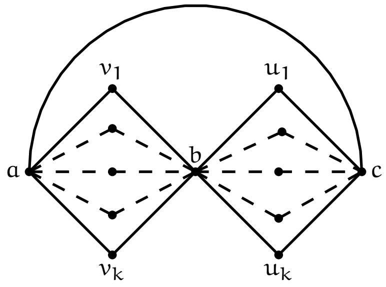

Figure 28: Diamond graph.

DIFFICULT GRAPHS FOR JOHNSON'S ALGORITHM. It is worth observing that the analysis of the time complexity of Johnson's algorithm is not pessimistic and cannot match the one of our algorithm for listing cycles. For example, consider the sparse "diamond" graph $D_n = (V, E)$ in Fig. 28 with $n = 2k + 3$ vertices in $V = \{a, b, c, v_1, \dots, v_k, u_1, \dots, u_k\}$. There are $m = \Theta(n)$ edges in $E = \{(a, c), (a, v_i), (v_i, b), (b, u_i), (u_i, c)$, for $1 \leqslant i \leqslant k\}$, and three kinds of (simple) cycles: (1) $(a, v_i), (v_i, b), (b, u_j), (u_j, c), (c, a)$ for $1 \leqslant i, j \leqslant k$; (2) $(a, v_i), (v_i, b), (b, v_j), (v_j, a)$ for $1 \leqslant i < j \leqslant k$; (3) $(b, u_i), (u_i, c), (c, u_j), (u_j, b)$ for $1 \leqslant i < j \leqslant k$, totalizing $\eta = \Theta(n^2)$ cycles. Our algorithm takes $\Theta(n + k^2) = \Theta(\eta) = \Theta(n^2)$ time to list these cycles. On the other hand, Johnson's algorithm takes $\Theta(n^3)$ time, and the discovery of the $\Theta(n^2)$ cycles in (1) costs $\Theta(k) = \Theta(n)$ time each: the backtracking procedure in Johnson's algorithm starting at a, and passing through v_i, b and u_j for some i, j, arrives at c: at that point, it explores all the vertices u_l $(l \neq i)$ even if they do not lead to cycles when coupled with a, v_i, b, u_j, and c.

STRUCTURE OF THE CHAPTER. This chapter is organised as follows: after introducing the main definitions and notations in Section 6.2, in Section 6.3 we show the main ideas of our algorithm; in Section 6.4 the general amortization strategy of our analysis is reported and in Section 6.5 the maintenance of the certificate, a data structure used by the algorithm, is described; in Section 6.6 we show how the algorithm works through an example and in Section 6.7 we explain in detail the operations performed by the algorithm and its analysis; finally, we conclude in Section 6.8.

6.2 PRELIMINARIES

Let $G = (V, E)$ be an undirected connected graph with $n = |V|$ vertices and $m = |E|$ edges, without self-loops or parallel edges. Recall that $\mathcal{P}(G)$ is the set of all paths in G and $\mathcal{P}_{s,t}(G)$ is the set of all (s, t)-paths in G. When $s = t$ we have cycles, and $\mathcal{C}(G)$ denotes the set of all cycles in G. In this chapter, given an undirected graph $G = (V, E)$ we consider the problems of listing all the cycles

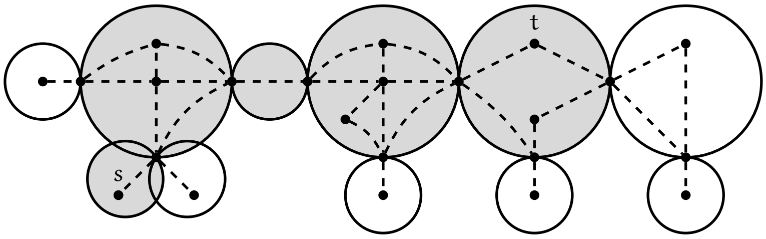

Figure 29: Block tree of G with bead string $B_{s,t}$ in gray.

$c \in \mathcal{C}(G)$ (*listing Cycles*) and all the paths $\pi \in \mathcal{P}_{s,t}(G)$ between two given distinct vertices $s, t \in V$ (*listing (s,t)-Paths*).

Our algorithms assume without loss of generality that the input graph G is connected, hence $m \geqslant n - 1$, and use the decomposition of G into biconnected components. Recall that an *articulation point* (or cut-vertex) is a vertex $u \in V$ such that the number of connected components in G increases when u is removed. G is *biconnected* if it has no articulation points. Otherwise, G can always be decomposed into a tree of biconnected components, called the *block tree*, where each biconnected component is a maximal biconnected subgraph of G (see Fig. 29), and two biconnected components are adjacent if and only if they share an articulation point.

6.3 overview and main ideas

While the basic approach is simple (see the binary partition in point 3), we use a number of non-trivial ideas to obtain our optimal algorithm for an undirected (connected) graph G as summarized in the steps below.

1. Prove the following reduction. If there exists an optimal algorithm to list the (s, t)-paths in G, there exists an optimal algorithm to list the cycles in G. This relates $\mathcal{C}(G)$ and $\mathcal{P}_{st}(G)$ for some choices s, t.

2. Focus on listing the (s, t)-paths. Consider the decomposition of the graph into biconnected components (bccs), thus forming a tree T where two bccs are adjacent in T iff they share an articulation point. Exploit (and prove) the property that if s and t belong to distinct bccs, then (i) there is a unique *sequence* $B_{s,t}$ of adjacent bccs in T through which each (s, t)-path must necessarily pass, and (ii) each (s, t)-path is the concatenation of paths connecting the articulation points of these bccs in $B_{s,t}$.

3. Recursively list the (s, t)-paths in $B_{s,t}$ using the classical binary partition (i.e. given an edge e in G, list all the cycles containing e, and then all the cycles not containing e): now it suffices to work on the *first* bcc in $B_{s,t}$, and efficiently maintain it when deleting an edge e, as required by the binary partition.

4. Use a notion of *certificate* to avoid recursive calls (in the binary partition) that do not list new (s,t)-paths. This certificate is maintained dynamically as a data structure representing the first BCC in $B_{s,t}$, which guarantees that there exists at least one *new* solution in the current $B_{s,t}$.

5. Consider the binary recursion tree corresponding to the binary partition. Divide this tree into *spines*: a spine corresponds to the recursive calls generated by the edges e belonging to the same adjacency list in $B_{s,t}$. The amortized cost for each listed (s,t)-path π is $O(|\pi|)$ when there is a guarantee that the amortized cost in each spine S is $O(\mu)$, where μ is a lower bound on the number of (s,t)-paths that will be listed from the recursive calls belonging to S. The (unknown) parameter μ, which is different for each spine S, and the corresponding cost $O(\mu)$, will drive the design of the proposed algorithms.

6.3.1 *Reduction to $(\mathbf{s},\mathbf{t})$-paths*

We now show that listing cycles reduces to listing (s,t)-paths while preserving the optimal complexity.

Lemma 7. *Given an algorithm that solves the problem of* listing (s,t)-Paths *in optimal* $O(m + \sum_{\pi \in \mathcal{P}_{s,t}(G)} |\pi|)$ *time, there exists an algorithm that solves the problem of* listing Cycles *in optimal* $O(m + \sum_{c \in \mathcal{C}(G)} |c|)$ *time.*

Proof. Compute the biconnected components of G and keep them in a list L. Each (simple) cycle is contained in one of the biconnected components and therefore we can treat each biconnected component individually as follows. While L is not empty, extract a biconnected component $B = (V_B, E_B)$ from L and repeat the following three steps: (i) compute a DFS traversal of B and take any back edge $b = (s,t)$ in B; (ii) list all (s,t)-paths in $B - b$, i.e. the cycles in B that include edge b; (iii) remove edge b from B, compute the new biconnected components thus created by removing edge b, and append them to L. When L becomes empty, all the cycles in G have been listed.

Creating L takes $O(m)$ time. For every $B \in L$, steps (i) and (iii) take $O(|E_B|)$ time. Note that step (ii) always outputs distinct cycles in B (i.e. (s,t)-paths in $B - b$) in $O(|E_B| + \sum_{\pi \in \mathcal{P}_{s,t}(B-b)} |\pi|)$ time. However, $B - b$ is then decomposed into biconnected components whose edges are traversed again. We can pay for the latter cost: for any edge $e \neq b$ in a biconnected component B, there is always a cycle in B that contains both b and e (i.e. it is an (s,t)-path in $B - b$), hence $\sum_{\pi \in \mathcal{P}_{s,t}(B-b)} |\pi|$ dominates the term $|E_B|$, i.e. $\sum_{\pi \in \mathcal{P}_{s,t}(B-b)} |\pi| = \Omega(|E_B|)$. Therefore steps (i)–(iii) take $O(\sum_{\pi \in \mathcal{P}_{s,t}(B-b)} |\pi|)$ time. When L becomes empty, the whole task has taken $O(m + \sum_{c \in \mathcal{C}(G)} |c|)$ time. □

6.3.2 *Decomposition in biconnected components*

We now focus on listing (s,t)-paths. We use the decomposition of G into a block tree of biconnected components. Given vertices s,t, define its *bead string*, denoted by $B_{s,t}$, as the unique sequence of one or more adjacent biconnected components (the *beads*) in the block tree, such that the first one contains s and the last one contains t (see Fig. 29): these biconnected components are connected through articulation points, which must belong to all the paths to be listed.

Lemma 8. *All the (s,t)-paths in $\mathcal{P}_{s,t}(G)$ are contained in the induced subgraph $G[B_{s,t}]$ for the bead string $B_{s,t}$. Moreover, all the articulation points in $G[B_{s,t}]$ are traversed by each of these paths.*

Proof. Consider an edge $e = (u, v)$ in G such that $u \in B_{s,t}$ and $v \notin B_{s,t}$. Since the biconnected components of a graph form a tree and the bead string $B_{s,t}$ is a path in this tree, there are no paths $v \rightsquigarrow w$ in $G - e$ for any $w \in B_{s,t}$ because the biconnected components in G are maximal and there would be a larger one (a contradiction). Moreover, let $B_1, B_2, \dots, B_r$ be the biconnected components composing $B_{s,t}$, where $s \in B_1$ and $t \in B_r$. If there is only one biconnected component in the path (i.e. $r = 1$), there are no articulation points in $B_{s,t}$. Otherwise, all of the $r - 1$ articulation points in $B_{s,t}$ are traversed by each path $\pi \in \mathcal{P}_{s,t}(G)$: indeed, the articulation point between adjacent biconnected components B_i and B_{i+1} is their only vertex in common and there are no edges linking B_i and B_{i+1}.

□

We thus restrict the problem of listing the paths in $\mathcal{P}_{s,t}(G)$ to the induced subgraph $G[B_{s,t}]$, conceptually isolating it from the rest of G. For the sake of description, we will use interchangeably $B_{s,t}$ and $G[B_{s,t}]$ in the rest of the chapter.

6.3.3 *Binary partition scheme*

We list the set of (s,t)-paths in $B_{s,t}$, denoted by $\mathcal{P}_{s,t}(B_{s,t})$, by applying the binary partition method (where $\mathcal{P}_{s,t}(G) = \mathcal{P}_{s,t}(B_{s,t})$ by Lemma 8): we choose an edge $e = (s, v)$ incident to s and then list all the (s,t)-paths that include e and then all the (s,t)-paths that do not include e. Since we delete some vertices and some edges during the recursive calls, we proceed as follows.

Invariant: At a generic recursive step on vertex u (initially, $u := s$), let $\pi_s = s \rightsquigarrow u$ be the path discovered so far (initially, π_s is empty {}). Let $B_{u,t}$ be the current bead string (initially, $B_{u,t} := B_{s,t}$). More precisely, $B_{u,t}$ is defined as follows: (i) remove from $B_{s,t}$ all the vertices in π_s but u, and the edges incident to u and discarded so far; (ii) recompute the block tree on the resulting graph; (iii) $B_{u,t}$ is the unique bead string that connects u to t in the recomputed block tree.

Base case: When $u = t$, output the (s,t)-path π_s.

Recursive rule: Let $\mathcal{P}(\pi_s, u, B_{u,t})$ denote the set of (s,t)-paths to be listed by the current recursive call. Then, it is the union of the following two disjoint sets, for an edge $e = (u, v)$ incident to u:

- *Left branching:* the (s,t)-paths in $\mathcal{P}(\pi_s \cdot e, v, B_{v,t})$ that use e, where $B_{v,t}$ is the unique bead string connecting v to t in the block tree resulting from the deletion of vertex u from $B_{u,t}$.
- *Right branching:* the (s,t)-paths in $\mathcal{P}(\pi_s, u, B'_{u,t})$ that do *not* use e, where $B'_{u,t}$ is the unique bead string connecting u to t in the block tree resulting from the deletion of edge e from $B_{u,t}$.

Hence, $\mathcal{P}_{s,t}(B_{s,t})$ (and so $\mathcal{P}_{s,t}(G)$) can be computed by invoking $\mathcal{P}(\{\}, s, B_{s,t})$. The correctness and completeness of the above approach is discussed in Section 6.3.4.

At this point, it should be clear why we introduce the notion of bead strings in the binary partition. The existence of the partial path π_s and the bead string $B_{u,t}$ guarantees that there surely exists at least one (s,t)-path. But there are two sides of the coin when using $B_{u,t}$.

1. One advantage is that we can avoid useless recursive calls: If vertex u has only one incident edge e, we just perform the left branching; otherwise, we can safely perform both the left and right branching since the *first* bead in $B_{u,t}$ is always a biconnected component by definition (thus there exists both an (s,t)-path that traverses e and one that does not).
2. The other side of the coin is that we have to maintain the bead string $B_{u,t}$ as $B_{v,t}$ in the left branching and as $B'_{u,t}$ in the right branching by Lemma 8. Note that these bead strings are surely non-empty since $B_{u,t}$ is non-empty by induction (we only perform either left or left/right branching when there are solutions by item 1).

To efficiently address point 2, we need to introduce the notion of certificate as described next.

6.3.4 *Introducing the certificate*

Given the bead string $B_{u,t}$, we call the *head* of $B_{u,t}$, denoted by H_u, the first biconnected component in $B_{u,t}$, where $u \in H_u$. Consider a DFS tree of $B_{u,t}$ rooted at u that changes along with $B_{u,t}$, and classify the edges in $B_{u,t}$ as tree edges or back edges (there are no cross edges since the graph is undirected).

To maintain $B_{u,t}$ (and so H_u) during the recursive calls, we introduce a *certificate* C (see Fig. 30): It is a suitable data structure that uses the above classification of the edges in $B_{u,t}$, and supports the following operations, required by the binary partition scheme.

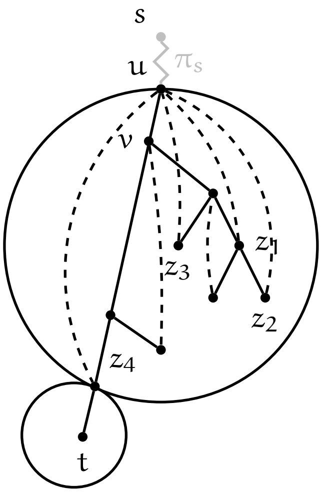

Figure 30: Example certificate of $B_{u,t}$

- `choose`(C, u): returns an edge $e = (u, v)$ with $v \in H_u$ such that $\pi_s \cdot (u, v) \cdot u \rightsquigarrow t$ is an (s, t)-path such that $u \rightsquigarrow t$ is inside $B_{u,t}$. Note that e always exists since H_u is biconnected. Also, the chosen v is the last one in DFS postorder among the neighbours of u: in this way, the (only) tree edge e is returned when there are no back edges leaving from u. (As it will be clear in Sections 6.4 and 6.5, this order facilitates the analysis and the implementation of the certificate.)

- `left_update`(C, e): for the given $e = (u, v)$, it obtains $B_{v,t}$ from $B_{u,t}$ as discussed in Section 6.3.3. This implies updating also H_u, C, and the block tree, since the recursion continues on v. It returns bookkeeping information I for what is updated, so that it is possible to revert to $B_{u,t}$, H_u, C, and the block tree, to their status before this operation.

- `right_update`(C, e): for the given $e = (u, v)$, it obtains $B'_{u,t}$ from $B_{u,t}$ as discussed in Section 6.3.3, which implies updating also H_u, C, and the block tree. It returns bookkeeping information I as in the case of `left_update`(C, e).

- `restore`(C, I): reverts the bead string to $B_{u,t}$, the head H_u, the certificate C, and the block tree, to their status before operation $I :=$ `left_update`(C, e) or $I :=$ `right_update`(C, e) was issued (in the same recursive call).

Note that a notion of certificate in listing problems has been introduced in [225], but it cannot be directly applied to our case due to the different nature of the problems and our use of more complex structures such as biconnected components.

Algorithm 23: list_paths$_{s,t}(\pi_s$, u, $C)$

```
1  if $u = t$ then
2      output($\pi_s$) ;
3      return ;
4  end
5  $e = (u,v) \leftarrow$ choose($C,u$) ;
6  if $e$ is back edge then
7      $I \leftarrow$ right_update($C,e$) ;
8      list_paths$_{s,t}$($\pi_s$, $u$, $C$) ;
9      restore($C,I$) ;
10 end
11 $I \leftarrow$ left_update($C,e$) ;
12 list_paths$_{s,t}$($\pi_s \cdot (u,v)$, $v$, $C$) ;
13 restore($C,I$) ;
```

Using our certificate and its operations, we can now formalize the binary partition and its recursive calls $\mathcal{P}(\pi_s, u, B_{u,t})$ described in Section 6.3.3 as Algorithm 23, where $B_{u,t}$ is replaced by its certificate C.

The base case ($u = t$) corresponds to lines 1–4 of Algorithm 23. During recursion, the left branching corresponds to lines 5 and 11-13, while the right branching to lines 5–10. Note that we perform only the left branching when there is only one incident edge in u, which is a tree edge by definition of choose. Also, lines 9 and 13 are needed to restore the parameters to their values when returning from the recursive calls.

Lemma 9. *Algorithm 23 correctly lists all the* (s,t)*-paths in* $\mathcal{P}_{s,t}(G)$.

Proof. For a given vertex u the function choose(C, u) returns an edge e incident to u. We maintain the invariant that π_s is a path $s \rightsquigarrow u$, since at the point of the recursive call in line 12: (i) is connected as we append edge (u, v) to π_s and; (ii) it is simple as vertex u is removed from the graph G in the call to left_update(C, e) in line 11. In the case of recursive call in line 8 the invariant is trivially maintained as π_s does not change. The algorithm only outputs (s,t)-paths since π_s is a $s \rightsquigarrow u$ path and $u = t$ when the algorithm outputs, in line 2.

The paths with prefix π_s that do not use e are listed by the recursive call in line 8. This is done by removing e from the graph (line 7) and thus no path can include e. Paths that use e are listed in line 12 since in the recursive call e is added to π_s. Given that the tree edge incident to u is the last one to be returned by choose(C, u), there is no path that does not use this edge, therefore it is not necessary to call line 8 for this edge.

□

A natural question is what is the time complexity: we must account for the cost of maintaining C and for the cost of the recursive calls of Algorithm 23. Since we cannot always maintain the certificate in $O(1)$ time, the ideal situation for attaining an optimal cost is taking $O(\mu)$ time if at least μ (s,t)-paths are listed in the current call (and its nested calls). Unfortunately, we cannot estimate μ efficiently and cannot design Algorithm 23 so that it takes $O(\mu)$ adaptively. We circumvent this by using a different cost scheme in Section 6.3.5 that is based on the recursion tree induced by Algorithm 23. Section 6.5 is devoted to the efficient implementation of the above certificate operations according to the cost scheme that we discuss next.

6.3.5 *Recursion tree and cost amortization*

We now show how to distribute the costs among the several recursive calls of Algorithm 23 so that optimality is achieved. Consider a generic execution on the bead string $B_{u,t}$. We trace this execution by using a binary recursion tree R. The nodes of R are labelled by the arguments of Algorithm 23: specifically, we denote a node in R by the triple $x = \langle \pi_s, u, C \rangle$ iff it represents the call with arguments π_s, u, and C.[1] The left branching is represented by the left child, and the right branching (if any) by the right child of the current node.

Lemma 10. *The binary recursion tree R for $B_{u,t}$ has the following properties:*

1. *There is a one-to-one correspondence between the paths in $\mathcal{P}_{s,t}(B_{u,t})$ and the leaves in the recursion tree rooted at node $\langle \pi_s, u, C \rangle$.*
2. *Consider any leaf and its corresponding (s,t)-path π: there are $|\pi|$ left branches in the corresponding root-to-leaf trace.*
3. *Consider the instruction $e := \texttt{choose}(C, u)$ in Algorithm 23: unary (i.e. single-child) nodes correspond to left branches (e is a tree edge) while binary nodes correspond to left and right branches (e is a back edge).*
4. *The number of binary nodes is $|\mathcal{P}_{s,t}(B_{u,t})| - 1$.*

Proof. We proceed in order as follows.

1. We only output a solution in a leaf and we only do recursive calls that lead us to a solution. Moreover every node partitions the set of solutions in the ones that use an edge and the ones that do not use it. This guarantees that the leaves in the left subtree of the node corresponding to the recursive call and the leaves in the right subtree do not intersect. This implies that different leaves correspond to different paths from s to t, and that for each path there is a corresponding leaf.
2. Each left branch corresponds to the inclusion of an edge in the path π.

[1] For clarity, we use "nodes" when referring to R and "vertices" when referring to $B_{u,t}$.

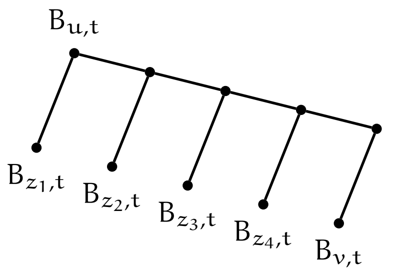

Figure 31: Spine of the recursion tree

3. Since we are in a biconnected component, there is always a left branch. There can be no unary node as a right branch: indeed for any edge of $B_{u,t}$ there exists always a path from s to t passing through that edge. Since the tree edge is always the last one to be chosen, unary nodes cannot correspond to back edges and binary nodes are always back edges.

4. It follows from point 1 and from the fact that the recursion tree is a binary tree. (In any binary tree, the number of binary nodes is equal to the number of leaves minus 1.)

□

We define a *spine* of R to be a subset of R's nodes linked as follows: the first node is a node x that is either the left child of its parent or the root of R, and the other nodes are those reachable from x by right branching in R. Let $x = \langle \pi_s, u, C \rangle$ be the first node in a spine S. The nodes in S correspond to the edges that are incident to vertex u in $B_{u,t}$: hence their number equals the degree $d(u)$ of u in $B_{u,t}$, and the deepest (last) node in S is always a tree edge in $B_{u,t}$ while the others are back edges. Fig. 31 shows the spine corresponding to $B_{u,t}$ in Fig. 30. Summing up, R can be seen as composed by spines, unary nodes, and leaves where each spine has a unary node as deepest node. This gives a global picture of R that we now exploit for the analysis.

We define the *compact head*, denoted by $H_X = (V_X, E_X)$, as the (multi)graph obtained by compacting the maximal chains of degree-2 vertices, except u, t, and the vertices that are the leaves of its DFS tree rooted at u.

The rationale behind the above definition is that the costs defined in terms of H_X amortize well, as the size of H_X and the number of (s, t)-paths in the subtree of R rooted at node $x = \langle \pi_s, u, C \rangle$ are intimately related (see Lemma 12 in Section 6.4) while this is not necessarily true for H_u.

Recall that each leaf corresponds to a path π and each spine corresponds to a compact head $H_X = (V_X, E_X)$. We now define the following abstract cost for spines, unary nodes, and leaves of R, for a sufficiently large constant $c_0 > 0$, that Algorithm 23 must fulfill:

$$T(r) = \begin{cases} c_0 & \text{if } r \text{ is unary} \\ c_0|\pi| & \text{if } r \text{ is a leaf} \\ c_0(|V_X| + |E_X|) & \text{if } r \text{ is a spine} \end{cases} \tag{6.1}$$

Lemma 11. *The sum of the costs in the nodes of the recursion tree* $\sum_{r \in R} T(r) = O(\sum_{\pi \in \mathcal{P}_{s,t}(B_{u,t})} |\pi|)$.

Section 6.4 contains the proof of Lemma 11 and related properties. Setting $u := s$, we obtain that the cost in Lemma 11 is optimal, by Lemma 8.

Theorem 19. *Algorithm 23 lists all the (s,t)-paths in optimal* $O(m + \sum_{\pi \in \mathcal{P}_{s,t}(G)} |\pi|)$ *time.*

By Lemma 7, we obtain an optimal result for listing cycles.

Theorem 20. *The cycles of an undirected graph can be optimally listed in* $O(m + \sum_{c \in \mathcal{C}(G)} |c|)$ *time.*

6.4 AMORTIZATION STRATEGY

We devote this section to prove Lemma 11. Let us split the sum in Eq. (6.1) in three parts, and bound each part individually, as

$$\sum_{r \in R} T(r) \leqslant \sum_{r:\,\text{unary}} T(r) + \sum_{r:\,\text{leaf}} T(r) + \sum_{r:\,\text{spine}} T(r). \tag{6.2}$$

We have that $\sum_{r:\,\text{unary}} T(r) = O(\sum_{\pi \in \mathcal{P}_{s,t}(G)} |\pi|)$, since there are $|\mathcal{P}_{s,t}(G)|$ leaves, and the root-to-leaf trace leading to the leaf for π contains at most $|\pi|$ unary nodes by Lemma 10, where each unary node has cost $O(1)$ by Eq. (6.1).

Also, $\sum_{r:\,\text{leaf}} T(r) = O(\sum_{\pi \in \mathcal{P}_{s,t}(G)} |\pi|)$, since the leaf r for π has cost $O(|\pi|)$ by Eq. (6.1).

It remains to bound $\sum_{r\,\text{spine}} T(r)$. By Eq. (6.1), we can rewrite this cost as $\sum_{H_X} c_0(|V_X| + |E_X|)$, where the sum ranges over the compacted heads H_X associated with the spines r. We use the following lemma to provide a lower bound on the number of (s,t)-paths descending from r.

Lemma 12. *Given a spine* r, *and its bead string* $B_{u,t}$ *with head* H_u, *there are at least* $|E_X| - |V_X| + 1$ (s,t)*-paths in* G *that have prefix* $\pi_s = s \rightsquigarrow u$ *and suffix* $u \rightsquigarrow t$ *internal to* $B_{u,t}$, *where the compacted head is* $H_X = (V_X, E_X)$.

Proof. H_X is biconnected. In any biconnected graph $B = (V_B, E_B)$ there are at least $|E_B| - |V_B| + 1$ xy-paths for any $x, y \in V_B$. Find an ear decomposition [214] of B and consider the process of forming B by adding ears one at the time, starting from a single cycle including x and y. Initially $|V_B| = |E_B|$ and there are

2 xy-paths. Each new ear forms a path connecting two vertices that are part of a xy-path, increasing the number of paths by at least 1. If the ear has k edges, its addition increases V by $k-1$, E by k, and the number of xy-paths by at least 1. The result follows by induction.

□

The implication of Lemma 12 is that there are at least $|E_X|-|V_X|+1$ leaves descending from the given spine r. Hence, we can charge to each of them a cost of $\frac{c_0(|V_X|+|E_X|)}{|E_X|-|V_X|+1}$. Lemma 13 allows us to prove that the latter cost is $O(1)$ when H_u is different from a single edge or a cycle. (If H_u is a single edge or a cycle, H_X is a single or double edge, and the cost is trivially a constant.)

Lemma 13. *For a compacted head* $H_X=(V_X,E_X)$*, its density is* $\frac{|E_X|}{|V_X|}\geqslant\frac{11}{10}$.

Proof. Consider the following partition $V_X=\{r\}\cup V_2\cup V_3$ where: r is the root; V_2 is the set of vertices with degree 2 and; V_3, the vertices with degree $\geqslant 3$. Since H_X is compacted DFS tree of a biconnected graph, we have that V_2 is a *subset* of the leaves and V_3 contains the set of internal vertices (except r). There are no vertices with degree 1 and $d(r)\geqslant 2$. Let $x=\sum_{v\in V_3}d(v)$ and $y=\sum_{v\in V_2}d(v)$. We can write the density as a function of x and y, namely,

$$\frac{|E_X|}{|V_X|}=\frac{x+y+d(r)}{2(|V_3|+|V_2|+1)}$$

Note that $|V_3|\leqslant\frac{x}{3}$ as the vertices in V_3 have at least degree 3, $|V_2|=\frac{y}{2}$ as vertices in V_2 have degree exactly 2. Since $d(r)\geqslant 2$, we derive the following bound

$$\frac{|E_X|}{|V_X|}\geqslant\frac{x+y+2}{\frac{2}{3}x+y+2}$$

Consider any graph with $|V_X|>3$ and its DFS tree rooted at r. Note that: (i) there are no tree edges between any two leaves, (ii) every vertex in V_2 is a leaf and (iii) no leaf is a child of r. Therefore, every tree edge incident in a vertex of V_2 is also incident in a vertex of V_3. Since exactly half the incident edges to V_2 are tree edges (the other half are back edges) we get that $y\leqslant 2x$.

With $|V_X|\geqslant 3$ there exists at least one internal vertex in the DFS tree and therefore $x\geqslant 3$.

$$\begin{aligned}\text{minimize}\quad & \frac{x+y+2}{\frac{2}{3}x+y+2}\\ \text{subject to}\quad & 0\leqslant y\leqslant 2x,\\ & x\geqslant 3.\end{aligned}$$

Since for any x the function is minimized by the maximum y s.t. $y\leqslant 2x$ and for any y by the minimum x, we get

$$\frac{|E_X|}{|V_X|}\geqslant\frac{9x+6}{8x+6}\geqslant\frac{11}{10}.$$

□

Specifically, let $\alpha = \frac{11}{10}$ and write $\alpha = 1 + 2/\beta$ for a constant β: we have that $|E_X| + |V_X| = (|E_X| - |V_X|) + 2|V_X| \leqslant (|E_X| - |V_X|) + \beta(|E_X| - |V_X|) = \frac{\alpha+1}{\alpha-1}(|E_X| - |V_X|)$. Thus, we can charge each leaf with a cost of $\frac{c_0(|V_X|+|E_X|)}{|E_X|-|V_X|+1} \leqslant c_0\frac{\alpha+1}{\alpha-1} = O(1)$. This motivates the definition of H_X, since Lemma 13 does not necessarily hold for the head H_u (due to the unary nodes in its DFS tree).

One last step to bound $\sum_{H_X} c_0(|V_X| + |E_X|)$: as noted before, a root-to-leaf trace for the string storing π has $|\pi|$ left branches by Lemma 10, and as many spines, each spine charging $c_0\frac{\alpha+1}{\alpha-1} = O(1)$ to the leaf at hand. This means that each of the $|\mathcal{P}_{s,t}(G)|$ leaves is charged for a cost of $O(|\pi|)$, thus bounding the sum as $\sum_{r\,\text{spine}} T(r) = \sum_{H_X} c_0(|V_X| + |E_X|) = O(\sum_{\pi\in\mathcal{P}_{s,t}(G)} |\pi|)$. This completes the proof of Lemma 11. As a corollary, we obtain the following result.

Lemma 14. *The recursion tree* R *with cost as in Eq.* (6.1) *induces an* $O(|\pi|)$ *amortized cost for each* (s,t)*-path* π.

6.5 CERTIFICATE IMPLEMENTATION AND MAINTENANCE

The certificate C associated with a node $\langle \pi_s, u, C\rangle$ in the recursion tree is a compacted and augmented DFS tree of bead string $B_{u,t}$, rooted at vertex u. The DFS tree changes over time along with $B_{u,t}$, and is maintained in such a way that t is in the leftmost path of the tree. We compact the DFS tree by contracting the vertices that have degree 2, except u, t, and the leaves (the latter surely have incident back edges). Maintaining this compacted representation is not a difficult data-structure problem. From now on we can assume w.l.o.g. that C is an augmented DFS tree rooted at u where internal nodes of the DFS tree have degree $\geqslant 3$, and each vertex v has associated the following information.

1. A doubly-linked list $lb(v)$ of back edges linking v to its descendants w sorted by postorder DFS numbering.
2. A doubly-linked list $ab(v)$ of back edges linking v to its ancestors w sorted by preorder DFS numbering.
3. An integer $\gamma(v)$, such that if v is an ancestor of w then $\gamma(v) < \gamma(w)$.
4. The smallest $\gamma(w)$ over all w, such that (h, w) is a back edge and h is in the subtree of v, denoted by *lowpoint*(v).

Given three vertices $v, w, x \in C$ such that v is the parent of w and x is not in the subtree[2] of w, we can efficiently test if v is an articulation point, i.e. *lowpoint*$(w) \leqslant \gamma(v)$. (Note that we adopt a variant of *lowpoint* using $\gamma(v)$ in place

[2] The second condition is always satisfied when w is not in the leftmost path, since t is not in the subtree of w.

of the preorder numbering [226]: it has the same effect whereas using $\gamma(v)$ is preferable since it is easier to dynamically maintain.)

Lemma 15. *The certificate associated with the root of the recursion can be computed in* $O(m)$ *time.*

Proof. In order to set t to be in the leftmost path, we perform a DFS traversal of graph G starting from s and stop when we reach vertex t. We then compute the DFS tree, traversing the path $s \rightsquigarrow t$ first. When visiting vertex v, we set $\gamma(v)$ to depth of v in the DFS. Before going up on the traversal, we compute the lowpoints using the lowpoints of the children. Let z be the parent of v. If *lowpoint*$(v) \leqslant \gamma(z)$ and v is not in the leftmost path in the DFS, we cut the subtree of v as it does not belong to $B_{s,t}$. When first exploring the neighbourhood of v, if w was already visited, i.e. $e = (u, w)$ is a back edge, and w is a descendant of v; we add e to $ab(w)$. This maintains the DFS preordering in the ancestor back edge list. Now, after the first scan of $N(v)$ is over and all the recursive calls returned (all the children were explored), we re-scan the neighbourhood of v. If $e = (v, w)$ is a back edge and w is an ancestor of v, we add e to $lb(w)$. This maintains the DFS postorder in the descendant back edge list. This procedure takes at most two DFS traversals in $O(m)$ time. This DFS tree can be compacted in the same time bound.

□

Lemma 16. *Operation* `choose(C,u)` *can be implemented in* $O(1)$ *time.*

Proof. If the list $lb(v)$ is empty, return the tree edge $e = (u, v)$ linking u to its only child v (there are no other children). Else, return the last edge in $lb(v)$.

□

We analyse the cost of updating and restoring the certificate C. We can reuse parts of C, namely, those corresponding to the vertices that are not in the compacted head $H_X = (V_X, E_X)$ as defined in Section 6.3.5. We prove that, given a unary node u and its tree edge $e = (u, v)$, the subtree of v in C can be easily made a certificate for the left branch of the recursion.

Lemma 17. *On a unary node,* `left_update(C,e)` *takes* $O(1)$ *time.*

Proof. Take edge $e = (u, v)$. Remove edge e and set v as the root of the certificate. Since e is the only edge incident in v, the subtree v is still a DFS tree. Cut the list of children of v keeping only the first child. (The other children are no longer in the bead string and become part of I.) There is no need to update $\gamma(v)$.

□

We now devote the rest of this section to show how to efficiently maintain C on a spine. Consider removing a back edge e from u: the compacted head $H_X = (V_X, E_X)$ of the bead string can be divided into smaller biconnected components. Many of those can be excluded from the certificate (i.e. they are no longer in the new bead string, and so they are bookkept in I) and additionally we have to update the lowpoints that change. We prove that this operation can be performed in $O(|V_X|)$ total time on a spine of the recursion tree.

Lemma 18. *The total cost of all the operations* `right_update`(C, e) *in a spine is* $O(|V_X|)$ *time.*

Proof. In the right branches along a spine, we remove all back edges in $\mathtt{lb}(u)$. This is done by starting from the last edge in $\mathtt{lb}(u)$, i.e. proceeding in reverse DFS postorder. For back edge $b_i = (z_i, u)$, we traverse the vertices in the path from z_i towards the root u, as these are the only lowpoints that can change. While moving upwards on the tree, on each vertex w, we update *lowpoint*(w). This is done by taking the endpoint y of the first edge in $\mathtt{ab}(w)$ (the back edge that goes the topmost in the tree) and choosing the minimum between $\gamma(y)$ and the lowpoint of each child[3] of w. We stop when the updated *lowpoint*$(w) = \gamma(u)$ since it implies that the lowpoint of the vertex can not be further reduced. Note that we stop before u, except when removing the last back edge in $\mathtt{lb}(u)$.

To prune the branches of the DFS tree that are no longer in $B_{u,t}$, consider again each vertex w in the path from z_i towards the root u and its parent y. We check if the updated *lowpoint*$(w) \leqslant \gamma(y)$ and w is not in the leftmost path of the DFS. If both conditions are satisfied, we have that $w \notin B_{u,t}$, and therefore we cut the subtree of w and keep it in I to restore later. We use the same halting criterion as in the previous paragraph.

The cost of removing all back edges in the spine is $O(|V_X|)$: there are $O(|V_X|)$ tree edges and, in the paths from z_i to u, we do not traverse the same tree edge twice since the process described stops at the first common ancestor of endpoints of back edges b_i. Additionally, we take $O(1)$ time to cut a subtree of an articulation point in the DFS tree.

□

To compute `left_update`(C, e) in the binary nodes of a spine, we use the fact that in every left branching from that spine, the graph is the same (in a spine we only remove edges incident to u and on a left branch from the spine we remove the vertex u) and therefore its block tree is also the same. However, the certificates on these nodes are not the same, as they are rooted at different vertices. Using the reverse DFS postorder of the edges, we are able to traverse each edge in H_X only a constant number of times in the spine.

Lemma 19. *The total cost of all operations* `left_update`(C, e) *in a spine is amortized* $O(|E_X|)$.

[3] If *lowpoint*(w) does not change we cannot pay to explore its children. For each vertex we dynamically maintain a list $l(w)$ of its children that have lowpoint equal to $\gamma(u)$. Then, we can test in constant time if $l(w) \neq \emptyset$ and y is not the root u. If both conditions are true *lowpoint*(w) changes, otherwise it remains equal to $\gamma(u)$ and we stop.

Proof. Let t' be the last vertex in the path $u \rightsquigarrow t$ s.t. $t' \in V_X$. Since t' is an articulation point, the subtree of the DFS tree rooted in t' is maintained in the case of removal of vertex u. Therefore the only modifications of the DFS tree occur in the compacted head H_X of $B_{u,t}$. Let us compute the certificate C_i: this is the certificate of the left branch of the ith node of the spine where we augment the path with the back edge $b_i = (z_i, u)$ of $lb(u)$ in the order defined by $\texttt{choose}(C, u)$.

For the case of C_1, we remove u and rebuild the certificate starting form z_1 (the last edge in $lb(u)$) using the algorithm from Lemma 15 restricted to H_X and using t' as target and $\gamma(t')$ as a baseline to γ (instead of the depth). This takes $O(|E_X|)$ time.

For the general case of C_i with $i > 1$ we also rebuild (part) of the certificate starting from z_i using the procedure from Lemma 15 but we use information gathered in C_{i-1} to avoid exploring useless branches of the DFS tree. The key point is that, when we reach the first bead in common to both $B_{z_i,t}$ and $B_{z_{i-1},t}$, we only explore edges internal to this bead. If an edge e leaving the bead leads to t, we can reuse a subtree of C_{i-1}. If e does not lead to t, then it has already been explored (and cut) in C_{i-1} and there is no need to explore it again since it will be discarded. Given the order we take b_i, each bead is not added more than once, and the total cost over the spine is $O(|E_X|)$.

Nevertheless, the internal edges E'_X of the first bead in common between $B_{z_i,t}$ and $B_{z_{i-1},t}$ can be explored several times during this procedure.[4] We can charge the cost $O(|E'_X|)$ of exploring those edges to another node in the recursion tree, since this common bead is the head of at least one certificate in the recursion subtree of the left child of the ith node of the spine. Specifically, we charge the first node in the *leftmost* path of the ith node of the spine that has exactly the edges E'_X as head of its bead string: (i) if $|E'_X| \leqslant 1$ it corresponds to a unary node or a leaf in the recursion tree and therefore we can charge it with $O(1)$ cost; (ii) otherwise it corresponds to a first node of a spine and therefore we can also charge it with $O(|E'_X|)$. We use this charging scheme when $i \neq 1$ and the cost is always charged in the leftmost recursion path of ith node of the spine. Consequently, we never charge a node in the recursion tree more than once.

□

Lemma 20. *On each node of the recursion tree,* $\texttt{restore}(C, I)$ *takes time proportional to the size of the modifications kept in* I.

Proof. We use standard data structures (i.e. linked lists) for the representation of certificate C. Persistent versions of these data structures exist that maintain a stack of modifications applied to them and that can restore its contents to their

[4] Consider the case where $z_i, \dots, z_j$ are all in the same bead after the removal of u. The bead strings are the same, but the roots $z_i, \dots, z_j$ are different, so we have to compute the corresponding DFS of the first component $|j - i|$ times.

previous states. Given the modifications in I, these data structures take $O(|I|)$ time to restore the previous version of C.

Let us consider the case of performing `left_update`(C, e). We cut at most $O(|V_X|)$ edges from C. Note that, although we conceptually remove whole branches of the DFS tree, we only remove edges that attach those branches to the DFS tree. The other vertices and edges are left in the certificate but, as they no longer remain attached to $B_{u,t}$, they will never be reached or explored. In the case of `right_update`(C, e), we have a similar situation, with at most $O(|E_X|)$ edges being modified along the spine of the recursion tree.

□

From Lemmas 16 and 18–20, it follows that on a spine of the recursion tree we have the costs: `choose`(u) on each node which is bounded by $O(|V_X|)$ time as there are at most $|V_X|$ back edges in u; `right_update`(C, e), `restore`(C, I) take $O(|V_X|)$ time; `left_update`(C, e) and `restore`(C, I) are charged $O(|V_X| + |E_X|)$ time. We thus have the following result, completing the proof of Theorem 19.

Lemma 21. *Algorithm 23 can be implemented with a cost fulfilling Eq.* (6.1)*, thus it takes total* $O(m + \sum_{r \in R} T(r)) = O(m + \sum_{\pi \in \mathcal{P}_{s,t}(B_{u,t})} |\pi|)$ *time.*

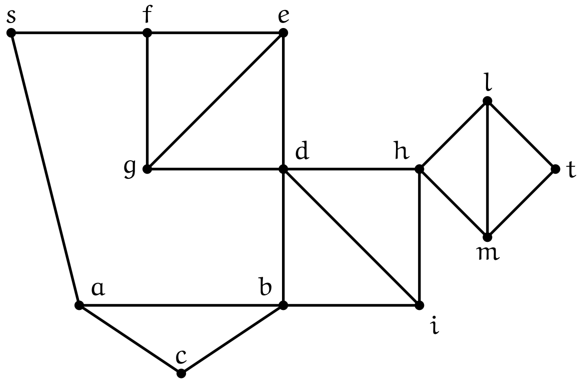

Figure 32: An undirected graph, whose biconnected components are B_1, that is the graph induced by $\{s, a, b, c, d, e, f, g, h, i\}$, and B_2, that is the graph induced by $\{h, l, m, t\}$.

6.6 enumerating paths: an example

Let us consider the graph in Figure 32. In this case Lemma 8 is witnessed by vertex h: indeed the bead string $B_{s,t}$ is B_1, B_2, where B_1 is the graph induced by $\{s, a, b, c, d, e, f, g, h, i\}$ and B_2 is the graph induced by $\{h, l, m, t\}$, and h is an articulation point; all the paths between s and t pass through h.

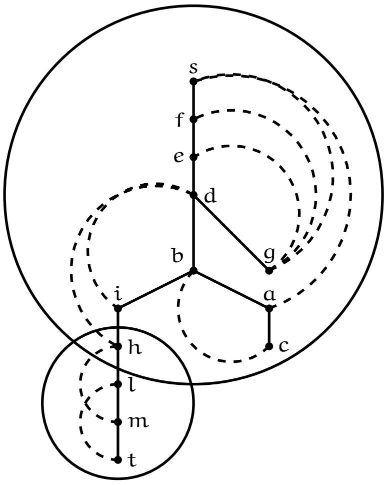

Vertex	γ	Post-order Number	Pre-order Number	lb	ab	*lowpoint*
s	0	1	13	(s,a),(s,g)	∅	$\gamma(s) = 0$
a	5	11	7	∅	(a,s)	$\gamma(s) = 0$
b	4	5	8	(b,c)	∅	$\gamma(s) = 0$
c	2	12	6	∅	(c,b)	$\gamma(b) = 4$
d	3	4	10	(d,h),(d,i)	∅	$\gamma(s) = 0$
e	2	3	11	(e,g)	∅	$\gamma(s) = 0$
f	1	2	12	(f,g)	∅	$\gamma(s) = 0$
g	4	13	9	∅	(g,s),(g,f),(g,e)	$\gamma(s) = 0$
h	6	7	4	(h,m)	(h,d)	$\gamma(d) = 3$
i	5	8	5	∅	(i,d)	$\gamma(d) = 3$
l	7	8	3	(l,t)	∅	$\gamma(h) = 6$
m	8	9	2	∅	(m,h)	$\gamma(h) = 6$
t	9	10	1	∅	(t,l)	$\gamma(l) = 7$

Figure 33: DFS tree starting from s, of the graph in Figure 32, with t in the leftmost path. Each biconnected component is enclosed in a circle. For any vertex the properties included by the certificate are reported in the table.

By considering as V_X and E_X respectively the vertices and edges in B_1, Lemma 12 with $u = s$ states that there are at least $|E_X| - |V_X| + 1 = 16 - 10 + 1 = 7$ paths between s and t. Indeed observe that in the DFS in Figure 33, B_1 is already compacted since the unique vertex with degree two is c, that is a leaf. Moreover, observe that $|E_X|/|V_X| = 16/10 \geqslant 11/10$, as stated by Lemma 13.

Lemma 15 builds the certificate shown in Figure 33. Observe that for any vertex v, whose children are $z_1, \ldots, z_k$,

$$\mathit{lowpoint}(v) = \min\{\mathit{lowpoint}(z_1), \ldots, \mathit{lowpoint}(z_k), \min_{(v,w) \in ab(v)} \{\gamma(w)\}\}.$$

Moreover the elements in any set lb are put in the ascending order defined by the post-order DFS numbering of their extremes. The elements in any set ab are put in the ascending order defined by the pre-order DFS numbering of their extremes.

The first bipartition is applied by considering the edge (s, g), that is the last edge in the list $lb(s)$. The right branch operation simply deletes this edge, and

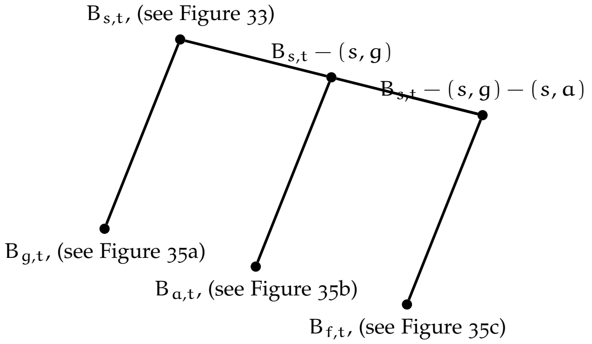
$B_{s,t}$, (see Figure 33)
$B_{s,t} - (s, g)$
$B_{s,t} - (s, g) - (s, a)$
$B_{g,t}$, (see Figure 35a)
$B_{a,t}$, (see Figure 35b)
$B_{f,t}$, (see Figure 35c)

Figure 34: Spine of the recursion tree starting from s

modifies the certificate by applying the method described in Section 6.7.1. In general by deleting an edge, some vertices could not reach t, but this is not the case. Moreover this edge has to be removed also from the ab lists and this can be easily done when removing the edge from lb; finally the *lowpoint*s have to be updated. The unique vertices, whose *lowpoint*s change, are on the path of tree edges from g to the root s. Lemma 23, in the following section, states that the sum of these costs along the entire spine of s is $O(|V_X|)$, where V_X is the set of vertices in the bead of s and g.

The left branch operation removes the vertex s and performs a DFS from g, as shown by Figure 35a. Observe that, since the entry point of the component h, l, m, and t remains h, it is sufficient to perform the visit just inside the biconnected component of s and g. In particular, since this is the first back edge of a spine, i.e. we are computing C_1 referring to Lemma 19, we have to rebuild the certificate from scratch by applying Lemma 15 (see Lemma 26). Observe that the component a, b, c is cut since it does not lead to t and b is compacted.

The second bipartition along the same spine considers the paths from s to t in the graph induced by $B_{s,t} - (s, g)$ and the edge (s, a), that is the remaining edge in $lb(s)$. Once again, the right update operation simply deletes the edge (s, a), removes (s, a) from both lb and ab, updates the *lowpoint*s along the path of tree edges from s to a, and checks whether branches have to be compressed or cut. In this case, by removing the edge (s, a), the vertices a, b, c do not belong anymore to the same biconnected component of s and each path from s to t in $B_{s,t} - (s, g) - (s, a)$, using a or c, should pass more than once through b. This implies that a and c have to be cut (see also Lemma 24). By considering the vertices w along the path of tree edges from a to s, that are a, b, d, e, f, s, a vertex y along this path is an articulation point if the updated child w is such that $\mathit{lowpoint}(w) \leqslant \gamma(y)$ (and there exists at least another vertex not descendant of y). Once again Lemma 24 states that the sum of these costs along the entire spine of s is $O(|V_X|)$, where V_X is the set of vertices in the bead of s and a. Moreover,

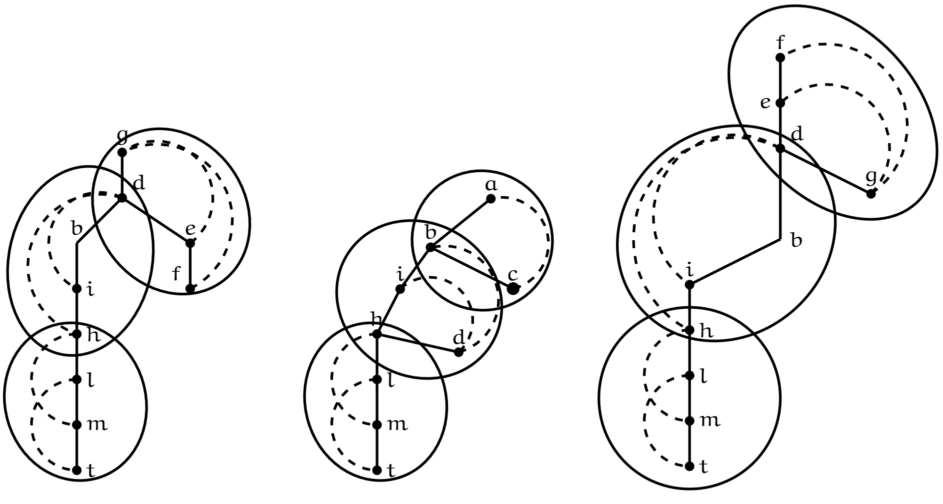

(a) $B_{g,t}$ (b) $B_{a,t}$ (c) $B_{f,t}$

Figure 35: Certificates in the spine of s

the vertex b has to be compressed, since by cutting its right subtree, its degree is just two. This operation takes constant time.

By following Lemma 19, the left update operation builds the certificate C_2 shown in Figure 35b, by reusing information from C_1. Indeed observe that the certificates C_1, in Figure 35a (plus the cut component a, b, c), and C_2, in Figure 35b, are DFSs defined on the same graph but with different roots. The first bead in common between these two certificates is d, b, i, h. In order to build the certificate in Figure 35b, the information about the components after d, b, i, h in the path of beads from s to t, can be inherited by C_1. However, as stated by Lemma 19, the visit of the bead intersection has to be performed, since the entry points, i.e. respectively d and b, are different: this implies that the visit of the component d, b, i, h has to be performed more than once along the spine. Lemma 19 (and 27) says that these extra costs can be amortized in the cost of the spines of d and b, since, when performing the recursion in d and b, the cost along their spine is at least the size of this component.

The third and last bipartition of the spine considers the tree edge (s, f), by looking for paths from s to t in $B_{s,t} - (s, g) - (s, a)$. Observe that, by deleting (s, g) and (s, a), all the paths from s to t have to pass through f. This implies that the set of paths in $B_{s,t} - (s, g) - (s, a)$ not using the edge (s, f) is empty and the right update operation does not have to be performed. The left update operation shown in Lemma 17 takes constant time, since the certificate shown in Figure 35c is simply obtained by $B_{s,t} - (s, g) - (s, a)$ by removing the vertex s and the edge (s, f). If f has two or more children, we should consider just the first child, since it is the unique one leading to t, and cut all the other children;

but since f has just one child this operation is not performed. The lb, ab, γ and *lowpoint* do not need to be updated.

6.7 extended analysis of operations

In this section, we present all details and illustrate with figures the operations `right_update`(C, e) and `left_update`(C, e) that are performed along a spine of the recursion tree. In order to better detail the procedures in Lemma 18 and Lemma 19, we divide them in smaller parts. We use bead string $B_{u,t}$ from Fig. 30 and the respective spine from Fig. 31 as the base for the examples. This spine contains four binary nodes corresponding to the back edges in $\mathrm{lb}(u)$ and an unary node corresponding to the tree edge (u, v). Note that edges are taken in order of the endpoints z_1, z_2, z_3, z_4, v as defined in operation `choose`(C, u).

By Lemma 8, the impact of operations `right_update`(C, e) and `left_update`(C, e) in the certificate is restricted to the biconnected component of u. Thus we mainly focus on maintaining the compacted head $H_X = (V_X, E_X)$ of the bead string $B_{u,t}$.

6.7.1 *Operation right_update(C,e)*

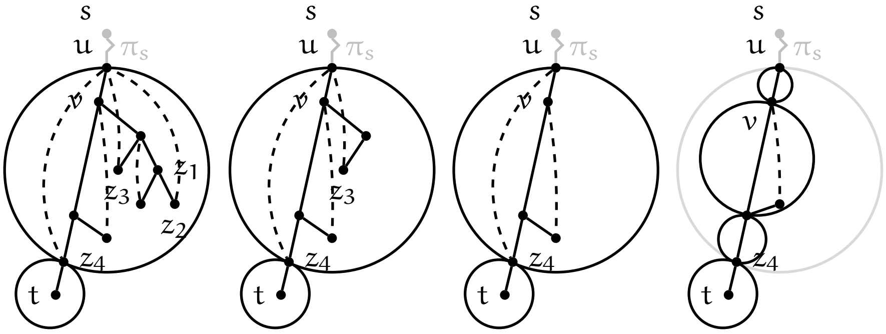

(a) Step 1 (b) Step 2 (c) Step 3 (d) Step 4 (final)

Figure 36: Example application of `right_update`(C, e) on a spine of the recursion tree

Lemma 22. (Lemma 18 restated) *In a spine of the recursion tree, operations* `right_update`(C, e) *can be implemented in* $O(|V_X|)$ *total time.*

In the right branches along a spine, we remove all back edges in $\mathrm{lb}(u)$. This is done by starting from the last edge in $\mathrm{lb}(u)$, i.e. proceeding in reverse DFS postorder. In the example from Fig. 30, we remove the back edges $(z_1, u) \ldots (z_4, u)$. To update the certificate corresponding to $B_{u,t}$, we have to (i) update the lowpoints in each vertex of H_X; (ii) prune vertices that cease to be in $B_{u,t}$ after removing a back edge. For a vertex w in the tree, there is no need to update $\gamma(w)$.

Consider the update of lowpoints in the DFS tree. For a back edge $b_i = (z_i, u)$, we traverse the vertices in the path from z_i towards the root u. By definition of lowpoint, these are the only lowpoints that can change. Suppose that we remove back edge (z_4, u) in the example from Fig. 30, only the lowpoints of the vertices in the path from z_4 towards the root u change. Furthermore, consider a vertex w in the tree that is an ancestor of at least two endpoints z_i, z_j of back edges b_i, b_j. The lowpoint of w does not change when we remove b_i. These observations lead us to the following lemma.

Lemma 23. *In a spine of the recursion tree, the update of lowpoints in the certificate by operation* `right_update`(C, e) *can be done in* $O(|V_X|)$ *total time.*

Proof. Take each back edge $b_i = (z_i, u)$ in the order defined by `choose`(C, u). Remove b_i from $lb(u)$ and $ab(z_i)$. Starting from z_i, consider each vertex w in the path from z_i towards the root u. On vertex w, we update *lowpoint*(w) using the standard procedure: take the endpoint y of the first edge in $ab(w)$ (the back edge that goes the nearest to the root of the tree) and choosing the minimum between $\gamma(y)$ and the lowpoint of each child of w. When the updated *lowpoint*$(w) = \gamma(u)$, we stop examining the path from z_i to u since it implies that the lowpoint of the vertex can not be further reduced (i.e. w is both an ancestor to both z_i and z_{i+1}).

If *lowpoint*(w) does not change we cannot pay to explore its children. In order to get around this, for each vertex we dynamically maintain, throughout the spine, a list $l(w)$ of its children that have lowpoint equal to $\gamma(u)$. Then, we can test in constant time if $l(w) \neq \emptyset$ and y (the endpoint of the first edge in $ab(w)$) is not the root u. If both conditions are satisfied *lowpoint*(w) changes, otherwise it remains equal to $\gamma(u)$ and we stop. The total time to create the lists is $O(|V_X|)$ and the time to update is bounded by the number of tree edges traversed, shown to be $O(|V_X|)$ in the next paragraph.

The cost of updating the lowpoints when removing all back edges b_i is $O(|V_X|)$: there are $O(|V_X|)$ tree edges and we do not traverse the same tree edge twice since the process described stops at the first common ancestor of endpoints of back edges b_i and b_{i+1}. By contradiction: if a tree edge (x, y) would be traversed twice when removing back edges b_i and b_{i+1}, it would imply that both x and y are ancestors of z_i and z_{i+1} (as edge (x, y) is both in the path z_i to u and the path z_{i+1} to u) but we stop at the first ancestor of z_i and z_{i+1}.

□

Let us now consider the removal of vertices that are no longer in $B_{u,t}$ as consequence of operation `right_update`(C, e) in a spine of the recursion tree. By removing a back edge $b_i = (z_i, u)$, it is possible that a vertex w previously in H_X is no longer in the bead string $B_{u,t}$ (e.g. w is no longer biconnected to u and thus there is no simple path $u \rightsquigarrow w \rightsquigarrow t$).

Lemma 24. *In a spine of the recursion tree, the branches of the DFS that are no longer in* $B_{u,t}$ *due to operation* `right_update(C, e)` *can be removed from the certificate in* $O(|V_X|)$ *total time.*

Proof. To prune the branches of the DFS tree that are no longer in H_X, consider again each vertex w in the path from z_i towards the root u and the vertex y, parent of w. It is easy to check if y is an articulation point by verifying if the updated *lowpoint*$(w) \leqslant \gamma(y)$ and there exists x not in the subtree of w. If w is not in the leftmost path, then t is not in the subtree of w. If that is the case, we have that $w \notin B_{u,t}$, and therefore we cut the subtree of w and bookkeep it in I to restore later. Like in the update the lowpoints, we stop examining the path z_i towards u in a vertex w when *lowpoint*$(w) = \gamma(u)$ (the lowpoints and biconnected components in the path from w to u do not change). When cutting the subtree of w, note that there are no back edges connecting it to $B_{u,t}$ (w is an articulation point) and therefore there are no updates to the lists lb and ab of the vertices in $B_{u,t}$. Like in the case of updating the lowpoints, we do not traverse the same tree edge twice (we use the same halting criterion).

□

With Lemma 23 and Lemma 24 we finalize the proof of Lemma 18. Fig. 36 shows the changes the bead string $B_{u,t}$ from Fig. 30 goes through in the corresponding spine of the recursion tree.

6.7.2 *Operation left_update(C,e)*

In the binary nodes of a spine, we use the fact that in every left branching from that spine the graph is the same (in a spine we only remove edges incident to u and on a left branch from the spine we remove the vertex u) and therefore its block tree is also the same. In Fig. 37, we show the resulting block tree of the graph from Fig. 30 after having removed vertex u. However, the certificates on these left branches are not the same, as they are rooted at different vertices. In the example we must compute the certificates $C_1 \dots C_4$ corresponding to bead strings $B_{z_1,t} \dots B_{z_4,t}$. We do not account for the cost of the left branch on the last node of spine (corresponding to $B_{v,t}$) as the node is unary and we have shown in Lemma 17 how to maintain the certificate in $O(1)$ time.

By using the reverse DFS postorder of the back edges, we are able to traverse each edge in H_X only an amortized constant number of times in the spine.

Lemma 25. (Lemma 19 restated) *The calls to operation* `left_update(C, e)` *in a spine of the recursion tree can be charged with a time cost of* $O(|E_X|)$ *to that spine.*

To achieve this time cost, for each back edge $b_i = (z_i, u)$, we compute the certificate corresponding to $B_{z_i,t}$ based on the certificate of $B_{z_{i-1},t}$. Consider the compacted head $H_X = (V_X, E_X)$ of the bead string $B_{u,t}$. We use $O(|E_X|)$ time to compute the first certificate C_1 corresponding to bead string $B_{z_1,t}$. Fig. 38 shows bead string $B_{z_1,t}$ from the example of Fig. 30.

Lemma 26. *The certificate* C_1*, corresponding to bead string* $B_{z_1,t}$*, can be computed in* $O(|E_X|)$ *time.*

Proof. Let t' be the last vertex in the path $u \rightsquigarrow t$ s.t. $t' \in V_X$. Since t' is an articulation point, the subtree of the DFS tree rooted in t' is maintained in the case of removal vertex u. Therefore the only modifications of the DFS tree occur in head H_X of $B_{u,t}$.

To compute C_1, we remove u and rebuild the certificate starting form z_1 using the algorithm from Lemma 15 restricted to H_X and using t' as target and $\gamma(t')$ as a baseline to γ (instead of the depth). In particular we do the following. To set t' to be in the leftmost path, we perform a DFS traversal of graph H_X starting from z_1 and stop when we reach vertex t'. Then compute the DFS tree, traversing the path $z_1 \rightsquigarrow t'$ first.

Update of γ. For each tree edge (v, w) in the $t' \rightsquigarrow z_1$ path, we set $\gamma(v) = \gamma(w) - 1$, using $\gamma(t')$ as a baseline. During the rest of the traversal, when visiting vertex v, let w be the parent of v in the DFS tree. We set $\gamma(v) = \gamma(w) + 1$. This maintains the property that $\gamma(v) > \gamma(w)$ for any w ancestor of v.

Lowpoints and pruning the tree. Bottom-up in the DFS-tree, compute the lowpoints using the lowpoints of the children. For z the parent of v, if *lowpoint*$(v) \leqslant \gamma(z)$ and v is not in the leftmost path in the DFS, cut the subtree of v as it does not belong to $B_{z_1,t}$.

Computing lb *and* ab. In the traversal, when finding a back edge $e = (v, w)$, if w is a descendant of v we append e to $ab(w)$. This maintains the DFS preorder in the ancestor back edge list. After the first scan of $N(v)$ is over and all the recursive calls returned, re-scan the neighbourhood of v. If $e = (v, w)$ is a back edge and w is an ancestor of v, we add e to $lb(w)$. This maintains the DFS postorder in the descendant back edge list. This procedure takes $O(|E_X|)$ time. □

To compute each certificate C_i, corresponding to bead string $B_{z_i,t}$, we are able to avoid visiting most of the edges that belong $B_{z_{i-1},t}$. Since we take z_i in reverse DFS postorder, on the spine of the recursion we visit $O(|E_X|)$ edges plus a term that can be amortized.

Lemma 27. *For each back edge* $b_i = (z_i, u)$ *with* $i > 1$*, let* $E_X{}'_i$ *be the edges in the first bead in common between* $B_{z_i,t}$ *and* $B_{z_{i-1},t}$*. The total cost of computing all certificates* $B_{z_i,t}$ *in a spine of the recursion tree is:* $O(|E_X| + \sum_{i>1} |E_X{}'_i|)$.

Proof. Let us compute the certificate C_i: the certificate of the left branch of the ith node of the spine where we augment the path with back edge $b_i = (z_i, u)$ of $lb(u)$.

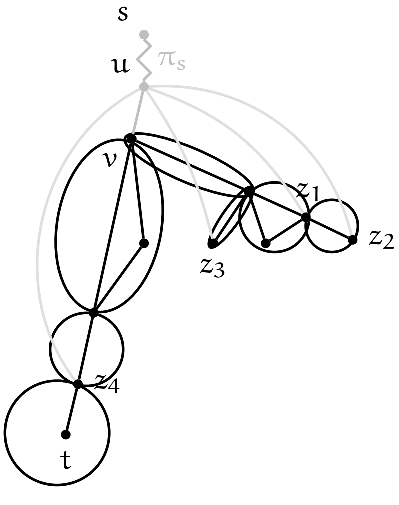

Figure 37: Block tree after removing vertex u

For the general case of C_i with $i > 1$ we also rebuild (part) of the certificate starting from z_i using the procedure from Lemma 15 but we use information gathered in C_{i-1} to avoid exploring useless branches of the DFS tree. The key point is that, when we reach the first bead in common to both $B_{z_i,t}$ and $B_{z_{i-1},t}$, we only explore edges internal to this bead. If an edge e that leaves the bead leads to t, we can reuse a subtree of C_{i-1}. If e does not lead to t, then it has already been explored (and cut) in C_{i-1} and there is no need to explore it again since it is going to be discarded.

In detail, we start computing a DFS from z_i in $B_{u,t}$ until we reach a vertex $t' \in B_{z_{i-1},t}$. Note that the bead of t' has one entry point and one exit point in C_{i-1}. After reaching t' we proceed with the traversal using only edges already in C_{i-1}. When arriving at a vertex w that is not in the same bead of t', we stop the traversal. If w is in a bead towards t, we reuse the subtree of w and use $\gamma(w)$ as a baseline of the numbering γ. Otherwise w is in a bead towards z_{i-1} and we cut this branch of the certificate. When all edges in the bead of t' are traversed, we proceed with visit in the standard way.

Given the order we take b_i, each bead is not added more than once to a certificate C_i, therefore the total cost over the spine is $O(|E_X|)$. Nevertheless, the internal edges E_{X_i}' of the first bead in common between $B_{z_i,t}$ and $B_{z_{i-1},t}$ are explored for each back edge b_i.

□

Although the edges in E_{X_i}' are in a common bead between $B_{z_i,t}$ and $B_{z_{i-1},t}$, these edges must be visited. The entry point in the common bead can be different for z_i and z_{i-1}, the DFS tree of that bead can also be different. For an example, consider the case where $z_i, \ldots, z_j$ are all in the same bead after the removal of u. The bead strings $B_{z_i,t} \ldots B_{z_j,t}$ are the same, but the roots $z_i, \ldots, z_j$ of the

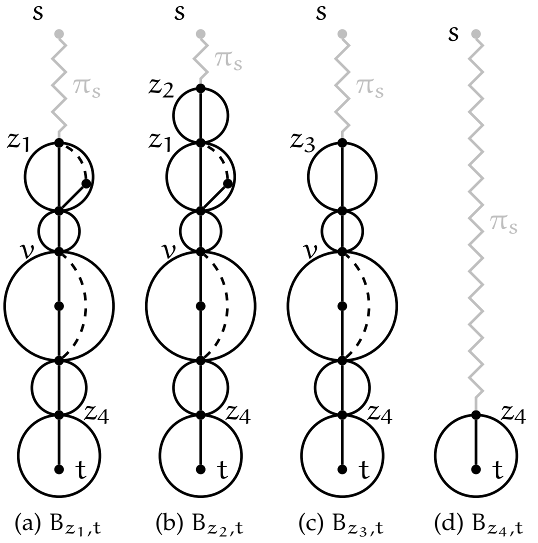

Figure 38: Certificates of the left branches of a spine

certificate are different, so we have to compute the corresponding DFS of the first bead $|j-i|$ times. Note that this is not the case for the other beads in common: the entry point is always the same.

Lemma 28. *The cost* $O(|E_X| + \sum_{i>1} |E_{X'_i}|)$ *on a spine of the recursion tree can be amortized to* $O(|E_X|)$*.*

Proof. We can charge the cost $O(|E_{X'_i}|)$ of exploring the edges in the first bead in common between $B_{z_i,t}$ and $B_{z_{i-1},t}$ to another node in the recursion tree. Since this common bead is the head of at least one certificate in the recursion subtree of the left child of the ith node of the spine. Specifically, we charge the first and only node in the *leftmost* path of the ith child of the spine that has exactly the edges $E_{X'_i}$ as head of its bead string: (i) if $|E_{X'_i}| \leqslant 1$ it corresponds to a unary node or a leaf in the recursion tree and therefore we can charge it with $O(1)$ cost; (ii) otherwise it corresponds to a first node of a spine and therefore we can also charge it with $O(|E_{X'_i}|)$. We use this charging scheme when $i \neq 1$ and the cost is always charged in the leftmost recursion path of ith node of the spine, consequently we never charge a node in the recursion tree more than once. □

Lemmas 27 and 28 finalize the proof of Lemma 19. Fig. 38 shows the certificates of bead strings $B_{z_i,t}$ on the left branches of the spine from Figure 31.

6.8 conclusion and open problems

We showed in this chapter the first optimal solution to list all the cycles of an undirected graph and all the paths from a given source to a given target. This result improves the Johnson's algorithm, that was still the theoretically most efficient in the case of undirected graphs. The main question arising from our work is whether it is possible to obtain an optimal algorithm to list all the paths and cycles in a directed graph.

7

ENUMERATING BUBBLES: LISTING PAIRS OF VERTEX DISJOINT PATHS

Polymorphisms in DNA- or RNA-seq data lead to recognisable patterns in a de Bruijn graph representation of the reads obtained by sequencing. Such patterns have been called mouths, or bubbles in the literature. They correspond to two vertex-disjoint directed paths between a source s *and a target* t*. Due to the high number of such bubbles that may be present in real data, their enumeration is a major issue concerning the efficiency of dedicated algorithms. We propose the first linear delay algorithm to enumerate all bubbles with a given source, by properly transforming the graph in input and enumerating special cycles.*

7.1 INTRODUCTION

In recent papers [20, 227], algorithms for identifying two types of polymorphism, respectively SNPs (Single Nucleotide Polymorphisms) in DNA, and alternative splicing in RNA-seq data were introduced. Both correspond to recognisable patterns in a de Bruijn graph (DBG) built from the reads provided by a sequencing project. In both cases, the pattern corresponds to two vertex-disjoint paths between a pair of source and target vertices s and t. Properties on the lengths or sequence similarity of the paths then enable to differentiate between different types of polymorphism.

Such patterns have been studied before in the context of genome assembly where they have been called bulges [228] or bubbles [229, 230, 231]. However, the purpose in these works was not to enumerate all these patterns, but "only" to remove them from the graph, in order to provide longer contigs for the genome assembly. More recently, ad-hoc enumeration methods have been proposed but are restricted to non-branching bubbles [232], i.e., each vertex from the bubble has in-degree and out-degree 1, except for s and t. Furthermore, in all these applications [229, 230, 232, 228, 231] since the patterns correspond to SNPs or sequencing errors, the authors only considered paths of length smaller than a constant. On the other hand, bubbles of arbitrary length have been considered in the context of splicing graphs [233]. However, in this context, a notable difference is that the graph is a DAG. Additionally, vertices are coloured and only unicolour paths are then considered for forming bubbles. Finally, the concept of bubble also applies to the area of phylogenetic networks [234], where it corresponds to the notion of a recombination cycle. Again for this application, the graph is a DAG.

In this chapter, we adopt the term bubble, which is being most used in the community, and this will denote two vertex-disjoint paths between a pair of source and target vertices with no condition on the path length or the degrees of the internal vertices. We then consider the more general problem of enumerating all bubbles in a arbitrary directed graph. That is, our solution is not restricted to acyclic or de Bruijn graphs. This problem is quite general but it was still an open question whether a polynomial-delay algorithm could be proposed for solving it. The algorithm presented in [20] was an adaptation of Tiernan's algorithm for cycle enumeration [21] which does not have a polynomial delay, in the worst case the time elapsed between the output of two solutions is proportional to the number of paths in the graph, i.e. exponential in the size of the graph. It was not clear at the time if more efficient cycle enumeration methods in directed graphs such as Tarjan's [60] or Johnson's [18] could be adapted to efficiently enumerate bubbles in directed graphs.

CONTRIBUTION. The aim of this chapter is to show a non trivial adaptation of Johnson's cycle (what he called elementary circuit) enumeration algorithm to identify all bubbles in a directed graph in the same theoretical complexity. Notably, the method we propose enumerates all bubbles with a given source with $O(|V| + |E|)$ delay. The algorithm requires an initial transformation, described in Section 7.3, of the graph for each source s that takes $O(|V| + |E|)$ time and space. Our work appeared in [22].

STRUCTURE OF THE CHAPTER. The chapter is organised as follows. We start by recalling in Section 7.2 what is a de Bruijn graph representation of a set of reads, and how polymorphisms in DNA- and RNA-seq data correspond to bubbles in this graph. We then explain in Section 7.3 how to transform the original graph into a new graph where bubbles will correspond to cycles with some properties. We present in Section 7.4 the algorithm for enumerating all cycles corresponding to bubbles in the initial graph and we provide an example in Section 7.5. We prove in Section 7.6 that this algorithm is correct and has linear delay; in Section 7.7 we explain how to avoid duplicate bubbles with no additional cost. Finally in Section 7.8 we conclude with some open problems.

7.2 PRELIMINARIES

Recall that a de Bruijn graph (DBG) is a directed graph $G = (V, E)$ whose set of vertices V are labelled by k-mers, i.e. words of length k. An arc in E links a vertex u to a vertex v if the suffix of length $k-1$ of u is a prefix of v. By an (s, t)-bubble, we mean two vertex-disjoint (s, t)-paths that only shares s and t.

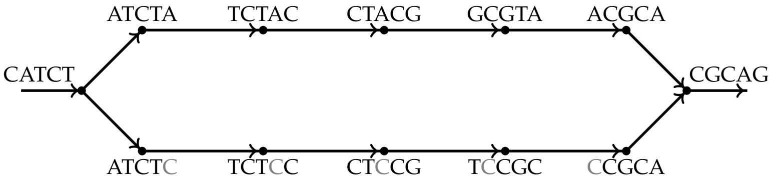

Figure 39: Bubble due to a substitution (gray letter).

In the case of next generation sequencing (NGS) data, the k-mers correspond to all words of length k present in the reads (strings) of the input dataset, and only those. In relation to the classical de Bruijn graph for all possible words of size k, the DBG for NGS data may then not be complete. Vertices may also be labelled by the number of times each k-mer is present in the reads. In general a vertex will be labelled by both a k-mer and its reverse complement, and the DBG used in practice will thus be a bi-directed multigraph. Figure 39 gives an example of a portion of a DBG that corresponds to a bubble generated by a SNP or a sequencing error.

In this chapter, we ignore all details related to the treatment of NGS data using De Bruijn graphs that are not essential for the algorithm described, and consider instead the more general case of finding all (s, t)-bubbles in an arbitrary directed graph.

7.3 turning bubbles into cycles

Let $G = (V, E)$ be a directed graph, and let $s \in V$. We want to find all (s, t)-bubbles for all possible target vertices t. We transform G into a new graph $G'_s = (V'_s, E'_s)$ where $|V'_s| = 2|V|$ and $|E'_s| = O(|V| + |E|)$. Namely,

$$V'_s = \{v, \bar{v} \mid v \in V\}$$

$$E'_s = \{(u, v), (\bar{v}, \bar{u}) \mid (u, v) \in E \text{ and } v \neq s\} \cup \{(v, \bar{v}) \mid v \in V \text{ and } v \neq s\} \cup \{(\bar{s}, s)\}$$

Let us denote by $\overline{V}$ the set of vertices of G'_s that were not already in G, that is $\overline{V} = V'_s \setminus V$. The two vertices $x \in V$ and $\bar{x} \in \overline{V}$ are said to be *twin vertices*. Observe that the graph G'_s is thus built by adding to G a reversed copy of itself, where the copy of each vertex is referred to as its *twin*. The arcs incoming to s (and outgoing from $\bar{s}$) are not included so that the only cycles in G'_s that contain s also contain $\bar{s}$. New arcs are also created between each pair of twins: the new arcs are the ones leading from a vertex u to its twin $\bar{u}$ for all u except for s where the arc goes from $\bar{s}$ to s. An example of a transformation is given in Figure 40.

We define a cycle of G'_s as being *bipolar* if it contains vertices of both V and $\overline{V}$. As the only arc from $\overline{V}$ to V is $(\bar{s}, s)$, then every bipolar cycle C contains also only one arc from V to $\overline{V}$. This arc, which is the arc $(t, \bar{t})$ for some $t \in V$, is called the *swap arc* of C. Moreover, since $(\bar{s}, s)$ is the only incoming arc of s, all

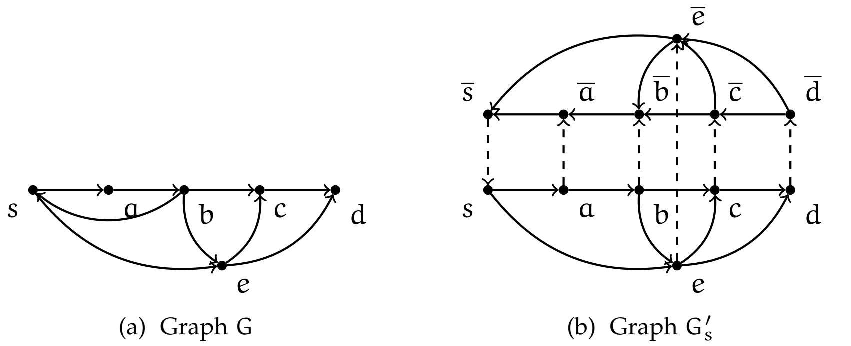

Figure 40: Graph G and its transformation $G'{}_s$. We have that $\langle s, e, \overline{e}, \overline{b}, \overline{a}, \overline{s}, s\rangle$ is a bubble-cycle with swap arc $(e, \overline{e})$ that has a correspondence to the (s, e)-bubble composed by the two vertex-disjoint paths $\langle s, e\rangle$ and $\langle s, a, b, e\rangle$.

the cycles containing s are bipolar. We say that C is *twin-free* if it contains no pair of twins except for $(s, \overline{s})$ and $(t, \overline{t})$.

Definition 3 (Bubble-cycle)**.** *A* bubble-cycle *in* G'_s *is a twin-free cycle of size greater than four*[1]*.*

Proposition 2. *Given a vertex* s *in* G*, there is a one-to-two correspondence between the set of* (s, t)*-bubbles in* G *for all* $t \in V$*, and the set of bubble-cycles of* G'_s*.*

Proof. Let us consider an (s, t)-bubble in G formed by two vertex-disjoint (s, t)-paths P and Q. Consider the cycle of G'_s obtained by concatenating P (resp. Q), the arc $(t, \overline{t})$, the inverted copy of Q (resp. P), and the arc $(\overline{s}, s)$. Both cycles are bipolar, twin-free, and have $(t, \overline{t})$ as swap arc. Therefore both are bubble-cycles.

Conversely, consider any bubble-cycle C and let $(t, \overline{t})$ be its swap arc. C is composed by a first subpath P from s to t that traverses vertices of V and a second subpath $\overline{Q}$ from $\overline{t}$ to $\overline{s}$ composed of vertices of $\overline{V}$ only. By definition of G'_s, the arcs of the subpath P form a path from s to t in the original graph G; given that the vertices in the subpath $\overline{Q}$ from $\overline{t}$ to $\overline{s}$ are in $\overline{V}$ and use arcs that are those of E inverted, then Q corresponds to another path from s to t of the original graph G. As no internal vertex of $\overline{Q}$ is a twin of a vertex in P, these two paths from s to t are vertex-disjoint, and hence they form an (s, t)-bubble.

Notice that there is a cycle $s, v, \overline{v}, \overline{s}$ for each v in the out-neighbourhood of s. Such cycles do not correspond to any bubble in G, and the condition on the size of C allows us to rule them out. □

[1] The only twin-free cycles in of size four in G'_s are generated by the outgoing arcs of s. There are $O(|V|)$ of such cycles.

7.4 THE ALGORITHM

In the previous chapter we have seen several techniques to enumerate cycles, and in particular the Johnson's Algorithm [18], that is a polynomial delay algorithm for the cycle enumeration problem that works also in the case of directed graphs. We propose to adapt the principle of this latter algorithm because, since the graphs in which we are interested in are directed, we cannot apply the algorithm presented in Chapter 6 .

In particular we will use the idea of the pruned backtracking, to enumerate bubble-cycles in G'_s, modified to take into account the twin vertices. Proposition 2 then ensures that running our algorithm on G'_s for every $s \in V$ is equivalent to the enumeration of (twice) all the bubbles of G. To do so, we explore G'_s by recursively traversing it while maintaining the following three variables. We denote by $N^+(v)$ the set of out-neighbours and $N^-(v)$ as the set of in-neighbours of v.

1. A variable *stack* which contains the vertices of a path (with no repeated vertices) from s to the current vertex. Each time it is possible to reach $\bar{s}$ from the current vertex by satisfying all the conditions to have a bubble-cycle, this stack is completed into a bubble-cycle and its content output.
2. A variable *status(v)* for each vertex v which can take three possible values:
   - $\mathtt{free}$*:* v should be explored during the traversal of G'_s;
   - $\mathtt{blocked}$*:* v should not be explored because it is already in the stack or because it is not possible to complete the current stack into a cycle by going through v – notice that the key idea of the algorithm is that a vertex may be blocked without being on the stack, avoiding thus useless explorations;
   - $\mathtt{twinned}$*:* $v \in \overline{V}$ and its twin is already in the stack, so that v should not be explored.
3. A set $B(v)$ of in-neighbours of v where vertex v is blocked and for each vertex $w \in B(v)$ there exists an arc (w, v) in G'_s (that is, $w \in N^-(v)$). If a modification in the stack causes that v is unblocked and it is possible to go from v to $\bar{s}$ using free vertices, then w should be unblocked if it is currently blocked.

Algorithm 24 enumerates all the bubble-cycles in G by fixing the source s of the (s, t)-bubble, computing the transformed graph G'_s and then listing all bubble-cycles with source s in G'_s. This procedure is repeated for each vertex $s \in V$. To list the bubble-cycles with source s, procedure CYCLE(s) is called. As a general approach, Algorithm 26 uses classical backtracking with a pruned search tree. The root of the recursion corresponds to the enumeration of all bubble-cycles in G'_s with starting point s. The algorithm then proceeds recursively:

for each free out-neighbour w of v the algorithm enumerates all bubble-cycles that have the vertices in the current stack plus w as a prefix. If $v \in V$ and $\bar{v}$ is twinned, the recursion is also applied to the current stack plus $\bar{v}$, $(v, \bar{v})$ becoming the current swap arc. A base case of the recursion happens when $\bar{s}$ is reached and the call to CYCLE$(\bar{s})$ completed. In this case, the path in *stack* is a twin-free cycle and, if this cycle has more than 4 vertices, it is a bubble-cycle to output.

The key idea that enables to make this pruned backtracking efficient is the block-unblock strategy. Observe that when CYCLE(v) is called, v is pushed in the stack and to ensure twin-free extensions, v is blocked and $\bar{v}$ is twinned if $v \in V$. Later, when backtracking, v is popped from the stack but it is *not necessarily* marked as free. If there were no twin-free cycles with the vertices in the current stack as a prefix, the vertex v would remain blocked and its status would be set to free only at a later stage. The intuition is that either v is a dead-end or there remain vertices in the stack that block all twin-free paths from v to $\bar{s}$. In order to manage the status of the vertices, the sets $B(w)$ are used. When a vertex v remains blocked while backtracking, it implies that every out-neighbour w of v has been previously blocked or twinned. To indicate that each out-neighbour $w \in N^+(v)$ (also, $v \in N^-(w)$ is an *in-neighbour* of w) blocks vertex v, we add v to each $B(w)$. When, at a later point in the recursion, a vertex $w \in N^+(v)$ becomes unblocked, v must also be unblocked as possibly there are now bubble-cycles that include v. Algorithm 25 implements this recursive unblocking strategy.

Algorithm 24: Main algorithm

```
Input: A graph $G = (V, E)$
Output: All the bubbles in $G$
for $s \in V$ do
    stack ← $\emptyset$;
    for $v \in G'_s$ do
        status← free;
        $B(v) = \emptyset$;
    end
    CYCLE(s);
end
```

An important difference between the algorithm introduced here and Johnson's is that we now have three possible states for any vertex, i.e. free, blocked and twinned, instead of only the first two. The twinned state is necessary to ensure that the two paths of the bubble share no internal vertex. Whenever $\bar{v}$ is twinned, it can only be explored from v. On the other hand, a blocked vertex should never be explored. A twin vertex $\bar{v}$ can be already blocked when the algorithm is exploring v, since it could have been unsuccessfully explored by some other call. In this case, it is necessary to verify the status of $\bar{v}$, as it is shown in the graph of

Algorithm 25: Procedure UNBLOCK(v)

```
Input: A vertex $v \in V$
/* recursive unblocking of vertices for which popping $v$ creates
   a path to $\bar{s}$                                            */
status($v$)$\leftarrow$ free;
for $w \in B(v)$ do
    delete $w$ from $B(v)$;
    if status($w$)= blocked then
        UNBLOCK($w$);
    end
end
```

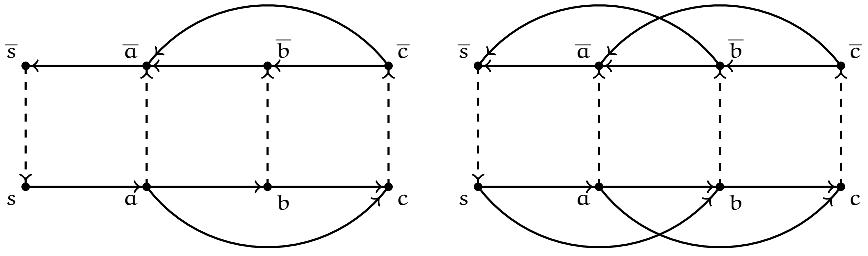

(a)

(b)

Figure 41: (a) Example where the twin $\bar{v}$ is already blocked when the algorithm starts exploring v. By starting in s and visiting first (s, a) and (a, b), the vertex $\bar{c}$ is already blocked when the algorithm starts exploring c. (b) Counterexample for the variant of the algorithm visiting first the twin and then the regular neighbours. By starting in s and visiting first (s, a) and (a, b), the algorithm misses the bubble-cycle $\langle s, a, c, \bar{c}, \bar{b}, \bar{s} \rangle$.

Figure 41a. Indeed, consider the algorithm starting from s with (s, a) and (a, b) being the first two arcs visited in the lower part. Later, when the calls CYCLE($\bar{c}$) and CYCLE($\bar{b}$) are made, since $\bar{a}$ is twinned, both $\bar{b}$ and $\bar{c}$ remain blocked. When the algorithm backtracks to a and explores (a, c), the call CYCLE(c) is made and $\bar{c}$ is already blocked.

Another important difference with respect to Johnson's algorithm is that there is a specific order in which the out-neighbourhood of a vertex should be explored. In particular, notice that the order in which Algorithm 26 explores the neighbours of a vertex v is: first the vertices in $N^+(v) \setminus \{\bar{v}\}$ and then $\bar{v}$. A variant of the algorithm where this order would be reversed, visiting first $\bar{v}$ and then the vertices in $N^+(v) \setminus \{\bar{v}\}$, would fail to enumerate all the bubbles. Indeed, intuitively a vertex can be blocked because the only way to reach $\bar{s}$ is through a twinned vertex and when that vertex is untwinned the first one is not unblocked. Indeed, consider the graph in Figure 41b and the twin-first variant starting in

Algorithm 26: Procedure CYCLE(v)

```
Input: A vertex $v \in V$
Output: All the bubbles in G starting from $v$
f ← false;
push $v$;
status($v$) ← blocked;
/* Exploring forward the arcs going out from $v \in V$ */
if $v \in V$ then
    if status($\overline{v}$) = free then status($\overline{v}$)← twinned
    for $w \in N^+(v) \cap V$ do
        if status($w$) = free then
            if CYCLE($w$) then f ← true
        end
    end
    if status($\overline{v}$) = twinned then
        if CYCLE($\overline{v}$) then f ← true
    end

/* Exploring forward the arcs going out from $v \in \overline{V}$ */
else
    for $w \in N^+(v)$ do
        if $w = \overline{s}$ then
            output the cycle composed by the stack followed by $\overline{s}$ and $s$;
            f ← true;
        else if status($w$) = free then
            if CYCLE($w$) then f ← true
        end
    end
end
if f then UNBLOCK($v$) else
    for $w \in N^+(v)$ do
        if $v \notin B(w)$ then $B(w) = B(w) \cup \{v\}$
    end
end
pop $v$;
return f;
```

s with (s, a) and (a, b) being the first two arcs explored in the lower part of the graph. When the algorithm starts exploring b the stack contains $\langle s, a, b \rangle$. After, the call CYCLE($\bar{b}$) returns *true* and CYCLE(c) returns *false* because $\bar{a}$ and $\bar{b}$ are twinned. After finishing exploring b, the blocked list $B(b)$ is empty. Thus, the only vertex unblocked is b, c (and $\bar{c}$) remaining blocked. Finally, the algorithm backtracks to a and explores the arc (a, c), but c is blocked, and it fails to enumerate $\langle s, a, c, \overline{c}, \overline{b}, \overline{s} \rangle$.

One way to address the problem above would be to modify the algorithm so that every time a vertex $\bar{v}$ is untwinned, a call to UNBLOCK($\bar{v}$) is made. All the bubble-cycles would be correctly enumerated. However, in this case, it is not hard to find an example where the delay would then no longer be linear. Intuitively, visiting first $N^+(v) \setminus \{\bar{v}\}$ and, then $\bar{v}$, works because every vertex u that was blocked (during the exploration of $N^+(v) \setminus \{\bar{v}\}$) should remain blocked when the algorithm explores $\bar{v}$. Indeed, a bubble would be missed only if there existed a path starting from $\bar{v}$, going to $\bar{s}$ through u and avoiding the twinned vertices. This is not possible if no path from $N^+(v) \setminus \{\bar{v}\}$ to u could be completed into a bubble-cycle by avoiding the twinned vertices, as we will show later on.

7.5 enumerating bubbles: an example

Consider the graph in Figure 40a and its transformation in Figure 40b. We want to enumerate all the bubble-cycles of the graph in Figure 40b by using Algorithm 24 and thus Algorithms 25 and 26. At the beginning every vertex has a status that is free, the stack is empty and Algorithm 26 is called with input s. At this point s is put on the stack, its status is now blocked and the status of $\bar{s}$ is now twinned. Then CYCLE(a), CYCLE(b), CYCLE(c), CYCLE(d) are called in this order, blocking and putting on the stack the vertices a, b, c, d, respectively, and twinning the vertices $\bar{a}$, $\bar{b}$, $\bar{c}$, $\bar{d}$, respectively. Observe that, since s is already blocked, CYCLE(c) does not call again CYCLE(s). At this point the stack is s, a, b, c, d. Since the unique neighbour of d is $\bar{d}$, CYCLE($\bar{d}$) is called and $\bar{d}$ is blocked and put on the stack. This corresponds to the code after line 15 in Algorithm 26. Since $\bar{c}$ is twinned, CYCLE($\bar{c}$) is not called, while, since $\bar{e}$ is free, CYCLE($\bar{e}$) is called and $\bar{e}$ is thus blocked and put on the stack. Once again, since $\bar{b}$ is twinned, CYCLE($\bar{b}$) is not called, and $\bar{s}$ is reached: the cycle containing the vertex on the stack plus $\bar{s}$, $s, a, b, c, d, \bar{d}, \bar{e}, \bar{s}$, is output.

After the output, the call CYCLE($\bar{e}$) returns and $\bar{e}$ is unblocked and removed from the stack. The same happens for the calls CYCLE($\bar{d}$) and CYCLE(d). At this point the stack is s, a, b, c and CYCLE($\bar{c}$) is called: $\bar{c}$ is thus blocked and put on the stack. Since $\bar{b}$ is twinned, CYCLE($\bar{b}$) is not called, while since $\bar{e}$ is free, CYCLE($\bar{e}$) is called and $\bar{e}$ is thus blocked and put on the stack. Once again, since $\bar{b}$ is twinned, CYCLE($\bar{b}$) is not called, and $\bar{s}$ is reached: the cycle containing the vertex on the stack plus $\bar{s}$, $s, a, b, c, \bar{c}, \bar{e}, \bar{s}$, is output.

After this latter output, the call CYCLE($\bar{e}$), and after CYCLE($\bar{c}$) and CYCLE(c), return, so that $\bar{e}$, $\bar{c}$, and c are unblocked and removed from the stack. Now the stack is s, a, b and we are exploiting other feasible neighbours of b: in particular CYCLE(e) is called. We have that e is now blocked and put on the stack. Since c is free, CYCLE(c) is called; this latter calls CYCLE(d), that calls CYCLE($\bar{d}$). At this point the stack is $s, a, b, e, c, d, \bar{d}$ and it is not possible to complete the stack in order to get a bubble-cycle. Thus f is false, and for any out-neighbour w of $\bar{d}$, v is added to $B(w)$, so that $\bar{d}$ is added to $B(\bar{c})$ and to $B(\bar{e})$. Hence CYCLE($\bar{d}$) returns and, also in CYCLE(d), f remains false, so that $\bar{d}$ is added to $B(d)$. At this point CYCLE(d) returns, we are in CYCLE(c) and we have to finish to exploit the neighbours of c. The stack is s, a, b, e, c, the vertices $s, a, b, c, d, e, \bar{d}$ are blocked, the vertices $\bar{s}, \bar{a}, \bar{b}, \bar{c}, \bar{e}$ are twinned. With this settings, CYCLE(c) calls CYCLE($\bar{c}$) that returns false; $\bar{c}$ is thus added to $B(\bar{b})$ and $B(\bar{e})$. Also CYCLE(c) returns false, so that c is added to $B(d)$ and $B(\bar{c})$. We are thus in CYCLE(e): c has been already considered and d is blocked, CYCLE($\bar{e}$) is thus called. Observe that CYCLE(e) never calls directly CYCLE(d) because it is known that it would return false, thanks to the previous calls from CYCLE(c). This avoids useless computation by realizing the so-called pruning strategy. At this point CYCLE($\bar{e}$) reaches $\bar{s}$ and a bubble-cycle is output: $s, a, b, e, \bar{e}, \bar{s}$. Summarizing, $s, a, b, c, d, e, \bar{c}, \bar{d}$ are blocked, $\bar{s}, \bar{a}, \bar{b}, \bar{e}$ are twinned. In particular $B(d) = \{c\}$, $B(\bar{b}) = \{\bar{c}\}$, $B(\bar{c}) = \{\bar{d}, c\}$, $B(\bar{d}) = \{d\}$, $B(\bar{e}) = \{\bar{d}, \bar{c}\}$, and the other B sets are empty.

After the output, vertex $\bar{e}$ is removed from the stack, unblocked, and any vertex $w \in B(\bar{e})$ is recursively unblocked, so that $\bar{d}$ and $\bar{c}$ are unblocked, and successively also d and c are unblocked. Thus $B(x)$ is empty for any vertex x except for $B(\bar{b}) = \{\bar{c}\}$. CYCLE($\bar{e}$) returns inside CYCLE(e), also e is removed from the stack and unblocked and CYCLE(e) returns inside CYCLE(b). Now the unique blocked vertices are s, a, b and $\bar{s}, \bar{a}, \bar{c}$ are the unique twinned vertices: the algorithm continues by calling CYCLE($\bar{b}$) and after CYCLE($\bar{a}$). Then it returns inside CYCLE($\bar{s}$), where, with empty stack, no blocked vertices, empty B sets, and no twinned vertices, CYCLE(e) is called.

By proceeding in the same way, also the bubble-cycles:

- $s, e, c, \bar{c}, \bar{b}, \bar{a}, \bar{s}$,
- $s, e, d, \bar{d}, \bar{c}, \bar{b}, \bar{a}, \bar{s}$, and
- $s, e, \bar{e}, \bar{b}, \bar{a}, \bar{s}$

are outputted.

7.6 PROOF OF CORRECTNESS AND COMPLEXITY ANALYSIS

The first part of this section is devoted to prove that Algorithm 26 enumerates all bubbles with source s.

Lemma 29. *Let v be a vertex of G'_s such that* $\mathtt{status}(v) = \mathtt{blocked}$*, S the set of vertices currently in the stack, and T the set of vertices whose status is equal to twinned. Then $S \cup T$ is a $(v, \bar{s})$ separator, that is, each path, if any exists, from v to $\bar{s}$ contains at least one vertex in $S \cup T$.*

Proof. The result is obvious for the vertices in $S \cup T$. Let v be a vertex of G'_s such that $\mathtt{status}(v) = \mathtt{blocked}$ and $v \notin S \cup T$. This means that when v was popped for the last time, CYCLE(v) was equal to *false* since v remained blocked.

Let us prove by induction on k that each path to $\bar{s}$ of length k from a blocked vertex not in $S \cup T$ contains at least one vertex in $S \cup T$.

We first consider the base case $k = 1$. Suppose that v is a counter-example for $k = 1$. This means that there is an arc from v to $\bar{s}$ ($\bar{s}$ is an out-neighbour of v). However, in that case the output of CYCLE(v) is *true*, a contradiction because v would then be unblocked.

Suppose that the result is true for $k - 1$ and, by contradiction, that there exists a blocked vertex $v \notin S \cup T$ and a path $(v, w, \dots, \bar{s})$ of length k avoiding $S \cup T$. Since $(w, \dots, \bar{s})$ is a path of length $k - 1$, we can then assume that w is free. Otherwise, if w were blocked, by induction, the path $(w, \dots, \bar{s})$ would contain at least one vertex in $S \cup T$, and so would the path $(v, w, \dots, \bar{s})$.

Since the call to CYCLE(v) returned *false* (v remained blocked), either w was already blocked or twinned, or the call to CYCLE(w) made inside CYCLE(v) gave an output equal to *false*. In any case, after the call to CYCLE(v), w was blocked or twinned and v put in $B(w)$.

The conditional at line 11 of the CYCLE procedure ensures that when untwinned, a vertex immediately becomes blocked. Thus, since w is now free, a call to UNBLOCK(w) was made in any case, yielding a call to UNBLOCK(v). This contradicts the fact that v is blocked. □

Theorem 21. *The algorithm returns only bubble-cycles. Moreover, each of those cycles is returned exactly once.*

Proof. Let us first prove that only bubble-cycles are output. As any call to UNBLOCK (either inside the procedure CYCLE or inside the procedure UNBLOCK itself) is immediately followed by the popping of the considered vertex, no vertex can appear twice in the stack. Thus, the algorithm returns only cycles. They are trivially bipolar as they have to contain s and $\bar{s}$ to be output.

Consider now a cycle C output by the algorithm with swap arc $(t, \bar{t})$. Let (v, w) in C with $v \neq s$ and $v \neq t$. If $\bar{v}$ is free when v is put on the stack, then $\bar{v}$ is twinned before w is put on the stack and cannot be explored until w is popped. If $\bar{v}$ is blocked when v is put on the stack, then by Lemma 29 it remains blocked at least until v is popped. Thus, $\bar{v}$ cannot be in C, and consequently the output cycles are twin-free.

So far we have proven that the output produces bubble-cycles. Let us now show that all cycles $C = \{v_0 = s, v_1, \ldots, v_{l-1}, v_l = \bar{s}, v_0\}$ satisfying those conditions are output by the algorithm, and each is output exactly once.

The fact that C is not returned twice is a direct consequence of the fact that the stack is different in all the leaves of a backtracking procedure. To show that C is output, let us prove by induction that the stack is equal to $\{v_0, \ldots, v_i\}$ at some point of the algorithm, for every $0 \leqslant i \leqslant l-1$. Indeed, it is true for $i = 0$. Moreover, suppose that at some point, the stack is $\{v_0, \ldots, v_{i-1}\}$.

Suppose that v_{i-1} is different from t. As the cycle contains no pair of twins except for those composing the arcs $(s, \bar{s})$ and $(t, \bar{t})$, the path $\{v_i, v_{i+1}, \ldots, v_l\}$ contains no twin of $\{v_0, \ldots, v_{i-1}\}$ and therefore no twinned vertex. Thus, it is a path from v_i to $\bar{s}$ avoiding $S \cup T$. Lemma 29 then ensures that at this point v_i is not blocked. As it is also not twinned, its status is free. Therefore, it will be explored by the backtracking procedure and the stack at some point will be $\{v_0, \ldots, v_i\}$. If $v_{i-1} = t$, $v_i = \bar{t}$ is not blocked using the same arguments. Thus it was twinned by the call to CYCLE(t) and is therefore explored at Line 12 of this procedure. Again, the stack at some point will be $\{v_0, \ldots, v_i\}$.

□

As in [18], we show that Algorithm 26 has delay $O(|V| + |E|)$ by proving that a cycle has to be output between two successive unblockings of the same vertex and that with linear delay some vertex has to be unblocked again. To do so, let us first prove the following lemmas.

Lemma 30. *Let v be a vertex such that CYCLE(v) returns true. Then a cycle is output after that call and before any call to UNBLOCK.*

Proof. Let y be the first vertex such that UNBLOCK(y) is called inside CYCLE(v). Since CYCLE(v) returns true, there is a call to UNBLOCK(v) before it returns, so that y exists. Certainly, UNBLOCK(y) was called before UNBLOCK(v) if $y \neq v$. Moreover, the call UNBLOCK(y) was done inside CYCLE(y), from line 25, otherwise it would contradict the choice of y. So, the call to CYCLE(y) was done within the recursive calls inside the call to CYCLE(v). CYCLE(y) must then return true as y was unblocked from it.

All the recursive calls CYCLE(z) made inside CYCLE(y) must return false, otherwise there would be a call to UNBLOCK(z) before UNBLOCK(y), contradicting the choice of y. Since CYCLE(y) must return true and the calls to all the neighbours returned false, the only possibility is that $\bar{s} \in N^+(y)$. Therefore, a cycle is output before UNBLOCK(y). □

Lemma 31. *Let v be a vertex such that there is a $(v, \bar{s})$-path P avoiding $S \cup T$ at the moment a call to CYCLE(v) is made. Then the return value of CYCLE(v) is true.*

Proof. First notice that if there is such a path P, then v belongs to a cycle in G'_s. This cycle may however not be a bubble-cycle in the sense that it may not be twin-free, that is, it may contain more than two pairs of twin vertices. Indeed, since the only constraint that we have on P is that it avoids all vertices that are in S and T when v is reached, then if $v \in V$, it could be that the path P from v to $\bar{s}$ contains, besides s and $\bar{s}$, at least two more pairs of twin vertices. An example is given in Figure 40b. It is however always possible, by construction of G'_s from G, to find a vertex $y \in V$ such that y is the first vertex in P with $\overline{y}$ also in P. Let P' be the path that is a concatenation of the subpath $s \rightsquigarrow y$ of P, the arc $(y, \overline{y})$, and the subpath $\overline{y} \rightsquigarrow \bar{s}$ in P. This path is twin-free, and a call to CYCLE(v) will, by correctness of the algorithm, return true. □

Theorem 22. *Algorithm 26 has linear delay.*

Proof. Let us first prove that between two successive unblockings of any vertex v, a cycle is output. Let w be the vertex such that a call to UNBLOCK(w) at line 25 of Algorithm 26 unblocks v for the first time. Let S and T be, respectively, the current sets of stack and twinned vertices after popping w. The recursive structure of the unblocking procedure then ensures that there exists a (v, w)-path avoiding $S \cup T$. Moreover, as the call to UNBLOCK(w) was made at line 25, the answer to CYCLE(w) is *true* so there exists also a $(w, \bar{s})$-path avoiding $S \cup T$. The concatenation of both paths is a again a $(v, \bar{s})$-path avoiding $S \cup T$. Let x be the first vertex of this path to be visited again. Note that, if no vertex in this path is visited again there is nothing to prove, since v is free, CYCLE(v) needs to be called before any UNBLOCK(v) call. When CYCLE(x) is called, there is a $(x, \bar{s})$-path avoiding the current $S \cup T$. vertices. Thus, applying Lemma 31 and then Lemma 30, we know that a cycle is output before any call to UNBLOCK. As no call to UNBLOCK(v) can be made before the call to CYCLE(x), a cycle is output before the second call to UNBLOCK(v).

Let us now consider the delay of the algorithm. In both its exploration and unblocking phases, the algorithm follows the arcs of the graph and transforms the status or the B lists of their endpoints, which overall require constant time. Thus, the delay only depends on the number of arcs which are considered during two successive outputs. An arc (u, v) is considered once by the algorithm in the three following situations: the exploration part of a call to CYCLE(u); an insertion of u in $B(v)$; a call to UNBLOCK(v). As shown before, UNBLOCK(v) is called only once between two successive outputs. CYCLE(u) cannot be called more than twice. Thus the arc (u, v) is considered at most 5 times between two outputs. This ensures that the delay of the algorithm is $\mathcal{O}(|V| + |E|)$.

□

7.7 AVOIDING DUPLICATE BUBBLES.

The one-to-two correspondence between cycles in G'_s and bubbles starting from s in G, claimed by Proposition 2, can be reduced to a one-to-one correspondence in the following way. Consider an arbitrary order on the vertices of V, and assign to each vertex of $\overline{V}$ the order of its twin. Let C be a cycle of G'_s that passes through s and contains exactly two pairs of twin vertices. Denote again by t the vertex such that $(t, \overline{t})$ is the arc through which C swaps from V to $\overline{V}$. Denote by *swap predecessor* the vertex before t in C and by *swap successor* the vertex after $\overline{t}$ in C.

Proposition 3. *There is a one-to-one correspondence between the set of* (s, t)*-bubbles in* G *for all* $t \in V$*, and the set of cycles of* G'_s *that pass through* s*, contain exactly two pairs of twin vertices and such that the swap predecessor is greater than the swap successor.*

Proof. The proof follows the one of Proposition 2. The only difference is that, if we consider a bubble composed of the paths P_1 and P_2, one of these two paths, say P_1, has a next to last vertex greater than the next to last vertex of P_2. Then the cycle of G'_s made of P_1 and $\overline{P_2}$ is still considered by the algorithm whereas the cycle made of P_2 and $\overline{P_1}$ is not. Moreover, the cycles of length four which are of the type $\{s, t, \overline{t}, \overline{s}\}$ are ruled out as $\overline{s}$ is of the same order as s. □

7.8 CONCLUSION AND OPEN PROBLEMS

We showed in this chapter that it is possible (Algorithm 26) to enumerate all bubbles with a given source in a directed graph with linear delay. Moreover, it is possible to enumerate all bubbles, for all possible sources (Algorithm 24), in $O((|E| + |V|)(|C| + |V|))$ total time, where $|C|$ is the number of bubbles. This required a non trivial adaptation of Johnson's algorithm [18]. The main question arising from our work is whether it is possible to generalize our result, by finding a linear delay algorithm enumerating k-tuple of vertex disjoint paths.

8 CONCLUSIONS

Biological networks models introduce several biases: arc dependencies are neglected and underlying hyper-graph behaviours are forced in simple graph representations to avoid intractability. Moreover regulatory interactions between all the biological networks are omitted, even if none of the different biological layers is truly isolated. Last but not least, the dynamical behaviours of biological networks are often not considered: indeed most of the currently available biological network reconstructions are potential networks, where all the possible connections are indicated, even if edges/arcs and vertices are hardly present all together at the same time. In this scenario, we have seen that very often enumeration algorithms can be helpful so that the solutions can be checked *a posteriori*, and in Chapter 3 we have resumed the main schemas to design enumeration algorithms.

In Chapter 4 we have described and experimented new algorithms for enumerating all the diametral and radial vertices and computing the diameter and radius of directed and undirected (weighted) graphs. Even though these algorithms have $O(nm)$ time complexity in the worst case, our experiments suggest that their execution for real-world networks requires time $O(m)$ in the case of the diameter and almost $O(m)$ in the case of the radius. The computation of the radius with our algorithm is affected by the choice of the starting vertices x, y so that the best performances are achieved whenever x and y are both diametral targets. The performance of DiFUB depends on the choice of the starting vertex u (indeed, it could be interesting to experimentally analyse its behaviour depending on this choice). The main fundamental questions are now the followings. Why the double sweep heuristic, both in the directed and in the undirected version, is so effective in finding tight lower bounds for the diameter and vertices with low eccentricity? Which one is the topological underlying property that can lead us to these results? Why real world graphs exhibit this property? Some progress has been done by [184], but still a lot has to be done. Finally, it could be interesting to analyse a parallel implementation of the DiFUB algorithm. Indeed, the eccentricities of the vertices belonging to the same fringe set can be computed in parallel. Moreover, a variety of parallel BFS algorithms have been explored in the literature and can be integrated in the implementation of our algorithm.

In Chapter 5 we have introduced the new notion of a story, which is a maximal acyclic subgraph of a directed graph in which only specified vertices can be sources or targets. We have proved some complexity results and designed some algorithms for enumerating all possible stories of a graph. From a theoretical point of view the main question left open is to establish the complexity of the enumeration problem. Indeed the enumeration algorithm presented, even if it works well in practice, gives no guarantee on the delay between the output of two consecutive solutions. We address as a future work, exploiting the relationship between stories and subset feedback vertex sets, that has been studied in [206] by applying *Measure and Conquer* approach [207]. From a practical point of view, for some graphs the number of solutions found is extremely large and therefore the analysis of the results is compromised. Adding more constraints to the model could be a way to filter a priori the set of solutions. This observation on the size of the output leads us to consider the problem from a modelling point of view. For instance, the acyclicity constraint could be relaxed allowing cycles between white vertices. Moreover, the model could be enriched by exploring the information on the concentrations given by the metabolomics experiment. Notice that in this case the nature of the problem changes into an optimization problem. Another alternative is to consider integrated models, adding to the Metabolic network other layers of information such as regulation, or taking the stoichiometry of the reactions into account.

In Chapter 6 we showed the first optimal solution to list all the cycles of an undirected graph and all the paths from a given source to a given target. This result improves the Johnson's algorithm, that was still the theoretically most efficient in the case of undirected graphs. The main question arising from our work is whether it is possible to obtain an optimal algorithm to list all the paths and cycles in a directed graph in order to deal more efficiently with directed biological interaction networks, like gene regulatory networks, where the cycle enumeration have been discovered to be useful for several purposes.

In Chapter 7 we showed that it is possible to enumerate all the bubbles, i.e. pairs of vertex disjoint paths, with a given source in a directed graph with linear delay. Moreover, it is possible to enumerate all bubbles, for all possible sources, in $O((|E|+|V|)(|C|+|V|))$ total time, where $|C|$ is the number of bubbles. This has required a non trivial adaptation of Johnson's algorithm [18]. The main question arising from our work is whether it is possible to generalize our result, by finding a linear delay algorithm enumerating k-tuple of vertex disjoint paths, or finding an algorithm to enumerate efficiently bubbles of a given size.

BIBLIOGRAPHY

[1] Cecilia Klein, Andrea Marino, Marie-France Sagot, Paulo Vieira Milreu, and Matteo Brilli. Structural and dynamical analysis of biological networks. *Briefings in functional genomics*, August 2012. (Cited on pages 3, 13, and 50.)

[2] M. E. J. Newman. The structure and function of complex networks. *SIAM REVIEW*, 45:167–256, 2003. (Cited on pages 4 and 48.)

[3] Pierluigi Crescenzi, Roberto Grossi, Leonardo Lanzi, and Andrea Marino. On computing the diameter of real-world directed (weighted) graphs. In *SEA*, pages 99–110, 2012. (Cited on pages 5 and 49.)

[4] P. Crescenzi, R. Grossi, C. Imbrenda, L. Lanzi, and A. Marino. Finding the Diameter in Real-World Graphs: Experimentally Turning a Lower Bound into an Upper Bound. In Mark de Berg and Ulrich Meyer, editor, *Algorithms - ESA 2010, 18th Annual European Symposium. Proceedings, Part I*, volume 6346 of *Lecture Notes in Computer Science*. Springer, 2010. (Cited on pages 5, 49, 58, and 89.)

[5] P. Crescenzi, R. Grossi, M. Habib, L. Lanzi, and A. Marino. On Computing the Diameter of Real-World Undirected Graphs. Presented at Workshop on Graph Algorithms and Applications (Zurich–July 3, 2011) and selected for submission to the special issue of Theoretical Computer Science in honor of Giorgio Ausiello in the occasion of his 70th birthday, 2011. (Cited on pages 5, 49, and 78.)

[6] P. Crescenzi, R. Grossi, M. Habib, L. Lanzi, and A. Marino. On computing the diameter of real-world undirected graphs. *Theoretical Computer Science*, 2012. (Cited on pages 5, 49, 78, 83, and 88.)

[7] Lars Backstrom, Paolo Boldi, Marco Rosa, Johan Ugander, and Sebastiano Vigna. Four Degrees of Separation. *arXiv:1111.4570v1*, 2011. (Cited on pages 5, 48, and 49.)

[8] Lars Backstrom, Paolo Boldi, Marco Rosa, Johan Ugander, and Sebastiano Vigna. Four degrees of separation. In *WebSci*, pages 33–42, 2012. (Cited on pages 5, 48, and 49.)

[9] Geoffrey Madalinski, Emmanuel Godat, Sandra Alves, Denis Lesage, Eric Genin, Philippe Levi, Jean Labarre, Jean-Claude Tabet, Eric Ezan, and Christophe Junot. Direct introduction of biological samples into a ltq-orbitrap hybrid mass spectrometer as a tool for fast metabolome analysis.

Analytical Chemistry, 80(9):3291–3303, 2008. PMID: 18351782. (Cited on pages 5, 95, and 96.)

[10] Vicente Acuña, Etienne Birmelé, Ludovic Cottret, Pierluigi Crescenzi, Vincent Lacroix, Alberto Marchetti-Spaccamela, Andrea Marino, Paulo Vieira Milreu, Marie-France Sagot, and Leen Stougie. Telling stories. Presented at Workshop on Graph Algorithms and Applications (Zurich–July 3, 2011) and selected for submission to the special issue of Theoretical Computer Science in honor of Giorgio Ausiello in the occasion of his 70th birthday, 2011. (Cited on pages 6 and 98.)

[11] Vicente Acuña, Etienne Birmelé, Ludovic Cottret, Pierluigi Crescenzi, Fabien Jourdan, Vincent Lacroix, Alberto Marchetti-Spaccamela, Andrea Marino, Paulo Vieira Milreu, Marie-France Sagot, and Leen Stougie. Telling stories: Enumerating maximal directed acyclic graphs with a constrained set of sources and targets. *Theor. Comput. Sci.*, 457:1–9, October 2012. (Cited on pages 6 and 98.)

[12] Benno Schwikowski and Ewald Speckenmeyer. On enumerating all minimal solutions of feedback problems. *Discrete Applied Mathematics*, 117(1-3):253 – 265, 2002. (Cited on pages 6, 97, and 99.)

[13] V. Acuña, E. Birmelé, L. Cottret, P. Crescenzi, F. Jourdan, V. Lacroix, A. Marchetti-Spaccamela, A. Marino, P.V. Milreu, M.-F.Sagot, and L. Stougie. Metabolic stories: uncovering all possible scenarios for interpreting metabolomics data. In First RECOMB Satellite Conference on Open Problems in Algorithmic Biology (RECOMB-AB), August 27-29, 2012, St. Petersburg, Russia., 2012. (Cited on pages 6 and 98.)

[14] S. Klamt and A. von Kamp. Computing paths and cycles in biological interaction graphs. *BMC Bioinformatics*, 10:181, 2009. (Cited on pages 7, 21, and 113.)

[15] Olivier Cinquin and Jacques Demongeot. Positive and negative feedback: Striking a balance between necessary antagonists. *J. Theor. Biol*, 216:229–241, 2002. (Cited on pages 7, 113, and 114.)

[16] Denis Thieffry. Dynamical roles of biological regulatory circuits. *Briefings in Bioinformatics*, 8(4):220–225, 2007. (Cited on pages 7, 113, and 114.)

[17] Yung-Keun Kwon and Kwang-Hyun Cho. Coherent coupling of feedback loops: a design principle of cell signaling networks. *Bioinformatics*, 24(17):1926–1932, September 2008. (Cited on pages 7 and 114.)

[18] D.B. Johnson. Finding all the elementary circuits of a directed graph. *SIAM J. Comput.*, 4(1):77–84, 1975. (Cited on pages 7, 9, 29, 113, 115, 144, 147, 154, 156, and 158.)

[19] E. Birmelé, R. Ferreira, R. Grossi, A. Marino, N. Pisanti, R. Rizzi, and G. Sacomoto. Optimal listing of cycles and st-paths in undirected graphs. In *ACM-SIAM Symposium on Discrete Algorithms, SODA 2013*, 2013 (to appear). (Cited on pages 8, 29, and 115.)

[20] Gustavo Sacomoto, Janice Kielbassa, Rayan Chikhi, Raluca Uricaru, Pavlos Antoniou, Marie F. Sagot, Pierre Peterlongo, and Vincent Lacroix. KISSPLICE: de-novo calling alternative splicing events from RNA-seq data. *BMC Bioinformatics*, 13(Suppl 6):S5+, 2012. (Cited on pages 8, 143, and 144.)

[21] James C. Tiernan. An efficient search algorithm to find the elementary circuits of a graph. *Communonications ACM*, 13:722–726, 1970. (Cited on pages 8, 29, 115, and 144.)

[22] Etienne Birmelé, Pierluigi Crescenzi, Rui A. Ferreira, Roberto Grossi, Vincent Lacroix, Andrea Marino, Nadia Pisanti, Gustavo Akio Tominaga Sacomoto, and Marie-France Sagot. Efficient bubble enumeration in directed graphs. In *SPIRE*, pages 118–129, 2012. (Cited on pages 9, 115, and 144.)

[23] Vincent Lacroix, Ludovic Cottret, Patricia Thébault, and Marie-France Sagot. An introduction to metabolic networks and their structural analysis. *IEEE/ACM Trans. Comput. Biology Bioinform.*, 5(4):594–617, 2008. (Cited on page 15.)

[24] Ludovic Cottret and Fabien Jourdan. Graph methods for the investigation of metabolic networks in parasitology. *Parasitology*, 137(9):1393–1407, August 2010. (Cited on pages 15, 69, 73, and 99.)

[25] Steffen Klamt, Utz-Uwe Haus, and Fabian Theis. Hypergraphs and Cellular Networks. *PLoS Comput Biol*, 5(5), May 2009. (Cited on page 15.)

[26] Vincent Lacroix, Ludovic Cottret, Patricia Thébault, and Marie-France Sagot. An introduction to metabolic networks and their structural analysis. *IEEE/ACM Trans. Comput. Biology Bioinform.*, 5(4):594–617, 2008. (Cited on page 15.)

[27] Hidde De Jong. Modeling and simulation of genetic regulatory systems: A literature review. *Journal of Computational Biology*, 9:67–103, 2002. (Cited on page 17.)

[28] Steffen Klamt, Julio Saez-Rodriguez, Jonathan A. Lindquist, Luca Simeoni, and Ernst Dieter Gilles. A methodology for the structural and functional analysis of signaling and regulatory networks. *BMC Bioinformatics*, 7:56, 2006. (Cited on pages 17, 113, and 114.)

[29] Rui S. Wang and Reka Albert. Elementary signaling modes predict the essentiality of signal transduction network components. *BMC Systems Biology*, 5(1):44+, 2011. (Cited on page 17.)

[30] E. R. Mardis. The impact of next-generation sequencing technology on genetics. *Trends in genetics*, 24(3):133–41+, 2008. (Cited on page 19.)

[31] Ralf Steuer, Thilo Gross, Joachim Selbig, and Bernd Blasius. Structural kinetic modeling of metabolic networks. *Proceedings of the National Academy of Sciences*, 103(32):11868–11873, August 2006. (Cited on page 19.)

[32] Sergio Grimbs, Joachim Selbig, Sascha Bulik, Hermann-Georg G. Holzhütter, and Ralf Steuer. The stability and robustness of metabolic states: identifying stabilizing sites in metabolic networks. *Molecular systems biology*, 3, November 2007. (Cited on page 19.)

[33] Ralf Steuer. Computational approaches to the topology, stability and dynamics of metabolic networks. *Phytochemistry*, 68(16-18):2139–2151, August 2007. (Cited on page 19.)

[34] Valentina Baldazzi, Delphine Ropers, Yves Markowicz, Daniel Kahn, Johannes Geiselmann, and Hidde de Jong. The carbon assimilation network in escherichia coli is densely connected and largely sign-determined by directions of metabolic fluxes. *PLoS Computational Biology*, 6(6), 2010. (Cited on page 19.)

[35] Valentina Baldazzi, Delphine Ropers, Johannes Geiselmann, Daniel Kahn, and Hidde de Jong. Importance of metabolic coupling for the dynamics of gene expression following a diauxic shift in escherichia coli. *J Theor Biol*, 2011. (Cited on page 19.)

[36] Oliver Kotte, Judith B Zaugg, and Matthias Heinemann. Bacterial adaptation through distributed sensing of metabolic fluxes. *Mol Syst Biol*, 6:355, 2010. (Cited on page 19.)

[37] S. Coulomb, M. Bauer, D. Bernard, and Marsolier M. C. Kergoat. Gene essentiality and the topology of protein interaction networks. *Proc. R. Soc. Lond. B*, 272(1573):1721–1725, August 2005. (Cited on page 20.)

[38] E. Costenbader. The stability of centrality measures when networks are sampled. *Social Networks*, 25(4):283–307, October 2003. (Cited on pages 20 and 92.)

[39] Eric de Silva, Thomas Thorne, Piers Ingram, Ino Agrafioti, Jonathan Swire, Carsten Wiuf, and Michael P. Stumpf. The effects of incomplete protein interaction data on structural and evolutionary inferences. *BMC biology*, 4:39+, November 2006. (Cited on page 20.)

[40] Jing-Dong J. Han, Nicolas Bertin, Tong Hao, Debra S. Goldberg, Gabriel F. Berriz, Lan V. Zhang, Denis Dupuy, Albertha J. M. Walhout, Michael E. Cusick, Frederick P. Roth, and Marc Vidal. Evidence for dynamically organized modularity in the yeast protein–protein interaction network. *Nature*, 430(6995):88–93, 2004. (Cited on pages 20, 50, and 51.)

[41] Nicholas M. Luscombe, Madan M. Babu, Haiyuan Yu, Michael Snyder, Sarah A. Teichmann, and Mark Gerstein. Genomic analysis of regulatory network dynamics reveals large topological changes. *Nature*, 431(7006):308–312, 2004. (Cited on page 20.)

[42] Arun S. Konagurthu and Arthur M. Lesk. Single and multiple input modules in regulatory networks. *Proteins*, 73(2):320–4, November 2008. (Cited on page 20.)

[43] P. V. Gopalacharyulu, V. R. Velagapudi, E. Lindfors, E. Halperin, and M. Oresic. Dynamic network topology changes in functional modules predict responses to oxidative stress in yeast. *Molecular Biosystems*, 5(3):276–287+, 2009. (Cited on page 20.)

[44] Trey Ideker and Nevan J. Krogan. Differential network biology. *Molecular systems biology*, 8(1), January 2012. (Cited on page 20.)

[45] Michael P. H. Stumpf, Carsten Wiuf, and Robert M. May. Subnets of scale-free networks are not scale-free: Sampling properties of networks. *Proceedings of the National Academy of Sciences of the United States of America*, 102(12):4221–4224, March 2005. (Cited on page 20.)

[46] Jing-Dong D. Han, Denis Dupuy, Nicolas Bertin, Michael E. Cusick, and Marc Vidal. Effect of sampling on topology predictions of protein-protein interaction networks. *Nature biotechnology*, 23(7):839–844, July 2005. (Cited on page 20.)

[47] Vicente Acuña, Paulo Vieira Milreu, Ludovic Cottret, Alberto Marchetti-Spaccamela, Leen Stougie, and Marie-France Sagot. Algorithms and complexity of enumerating minimal precursor sets in genome-wide metabolic networks. *Bioinformatics*, 28(19):2474–2483, 2012. (Cited on page 21.)

[48] Elisabeth Wong, Brittany Baur, Saad Quader, and Chun-Hsi Huang. Biological network motif detection: principles and practice. *Briefings in Bioinformatics*, 13(2):202–215, March 2012. (Cited on page 21.)

[49] Giovanni Ciriello and Concettina Guerra. A review on models and algorithms for motif discovery in proteinâĂŞprotein interaction networks. *Briefings in Functional Genomics & Proteomics*, 7(2):147–156, March 2008. (Cited on page 21.)

[50] Joshua A. Grochow and Manolis Kellis. M: Network motif discovery using subgraph enumeration and symmetry breaking. In *In Proceedings of the 11th International Conference on Research in Computational Molecular Biology (RECOMB*, pages 21–25. Springer, 2007. (Cited on page 21.)

[51] Karoline Faust, Pierre Dupont, Jérôme Callut, and Jacques van Helden. Pathway discovery in metabolic networks by subgraph extraction. *Bioinformatics*, 26(9):1211–1218, May 2010. (Cited on pages 21 and 95.)

[52] Mehmet Koyutürk, Ananth Grama, and Wojciech Szpankowski. An efficient algorithm for detecting frequent subgraphs in biological networks. *Bioinformatics*, 20(1):200–207, January 2004. (Cited on page 21.)

[53] Shi-Hua Zhang, Xue-Mei Ning, and Xiang-Sun Zhang. Identification of functional modules in a ppi network by clique percolation clustering. *Computers & Chemistry*, 30(6):445–451, 2006. (Cited on page 21.)

[54] Elisabeth Georgii, Sabine Dietmann, Takeaki Uno, Philipp Pagel, and Koji Tsuda. Enumeration of condition-dependent dense modules in protein interaction networks. *Bioinformatics*, 25(7):933–940, April 2009. (Cited on page 21.)

[55] John D. Eblen, Charles A. Phillips, Gary L. Rogers, and Michael A. Langston. The maximum clique enumeration problem: Algorithms, applications and implementations. In Jianer Chen, Jianxin Wang, and Alexander Zelikovsky, editors, *Bioinformatics Research and Applications - 7th International Symposium, ISBRA 2011, Changsha, China, May 27-29, 2011. Proceedings*, volume 6674 of *Lecture Notes in Computer Science*, pages 306–319. Springer, 2011. (Cited on page 21.)

[56] David S. Johnson, Christos H. Papadimitriou, and Mihalis Yannakakis. On generating all maximal independent sets. *Inf. Process. Lett.*, 27(3):119–123, 1988. (Cited on page 26.)

[57] Pang-Ning Tan, Michael Steinbach, and Vipin Kumar. *Introduction to Data Mining, (First Edition)*. Addison-Wesley Longman Publishing Co., Inc., Boston, MA, USA, 2005. (Cited on page 27.)

[58] Takeaki Uno. A fast algorithm for enumerating bipartite perfect matchings. In *ISAAC*, pages 367–379, 2001. (Cited on pages 28 and 44.)

[59] Akiyoshi Shioura, Akihisa Tamura, and Takeaki Uno. An optimal algorithm for scanning all spanning trees of undirected graphs. *SIAM J. Comput.*, 26(3):678–692, 1997. (Cited on page 28.)

[60] R. E. Tarjan. Enumeration of the elementary circuits of a directed graph. *SIAM Journal on Computing*, 2(3):211–216, 1973. (Cited on pages 29, 115, and 144.)

[61] R C Read and Robert E Tarjan. Bounds on backtrack algorithms for listing cycles, paths, and spanning trees. *Networks*, 5(3):237–252, 1975. (Cited on pages 29 and 115.)

[62] David Eppstein. Finding the k shortest paths. *SIAM J. Comput.*, 28(2):652–673, February 1999. (Cited on page 29.)

[63] David Avis and Komei Fukuda. Reverse search for enumeration. *Discrete Applied Mathematics*, 65:21–46, 1993. (Cited on page 29.)

[64] Takeaki Uno. Two general methods to reduce delay and change of enumeration algorithms. NII Technical Report., 2003. (Cited on page 30.)

[65] Richard M. Karp. Reducibility among combinatorial problems. In *Complexity of Computer Computations*, pages 85–103, 1972. (Cited on page 31.)

[66] Kazuhisa Makino and Takeaki Uno. New algorithms for enumerating all maximal cliques. In *SWAT*, pages 260–272, 2004. (Cited on page 31.)

[67] Toshinobu Kashiwabara, Sumio Masuda, Kazuo Nakajima, and Toshio Fujisawa. Generation of maximum independent sets of a bipartite graph and maximum cliques of a circular-arc graph. *J. Algorithms*, 13(1):161–174, 1992. (Cited on page 31.)

[68] E. A. Akkoyunlu. The enumeration of maximal cliques of large graphs. *SIAM J. Comput.*, 2(1):1–6, 1973. (Cited on page 31.)

[69] Etsuji Tomita, Akira Tanaka, and Haruhisa Takahashi. The worst-case time complexity for generating all maximal cliques and computational experiments. *Theor. Comput. Sci.*, 363(1):28–42, October 2006. (Cited on page 32.)

[70] Tatsuya Asai, Hiroki Arimura, Takeaki Uno, and Shin-Ichi Nakano. Discovering frequent substructures in large unordered trees. In *Discovery Science*, pages 47–61, 2003. (Cited on page 33.)

[71] Katsuhisa Yamanaka, Yota Otachi, and Shin-Ichi Nakano. Efficient enumeration of ordered trees with kleaves (extended abstract). In *WALCOM*, pages 141–150, 2009. (Cited on page 33.)

[72] Takeaki Uno and Shin-Ichi Nakano. Efficient generation of rooted trees. NII Technical Report., 2003. (Cited on page 35.)

[73] Shin-Ichi Nakano and Takeaki Uno. Constant time generation of trees with specified diameter. In *WG*, pages 33–45, 2004. (Cited on page 35.)

[74] Shin-Ichi Nakano and Takeaki Uno. Generating colored trees. In *WG*, pages 249–260, 2005. (Cited on page 35.)

[75] Komei Fukuda and Tomomi Matsui. Finding all the perfect matchings in bipartite graphs. *Appl. Math. Lett*, 7:15–18, 1989. (Cited on page 44.)

[76] Komei Fukuda and Tomomi Matsui. Finding all minimum-cost perfect matchings in bipartite graphs. *Networks*, 22(5):461–468, 1992. (Cited on page 44.)

[77] Takeaki Uno. Algorithms for enumerating all perfect, maximum and maximal matchings in bipartite graphs. In *ISAAC*, pages 92–101, 1997. (Cited on page 44.)

[78] Chandra R. Chegireddy and Horst W. Hamacher. Algorithms for finding k-best perfect matchings. *Discrete Applied Mathematics*, 18(2):155 – 165, 1987. (Cited on page 44.)

[79] T. Uno. A fast algorithm for enumerating non-bipartite maximal matchings. *J. National Institute of Informatics*, 3:89–97, 2001. (Cited on page 44.)

[80] Bjőrn H. Junker and Falk Schreiber. *Analysis of Biological Networks (Wiley Series in Bioinformatics)*. Wiley-Interscience, 2008. (Cited on page 48.)

[81] Jure Leskovec, Kevin J. Lang, Anirban Dasgupta, and Michael W. Mahoney. Community structure in large networks: Natural cluster sizes and the absence of large well-defined clusters. *Internet Mathematics*, 6(1):29–123, 2009. (Cited on pages 48 and 49.)

[82] Shweta Bansal, Shashank Khandelwal, and Lauren Meyers. Exploring biological network structure with clustered random networks. *BMC Bioinformatics*, 10(1):405+, 2009. (Cited on page 48.)

[83] N. Pržulj, D. G. Corneil, and I. Jurisica. Efficient estimation of graphlet frequency distributions in protein–protein interaction networks. *Bioinformatics*, 22:974–980, April 2006. (Cited on page 48.)

[84] Alan Mislove, Massimiliano Marcon, Krishna P. Gummadi, Peter Druschel, and Bobby Bhattacharjee. Measurement and analysis of online social networks. In *Proceedings of the 7th ACM SIGCOMM conference on Internet measurement*, IMC '07, pages 29–42, New York, NY, USA, 2007. ACM. (Cited on pages 48 and 49.)

[85] Christo Wilson, Bryce Boe, Alessandra Sala, Krishna P.N. Puttaswamy, and Ben Y. Zhao. User interactions in social networks and their implications. In *Proceedings of the 4th ACM European conference on Computer systems*, EuroSys '09, pages 205–218, New York, NY, USA, 2009. ACM. (Cited on page 48.)

[86] Fang Wang, Yamir Moreno, and Yaoru Sun. Structure of peer-to-peer social networks. *Phys. Rev. E*, 73:036123, Mar 2006. (Cited on page 48.)

[87] Zheng-Bin Dong, Guo-Jie Song, Kun-Qing Xie, and Jing-Yao Wang. An experimental study of large-scale mobile social network. In *Proceedings of the 18th international conference on World wide web*, WWW '09, pages 1175–1176, New York, NY, USA, 2009. ACM. (Cited on page 48.)

[88] M. E. J. Newman. The structure of scientific collaboration networks. *Proceedings of the National Academy of Sciences of the United States of America*, 98(2):404–409, January 2001. (Cited on pages 48 and 80.)

[89] Andrei Z. Broder, Ravi Kumar, Farzin Maghoul, Prabhakar Raghavan, Sridhar Rajagopalan, Raymie Stata, Andrew Tomkins, and Janet L. Wiener. Graph structure in the web. *Computer Networks*, 33(1-6):309–320, 2000. (Cited on pages 48 and 49.)

[90] U. Kang, Charalampos E. Tsourakakis, and Christos Faloutsos. PEGASUS: A Peta-Scale graph mining system implementation and observations. In *2009 Ninth IEEE International Conference on Data Mining*, pages 229–238. IEEE, December 2009. (Cited on page 48.)

[91] U. Zwick. All Pairs Shortest Paths using Bridging Sets and Rectangular Matrix Multiplication. *Journal of the ACM*, 49:2002, 2000. (Cited on page 49.)

[92] Christopher R. Palmer, Phillip B. Gibbons, and Christos Faloutsos. ANF: a Fast and Scalable Tool for Data Mining in Massive Graphs. In *Proceedings of the 8th ACM SIGKDD International Conference on Knowledge Discovery and Data Mining*, pages 81–90, 2002. (Cited on pages 49 and 93.)

[93] Paolo Boldi, Marco Rosa, and Sebastiano Vigna. Hyperanf: approximating the neighbourhood function of very large graphs on a budget. In *WWW*, pages 625–634, 2011. (Cited on pages 49, 93, and 94.)

[94] U. Kang, Charalampos E. Tsourakakis, Ana Paula Appel, Christos Faloutsos, and Jure Leskovec. Hadi: Mining radii of large graphs. *TKDD*, 5(2):8, 2011. (Cited on page 49.)

[95] E. Cohen. Estimating the size of the transitive closure in linear time. *Foundations of Computer Science, Annual IEEE Symposium on*, 0:190–200, 1994. (Cited on pages 49 and 93.)

[96] E. Cohen and H. Kaplan. Summarizing data using bottom-k sketches. In *Proceedings of the twenty-sixth annual ACM symposium on Principles of distributed computing*, PODC '07, pages 225–234, New York, NY, USA, 2007. ACM. (Cited on pages 49 and 93.)

[97] E. Cohen. Size-Estimation Framework with Applications to Transitive Closure and Reachability. *J. Comput. Syst. Sci.*, 55(3):441–453, 1997. (Cited on pages 49 and 93.)

[98] E. Cohen and H. Kaplan. Tighter estimation using bottom k sketches. *PVLDB*, 1(1):213–224, 2008. (Cited on pages 49 and 93.)

[99] E. Cohen and H. Kaplan. Bottom-k sketches: better and more efficient estimation of aggregates. In Golubchik, L. and Ammar, M.H. and Harchol-Balter, M., editor, *Proceedings of the 2007 ACM International Conference on Measurement and Modeling of Computer Systems, SIGMETRICS 2007*, pages 353–354, San Diego, CA, USA, 2007. ACM. (Cited on pages 49 and 93.)

[100] E. Cohen. Size-estimation framework with applications to transitive closure and reachability. *J. Comput. System Sci. (special issue of selected papers from FOCS'94)*, 55:441–453, 1997. (Cited on pages 49 and 93.)

[101] J. Leskovec and C. Faloutsos. Sampling from large graphs. In *Proceedings of the 12th ACM SIGKDD international conference on Knowledge discovery and data mining*, KDD '06, pages 631–636, New York, NY, USA, 2006. ACM. (Cited on page 49.)

[102] M. Latapy and C. Magnien. Measuring Fundamental Properties of Real-World Complex Networks. *CoRR*, abs/cs/0609115, 2006. (Cited on page 49.)

[103] Frank W. Takes and Walter A. Kosters. Determining the diameter of small world networks. In *CIKM*, pages 1191–1196, 2011. (Cited on pages 49 and 90.)

[104] P. Boldi and S. Vigna. The WebGraph Framework I: Compression Techniques. In *Proceedings of the 13th International World Wide Web Conference*, pages 595–601, Manhattan, USA, 2003. ACM Press. (Cited on page 49.)

[105] P. Crescenzi, R. Grossi, L. Lanzi, and A. Marino. A Comparison of Three Algorithms for Approximating the Distance Distribution in Real-World Graphs. In *Proceedings of the 1st International ICST Conference on Theory and Practice of Algorithms in (Computer) Systems, TAPAS 2011*, volume 6595 of *Lecture Notes in Computer Science*, 2011. (Cited on pages 50 and 93.)

[106] Björn H. Junker, Dirk Koschützki, and Falk Schreiber. Exploration of biological network centralities with centibin. *BMC Bioinformatics*, 7:219, 2006. (Cited on page 50.)

[107] Johannes Gräßler, Dirk Koschützki, and Falk Schreiber. Centilib: comprehensive analysis and exploration of network centralities. *Bioinformatics*, 28(8):1178–1179, 2012. (Cited on page 50.)

[108] Dirk Koschützki and Falk Schreiber. Centrality analysis methods for biological networks and their application to gene regulatory networks. *Gene regulation and systems biology*, 2:193–201, 2008. (Cited on page 50.)

[109] Georgios Pavlopoulos, Maria Secrier, Charalampos Moschopoulos, Theodoros Soldatos, Sophia Kossida, Jan Aerts, Reinhard Schneider, and Pantelis Bagos. Using graph theory to analyze biological networks. *BioData mining*, 4(1):10+, April 2011. (Cited on page 50.)

[110] O. Mason and M. Verwoerd. Graph theory and networks in Biology. *Systems Biology, IET*, 1(2):89–119, March 2007. (Cited on page 50.)

[111] Giovanni Scardoni and Carlo Laudanna. Centralities based analysis of complex networks. *New Frontiers in Graph Theory, Yagang Zhang (Ed.)*, 2012. (Cited on pages 50 and 52.)

[112] Z. J. Hu, J. H. Hung, Y. Wang, Y. C. Chang, C. L. Huang, M. Huyck, and C. DeLisi. VisANT 3.5: multi-scale network visualization, analysis and inference based on the gene ontology. *Nucleic Acids Research*, 37:W115–W121+, 2009. (Cited on page 50.)

[113] Michael Baur, Marc Benkert, Ulrik Brandes, Sabine Cornelsen, Marco Gaertler, Boris KÃűpf, JÃijrgen Lerner, and Dorothea Wagner. Visone. In Petra Mutzel, Michael JÃijnger, and Sebastian Leipert, editors, *Graph Drawing, 9th International Symposium, GD 2001 Vienna, Austria, September 23-26, 2001, Revised Papers*, volume 2265 of *Lecture Notes in Computer Science*, pages 463–464. Springer, 2001. (Cited on page 50.)

[114] V. Batagelj and A. Mrvar. PAJEK – Program for large network analysis, 1998. (Cited on page 50.)

[115] Johannes Gräßler, Dirk Koschützki, and Falk Schreiber. CentiLib: comprehensive analysis and exploration of network centralities. *Bioinformatics (Oxford, England)*, 28(8):1178–1179, April 2012. (Cited on page 50.)

[116] H. Jeong, S. P. Mason, A. L. Barabási, and Z. N. Oltvai. Lethality and centrality in protein networks. *Nature*, 411(6833):41–42, May 2001. (Cited on page 50.)

[117] Xionglei He and Jianzhi Zhang. Why Do Hubs Tend to Be Essential in Protein Networks? *PLoS Genet*, 2(6):e88+, June 2006. (Cited on page 50.)

[118] Reka Albert, Hawoong Jeong, and Albert-Laszlo Barabasi. Error and attack tolerance of complex networks. *Nature*, 406(6794):378–382, July 2000. (Cited on pages 50 and 51.)

[119] Stefan Wuchty and Eivind Almaas. Peeling the yeast protein network. *Proteomics*, 5(2):444–449, February 2005. (Cited on page 50.)

[120] S. Wuchty. Interaction and domain networks of yeast. *Proteomics*, 2(12):1715–23, December 2002. (Cited on page 50.)

[121] Elena Zotenko, Julian Mestre, Dianne P. O'Leary, and Teresa M. Przytycka. Why Do Hubs in the Yeast Protein Interaction Network Tend To Be Essential: Reexamining the Connection between the Network Topology and Essentiality. *PLoS Comput Biol*, 4(8):e1000140+, August 2008. (Cited on page 50.)

[122] Stratus Not Altocumulus: A New View of the Yeast Protein Interaction Network. (Cited on page 50.)

[123] Teresa Reguly, Ashton Breitkreutz, Lorrie Boucher, Bobby-Joe J. Breitkreutz, Gary C. Hon, Chad L. Myers, Ainslie Parsons, Helena Friesen, Rose Oughtred, Amy Tong, Chris Stark, Yuen Ho, David Botstein, Brenda Andrews, Charles Boone, Olga G. Troyanskya, Trey Ideker, Kara Dolinski, Nizar N. Batada, and Mike Tyers. Comprehensive curation and analysis of global interaction networks in Saccharomyces cerevisiae. *Journal of biology*, 5(4):11+, June 2006. (Cited on page 51.)

[124] Diana Ekman, Sara Light, Asa Bjorklund, and Arne Elofsson. What properties characterize the hub proteins of the protein-protein interaction network of Saccharomyces cerevisiae? *Genome Biology*, 7(6):R45+, June 2006. (Cited on pages 51 and 92.)

[125] Ramon Aragues, Andrej Sali, Jaume Bonet, Marc A. Marti-Renom, and Baldo Oliva. Characterization of protein hubs by inferring interacting motifs from protein interactions. *PLoS computational biology*, 3(9):1761–1771, September 2007. (Cited on page 51.)

[126] Albert-Laszlo Barabasi and Zoltan N. Oltvai. Network biology: understanding the cell's functional organization. *Nature Reviews Genetics*, 5(2):101–113, February 2004. (Cited on page 51.)

[127] Gipsi Lima-Mendez and Jacques van Helden. The powerful law of the power law and other myths in network biology. *Molecular bioSystems*, 5(12):1482–1493, December 2009. (Cited on page 51.)

[128] Mark E. Newman. Assortative mixing in networks. *Phys. Rev. Lett.*, 89(20):208701, 2002. (Cited on page 51.)

[129] Sergei Maslov and Kim Sneppen. Specificity and Stability in Topology of Protein Networks. *Science*, 296(5569):910–913, May 2002. (Cited on page 51.)

[130] Juyong Park and Albert-László Barabási. Distribution of node characteristics in complex networks. In *Proceedings of the National Academy of Sciences*, 2007. (Cited on page 51.)

[131] X. Jiang, B. Liu, J. Jiang, H. Zhao, M. Fan, J. Zhang, Z. Fan, and T. Jiang. Modularity in the genetic disease-phenotype network. *FEBS letters*, 582(17):2549–2554, July 2008. (Cited on page 51.)

[132] J Nacher and N. Araki. On the Relation between Structure and Biological Function in Transcriptional Networks and ncRNA-Mediated Interactions. *2011 International Conference on Bioscience, Biochemistry and Bioinformatics IPCBEE*, 5:348–352, 2011. (Cited on page 51.)

[133] V. Latora and M. Marchiori. A measure of centrality based on network efficiency. *New Journal of Physics*, 9(6):188, June 2007. (Cited on page 51.)

[134] Linton C. Freeman. A Set of Measures of Centrality Based on Betweenness. *Sociometry*, 40(1):35–41, March 1977. (Cited on page 51.)

[135] See-Kiong Ng and Xiao-Li Li. *Biological Data Mining in Protein Interaction Networks*. Information Science Reference - Imprint of: IGI Publishing, Hershey, PA, 2009. (Cited on page 51.)

[136] Chia-Lang Hsu, Yen-Hua Huang, Chien-Ting Hsu, and Ueng-Cheng Yang. Prioritizing disease candidate genes by a gene interconnectedness-based approach. *BMC Genomics*, 12(Suppl 3):S25, 2011. (Cited on page 52.)

[137] D. Eppstein and J. Wang. Fast approximation of centrality. In *SODA 2001: Proceedings of the twelfth annual ACM-SIAM Symposium On Discrete Algorithms*, pages 228–229, Philadelphia, PA, USA, 2001. Society for Industrial and Applied Mathematics. (Cited on page 52.)

[138] Stefan Wuchty and Peter F. Stadler. Centers of complex networks. *J Theor Biol*, 223:2003, 2003. (Cited on page 52.)

[139] Sreenivas Chavali, Fredrik Barrenas, Kartiek Kanduri, and Mikael Benson. Network properties of human disease genes with pleiotropic effects. *BMC systems biology*, 4(1):78+, 2010. (Cited on page 52.)

[140] Haiyuan Yu, Philip M. Kim, Emmett Sprecher, Valery Trifonov, and Mark Gerstein. The Importance of Bottlenecks in Protein Networks: Correlation with Gene Essentiality and Expression Dynamics. *PLoS Comput Biol*, 3(4):e59+, April 2007. (Cited on page 52.)

[141] Jason E. McDermott, Ronald C. Taylor, Hyunjin Yoon, and Fred Heffron. Bottlenecks and hubs in inferred networks are important for virulence in Salmonella typhimurium. *Journal of computational biology : a journal of computational molecular cell biology*, 16(2):169–180, February 2009. (Cited on page 52.)

[142] Cécile Caretta-Cartozo, Paolo De Los Rios, Francesco Piazza, and Pietro Liò. Bottleneck genes and community structure in the cell cycle network of *s. pombe*. *PLoS Computational Biology*, 3(6), 2007. (Cited on page 52.)

[143] Ravishankar R. Vallabhajosyula and Alpan Raval. Computational Modeling in Systems Biology. In John M. Walker and Qing Yan, editors, *Systems Biology in Drug Discovery and Development*, volume 662 of *Methods in Molecular Biology*, chapter 5, pages 97–120. Humana Press, Totowa, NJ, 2010. (Cited on page 52.)

[144] Arvind K. Chavali, Anna S. Blazier, Jose L. Tlaxca, Paul A. Jensen, Richard D. Pearson, and Jason A. Papin. Metabolic network analysis predicts efficacy of FDA-approved drugs targeting the causative agent of a neglected tropical disease. *BMC systems biology*, 6(1):27+, April 2012. (Cited on page 52.)

[145] Liang C. Chen, Hsiang Y. Yeh, Cheng Y. Yeh, Carlos Arias, and Von W. Soo. Identifying co-targets to fight drug resistance based on a random walk model. *BMC Systems Biology*, 6(1):5+, 2012. (Cited on page 52.)

[146] Syed A. Rahman and Dietmar Schomburg. Observing local and global properties of metabolic pathways: 'load points' and 'choke points' in the metabolic networks. *BIOINFORMATICS*, 22(14), July 2006. (Cited on page 52.)

[147] Todd G Smith and Timothy R Hoover. Deciphering bacterial flagellar gene regulatory networks in the genomic era. *Adv Appl Microbiol*, 67:257–95, 2009. (Cited on page 53.)

[148] M.E.J. Newman. A measure of betweenness centrality based on random walks. *Social networks*, 27(1):39–54, 2005. (Cited on page 53.)

[149] Phillip Bonacich. Some unique properties of eigenvector centrality. *Social Networks*, 29(4):555–564, October 2007. (Cited on page 53.)

[150] Nicola Perra and Santo Fortunato. Spectral centrality measures in complex networks. *Physical Review E (Statistical, Nonlinear, and Soft Matter Physics)*, 78(3):036107+, 2008. (Cited on page 53.)

[151] De-wu Ding and Xiao-qing He. Application of eigenvector centrality in metabolic networks. In *Proceedings of the 2nd International Conference on Computer Engineering and Technology*, pages V1–89–V1–91, 2010. (Cited on page 53.)

[152] Ernesto Estrada. Virtual identification of essential proteins within the protein interaction network of yeast. *Proteomics*, 6(1):35–40, January 2006. (Cited on page 53.)

[153] E. Estrada and J. A. Rodríguez-Velázquez. Subgraph centrality in complex networks. *Phys Rev E Stat Nonlin Soft Matter Phys*, 71(5 Pt 2), May 2005. (Cited on page 53.)

[154] Min Li, Hanhui Zhang, Jianxin Wang, and Yi Pan. A new essential protein discovery method based on the integration of protein-protein interaction and gene expression data. *BMC Systems Biology*, 6(1):15+, 2012. (Cited on page 53.)

[155] Jianxin Wang, Min Li, Huan Wang, and Yi Pan. Identification of Essential Proteins Based on Edge Clustering Coefficient. *IEEE/ACM Transactions on Computational Biology and Bioinformatics*, 99(PrePrints), 2011. (Cited on page 53.)

[156] Leonardo Lanzi. Complex networks: Algorithms, analysis, and models. PhD Dissertation Thesis, 2012. (Cited on pages 58, 78, and 88.)

[157] C. Magnien, M. Latapy, and M. Habib. Fast computation of empirically tight bounds for the diameter of massive graphs. *Journal of Experimental Algorithmics*, 13, 2009. (Cited on pages 58 and 89.)

[158] Edsger Dijkstra. A note on two problems in connexion with graphs. *Numerische Mathematik*, 1:269–271, 1959. (Cited on page 60.)

[159] Research Group on Graph Theory and Department of the Universitat Politècnica de Catalunya (UPC) Combinatorics. The degree diameter problem for general graphs. `http://www-mat.upc.es/grup_de_grafs/`, 2010. (Cited on pages 66 and 67.)

[160] MetExplore. MetExplore: a web server to link metabolomic experiments and genome-scale metabolic networks. `http://metexplore.toulouse.inra.fr/metexplore/`, 2010. (Cited on pages 69, 73, and 99.)

[161] SNAP. Stanford Network Analysis Package (SNAP) Website. `http://snap.stanford.edu`, 2009. (Cited on pages 74, 75, 76, 77, 80, and 82.)

[162] WebGraph. WebGraph. `http://webgraph.dsi.unimi.it/`, 2001. (Cited on pages 74, 75, 76, 77, and 78.)

[163] C. Sommer. Christian Sommer's homepage. `http://www.sommer.jp/graphs/`, 2009. (Cited on pages 79, 80, and 82.)

[164] HPRD. Human Protein Reference Database. `http://www.hprd.org/`, 2003. (Cited on page 79.)

[165] The Jena Protein-Protein Interaction Website. `http://ppi.fli-leibniz.de/`, 2009. (Cited on page 79.)

[166] iPfam. iPfam: the Protein Domain Interactions Database. http://ipfam.sanger.ac.uk/, 2009. (Cited on page 79.)

[167] J. Wu, T. Vallenius, K. Ovaska, J. Westermarck, T.P. Makela, and S. Hautaniemi. Integrated network analysis platform for protein-protein interactions. *Nature methods*, 6:75–77, 2009. (Cited on page 79.)

[168] Pierluigi Crescenzi, Leonardo Lanzi, and Andrea Marino. Lasagne: Laboratory of algorithms, models, and analysis of graphs and networks. http://amici.dsi.unifi.it/lasagne/, 2012. (Cited on pages 79 and 80.)

[169] Integrated protein-protein interaction database of Synechocystis sp. PC 6803. http://bioportal.kobic.re.kr/SynechoNET/, 2007. (Cited on page 79.)

[170] Gergely Palla, Illés J. Farkas, Péter Pollner, Imre Derényi, and Tamás Vicsek. Fundamental statistical features and self-similar properties of tagged networks. *New Journal of Physics*, 10(12):123026+, December 2008. (Cited on page 79.)

[171] K. Norlen, G. Lucas, M. Gebbie, and J. Chuang. EVA: Extraction, Visualization and Analysis of the Telecommunications and Media Ownership Network, August 2002. (Cited on page 80.)

[172] TrustLet. TrustLet Website. ://www.trustlet.org, 2007. (Cited on page 80.)

[173] Pablo Gleiser and Leon Danon. Community Structure in Jazz. *Advances in Complex Systems*, 6(4):565–573, July 2003. (Cited on page 80.)

[174] Marian Boguna, Romualdo Pastor-Satorras, Albert D. Guilera, and Alex Arenas. Models of social networks based on social distance attachment. *Physical Review E*, 70(5):056122+, November 2004. (Cited on page 80.)

[175] Clusters and Communities, overlapping dense groups in networks. http://hal.elte.hu/cfinder/, 2005. (Cited on page 80.)

[176] Pajek dataset. http://vlado.fmf.uni-lj.si/pub/networks/data/default.htm, 2006. (Cited on pages 80 and 83.)

[177] J. Duch and A. Arenas. Community identification using Extremal Optimization. *Physical Review E*, 72:027104, 2005. (Cited on page 80.)

[178] tnet. tnet package, analysis of wieghted, two-mode, and longitudinal networks. http://opsahl.co.uk/tnet/datasets/. (Cited on page 80.)

[179] Sandbox. Webscope from Yahoo! Labs. Data available, as explained at http://sandbox.yahoo.com/, 2010. (Cited on pages 80, 81, and 83.)

[180] Ben Y. Zhao. CURRENT LAB: social networking project. Data available, as explained at http://current.cs.ucsb.edu/facebook/, 2010. (Cited on page 81.)

[181] U. Aron. Uri Alon Lab. http://www.weizmann.ac.il/mcb/UriAlon/, 2002. (Cited on page 83.)

[182] Deepak Ajwani, Ulrich Meyer, and David Veith. I/o-efficient hierarchical diameter approximation. In *ESA*, pages 72–83, 2012. (Cited on page 84.)

[183] Deepak Ajwani, Andreas Beckmann, Ulrich Meyer, and David Veith. I/o-efficient approximation of graph diameters by parallel cluster growing - a first experimental study. In *ARCS Workshops*, pages 493–504, 2012. (Cited on page 84.)

[184] V. Chepoi, F. Dragan, B. Estellon, M. Habib, and Y. Vaxès. Diameters, centers, and approximating trees of delta-hyperbolic geodesic spaces and graphs. In *Proceedings of the 24th Annual Symposium on Computational Geometry*, SCG '08, pages 59–68, New York, NY, USA, 2008. ACM. (Cited on pages 91 and 157.)

[185] R. Albert, H. Jeong, and A. L. Barabási. The diameter of the world wide web. *Nature*, 401:130–131, 1999. (Cited on page 92.)

[186] L. A. N. Amaral, A. Scala, M. Barthélémy, and H. E. Stanley. Classes of small-world networks. *Proceedings of the National Academy of Sciences*, 97(21):11149–11152, October 2000. (Cited on page 92.)

[187] T. W. Valente. *Social Networks and Health: Models, Methods, and Applications*. Oxford University Press, 2010. (Cited on page 92.)

[188] D. J. Watts and S. H. Strogatz. Collective dynamics of'small-world'networks. *Nature*, 393(6684):409–10, 1998. (Cited on page 92.)

[189] H. Jeong, B. Tombor, R. Albert, Z. N. Oltvai, and A. L. Barabási. The large-scale organization of metabolic networks. *Nature*, 407(6804):651–654, October 2000. (Cited on page 92.)

[190] David A. Fell and Andreas Wagner. The small world of metabolism. *Nature Biotechnology*, 18(11):1121–1122, November 2000. (Cited on page 92.)

[191] A. Wagner and D. A. Fell. The small world inside large metabolic networks. *Proc R Soc Lond B Biol Sci*, 268(1478):1803–1810, September 2001. (Cited on page 92.)

[192] E. Ravasz, A. L. Somera, D. A. Mongru, Z. N. Oltvai, and A. L. Barabási. Hierarchical organization of modularity in metabolic networks. *Science*, 297(5586):1551–1555, 2002. (Cited on page 92.)

[193] H. Ma and A. P. Zeng. Reconstruction of metabolic networks from genome data and analysis of their global structure for various organisms. *Bioinformatics*, 19(2):270–277, January 2003. (Cited on page 92.)

[194] Soon-Hyung Yook, Zoltan N Oltvai, and Albert-László Barabási. Functional and topological characterization of protein interaction networks. *Proteomics.*, 4:928–42, 2004. (Cited on page 92.)

[195] Masanori Arita. The metabolic world of Escherichia coli is not small. *Proceedings of the National Academy of Sciences of the United States of America*, 101(6):1543–1547, February 2004. (Cited on page 92.)

[196] Esa Pitkänen, Ari Rantanen, Juho Rousu, and Esko Ukkonen. Finding feasible pathways in metabolic networks. In *Proceedings of the 10th Panhellenic conference on Advances in Informatics*, PCI'05, pages 123–133, Berlin, Heidelberg, 2005. Springer-Verlag. (Cited on page 92.)

[197] Zhihua Zhang and Jianzhi Zhang. A Big World Inside Small-World Networks. *PLoS ONE*, 4(5):e5686+, May 2009. (Cited on pages 92 and 93.)

[198] J. Leskovec, J. Kleinberg, and C. Faloutsos. Graph Evolution: Densification and Shrinking Diameters. *ACM Trans. Knowl. Discov. Data*, 1(1), 2007. (Cited on page 93.)

[199] Wassily Hoeffding. Probability Inequalities for Sums of Bounded Random Variables. *Journal of the American Statistical Association*, 58(301):13–30, 1963. (Cited on page 93.)

[200] Alexey V. Antonov, Sabine Dietmann, Philip Wong, and Hans W. Mewes. Ticl – a web tool for network-based interpretation of compound lists inferred by high-throughput metabolomics. *FEBS Journal*, 276(7):2084–2094, 2009. (Cited on page 95.)

[201] David P. Leader, Karl Burgess, Darren Creek, and Michael P. Barrett. Pathos: A web facility that uses metabolic maps to display experimental changes in metabolites identified by mass spectrometry. *Rapid Communications in Mass Spectrometry*, 25(22):3422–3426, 2011. (Cited on page 95.)

[202] Betzler N. Steiner tree problems in the analysis of biological networks. PhD Dissertation Thesis, 2005. (Cited on page 97.)

[203] Paulo Vieira Milreu. Enumerating functional substructures of genome-scale metabolic networks: Stories, precursors and organisations. PhD Dissertation Thesis, 2012. (Cited on pages 98 and 112.)

[204] Michael R. Garey and David S. Johnson. *Computers and Intractability; A Guide to the Theory of NP-Completeness*. W. H. Freeman & Co., New York, NY, USA, 1990. (Cited on page 103.)

[205] Thomas Eiter, Kazuhisa Makino, and Georg Gottlob. Computational aspects of monotone dualization: A brief survey. *Discrete Applied Mathematics*, 156(11):2035–2049, 2008. (Cited on page 110.)

[206] Fedor V. Fomin, Pinar Heggernes, Dieter Kratsch, Charis Papadopoulos, and Yngve Villanger. Enumerating minimal subset feedback vertex sets. In *WADS*, pages 399–410, 2011. (Cited on pages 112 and 158.)

[207] Fedor V. Fomin, Fabrizio Grandoni, and Dieter Kratsch. A measure & conquer approach for the analysis of exact algorithms. *J. ACM*, 56(5), 2009. (Cited on pages 112 and 158.)

[208] Mano Ram Maurya, Raghunathan Rengaswamy, and Venkat Venkatasubramanian. A systematic framework for the development and analysis of signed digraphs for chemical processes. 1. algorithms and analysis. *Industrial & Engineering Chemistry Research*, 42(20):4789–4810, 2003. (Cited on page 113.)

[209] Eduardo D. Sontag. Molecular systems biology and control. In *European Journal of Control*, volume 11, page 396âĂŞ435, 2005. (Cited on page 114.)

[210] E.H. Sussenguth. A graph-theoretical algorithm for matching chemical structures. *J. Chem. Doc.*, 5:36–43, 1965. (Cited on page 114.)

[211] John T. Welch, Jr. A mechanical analysis of the cyclic structure of undirected linear graphs. *J. ACM*, 13:205–210, 1966. (Cited on page 114.)

[212] G.J. Bezem and J. van Leeuwen. Enumeration in graphs. Technical Report RUU-CS-87-07, Utrecht University, 1987. (Cited on page 114.)

[213] Prabhaker Mateti and Narsingh Deo. On algorithms for enumerating all circuits of a graph. *SIAM J. Comput.*, 5(1):90–99, 1976. (Cited on page 114.)

[214] Reinhard Diestel. *Graph Theory (Graduate Texts in Mathematics)*. Springer, 2005. (Cited on pages 114 and 125.)

[215] Maciej M. Syslo. An efficient cycle vector space algorithm for listing all cycles of a planar graph. *SIAM J. Comput.*, 10(4):797–808, 1981. (Cited on page 114.)

[216] Jayme L. Szwarcfiter and Peter E. Lauer. A search strategy for the elementary cycles of a directed graph. *BIT Numerical Mathematics*, 16, 1976. (Cited on page 115.)

[217] J. Ponstein. Self-avoiding paths and the adjacency matrix of a graph. *SIAM Journal on Applied Mathematics*, 14:600–609, 1966. (Cited on page 115.)

[218] S.S. Yau. Generation of all hamiltonian circuits, paths, and centers of a graph, and related problems. *IEEE Transactions on Circuit Theory*, 14:79–81, 1967. (Cited on page 115.)

[219] T. R. Halford and K. M. Chugg. Enumerating and counting cycles in bipartite graphs. In *IEEE Communication Theory Workshop*, 2004. (Cited on page 115.)

[220] Tamás Horváth, Thomas Gärtner, and Stefan Wrobel. Cyclic pattern kernels for predictive graph mining. In *Proc. of 10th ACM SIGKDD*, pages 158–167, 2004. (Cited on page 115.)

[221] Hongbo Liu and Jiaxin Wang. A new way to enumerate cycles in graph. In *AICT and ICIW*, pages 57–59, 2006. (Cited on page 115.)

[222] K. Sankar and A.V. Sarad. A time and memory efficient way to enumerate cycles in a graph. In *Intelligent and Advanced Systems*, pages 498–500, 2007. (Cited on page 115.)

[223] Marcel Wild. Generating all cycles, chordless cycles, and hamiltonian cycles with the principle of exclusion. *J. of Discrete Algorithms*, 6:93–102, 2008. (Cited on page 115.)

[224] R. Schott and George Stacey Staples. Complexity of counting cycles using Zeons. *Computers and Mathematics with Applications*, 62:1828–1837, 2011. (Cited on page 115.)

[225] Rui A. Ferreira, Roberto Grossi, and Romeo Rizzi. Output-sensitive listing of bounded-size trees in undirected graphs. In *ESA*, pages 275–286, 2011. (Cited on page 121.)

[226] Robert Endre Tarjan. Depth-first search and linear graph algorithms. *SIAM J. Comput.*, 1(2):146–160, 1972. (Cited on page 128.)

[227] Pierre Peterlongo, Nicolas Schnel, Nadia Pisanti, Marie-France Sagot, and Vincent Lacroix. Identifying snps without a reference genome by comparing raw reads. In *SPIRE*, pages 147–158, 2010. (Cited on page 143.)

[228] P.A. Pevzner, H. Tang, and G. Tesler. *D*e novo repeat classification and fragment assembly. In *RECOMB*, pages 213–222, 2004. (Cited on page 143.)

[229] Gordon Robertson, Jacqueline Schein, Readman Chiu, Richard Corbett, Matthew Field, Shaun D. Jackman, Karen Mungall, Sam Lee, Hisanaga Mark M. Okada, Jenny Q. Qian, Malachi Griffith, Anthony Raymond, Nina Thiessen, Timothee Cezard, Yaron S. Butterfield, Richard Newsome, Simon K. Chan, Rong She, Richard Varhol, Baljit Kamoh, Anna-Liisa L. Prabhu, Angela Tam, YongJun Zhao, Richard A. Moore, Martin Hirst,

Marco A. Marra, Steven J. Jones, Pamela A. Hoodless, and Inanc Birol. De novo assembly and analysis of RNA-seq data. *Nature methods*, 7(11):909–912, November 2010. (Cited on page 143.)

[230] Jared T. Simpson, Kim Wong, Shaun D. Jackman, Jacqueline E. Schein, Steven J. M. Jones, and İnanç Birol. ABySS: A parallel assembler for short read sequence data. *Genome Research*, 19(6):1117–1123, June 2009. (Cited on page 143.)

[231] D.R. Zerbino and E. Birney. Velvet: Algorithms for de novo short read assembly using de bruijn graphs. *Genome Research*, 18(5):821–829, 2008. (Cited on page 143.)

[232] Z. Iqbal, M. Caccamo, I. Turner, P. Flicek, and G. McVean. De novo assembly and genotyping of variants using colored de bruijn graphs. *Nature genetics*, 2012. (Cited on page 143.)

[233] M. Sammeth. Complete alternative splicing events are bubbles in splicing graphs. *J. Comput. Biol.*, 16(8):1117–1140, 2009. (Cited on page 143.)

[234] D. Gusfield, S. Eddhu, and C.H. Langley. Optimal, efficient reconstruction of phylogenetic networks with constrained recombination. *J. Bioinf. and Comput. Biol.*, 2(1):173–214, 2004. (Cited on page 143.)